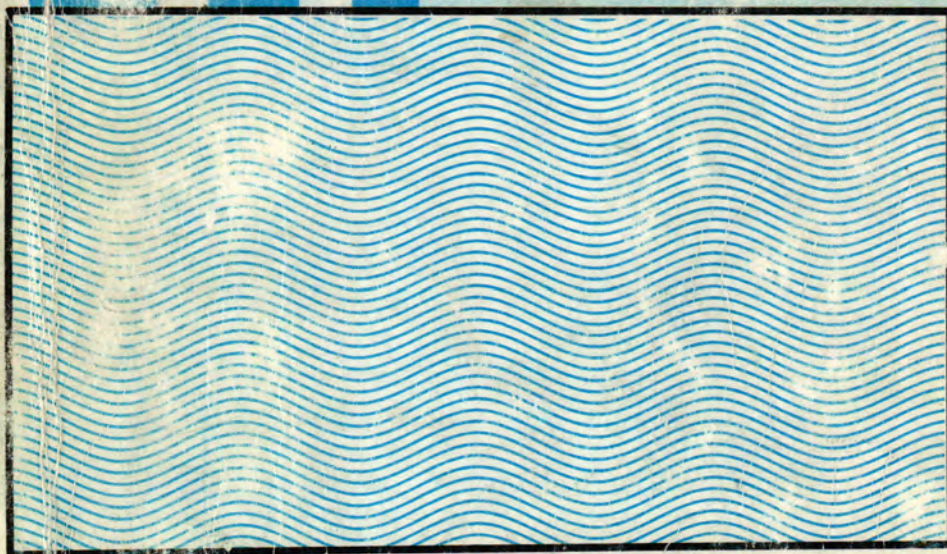


Al-Mustansiriya Journal of Science

Vol. 11

No. 1

Year 2000



**Issued by College of Science
Al-Mustansiriya University**

AL-MUSTANSIRIYA JOURNAL OF SCIENCE

Head Editor

Dr. Rasheed H. Al-Naimi

Prof. Physics

General Editor

Dr. Abdul Wahid Baqir

Prof. Microbiology

EDITORIAL BOARD

Dr. Ridha I. Al-Bayaty

Prof. Chemistry

Dr. Ihsan Sh. Tawfiq

Prof. Biology

Dr. Abdul Samie A. R. Al-Janaby

Asst. Prof. Mathematics

Dr. Kais J. Latif

Asst. Prof. Meteorology

Dr. Hashim H. Jawad

Asst. Prof. Physics

Dr. Mohammad A. Ali

Asst. Prof. Computer

List of Contents

Subject	Page No.
Study of the Inhibitory Effect of Lactobacillus on Some Food Pathogenic Bacteria NIBRAS N. MAHMOOD & ABDUL W. BAQIR	1
A Comparative Study of Coxsacki Bx. Virus IgM Response in Elisa and IgM Nutralization Test RAGHAD AL -SUHAIL	11
Fibrinolytic Activity of Thermostable Alkaline Proteases from Alkalophilic and Thermophilic <i>Bacillus sp.</i> SHADAN AL-WANDWAI	21
Effect of Decomposing Wheat Residue on Growth of Chickpea and its Possible Modes of Action KADHUM H.Y. ZWAIN	31
Use of Oleander and Tobacco Extracts As An Insecticide BADIR M. AL-AZAWI, WALA SHAWKET AL-MASHADANI AND SUADAD A.E. AL-SAMARAIE	41
Inhibition of Colony Growth of Some Dermatophytes by Some Plant Extracts IHSAN S. DAMIRDAGH AND ALI A.H. AL-JANABI	53
A Modified <i>Salomonella typhi</i> Ty21a Strain which Encoded to Colonization Factor Antigen SHAYMA J. AHMED	65

Subject	Page No.
Study on Fruit Scab Disease of Cucumber (<i>Cucumis Sativus</i> , L.) Caused by <i>Cladosporium</i> <i>Cladosporioides</i> and its Control ABDULAZEEZ M. NOKHALAN	73
Isolation and Detection of <i>Clostridium</i> <i>Perfringens</i> and Study of its Physiological Characteristics and Sporulation with Comparison of the Sensory Quality of Beef ZAID K. KAMOUNA AND HAMEED M. AL-OBAIDY	79
Coherent States and the Classical Limit of the Hydrogen Atom MOHAMMED A. Z. HABEEB ZIYAD A. ABDEL-KADER AND KHALID A. AHMAD	95
The $SL(3,R)$ Group and Harmonic Oscillator with Variable Damping MOHAMMED A. Z. HABEEB AND ZIYAD KH. A. ABDEL-KADER	111
Comparison Between Normal Metal, Low and High Temperature Suprconductors D.N. Rouf, W.A. Latif, and K.A. Ahmed	123
EO, M1, E2 TRANSTITIONS OF COLLECTIVE LEVELS BELOW 1.821 MeV IN Pt-196 IMAN T. AL-ALAWY	147
The Variation of Probability Distributions with Atomic Number KHALIL H. AL-BAYATI AND MOHAMMED I. SANDUK	161

Subject	Page No.
Photostabilization of Polystyrene by Hindered Amines F.M. AL-SALAMI	175
Preparation of New Acetylenic Amines of Expected Pharmacological Activity ABDUL-HUSSAIN KHUTHEIR AND ADIL O. ABDEL BAGI	185
Synthesis of N-(2,4-Dinitrophenyl)-N'-(Substituted)-1,4-Diamino-2-Butynes MAZIN J. HABIB	195
The Role of Tide Modifying Factors in the NW Arabian Gulf HASSAN H. SALMAN	203
On Infinite Dimensional Leslie Matrices in Sequence Space ℓ_p , $p < \infty$ ABDUL SAMEE A. R. AL-JANABE AND OMER F. MUKHERIJ**	217
Finiteness of Fully Stable Modules MAHDY S. ABBAS	231
Direct Reduction of Some Nonlinear Evolution Equations INAAM A. MLLOKI AND AMAL K. AL-TAMIMI	239
Schedulign Job Classes on a Single Machine with batches to Minimize the Sum of the Weigted Completion Times TARIK S. ABDUL-RAZAQ AND KAWA A. ABDULLAH	253

Study of the Inhibitory Effect of Lactobacillus on Some Food Pathogenic Bacteria

NIBRAS N. MAHMOOD & ABDUL W. BAQIR

Department of Biology, College of Science, Al-Mustansiriya University, Baghdad, Iraq

(Received Apr. 21, 1999; Accepted May 16, 1999)

الخلاصة

جمعت (٥٠) عزلة من عصيات اللاكتيك (*Lactobacillus*) من مصادر مختلفة لاختيار فعاليتها كفاءتها في انتاج المواد المثبطة لنمو بعض انواع البكتريا المرضية في الاغذية. وقد شخصت (٢٠) عزلة منها بانها تعود للوع *L.bulgaricus* و (١٣) *L. plantarum* ، (١١) *L. casei* ، (٦) *L. brevis*. واعتمادا على افضل فعالية تثبيطية انتخبت عزلة واحدة من كل الانواع *L. buigarius* و *L. plantrum* و *L. casei*، واعطت العزلات الثلاث افضل فعالية لتثبيط سلالات البكتريا الاختبارية المستخدمة، *Brucella* ، *Bacillus subtilis* *Pseudomonas aeruginosa* *Staphylococcus aureus* *Escherichia coli* ، *abortus* لفترات تراوحت بين (١٨، ٢٤، ٣٠، ٣٦، ٤٢) ساعة على وسط MRS الصلب، فيما لم تؤدي زيادة فترة التثبيط لغاية (٤٨) ساعة الى زيادة كفاءة التثبيط باستثناء العزلة *L. casei* عندما اعطت افضل فعالية تثبيطية ضد سلالة *Br. Abortus* بعد (٤٨) ساعة.

ABSTRACT

Fifty isolates of *Lactobacillus* were isolated from various food sources to investigate their antagonistic activity against some food pathogenic bacteria. Identification showed that 20,13,11 and 6 isolates were belonged to *L.bulgaricus*, *L. plantarum*, *L. casei* and *L. brevis*, respectively. Depending on the most efficient antibacterial effect, one isolate from each of the first three species were evaluated for their inhibitory effect on MRS agar against *Bacillus subtilis*, *Brucella abortus*, *E. coli*, *Ps. Aeruginosa* and *S. aureus*. Highest effects were achieved at various periods incubation up to 42 hr. With the exception

*Study of the Inhibitory Effect of Lactobacillus on Some Food
Pathogenic Bacteria*

N.N. Mahmood & A.W. Baqir

of *L. casei* inhibitory effect was not improved by any isolate even when incubation periods increased to 48 hr.

INTRODUCTION

Lactic acid bacteria are involved in the production of fermented foods constituting one quarter of our dairy diet. Such foods are characterized by a safe history, certain beneficial health effects, and an extended shelf life when compared with others⁽¹⁾.

As a primary effects they reduce the (pH, and capable to produce organic acids, hydrogen peroxide, lactic peroxidase diacetyl and other inhibitory is probably due to combination of such factors⁽⁴⁾.

Bacteriocinogenicity, already determined within lactic acid bacteria, has been the subject of recent studies^(5,6).

The purpose of this study was to screen a number of lactic acid bacteria isolated from different sources for antagonistic activity against some food poisoning bacteria after incubation for various periods of time.

MATERIALS AND METHODS

Sources of Isolates and Strains

Fifty isolates of *Lactobacillus* were collected from dairy products in Baghdad and in Abu-Ghraib.

Lactobacillus bulgaricus were purified from a lyophilized double-strain culture obtained from a dairy factory near Baghdad.

Tested bacteria (*Bacillus subtilis*; *Brucella abortus* S₉₉; *Escherichia coli* ATCC25922; *Pseudomonas aeruginosa* ATCC27853 and *Staphylococcus aureus* ATCC25923 were obtained from Saddam hospital in Baghdad.

Cultivation of Lactobacilli from Food Samples

After preparing suspension from samples, 1ml of each was inoculated into 10ml of sterilized MRS broth (Man Rogosa Sharpe) in test tubes, then incubated at 37°C

for 48hr under anaerobic conditions. The process was repeated three times for purification purpose⁽⁷⁾. Slants of each isolates also were prepared on MRS agar.

Bacilli-Cocci Differentiation

Streaking technique was used to obtain individual colonies from lyophilized culture on the Rogosa SL agar plates were incubated at 37°C for 48hr under anaerobic conditions⁽⁸⁾. Selected colonies were then transferred into 10ml of SL broth and incubated at 37°C for 48hr⁽⁹⁾.

Identification of the Lactobacilli Isolates

Suspected lactobacilli were identified by colony morphology and microscopic characteristics; followed by the biochemical tests which included; gelatinase test⁽¹⁰⁾, acid production in litmus milk media⁽¹¹⁾, catalase test⁽¹²⁾, ammonia from arginine⁽¹³⁾, and sugars (glucose, fructose, lactose, sucrose, mannitol, xylose) fermentation⁽⁷⁾.

Detection of Antagonistic Activity

Petri dishes contained MRS agar were streaked by Lactobacillus isolates previously grown in the MRS broth. Dishes were incubated under anaerobic conditions at 37°C for 48hr⁽¹⁴⁾.

After incubation cork borer (5mm diameter) was used to transfer discs to plates contained MRS-Glucose agar⁽¹⁵⁾ previously spreaded by 0.1ml of each test bacteria.

Plates then, incubated at 37°C for 24hr, followed by measuring the inhibition zone⁽¹⁶⁾.

Three of the highest antagonistic activity isolates were selected and subjected to same above treatment but after incubation for (18,24,30,36,42 and 48)hr to determine the ideal incubation period for production of antagonistic materials.

RESULTS AND DISCUSSION

Cultural and Microscopic Examination

Typical colonies of Lactobacillus isolates grew well on both SL and MRS agar after incubation at 37°C for 48-

72hr. Rogosa et.al.⁽¹⁷⁾ stated that SL agar is a suitable and selected medium for *Lactobacillus* due to its acidity (pH=5.4) and high content of Na-acetate in its formula. MRS medium, on the other hand, encourages growth of most *Lactobacillus* species⁽⁷⁾.

Slide examination showed that cells of the isolates were long rods arranged in chains, gram (+) and non sporeformers.

Biochemical Tests

Biochemical results showed that all strains were gelatinase and catalase negative, but positive to the litmus test when they exhibited curd and acid in the milk which lowered the pH from 6.5 to 4.5. They were unable to produce ammonia from arginine.

Table (1) shows that the *Lactobacilli* isolates were differed in their ability to ferment sugar sources.

Isolates (Lb-7, Lb-8, Lb-25, Lb-29, Lb-37, Lb-44) were identified as *L. brevis*, while (Lb-6, Lb-9, Lb-10, Lb-17, Lb-21, Lb-22, Lb-23, Lb-24, Lb-30, Lb-38, Lb-39) as *L. casei*, (Lb-4, Lb-5, Lb-11, Lb-12, Lb-13, Lb-16, Lb-18, Lb-19, Lb-20, Lb-27, Lb-28, Lb-34, Lb-35, Lb-36, Lb-42, Lb-43, Lb-46, Lb-47, Lb-49, Lb-50) as *L. bulgaricus*. (Lb-1, Lb-2, Lb-14, Lb-15, Lb-26, Lb-31, Lb-32, Lb-33, Lb-40, Lb-41, Lb-45, Lb-48) were belonged to *L. plantarum*.

Efficiency of Antagonistic Activity

MRS agar was found to be the suitable medium for studying the ability of *Lactobacilli* isolates to produce antagonistic substances against test bacteria⁽¹⁶⁾.

Results in table (2) show that *Lactobacillus* isolates exhibited various antagonistic activities against the test bacteria. Lb-3, Lb-24 and Lb-43 isolates of *Lactobacillus* possessed highest antagonistic activity against the test bacteria.

Sixteen other isolates exhibited such activity against four of the test bacteria but not against *Br. Abortus*⁽¹⁸⁾.

Depending on the best antimicrobial activity, three isolates; namely (Lb-3) belong to *L. plantarum*, (Lb-24) to

L. casei and (Lb-43) to *L. bulgaricus* were selected for further experiments.

Table 1: Ability of Lactobacillus isolates to ferment carbon sources

Fermentation ability						Isolates symbol
Xyl.	Mann	Suc	Lac	Fru	Glu	
-	+(3)	+1	+1	+1	+1	Lb-1
+1	+2	+1	+1	+1	+1	Lb-2
+3	+1	+2	+1	+1	+1	Lb-3
-	-	-	+1	+1	+1	Lb-4
-	-	-	+1	+2	+1	Lb-5
-	+2	+1	+2w	+1	+1	Lb-6
+2	-	+2w	+1	+1	+1	Lb-7
+3w	-	+3w	+1	+1	+1	LB-8
-	+2	+2w	+1	+1	+1	Lb-9
-	+1	+2	+1	+1	+1	Lb-10
-	-	-	+1	+1	+1	Lb-11
-	-	-	+1	+1	+1	Lb-12
-	-	-	+2	+1	+1	Lb-13
+4w	+1	+2	+2	+1	+1	Lb-14
-	+1	+1	+1	+2	+1	Lb-15
-	-	-	+1	+1	+1	Lb-16
-	+1	+2w	+1	+1	+1	Lb-17
-	-	-	+1	+1	+1	Lb-18
-	-	-	+1	+1	+1	Lb-19
-	-	-	+2w	+1	+1	Lb-20
-	+1	+3w	+1	+1	+1	Lb-21
-	+1	+2w	+1	+1	+1	Lb-22
-	+1	+1	+2w	+1	+1	Lb-23
-	+1	+1	+3w	+1	+1	Lb-24
+2w	-	+1	+1	+1	+1	Lb-25
-	+2	+1	+1	+1	+1	Lb-26
-	-	-	+2	+1	+1	Lb-27
-	-	-	+1	+1	+1	Lb-28
+2w	-	+2w	+1	+1	+2	Lb-29
-	+1	+2w	+1	+1	+1	Lb-30

Study of the Inhibitory Effect of Lactobacillus on Some Food Pathogenic Bacteria

N.N. Mahmood & A.W. Baqir

+3w	+1	+1	+1	+1	+1	Lb-31
+2	+1	+1	+3	+1	+1	Lb-32
+3w	+1	+1	+1	+1	+1	Lb-33
-	-	-	+1	+1	+1	Lb-34
-	-	-	+1	+1	+1	Lb-35
-	-	-	+3w	+1	+1	Lb-36
+2	-	+2	+1	+1	+1	Lb-37
-	+3	+2	+1	+1	+1	Lb-38
-	+2	+2	+3	+1	+1	Lb-39
+3w	+1	+1	+2	+1	+1	Lb-40
-	+2	+1	+1	+1	+1	Lb-41
-	-	-	+1	+2	+1	Lb-42
-	-	-	+3w	+1	+1	Lb-43
+1	-	+1	+2	+2	+1	Lb-44
+4w	+1	+1	+2	+1	+1	Lb-45
-	-	-	+1	+2	+1	Lb-46
-	-	-	+2	+1	+1	Lb-47
+2	+2	+1	+2	+1	+1	Lb-48
-	-	-	+1	+1	+2	Lb-49
-	-	-	+1	+1	+1	Lb-50

Table 2: Antibacterial activity of lactobacillus isolates on MRS medium (by disc method)

Antimicrobial activity against					Isolates Symbol
G(-) bacteria			G(+) bacteria		
<i>Br. Abortus</i>	<i>Ps. Aerugi</i>	<i>E.coli</i>	<i>B.subtilis</i>	<i>S.aureus</i>	
+	++	++	+	+++	Lb-3, Lb-24, Lb-43
-	+	+	+	+	Lb-1, Lb-2, Lb-11, Lb-14, Lb-18, Lb-19, Lb-20, Lb-26, Lb-27, Lb-31, Lb-32, Lb-35, Lb-39, Lb-40, Lb-48, Lb-49
-	-	+	+	+	Lb-4, Lb-5, Lb-16, Lb-22, Lb-23, Lb-28, Lb-33, Lb-36, Lb-38, Lb-41, Lb-42, Lb-45, Lb-46, Lb-50
-	-	-	+	-	Lb-10, Lb-12, Lb-13, Lb-17, Lb-21, Lb-30, Lb-37
-	-	-	-	-	Lb-8
-	-	-	-	-	Lb-6, Lb-7, Lb-9, Lb-15, Lb-25, Lb-29, Lb-34, Lb-44, Lb-47

Disc diameter = 5mm

+= (6-14mm) inhibition diameter

++ = (15-20mm) inhibition diameter

+++ = (21-26mm) inhibition diameter

Effect of Incubation Periods on the Antagonistic Activity

All three isolates gave high antagonistic activity against all test bacteria (*B. subtilis*; *E.coli*; *S.aureus*; *Ps.aeruginosa* and *Br.abortus*) plated on MRS agar for the periods of (18,24,30,36 and 42)hr.

Unfortunately, extending incubation period to (48)hr. showed no increase in the inhibition efficiency except in the case of *L. casei* isolate when it gave best inhibitory activity against *B. subtilis* after only (18)hr of incubation when inhibition zone reached (11)mm (figure 1).

Best activity gave by *L. plantarum* against all test bacteria was achieved after (36)hr except against *B. subtilis* when occurred after (24)hr^(19,20).

L. bulgaricus gave best activity against *S. aureus* after (30)hr and against (*E.coli*, *Br. Abortus* and *B. subtilis*) after (36)hr, but after (48)hr against *Ps. Aeruginosa*^(21,22).

REFERENCES

1. Hammes, W.P. and Tichaczek, P.S. The potential of lactic acid bacteria for the production of safe and whole some food. Z-lebensm-Unters-Forsch., 198(3): 193-201 (1994).
2. Daeschel, M.A. Antimicrobial substances from lactic acid bacteria for use as food preservatives. Food Technology., 43(1): 164-167(1989).
3. Upreti, G.C. and Hinsdill, R.D. Production and mode of action of lactocin 27: bacteriocin form homofermentative lactobacillus. Antimicrobial Agents and Chemotherapy., 7(2): 139-45 (1975).
4. Schillinger, U. and Lucke, F.K. Antibacterial activity of *lactobacillus sake*-isolated from meat. Appl. Environ. Microbi., 55(8): 1901-1906(1989).
5. Klaenhammer, T.R. Bacteriocins of lactic acid bacteria Biochimie., 70: 337-349 (1988).

Study of the Inhibitory Effect of Lactobacillus on Some Food Pathogenic Bacteria
N.N. Mahmood & A.W. Baqir

6. Piard, J.C. and Desmazeaud, M. Inhibitory factors produced by lactic acid bacteria: 2 Bacteriocins and other antibacterial substances. *Lait*, 72: 13-142 (1992).
7. DeMan, J.C.; Rogosa, M. and Sharpe, M.E. A medium for the cultivation of Lactobacilli. *J. Appl. Bact.*, 23(1): 130-135 (1960).
8. Stainer, R.Y.; Ingraham, J.L.; Wheelis, M.L. and Painter, P.R. The microbial world, 5th. Ed. Prentic Hall New Jersey (1986).
9. Collins, C.H. and Lyne, P.M. Microbial mehtods. Balte Worth and Co. (Pub.) (1985).
10. Baron, E.J. and Finegold, S.M. Diagnostic Microbiology., 8th. Ed. The CV Mosby company, Baltimore (1990).
11. Kandler, O. and Weiss, N. Genus Lactobacillus In: Bergey's manual of systematic bacteriology. (Sneath, PHA; Mair, N.S. and Holt, J.G. ed). Vol. 2 Williams and Wilkins co., Baltimore M.D. USA (1986).
12. Tayler, W.L. and Achanzer, D. Catalase test as an aid in the Identification of Enterobacteriaceae. *Appl. Microbiol.*, 24(1): 58-61 (1972).
13. Briggs, M. The classification of lactobacilli by means of physiological test. *J. Gen. Microbiol.*, 9: 234-248 (1953).
14. Silva, M., Jacobus, N.V.; Deneke, C. and Gorbach, S.L. Antimicrobial substances from a human Lactobacillus strain. *Antimicrob. Agent and chemother.*, 31(8): 1231-1233 (1987).
15. Vignolo, G.M.; Suriani, F., Holgado, A.P.R. and Oliver, G. Antibacterial activity of Lactobacillus strains isolated from dry fermented sausages. *J. Appl. Bacteriol.*, 75: 344-349 (1993).

١٦. القصاب، عبد الجبار عمر و الخفاجي، زهرة محمود. تأثير الظروف المختلفة على الفعالية التثبيطية للعصيات اللبنية المعوية تجاه البكتيريا المعوية المسببة للإسهال. مجلة العلوم الزراعية العراقية. المجلد ٣، العدد (١) ص ١٨-٢٦ (١٩٩٢).

17. Rogosa, M.; Mitchell, J.A. and Wiseman, R.F. A selective medium for the isolation and enumeration of oral and fecal lactobacilli. J. Bacteriol., 62: 132-133 (1951).
18. Egorov, N.S. Antibiotics a scientific approach. Mir Publishers, Moscow (1985).
19. Vescovo, M; Torriani, S.; Orsi, C.; Macchiarolo, F. and Scolari, G. Application of antimicrobial-producing lactic acid bacterial to control pathogens in ready to use vegetables. J. Appl. Bacteriol., 81(2): 113-119 (1996). Abst.
20. Olasupo, N.A.; Olukoya, D.K. and Odunfa, S.A. Studies on bacteriogenic Lactobacillus isolated from selected Nigerian fermented foods. J. Basic Microbid., 35(5): 319-324 (1995). Abst.
21. Boycheva, S. Inhibitory activity of certain lactic acid bacteria against gram negative micro organisms in the raw milk. Abstracts fifth symposium on lactic acid bacteria FEMS. Microbiology., 8/12 (1996).
22. Fang, W.; Shi, M.; Hunag, L.; Chen, J. and Wang, Y. Antagonism of lactic acid bacteria towards *Staphylococcus aureus* and *Escherichia coli* on agar plates and in milk. Vet. Res., 27(1): 3-12 (1996). Abst.

A Comparative Study of Coxsackie Bx. Virus IgM Response in Elisa and IgM Neutralization Test

RAGHAD AL-SUHAIL

Biology Department, College of Science, Baghdad University, Al-Jadryah, Baghdad-Iraq

(Received May 19, 1997; Accepted Jan. 17, 1998)

الخلاصة

تمت دراسة التفاعلات التصالبية لفيروسات Coxsackie B. ووجد ان معظم المصلول الايجابية للضد IgM تفاعلت تصالبيا مع اثنان او اكثر من الانماط المصلية لفيروسات Coxsackie B. في اختبار ELISA-IgM وهذه النتائج كانت مقرونة بعزل الفيروس من عينات المرضى، لهذا اعيد فحص المصلول باختبار التعادل Neutralization Test مرتين، مرة بالاختبار الاعتيادي لقياس عيارية الاضداد الكنية ومرة لقياس عيارية الضد IgM مقابل كل نمط مصلي. ووجد ان المصلول التي كانت ايجابية التفاعل التصالبي باختبار ELISA. لم تكن كذلك باختبار التعادل لقياس الضد IgM لاي من الانماط المصلية لفيروسات Coxsackie B، اضافة الى انه العيارية العالية للاضداد الكلية باختبار التعادل قد تعكس نوعية النمط المصلي باختبار التعادل للضد IgM.

ABSTRACT

The cross reactivity among Coxsackie B viruses was investigated and found that most of the IgM positive sera cross reacted with two or more Coxsackie B virus serotypes in an ELISA IgM. These results were supported by virus isolation. Sera samples were re-tested by two neutralization tests, one was done with whole sera against five Coxsackie B virus and the other test was applied with the separated fractions of IgM, which was fractionated by the sucrose gradient method in order to demonstrate the

specific IgM against each serotype. It was found that several of ELISA cross reactive sera had no detectable Coxsackie B virus specific IgM neutralizing antibody to any serotype. Furthermore, the high titer of total neutralizing antibody may reflect the IgM neutralizing antibody with certain specific serotype.

INTRODUCTION

Viral aseptic meningitis (AM) continues to be common sporadic or epidemic manifestation of enterovirus infections. Most of the 69 Enterovirus serotypes have been isolated from patients with (AM) with the Echovirus and Coxsackie B virus being predominant^(1,2,3).

The diagnosis of Enterovirus infections by virus isolation procedure is usually not achieved until long after the patient has been discharged from the hospital^(4,5). Detecting rise in the antibody titer by the conventional neutralization tests (NT) with paired acute and convalescent phase sera from patients that is not always possible, since the acute sample must be collected early during viral infections⁽⁴⁾. On the other hand, early detection of Coxsackie B virus specific IgM indicating recent infection, provides an attractive diagnostic technique. The Coxsackie B virus specific IgM enzyme linked immunoabsorbant assay (ELISA) developed by Banatvala and his coworkers in 1985⁽⁶⁾ have proved useful in their investigations. However, this ELISA IgM is known to cross react with other enteroviruses^(1,3). Thus, it is important to know the extent of this cross reactivity if we intent to provide a serotype specific diagnosis for enterovirus infection. For this purpose we have examined CSF, feces and sera samples from patients with (AM) and control patients by virus isolation, ELISA IgM, neutralization test and IgM neutralization test, for evidence of recent Coxsackie B virus infection.

MATERIALS AND METHODS

Samples

44 feces samples, 30 CSF samples, 25 single sera and 30 paired sera samples were collected from different hospital's laboratories in Baghdad for virological investigations. Six control samples were also included.

Viruses, Antigens and Cell Line

Coxsackie B virus⁽¹⁻⁵⁾ and vero cell line were kindly provided by Dr. Alex Pacsa of Microbiology Department in the Medical College-Hungary (personal communication). Purified (CBV (1-5)) for use as antigens in ELISA and neutralization test and control antigens were prepared as described by Hannington et al., 1983⁽⁷⁾.

Virus Isolation

Samples of CSF and Feces taken in the acute phase of illness were inoculated into tubes culture of vero cells. Culture tubes were kept for at least one week before being considered negative. Identification of virus serotype was achieved by neutralization with specific monovalent antiserum that was kindly supplied by Dr. Alex Pacsa of Microbiology Department in the Medical College-Hungary (personal communication).

ELISA IgM

The ELISA technique was performed as described by Hannington et al., 1989⁽⁸⁾. Briefly, 0.3ml of serum sample was diluted 1:100 with PBS containing Tween 20 at a concentration of 0.05%, was incubated at 4 C antigen and the control antigens. After washing, alkaline phosphatase test included known positive and negative IgM serum controls as well as serum free controls. The mean reading of the serum free control was subtracted from test readings to give the ELISA value for each sample. The cut off value was calculated in each test run from the value obtained for all the test sera against the control antigens. It was defined as the mean absorbance value +4 standard deviations. Sera

that gave positive results for Coxsackie B virus IgM were re-tested after removal of Rheumatoid factor.

Removal of Rheumatoid Factor

A 30 μ l sample of each serum was mixed with 200 μ l of 10% v/v suspension of heat aggregated human IgG and incubated at room temperature for 1 hour with shaking. After centrifugation for 1 minute in a microfuge the supernatant was removed for testing.

Sucrose Gradient Fractionation of Serum and Neutralization Test

One ml of 1:4 dilution of serum in PBS was layered onto continuous (12.5-37.5% w/v) sucrose gradient in PBS pH 7.2, centrifuged for 2 hours at 2500 rpm in a Beckman SW41 rotor. Ten one ml fractions were collected from each sample. The Neutralization test was done as described by Pozzetto et al., 1989⁽³⁾. The sucrose gradient fractions were tested in two fold dilutions from 2-256.

RESULTS AND DISCUSSIONS

Of the 44 samples studied a total of 23 (52.3%) yielded a CBV (1-5) by virus isolation procedure, whereas 36 (81.8%) produced a positive CBV-IgM response in ELISA IgM, table 1. All patients with virus in CSF and or feces were CBV IgM positive.

Twenty five single serum sample and 30 paired sample were examined, 13 of the single sera were CBV-IgM positive. Samples were taken 2-8 days after illness; whereas 18 paired samples showed a significant rise in antibody titer. The remaining 5 paired sera showed a moderate fall in antibody titer. This seroconversion was more obvious when 4 patients were following up weekly and their sera samples tested by ELISA IgM, table 2.

In all patients seroconversion for IgM antibodies was demonstrated by ELISA, the early samples taken within 1-4 weeks after illness had IgM for all five CBV

antigens. Thus, subsequently antibody level declined at different rates for different antigens. However IgM was detected for 5 months in sample No. 1 and for more than 4 months in sample No. 4. The exact information on the duration of IgM response to CBV is still limited, however it has been recorded as long as 6-8 weeks^(9,10) and 12-24 weeks⁽⁸⁾.

Sera samples were fractionated by sucrose density gradient to be tested by neutralization test against the five Coxsackie B viruses. The sera were also tested for the total neutralizing antibody activity against each CBV serotype. Table (3) illustrates results obtained with 20 of the sera, after the fractionation only 10 samples had detectable IgM neutralizing activity, while the other samples were negative by IgM neutralization test and showed a positive result by ELISA IgM to all five antigens, similarity with total neutralizing antibodies. From the 20 sera sample, 18 samples reacted with all five serotypes and gave considerably stronger readings in ELISA test, which probably indicates recent infection. This conclusion is supported by the previous results, table (2), which was obtained with the serial serum specimens from 4 patients in whom recent infection was confirmed by virus isolation. In all these samples, the early ELISA IgM response was group reactive against all five CBV serotypes but subsequently became progressively less so until after 17 and 4 weeks respectively their sera reacted with only one serotype and three serotypes respectively; this loss in broader cross reactivity was also associated with weaker absorbance readings in ELISA test. The neutralization test which was applied with whole serum (table 3) does not differentiate between IgG and IgM antibody activity but in each of the 10 IgM neutralizing antibody positive sera, the highest titer of the total neutralizing antibody reflected the IgM antibody specifically of the serum. However, a high titer of the total neutralizing antibody did not necessarily specify the presence of IgM neutralizing antibodies as sera No. 8,10. Similarly sera with high level of cross reactivity in the ELSIA IgM test had no detectable IgM neutralizing

A Comparative Study of Coxsackie B₁ Virus IgM Response in Elisa and IgM Neutralization Test

R. AL-Suhail

antibodies as sera No. 8,9,10. This may be due to the broader cross reactivity of ELISA IgM within the enteroviruses^(10,11) and this needs further investigation.

The method of antigen preparation appears to have little bearing on the specificity of the test in which the antigen is allowed to adsorb directly on to a solid phase. Since the purified virus prepared by heterotypic activity when used in such test^(7,8,12). The ELISA may be made type specific by using IgM capture technique or by using radiolabelled purified antigens^(13,14).

For the laboratory diagnostic purposes a test for broadly cross reactive enteroviral IgM would be of more practical value to recognize recent infection with only of the very large number of enteroviruses. The actual infecting virus could then be identified by a more specific immunoassays such as that presented in this study by type specific neutralization test.

Table 1: Results of 44 sample tested for recent Coxsackie B virus infection

Samples	CSF*	Feces*	Single Sera **	Paired Sera **
Total No.	30	44	25	30
No. +ve	10	13	13	23

* Tested by virus isolation CBV (1-5)

** Tested by ELISA - IgM

Table 2: The seroconversion and the cross reactivity among Coxsackie B virus shown by ELISA-IgM test in four samples

No. of patients	Weeks after illness	ELISA IgM					Control
		B ₁	B ₂	B ₃	B ₄	B ₅	
1	1-2	0.13	0.15	0.15	0.18	0.16	0.06
	3	0.43	0.44	0.51	0.49	0.6	0.06
	4	0.51	0.49	0.38	0.51	0.57	0.07
	6	0.28	0.41	0.29	0.31	0.55	0.05
	12	0.19	0.21	0.28	0.31	0.41	0.06
	20	0.19	0.2	0.2	0.25	0.28	0.09

2 ⁺⁺	1-2	0.1	0.12	0.18	0.19	0.19	0.07
	3	0.23	0.22	0.25	0.21	0.36	0.08
	4	0.18	0.29	0.19	0.26	0.27	0.08
	6	0.16	0.16	0.18	0.20	0.20	0.08
	10	0.16	0.15	0.14	0.19	0.20	0.07
	14	0.15	0.13	0.08	0.08	0.09	0.08
3 ⁺⁺	1-2	0.10	0.15	0.16	0.17	0.19	0.07
	4	0.23	0.21	0.23	0.29	0.23	0.06
	6	0.29	0.28	0.21	0.25	0.25	0.05
	10	0.19	0.20	0.16	0.18	0.21	0.06
	15	0.10	0.12	0.09	0.09	0.10	0.09
4 ⁺	1-2	0.15	0.17	0.16	0.18	0.11	0.06
	4	0.45	0.31	0.38	0.37	0.49	0.07
	6	0.37	0.25	0.26	0.29	0.29	0.07
	9	0.31	0.25	0.26	0.29	0.31	0.08
	17	0.13	0.15	0.21	0.23	0.20	0.08

* Positive reactings >20

⁺ CB₅ Isolated

⁺⁺ CB₄ Isolated

REFERENCES

1. Bell, E.J., McCartney, R.A., Bsquill, D. and Chaudhri, A.K.R. Antibody capture ELISA for the rapid diagnosis of enterovirus infections in patients with aspecific meningitis. *J. Med. Virol.* 19:217 (1986).
2. McCartney, R.A., Banatvala, J.E., Bell, E.J. Routine use of u antibody capture ELISA for the serological diagnosis of Cocksackie B virus infections. *J. Med. Virol.* 19: 205-212 (1986).
3. Potterro, B., Gaudin, O.G., Ros, A. Comparative evaluation of immunoglobulin M neutralizing antibody response in acute phase sera and virus isolation for the routine diagnosis of enterovirus infections. *J. Clin. Microbiol.* 27(4): 705-505 (1989).
4. Lan, R.C.H. Cocksackie B virus specific IgM responses in coronary care unit patients, *J. Med. Virol.* 18: 193-198 (1986).

*A Comparative Study of Coxsacki Bx Virus IgM Response in Elisa
and IgM Neutralization Test*
R. AL-Suhail

Table 3: Cross reactivity among coxsackie B viruses tested by ELISA-IgM neutralization and total antibody neutralization tested in 20 samples

Serum No.	ELISA IgM						Neutralization test									
							Specific IgM against Ag type					Total Ab against Ag type				
	B1	B2	B3	B4	B5	Cont.	B1	B2	B3	B4	B5	B1	B2	B3	B4	B5
1	1.04	0.70	1.60	1.40	1.31	0.19	-	-	32	-	-	32	128	>1024	512	256
2	0.47	0.30	0.71	0.79	0.71	0.11	-	4	-	-	-	256	512	<8	<8	<8
3	0.4	0.70	0.61	0.73	0.78	0.13	-	-	-	16	-	16	<8	<8	512	<8
4	0.5	0.56	0.61	0.53	0.68	0.06	-	-	-	16	-	<8	16	16	1024	<8
5	0.5	0.61	0.51	0.63	0.53	0.16	-	-	-	64	-	8	128	128	256	32
6	0.46	0.41	0.55	0.30	0.43	0.07	-	2	-	-	-	64	512	8	128	<8
7	1.31	0.31	0.31	0.30	0.43	0.14	-	-	-	8	-	<8	32	64	512	16
8	0.42	0.34	0.30	0.33	0.57	0.16	-	-	-	-	-	64	256	<8	<8	16
9	0.49	0.60	0.30	0.81	1.01	0.16	-	-	-	-	-	128	32	<8	8	<8
10	0.50	0.88	0.33	1.27	1.26	0.15	-	-	-	-	-	>8	512	1024	<8	8
11	0.70	0.30	0.33	0.36	0.31	0.16	-	-	-	-	-	512	128	8	256	<8
12	0.90	0.41	0.34	0.35	0.30	0.09	-	-	-	-	-	16	32	<8	64	<8
13	0.30	0.51	0.51	0.48	0.37	0.08	32	-	-	-	-	16	64	<8	512	<8
14	0.37	0.42	0.61	0.81	0.61	0.10	-	-	-	-	-	8	8	<8	<8	16
15	0.40	0.41	0.89	0.83	0.81	0.08	-	-	-	-	-	1024	32	<8	128	<8
16	0.47	0.47	0.28	0.70	0.35	0.08	-	-	-	-	-	16	64	512	16	128
17	0.40	0.40	0.28	0.31	0.36	0.06	-	-	-	-	-	128	<8	<8	16	32
18	0.32	0.30	0.41	0.49	0.51	0.07	-	-	-	-	-	32	32	512	64	1024
19	0.31	0.29	0.66	0.91	0.91	0.10	-	-	-	-	16	32	<8	<8	512	<8
20	0.88	0.40	0.80	0.71	0.83	0.06	16	-	-	-	-	1024	<8	128	64	32

5. Chan, D. and Hammond, G.W. Comparison of serodiagnosis of group B Cocksackie virus infections by an immunoglobulin M capture enzyme immunoassay versus microneutralization. *J. Clin Microbiol.* 21(5): 830-834 (1985).
6. Banatvala, J.E., Bryant, J., Schernthaner, G., Borkenstein, M. Schober, E., Brown, D., Desilvia, L.M., Menser, M.A., and Silink. Cocksackie B, mumps, rubella and cytomegalovirus specific IgM responses in patients with juvenile-onset insulin-dependent diabetes mellitus in Britain, Austria and Australia. *Lancet* i: 1409-1412 (1985).
7. Hanington, G., Booth, J.G., Wiblin, C.N., Stern, H. Indirect enzyme linked immunosorbent assay (ELISA) for detection of IgG antibodies against Cocksackie B viruses, *J. Med. Microbiol.* 16: 459-465 (1983).
8. Hannington, G., Booth, J.G., Bowes, R.J., Stern, H. Cocksackie B virus specific IgM antibody and myocardial infraction. *J. Med. Microbiol.* 21: 287-291 (1989).
9. El-Hagrassay, M.M.G., Banatvala, J.E. and Coltard, D.J. Cocksackie B virus specific IgM responses in patients with cardiac and other diseases. *Lancet* ii: 1160-1162.
10. King, M.L., Shaikh, A., Bidwell, D., Voller, A., Banatvala, J.E. Cocksackie B virus specific IgM responses in children with insulin dependent (Juvenile-onset type 1) diabetes mellitus. *Lancet* i: 1397-1399 (1983).
11. Yousef, G.E., Mann, G.F., Brown, I.N., Nowbray, J.F. Clinical and research application of enterovirus group reactive monoclonal antibody. *Interovirol.* 28: 119-205.
12. Brown, F., Wild, T.F., Rowe, L.W., Underwood, B.O., Harris, T.J.R. Comparison of swine vesicular disease virus and Cocksackie B5 virus by serological and RNA hybridiazation methods. *J. Gen. Virol.* 31: 231-237 (1976).
13. Katze, M.G. and Crowell, R.L. Immonological studies of the group B Cocksackie viruses by sandwich enzyme

*A Comparative Study of Coxsacki Bx Virus IgM Response in Elisa
and IgM Neutralization Test*

R. AL -Suhail

linked immunosorbent assay (ELISA) and immunoprecipitation. J. Gen. Virol. 50: 357-367 (1980).

14. Tofrasan, E.G., Frisk, G. Diderholm, H. Indirect and reverse radio immuno-assays and their apparent specificities in the detection of antibodies to enteroviruses in human sera. J. Med. Virol. 13: 13-31 (1984).

Fibrinolytic Activity of Thermostable Alkaline Proteases from Alkalophilic and Thermophilic *Bacillus* sp.

SHADAN AL-WANDWAI

Department of Biology, College of Science, University of Baghdad

(Received Nov., 1998; Accepted May 16, 1999)

الخلاصة

لأثبتت قابلية تحليل الليفين لبعض البروتيازات المايكروبية تم عزل انزيمين من البروتيازات الثابتة حراريا ولاقلوية (B_{60} , B_{52}) من عزلات التربة المحلية لبكتريا *Bacillus* sp. اظهرت الانزيمات باهاء ودرجات حرارة امثل عاليين لتحلل الكازئين، فكانت اعلى فعالية تحليلية للانزيم B_{52} عند باهاء (pH) 10 بدرجة حرارة 75°م وللانزيم B_{60} عند باهاء (pH) 11 بدرجة حرارة 70°م. والانزيمين اظهرا فعالية تحليلية لليفين من خلال تكوين مناطق الليفين المحلل بالاطباق وبفعالية تقدر بحوالي 400 وحدة/مللتر للانزيم B_{52} و 740 وحدة/مللتر للانزيم B_{60} بدرجة حرارة 40°م وفترة حضانة 3 ساعات.

ABSTRACT

To prove the fibrinolytic activity of some microbial proteases, two thermostable alkaline protease (B_{52} & B_{60}) were obtained from local soil *Bacillus* isolates. The optimum pH and temperture toward the hydrolysis of casein were pH 10 at 75°C and pH 11 at 70°C for proteas B_{52} and B_{60} respectively. The two enzymes possessed fibrinolytic activity that formed fibrin dissolution zones on plates. The fibrinolysis activity was about 400 FU/ml of protease B_{52} and 740FU/ml of protease B_{62} at 40°C within 3h.

INTRODUCTION

Enzymes are finding increasingly wide use in medicine. In particular a great number of studies are being carried out in the field of isolation of microbial proteolytic preparation which act as a natural fibrinolytic enzymes or can exert an activating action on the fibrinolytic blood factors (Szelenova and Bol'shakova, 1986). The most studied substances in this group is streptokinase from Streptococci which at present is manufactured by many firms (Wiseman, A.1980), also tricholysin which synthesized by the fungus *Trichothecium roseum* (Stephanova & Yulikova, 1977).

The study of fibrinolysis activity of the proteolytic enzymes of the genus *Bacillus* which is widely distributed in the nature is limited although the alkaline thermostable hydrolytic enzymes from soil *Bacillus* attracted attention of many microbiologists. Petroius and worker mentioned in 1966 that the dissolution of fibrin from some thermophilic soil *Bacillus* is more than casein and haemoglobin digestion, also (Imshenefski et al., 1988) pointed out the thrombolysis and fibrinolysis activity of proteolytic complexes of *Bacillus subtilis* and *Bacillus mesentericus*.

The purpose of this study was to investigate the fibrinolysis activity of local soil *Bacillus* sp. For its imprtunes in medical application's for the dissolution of blood thrombi.

MATERIALS AND METHODS

Screening Procedure

65 local soil samples were collected. The surface layer of sampled site was removed to 15cm in depth, the soil temperature was measured during sampling and pH values were measured using a pH-meter. The collected soil samples placed in sterile plastic bags. One gram from each sample was incubated in alkaline medium pH (10) (1% peptone, 5% yeast extract, 0.1% glucose and 1% Na_2CO_3) at 50°C for 24 hours with shaking. Then inoculated on

nutrient agar plates several time until pure culture were obtained. Preliminary assessment of extracellular protease production was conducted by spreading a heavy inoculum from each culture on skim-milk agar plates which was examined for clear zone formation after incubation at 40°C for 24h. Bacterial isolates which showed positive phenotype in skim-milk agar were analyzed for protease production by cultivating in production medium (pH 10) containing (2% glucose, 2% peptone, 0.1% KH_2PO_4 , 0.02% $\text{MgSO}_4 \cdot 7\text{H}_2\text{O}$, 0.5% yeast extract and 1% Na_2CO_3) at 40°C for 24h with shaking at 300rpm (Fujiwara and Yamamoto, 1995).

Measurement of Protease Activity

Protease activity was measured in cell-free supernatants by the method of McDonald and Chen (1975). For routine analyses, the enzyme was incubated with 0.6% casein solution as the substrate, in 10mM borax-NaOH buffer (pH10) at 40°C for 10min, the reaction was stopped by the addition of 5ml of 5% (w/vol) trichloroacetic acid, the reaction mixture kept at 30°C for 10min and filtered through Whatman No.6 filter paper. The optical density of filtrate was measured at 700nm. A unit of protease activity was defined as the amount of enzyme that produce TCA*-soluble materials equivalent to 1 microgram of tyrosin per minute from substrate (casein) at 30°C.

Effect of Temperature and Thermostability

Proteases activity at various temperature was determined with casein as the substrate, sample of 0.6% solution in 10mM borax-NaOH buffer (pH 10) were held at various temperature for 10min. Then 4 ml of substrate was added to 1ml of cell-free supernatant, and assay mixture was incubated at the selected temperature for 60min. The enzymes was stabilized at high temperature by 10mM Ca^{+2} .

To determine the heat stability, the enzyme solutions allowed to stand in water baths set at various temperature for 15min, the heat-treated enzyme solutions

Fibrinolytic Activity of Thermostable Alkaline Proteases from Alkalophilic and Thermophilic Bacillus sp. S. Al-Wandwai
were rapidly cooled and the residual activity (%) was determined at 30°C with casein as substrate.

Effect of pH and Stability to pH

The effect of hydrogen ion concentration on the activity of crude proteases was determined with casein, over the pH range 5 to 12 at 40°C. To determine the activity at various pH values, equal volume of 0.6% casein solution and appropriate buffer were mixed and equilibrated to 40°C. Then 1ml of cell-free supernatant was mixed with 4ml of substrate, and the assay mixture was incubated at 30°C for 30 min. The enzymes activity were estimated by the McDonald-Chen method (1975).

Stability to pH samples (1ml) of culture liquid were mixed with 5ml of buffer of the appropriate pH, the solutions were allowed to stand at 40°C in water bath for 30 min. The remaining activity (residual activity %) was assayed by mixing 1ml of enzyme with 4ml of 0.6% casein solution in 10mM borax-NaOH buffer pH(10) and incubating the mixture at 40°C for 60 min.

Fibrinolytic Activity Determination

Fibrinolytic activity was assayed on fibrin plates, using Selezneva and Shakova (1986) method. 10ml of 0.6% (w/vol) fibrinogen solution mixed with 0.3ml of 1% (w/vol) thrombin solution in a 50ml flask. Under the action of thrombin the fibrinogen was converted to insoluble gel fibrin. Then 0.5 ml of culture liquid added to the surface plate formed, the duration of incubation at 40°C was 3h. The fibrinolytic activity units (FU) was expressed in arbitrary units/ml culture liquid. One unit corresponded to fibrin lysis zone 10mm² in area. The lytic activity of fibrin dissolution was compared to that of casein digestion under the same conditions.

RESULTS AND DISCUSSION

Screening of Isolates

Protease activity was detected in 10 isolates (6.5% of total isolates) which formed a large clear zone on skim-milk agar. The productivity of protease production by each of ten isolates (B_{52} , B_{60}) were found to produce thermostable alkaline protease. The taxonomic characteristics of the two produces isolates are summarized in table (1). The isolates could be identified in the genus *Bacillus* according to Bergey's manual (Bachanan and Gibbons, 1978). The two isolates were a typical alkaliphilic bacteria because the cells could not grow at all in neutral medium (pH 7.0). The maximum growth temperature of the two bacteria (B_{52} , B_{60}) are 70°C and 65°C respectively.

The bacteria exhibited both a higher optimum growth pH and temperature than those of the mesophilic *Bacillus* sp.

Bacillus sp. Number AH-101 isolated from soil also produce thermostable protease but could not grow above 55°C as mentioned previously by (Takami & Horrikoshi, 1989).

Effect of Temperature & Thermostability

Figure 1, show that the optimum temperature of enzymes reaction were around 75°C and 70°C for B_{52} and B_{60} respectively in the presence of Ca^{++} . Thermostability of the protease detected by measuring residual activity %. The protease B_{52} was stable up to 75°C and B_{60} was stable up to 70 and both were inactivated by loosing about 90% of their activities after a 15 min. exposure at 85°C. Figure (2)

The data suggested that the casein substrate optimally hydrolyzed at high temperature about 70 and 75°C. These values is one of the highest among bacterial protease (Dann, G., 1970) and its higher than that of mesophilic protease of *Bacillus* sp. about 20°C (Levison and Arenson, 1979) heat stability of most microbial protease enhanced by Ca^{++} , the Ca^{++} protect the enzyme activity from heat inactivation to a certain extent but also

Fibrinolytic Activity of Thermostable Alkaline Proteases from Alkalophilic and Thermophilic Bacillus sp. S. Al-Wandwai
the two protease were irreversibly destroyed at 85°C showing a 90% loose of activity.

Two protease were irreversibly destroyed at 85°C showing a 90% loose of activity.

Effect of pH and Stability of Protease to pH

From the figure (3), the protease B₅₂ was optimally active at about pH 10 with casein substrate, but the optimum pH of protease B₆₀ was one unit higher it was about 11.

Figure (4) show the stability to pH. The protease B₅₂ was most stable (residual activity between 98-100%) at pH value 5-11 but protease B₆₀ showed a less stability value it was stable between pH 7 and 11.

The enzymes retained most of its activity after exposure to different hydrogen ion concentration.

(Millat, J., 1970) reported that alkaline protease of *Bacillus cereus* was active at pH level 9 to 10.5, (Muro et al., 1984) pointed out the protease complexes of *Ba Stearothmophilus* was active and stable at pH 8 to 10 for 30 min.

Fibrinolytic Activity

The result of fibrinolysis (FU/ml) in comparison to caseinolysis (CU/ml) are shown in table (2). The results indicated the highest activity of fibrin dissolution of protease B₅₂ was about 400 FU/ml. This protease distinguished by having high caseinolytic activity about 5.67 CU/ml at 40°C. The protease B₆₀ fibrinolytic activity was 740FU/ml, and this protease showed low caseinolytic activity (2.57CU/ml). It appears that the fibrinolysis of proteases does not always correlated with its casinolysis. This also was observed by (Imshenetski et al., 1988) who studied the fibrinolytic preparation obtained from the bacterial cultures of *B. subtilis* and *B. mesentericus*.

Table 1: Taxonomical properties of the bacterial isolates

Character	B ₅₂	B ₆₀
Form	Rods	Rods
Motility	Motile	Non motile
Spore	Central	Central
Gram stain	Positive	Positive
Gelatin liquifaction	Positive	Positive
Hydrolysis of starch	Positive	Positive
Utilization of nitrate	Positive	Positive
Catalase activity	Positive	Positive
Oxidase activity	Positive	Positive
Growth temperature	70°C	65°C
pH for cells growth	8-10.5	8-12

Table 2: The level of fibrinolysis and caseinolysis of protease B₅₂ and protease B₆₀

Protease	Fibrinolytic activity FU/ml	Caseinolytic activity CU/ml
B ₅₂	400	5.67
B ₆₀	740	2.57

REFERENCES

1. Bachanan, R.E. and Gibbons. Key to the species of genus *Bacillus*: In Bergeys manual of determinative bacteriology, 8th ed., Baltimore: Wiliams & Wilkins (1974).
2. Fujiwara, N. and Ymamoto, K. Purification of alkaline protease in low-cost medium by alkalophilic *Bacillus* sp. and properties of the enzymes. J. Ferment Technol. 65: 345-348 (1995).
3. Imshenetski, A.A., Nesterova, N.G. and Festisora, Z.S. Influence of inhibitors and certain Cations on proteolytic activity of *Bacillus mesentericus*, Microbiol. (USSR). 57(3): 324-327 (1988).
4. Levison, S.H., and Aronson, A.I. Regulation of extracellular protease production in *Bacillus cereus*. Bacterial. 33: 1023-1030 (1979).

*Fibrinolytic Activity of Thermostable Alkaline Proteases from
Alkalophilic and Thermophilic Bacillus sp.* S. Al-Wandwai

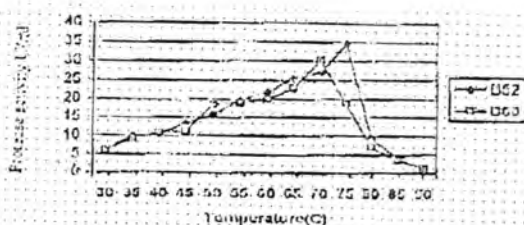


(Fig. 1)

Effect of temperature on the protease activity, the enzymes activity was measured in 10 mM borax - NaCl buffer (PH 10) with Ca^{++} at various temperature

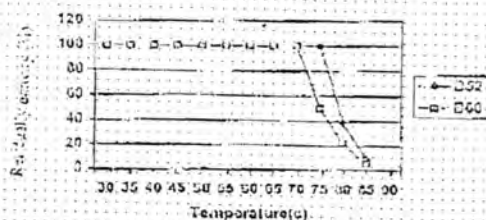


(Fig. 2)

Effect of heat on proteases stability.

After incubating the enzymes in buffer solution at each temperature with 10 mM Ca^{++} at PH 10 for 10 min, the remaining activities were measured at PH (10) and 40 °C

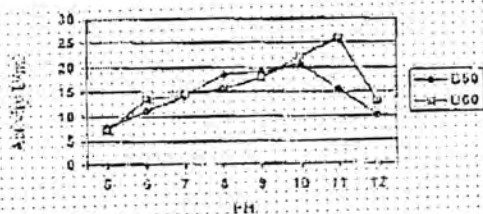


(Fig 3)

Effect of pH on proteases B_{50} , B_{60} activity.

The activities were measured in the buffer of each pH containing 0.5 % casein as a substrate at 30 °C. Buffer system : pH 5 – 8.5 phosphate buffer , pH 8.5 – 9 : 0.1 M Boric acid-NaOH buffer , pH 9.5 – 12 Borax – NaOH buffer .

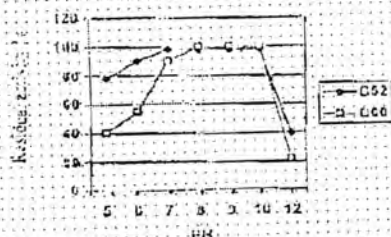


(Fig 4)

Stability of proteases B_{52} , B_{60} to pH . The enzymes were incubated at various pH values for 30 min at 40 °C before assay, the remaining activities were measured at pH 10 and 40 °C.

- Fibrinolytic Activity of Thermostable Alkaline Proteases from Alkalophilic and Thermophilic Bacillus sp.* S. Al-Wandwai
- McDonald, C.E., and Chen, L.L. The lowry modification of the folin reagent for determination of proteinase activity. *Anal. Biochem.* 10: 170-177 (1975).
6. Millet, J. Characterization of protease excreted by *B. subtilis* strains during sporulation *J. Appl. Bacteriol.* 33: 207-219 (1976).
 7. Muro, T., Tominago, Y., and Okada, S. Purification and some properties of protease from *B. stearothermophilus*. *Agri. Biol. Chem.* 43(5): 1223-1230 (1984).
 8. Pretorias, I.S., Dekock, M.J., and Lategam, P.M. Numerical taxonomy of proteinase producing *Bacillus* sp. *Appl. Bacteriol.* 60: 351-360 (1966).
 9. Selezneva, A.Ai., and Shakova, B.D. Proteolytic complex of *Aspergillus terricola*. *Microbiol. (USSR)*, 22(1): 3-11 (1986).
 10. Stepanova, A.T., and Yalikova, E.P. Fractionation of tricholysin by isoelectrofocusing. *Biochem. Micobiol.* 42(1): 167-170 (1977).
 11. Takami, H. and Horrikoshi, K. Production of extremely thermostable alkaline protease from *Bacillus* sp. No. AH. 101. *Appl. Microbiol. Biotechnol.* 30: 120-124. (1989).
 12. Wiseman, A. Handbook of enzymes. Biotechnology 2nd ed. Pp 66-69. John Wiley and Sons (1980).

Effect of Decomposing Wheat Residue on Growth of Chickpea and its Possible Modes of Action

KADHUM H.Y. ZWAIN

Department of Biology, College of Science, Al-Mustansiriya University, Baghdad, Iraq.

(Received Dec. 30, 1998; Accepted Feb. 24, 1999)

الخلاصة

في تجارب اجريت في البيت الزجاجي، وجد ان مخلفات الحنطة المضافة الى التربة تؤدي الى تثبيط النمو واخذ الايونات ومحتوى الكلوروفيل وفعالية الانزيم المختزل للنترات في اوراق نبات الحمص. وفي اغلب الحالات، يترافق الانخفاض في النمو بشكل واضح مع الانخفاض الحاصل في اخذ الايونات ومحتوى الكلوروفيل وفعالية الانزيم المختزل للنترات، مما يشير الى ان هذه المؤشرات الفسلجية هي من طرائق التأثير التي تثبط بها مخلفات الحنطة نمو نبات الحمص.

ABSTRACT

In a greenhouse experiments, it was found that incorporation of wheat residues into soil significantly inhibited growth, ion uptake, chlorophyll content and nitrate reductase activity in leaves of chickpea. In most cases, the reduction in growth appeared to be parallel with the reduction in the test physiological parameters. This suggests that inhibition of uptake, chlorophyll content and nitrate reductase activity are the modes of action by which wheat residues can inhibit growth of chickpea.

INTRODUCTION

There is a large volume of evidence that allelochemicals in plants are important in allelopathy^(1,2). The mode of action of allelochemical compounds could be directly on plant growth and development or indirectly through alteration of soil properties, nutrients availability and population of microorganisms⁽³⁾.

Wheat is reported to have allelopathic potential against corps and weeds⁽⁴⁻⁶⁾. Recently, it was found that

reduction in yield of rice cultivated after wheat was due to allelopathic potential of wheat straw left in soil after wheat harvest⁽⁷⁾. Also, wheat residues were found to affect rice growth indirectly through reduction of nitrogen fixation carried out by blue green algae living in rice fields⁽⁸⁾.

Preliminary field observations revealed that chickpea growth was reduced when cultivated after wheat harvests. We hypothesized that wheat residues has allelopathic effect on chickpea. Therefore, the present work was conducted to test this hypothesis and to study the possible modes of action by which wheat residues affect growth of chickpea.

MATERIALS AND METHODS

Soil Analysis

Soil from the field in Baghdad area was brought, air dried, mixed and sieved through a 2mm openings. Electrical conductivity and pH was determined using saturation past extract method⁽⁹⁾. Organic matter was determined according to the method outlined by Black⁽¹⁰⁾. Soil texture were determined by international pipette method⁽¹⁰⁾, total nitrogen by macro-kjeldahl method⁽¹¹⁾ and total phosphorus by the vanadomolybdo phosphoric colorimetric method⁽¹²⁾. Calcium, Mg, K, Fe, and Zn were determined by atomic absorption spectrophotometer according to Anonymous⁽¹³⁾.

Effects of Wheat Residues on Growth of Chickpea

Wheat residues were mixed with the soil at rates of 4 and 8g per kg soil and placed in plastic pots each of 2kg capacity. Some physical and chemical properties of soil are indicated in table 1. Controls were run similarly expect wheat residues were replaced by equal amounts of peatmoss to keep the organic matter the same⁽¹⁴⁾. Five chickpea seeds were planted in each pot and all pots were watered whenever necessary with equal amounts of tap water. Seedlings were thinned to three largest plants per pot and the pots were placed in a greenhouse and arranged in a

complete randomized design with six replications for each treatment. Twelve weeks after planting. The plants were harvested, separated into roots and tops and compared on the basis of oven dry weight.

Modes of Action of Wheat Residues

Separated experiment of the same treatments, experimental design and growth conditions as the previous one was initiated to test the following;

Effect on Mineral Uptake

Ten weeks after planting, shoot of chickpea was washed with distilled water, and oven-dried at 75°C for 3 days. The oven-dried materials were ground in an electrical grinder and used for determination of total nitrogen by the macro-kjeldahl method⁽¹¹⁾ and total phosphorus by the vanadomolybdophosphoric calorimetric method⁽¹²⁾. Calcium, Mg, K, Fe and Zn were also determined using a Perkin-Elmer model 305 atomic absorption spectrophotometer after digestion according to instructions in the analytical manual supplied with the instrument⁽¹³⁾.

Effect on Chlorophyll Content

Ten weeks after planting, chlorophyll was extracted from the two unifoliate leaves of chickpea following a method outlined by Knudson⁽¹⁵⁾. The leaves were weighed and immersed in 30ml of 95% ethanol for 24h. at room temperature. The ethanol-chlorophyll solutions were transferred to containers. The leaves were resoaked in a similar manner for two additional 24h. periods each time. Solutions of all treatments were pooled and taken to a final volume of 100ml. Absorbance (A) of each chlorophyll extract was read at 665 and 649nm on a Varian Cary 118CX Spectrophotometer. Chlorophylls a & b were computed using the following equations^(15,16).

$$\frac{\mu\text{g chlorophyll a}}{\text{ml solution}} = (13.70) (A_{665\text{nm}}) - (5.76) (A_{649\text{nm}}) \quad (1)$$

$$\frac{\mu\text{g chlorophyll b}}{\text{ml solution}} = (25.80) (A_{649\text{nm}}) - (7.60) (A_{665\text{nm}}) \quad (2)$$

Effect on Nitrate Reductase Activity

In Vivo nitrate reduction (NR) was determined by leaf-disc method⁽¹⁷⁾. The standard incubation medium used contained 50mM KNO₃, 100mM K-phosphate buffer (pH 7.5), and 1% (V/V) 1-propanol. Samples of leaf disc (approximately 200mg) were taken and placed in 100ml incubation medium, vacuum-infiltrated twice for 2min and incubated in a shaking water bath for 30 min. Following incubation, the concentration of nitrate released to the incubation medium was determined. The activity of NR was expressed as $\mu\text{mol NO}_2^- (\text{g fresh weight. h})^{-1}$.

RESULTS

The results showed that all rates of incorporated wheat residues into soil significantly inhibited growth of shoot and whole plant of chickpea (Table 2). On the other hand, root was not significantly affected by any of the test rate of residue. The reduction increased with the increased residue concentration and the reduction ranged from 26-34% for whole plant.

All test ratios of wheat residues in soil significantly reduced the concentrations of all test minerals with the exception of Na and Ca which were significantly reduced by the high rate only (Table 3).

Total chlorophyll concentration in the unifoliate leaves was significantly below that the control seedling (Table 4). Both chlorophyll a and b were reduced. Chlorophyll b was slightly more inhibited than chlorophyll a and this led to increase the a/b ratio.

Nitrate reductase activity in leaves significantly inhibited when compared to the control. The reduction in the activity of the enzyme was increased with the increased residue concentration (Table 5).

DISCUSSION

The inhibition in growth of chickpea due to addition of wheat residues to the soil suggests that the residues contain phytotoxins which released by irrigation and /or after it's decaying by microorganisms. Alsaadawi et al.⁽⁷⁾ isolated four phytotoxins which have considerable solubility in water.

Wheat residues incorporated in soil significantly inhibited chlorophyll content and ion uptake. It is possible that the reduction in chlorophyll content is due to the reduction in ion uptake since some of these ions tested are involved in chlorophyll structure and / or metabolic pathway of chlorophyll biosynthesis. Some of the phytotoxins isolated from wheat residues are reported to reduce chlorophyll content and ion uptake by cowpea⁽¹⁸⁾.

The reduction in growth of chickpea appeared to be apprralel with the reduction in ions uptake and chlorophyll content of leaves. This indicated that the reduction in growth may be attributed to the reduction in ions uptake and chlorophyll content since these two parameters are known to limit plant growth and productivity⁽¹⁹⁻²¹⁾.

The inhibition of NR activity and nitrogen uptake by chickpea due to wheat residues suggest that the residues after nitrogen metabolism in plant and this may lead to reduce the uptake of available nitrogen in soil.

The present study leads to the conclusion that wheat residues has an allelopathic potential against chickpea and the reduction of ion uptake, chlorophyll content and NR activity are the modes of action by which wheat residues can inhibit chickpea growth. However, the other possible mechanisms could not be excluded. Rice⁽¹⁾ reported that there are numerous modes of action by which action which plant growth and productivity can be inhibited.

Effect of Decomposing Wheat Residue on Growth of Chickpea and its Possible Modes of Action

K. H. Y. ZWAIN

Table 1: Some physical and chemical properties of the soil used in the experiment

*Soil Properties	Value
PH	7.90*
EC ds/m	1.95**
Organic matter %	0.15
Sand %	34.1
Silt %	36.8
Clay %	29.1
Total - N (ppm)	105.0
Total - P (ppm)	98.0
Na (ppm)	40.0
K (ppm)	8.5
Ca (ppm)	71.0
Mg (ppm)	18.0
Fe (ppm)	1.6
Zn (ppm)	2.8

* each value is an average of three replications

** In saturated past extract at 25°C

Table 2: Effect of wheat residues on growth of chickpea

Residue added* (g.kg ⁻¹ soil)	Dry weight (g) ^a			Reduction %
	Root	Shoot	Whole plant	
Control (peatmoss)	0.325	1.144	1.469	0.00
4	0.310	0.775**	1.085**	26.14
Control (peatmoss)	0.366	1.231	1.597	0.00
8	0.345	0.708**	1.053	34.06

* Controls had similar rate of peat moss only

^a Each value is an average of 3 replications and each replicate consists of 3 plants.

** Significant at 5% level from their respective control according to Student's t test

Table 3: Effects of wheat residues on minerals content of chickpea

Residue * Added (g.kg ⁻¹ soil)	Minerals (mg/g dry weight) ^a							
	Na	K	Ca	Mg	N	P	Fe	Zn
Control	6.80	7.20	18.70	6.60	27.40	4.80	1.20	2.80
Peat moss								
4	6.40	6.10 **	17.60	5.40 **	24.10 **	4.60	0.90 **	2.60
Control	7.80	8.40	19.30	6.80	28.80	5.10	1.40	2.90
peat moss								
8	5.10 *	5.20 **	12.80 *	4.20 **	22.80 **	5.00	0.90 **	2.10

* Controls had similar rate of peat moss only

^a Each value is an average of 3 replications and each replicate consists of 3 plants

** Significant at 5% level from their respective control according to Student's t test.

Table 4: Effects of wheat residues on chlorophyll content of chickpea

Residue added* (g.kg ⁻¹ soil)	Chlorophyll (µg/mg dry weight) ^a			Ratio (a/b)	Reduction (%)
	Chloro. a	Chloro. b	Total chloro. (a+b)		
Control	8.20	7.25	15.45	1.13	0.00
peat moss					
4	6.74 **	5.82 **	12.56 **	1.16	18.70
Control	9.80	7.85	17.65	1.25	0.00
Peat moss					
8	6.35**	4.35 **	10.70	1.46	39.38

* Controls had similar rate of peat moss only

^a Each value is an average of 3 replications and each replicate consists of 3 plants

** Significant at 5% level from their respective control according to Student's t test

Effect of Decomposing Wheat Residue on Growth of Chickpea and its Possible Modes of Action

K. H.Y. ZWAIN

Table 5: Effect of wheat residue on nitrate reductase activity in chickpea

Residue added * (g.kg ⁻¹ soil)	Nitrate Reductase Activity ^a μmoles NO ₂ ⁻¹ (g.fesh wt.hr) ⁻¹	Reduction %
Control peat moss	2.47	0.00
4	1.35 **	45.34
Control peat moss	3.87	0.00
8	1.05 **	72.89

* Controls had similar rate of peat moss only

^a Each values is an average of 3 replications and each replicate consists of 3 plants

** Significant at 5% level from their respective control according to Student's t test.

REFERENCES

1. Rice, E.L. Allelopathy. 2nd ed. Academic Press, New York. (1984).
2. Rizvi, S.J. and Rizvi, V. Allelopathy, Basic and Applied Aspects. Chapman and Hall Press. London (1992).
3. Whittaker, R.H. and Feeny, P.P. Allelochemicals: Chemical interactions between species. Science 171: 757-770 (1971).
4. Guenzi, W.D. and McCalla, T.M. Phenolic acids in oat, wheat, sorghum and corn residues. Agro. J. 59: 163-165 (1966a).
5. Guenzi, W.D. and McCalla, T.M. and Norstadt, F.A. Presence and Persistence of phytotoxic substances in wheat, oat, corn and sorghum residues. Agro. J. 59: 163-165 (1967).
6. Chou, C.H. and Patrick, Z.A. Identification and phytotoxic activity of compounds produced during decomposition of corn and rye residues in soil. J. of chem. Ecol. 2: 369-387 (1976).

7. Alsaadawi, I.S., Zwain, K.H.Y. and Shahata, H.A. Allelopathic inhibition of growth of rice by wheat residues. *Allelopathy Journal* 5(2): 163-169 (1998).
8. Zwain, K.H.Y. Alsaadawi, I.S., and Shahata, H.A. Effect of wheat residues on growth and nitrogen fixation of blue green algae. Accepted for publication in *Allelobathy Journal*. (1993).
9. Piper, C.S. Soil and plant analysis. University of Adlaide. Adelaide. Australia, pp. 368 (1942).
10. Black, C.A. Methods of soil analysis part 1. American society of agronomy. Madison, Wisconsin, USA p. 562 (1965).
11. Chapman, H.D. and Pratt. Methods of analysis for soils, Plants and Waters. Pp. 150-160 University of California, Riverside, California (1961).
12. Jackson, M.L. Soil chemical analysis. Prentice-Hall. Englewood cliffs. New Jersey. (1958).
13. Anonymous. Analytical methods for absorption spectrophotometry Perkin-Elmer. Norwalk, Connecticut. (1976).
14. Alsaadwi, I.S. and Rice, E.L. Allelopathic effects of *Polygonum aviculare* L. 1. Vegetation Patterning. *J. Chem. Ecol.* 8, 993-1009 (1982).
15. Knudson, L.L., Tibbitts, T.W. and Edwards, G.E. Measurement of ozone injury by determination of chlorophyll concentration. *Plant Physiol.*, 60, 606-608 (1977).
16. Wintermans, T.F. and Demots, A. spectrophotometry characteristics of chlorophylls a and b and their phenophytins in ethanol. *Biochem. Biophys. Acta*, 109, 448-453 (1965).
17. Harper, J.E., and Hageman, R.H. Canopy and seasonal profiles of nitrate reductase in soybeans (*Glycine max* L.) *Plant Physiol.* 49: 149-154 (1972).
18. Alsaadwi, I.S., Al-Hadithy, S.M. and Arif. Effect of three phenolic acids on chlorophyll content and ions uptake in cowpea seedlings, *J. Chem. Ecol.*, 12, 221-27 (1986).

Effect of Decomposing Wheat Residue on Growth of Chickpea and its Possible Modes of Action

K. H. Y. ZWAIN

19. Parks, J.M. and Rice, E.L. Effects of certain plants of old field succession on the growth of blue-green alga. Bull. Torrey Bot. Club, 96, 345-360 (1969).
20. Epstein, E. Mineral nutrition of plants: Principle and Perspectives. John Wiley and Sons. New York, USA (1976).
21. Colton, C.E. and Einhellig, F.A. Allelopathic mechanism of velvet leaf *Abutilon Theophrastii* Medi. Malvaceae on soybean. Am. J. Bot., 67, 14707-1413. (1980).

Use of Oleander and Tobacco Extracts As An Insecticide

BADIR M. AL-AZAWI, WALA SHAWKET AL-MASHADANI
AND SUADAD A.E. AL-SAMARAIE

Dept. of Biological Science / Science College Al-Mustansiriyah
University

(Received Mar. 9, 1998 ; Accepted May 5, 1999)

الخلاصة

استخلصت المادة القلوية من نبات الدفلة ومادة النيكوتين من نبات التبغ واختبرت على الاطوار المختلفة للصرصر الامريكي. التراكيز العالية للمادة القلوية والنيكوتين أعطت سمية ونسبة قتل عالية لطوري الحورية الثالث والسادس والطور البالغ على التوالي. وقد مزجت هذه المواد الفعالة لأول مرة مع مواد كيميائية حاملة وصنعت بشكل مبيد تجاري وأعطت نفس النتائج وقد صنعت لأول مرة في العراق كمبيد حشري.

ABSTRACT

The aqueous extracts of oleander plant *Nerium oleander* like alkaloids and nicotine from tobacco plant *Nicotiana tabacum* have given high mortality of different instars of american cockroaches *periplaneta americana*. The high concentration of both chemicals have given more toxic to 3 rd, 6th nymph of instars and adults on cockroaches respectively. The active gradient material mixed with carrying chemical and manufacturing as insecticides which have a good effect on cockroaches the first time in Iraq.

INTRODUCTION

The aqueous extracts of plants were used long time ago against insects, animal diseases and steroid and plant diseases⁽¹⁾. Many different groups of chemicals like alkaloid, nicotine which was extracted from different plants improved toxic or suitable insecticides to different insects⁽²⁾ recorded the extract alkaloid from cactus was very toxic to eight species of *Drosophila sonora* desert⁽³⁾. The pyrolizidine alkaloid extract from plant *Heliotropium indicum* was a very attractive chemical to different species of Lepidoptera like Aretiidae and Nymphalidae⁽⁴⁾ recorded that leaves powder of common oleander slightly toxic to melon worm, European and corn borer but he found the aqueous extracts were non effective against house flies but toxic against colding moths⁽⁵⁾ also found that the aqueous extract of oleander leaves were very toxic to american cockroaches and black carpet beetle larvae but non toxic to german cockroaches and mosquitoes⁽¹⁾ recorded that Nicotinoids and Nicotine were extracted from tobacco plant⁽⁶⁾ extracted toxin from tobacco plant *Nicotiana tabacum*. The leaves extracted of Nicotiana were very toxic to larvae of tobacco horn worm⁽⁶⁾. ⁽⁷⁾ found that the extracted stem, flower and leaves from oleander plant was effective of the cotton boll worm.

MATERIAL AND METHODS

The leaves of tobacco plant *Nicotiana tabacum* and oleander plant *Nerium oleander* were collected in 1995 from Baghdad.

1- Extract dried tissue of oleander leaves with 10% acetic acid in ethanol Leaving to stand for at least 4 hrs. In the lab. Filter the extract and concentrated to one quarter of the original volume by using Retor evaprate of temperature 40-50C.

The alkaloid precipitated by dropwise addition of NH_4OH . Collect the precipitate by centrifugation, washing with 1% NH_4OH . Then dissolve the residue in a few drops of ethanol or chloroform⁽⁸⁾. Chromatography an aliquot on silica gel G plates in methanol conc. NH_4OH (200 : 3).

Detect the presence of alkaloids on the paper and plate, first of all by any fluorescence in UV light and then by application of three spray reagents - Dragendorff, Iodo platinate and Marquis. Confirm the presence of alkaloid by measuring the UV. Length by using relative factor (RF) with this equation^{(9),(8)}.

$$\text{The equation RF} = \frac{\text{Distance traveled by pigment}}{\text{Distance traveled by solvent}}$$

2- The second extract dried leaf tissue of tobacco leaves which were extracted with 10% acetic acid an ethanol leaving to stand for 6 hrs. Concentrate the extract and precipitate the Nicotine by dropwise addition of dissolved residue of ethanol or chloroform or ammonia⁽¹⁾.

The american cockroach *Periplaneta americana* was collected from Baghdad and reared on cage 50×50×50 cm 3 cover with mesh with one open. The cage had a petridish containing 3 parts of bread mixed with apart of milk sugar in the lab. Condition⁽¹⁰⁾.

The experiment was designed by using three concentrations of alkaloid 1%, 0.1%, 100% with control, using contact and food contamination method. Three instars of cockroaches 3rd nymph instar, 6th nymphs and adults for each concentration treatment were used 20 cockroaches and replicated 3 times and the results were recorded for 3-4 days. The same procedures were used with nicotine extracts. The experiment was done in Entomology lab. of Biology Department and Chemistry Department, Science College, University of Al-Mustansiriyah. Both these extracted nicotine and alkaloid were mixed with wettable

chemical as carrying material change the extract to emulsion solution insecticides like any manufacturing insecticides.

RESULTS AND DISCUSSION

The wave length of alkaloid from oleander extract is shown in fig. (1). The wave length was 271, 227 (nm) and the absorption was 0.325, 1.400 (nm). Fig(2) shows the effect of different concentrations of alkaloid on the different instars of cockroach by contact method. The high concentration of alkaloid gave high peak mortality of nymph instar in different concentrations 1% > 0.15% > 0.1% respectively.

The immature 3 rd instar was high peak mortality in different concentrations of alkaloid more than 6 th and adult respectively compare with fig (2A, B, C). The immature (3rd and 6th) instars are very sensitive to the nicotine and other alkaloid because of the body wall of immature instars are more permeability than the adult instars when are using the contact method. The effect of these two extracts chemicals are more permeability in immature instars than the adult instars when are using feeding method⁽¹¹⁾.

Fig (3) shows the effect of different concentrations of alkaloid on the different instars of cockroach by contact method. 1% concentration of alkaloid showed low peak of mortality of different instars of cockroach lower than 100% concentration. Fig. (4A-B) showed the high concentration of Nicotine effective and high mortality of different instars of american cockroach in both ways digestive and contact. The adults of cockroach recorded 75%, 80% lower than 3 rd and 6 th instars which recorded 100%.

Fig (5 and 6) show that the LD 50 of 3 rd instars of cockroaches were higher than the LD 50 of the 6th and adult respectively in digestive method and in contract method.

The different chemicals extracted from different plants were very important to produce different insecticide

and play important role in controlling insects. The demonstrated data found the alkaloid extract effective and highly toxic different instars of american cockroach. Jacobson has the same result, who found the aqueous extracts of the leaves were very toxic to american cockroaches⁽⁵⁾ recorded that oleander extracts were very toxic to american cockroaches black beetle larva, and non toxic to german cockroaches, Mosquito *Anopheles* and *Aedes*⁽⁷⁾ found alkaloid extracts from oleander effective some agriculture insects like on american cockroach was toxic⁽⁶⁾ has same results but agriculture insects like horn tobacco worm.

CONCLUSION

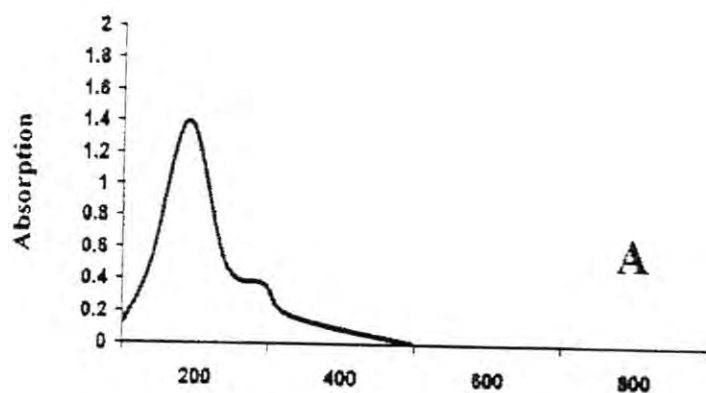
We recommended the alkaloid and Nicotine as good insecticides o different insects. We added carrying materials and preparing the first time in Iraq as new insecticides which have results on the cockroaches.

ACKNOWLEDGEMENT

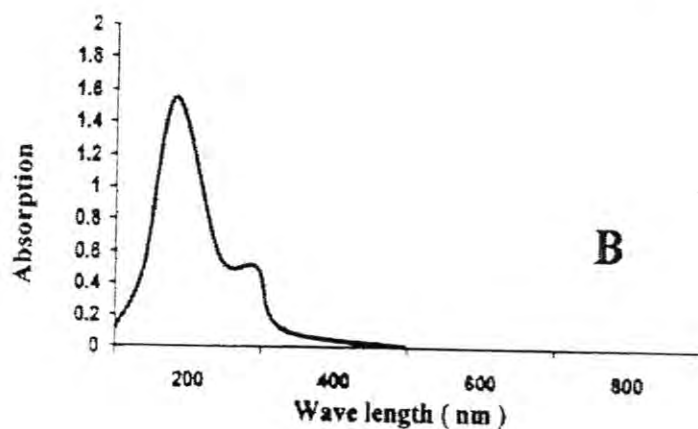
We would like to thank Prof. Adassie, S. The head of Chemistry Dept. in Science College, Al-Mustansiriyah for his help on preparing the carrying material, and Assistant Prof. Al-Shakali, M. for his efforts of help in this projects.

REFERENCES

1. Jacobson, M. Isolation and Identification of toxic agents from plants . ACS Symposium Series, No. 62, Hostplant Resistance to Pest, Paul Hedin Editor (1997).
2. Kircher, H.W. ; Heed, W.B.; Jeans, S.R. & John, G. Senita *Cacutus* alkaloids their significance to Sonoran desert *Drosophila*. *J. Insect. Physiol.* 13:/ 1864-1874 (1967).



Wave length (nm)
Wave length 271 , 227 nm
Absorption 0.325 , 1.4



Wave length 275 , 228 nm
Absorption 0.301 , 1.455

Fig . (1) Scanning profiles A , B and integration curve of
alkoloid plant extracts .

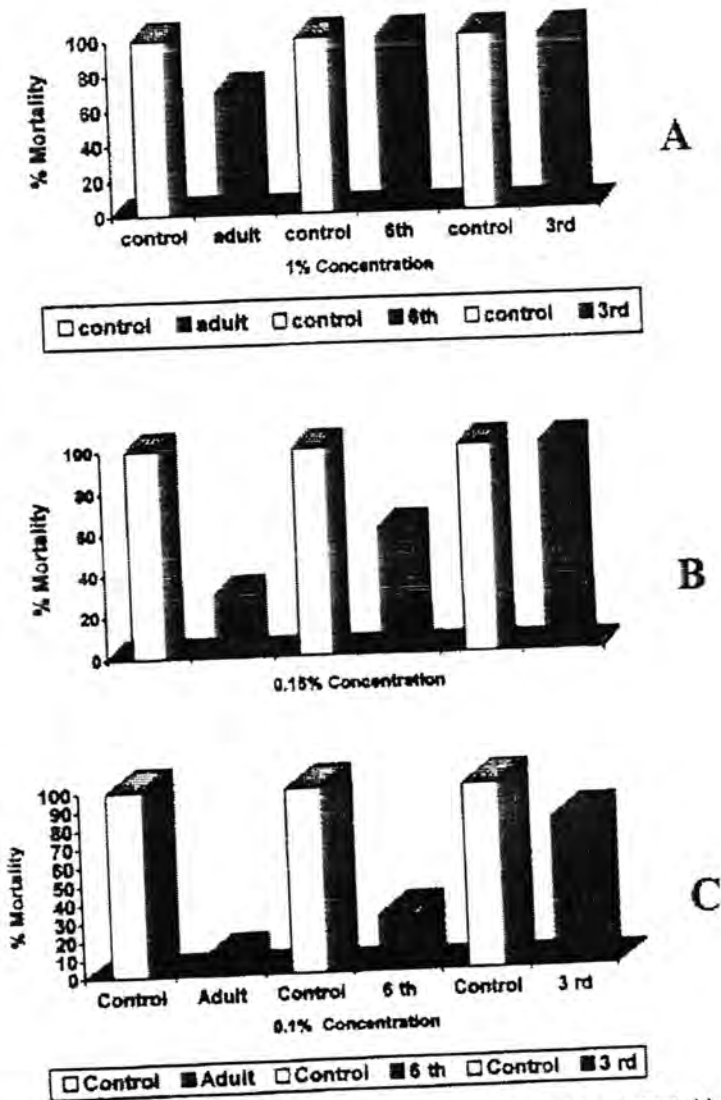


Fig (2) : A , B and C , The effect of different concentration of alkoid on the different instars of cockroaches by digestive method

Use of Oleander and Tobacco Extracts As An Insecticide

B.M. Al-Azawi, et al.

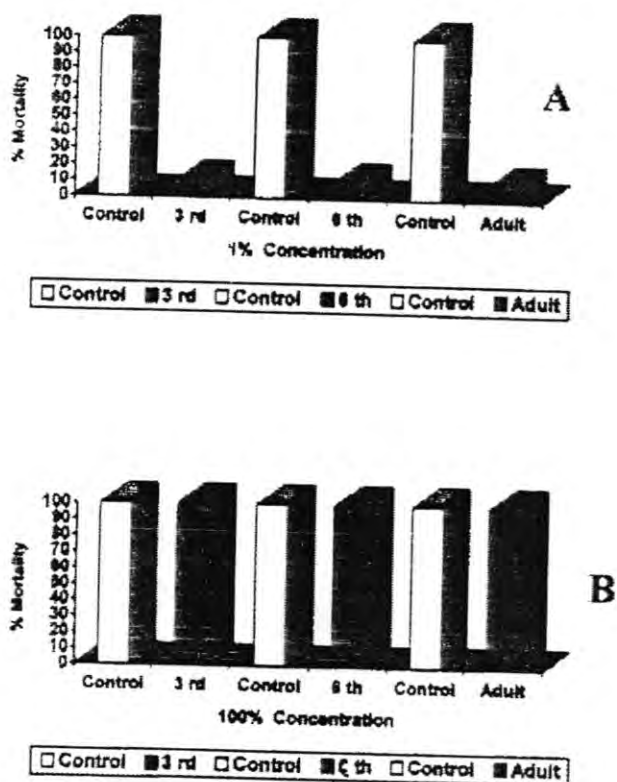


Fig (3) : A and B The effect of different concentration of alkoid on the different instars of cockroaches by contact method

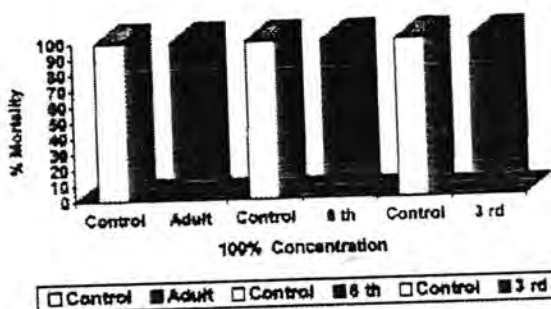
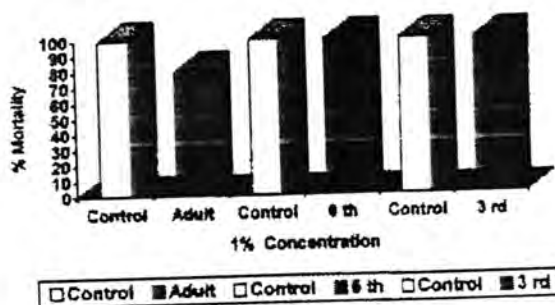


Fig (4-A) : The effect of different concentration of nicotine on the different instars of cockroaches by digestive method

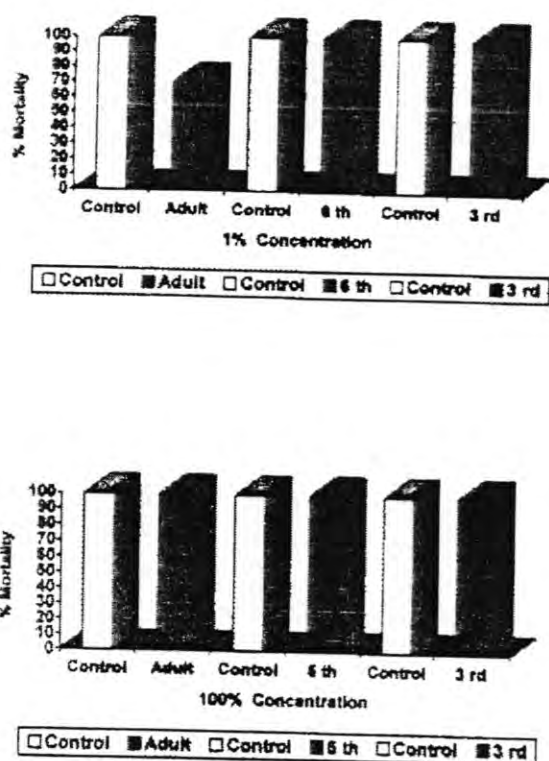


Fig (4-B) : The effect of different concentration of nicotine on the different instars of cockroaches by contact method

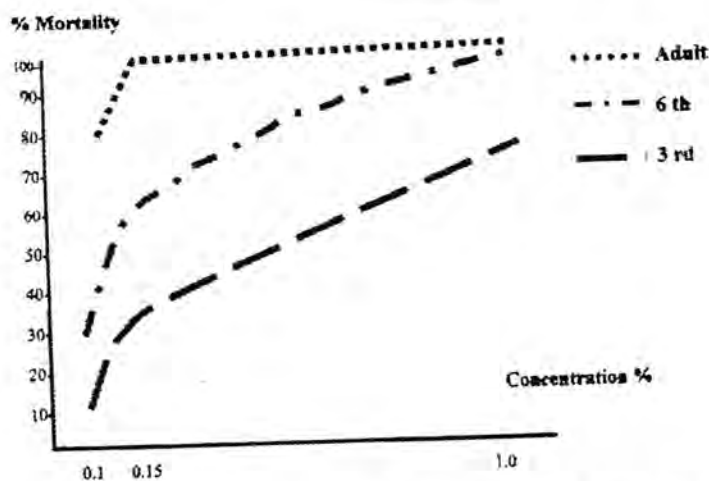


Fig. (5) The relationship between different concentrations of alkaloid and % mortality for each instars of cockroaches in digestive method

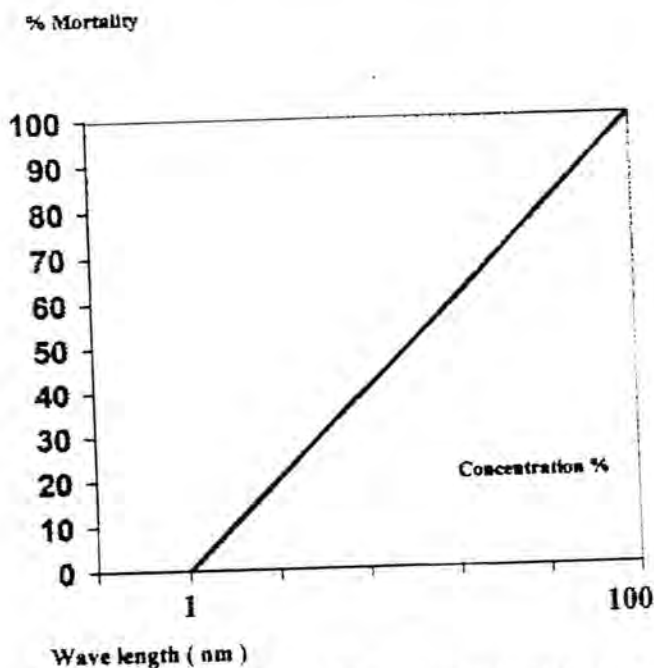


Fig. (6) The relationship between different concentrations of alkaloid and different instars of cockroaches by contact method

3. Pliske, T.E., Pollination of Pyrrolizidine alkaloid containing plants by male lepidoptera Environ. Ent 4 : 474-479 (1975).
4. Jacobson, M. Insecticides from plants. A review of the literature. United States, Department of Agriculture, No 154, 20 pp (1953).
5. Record E.F; Wallace R.T.; and Starves , O. A survey of plants for insecticidal activity. Liaydia 13 : 89-162 (1950).
6. Thruston, R. Toxicity of Trichome exudates on Nicotina and Petunis species to tobacco horn worm larva. J. Econ. Ent. 63 : 272-274 (1970).
7. Amir, K.A. Investigations on some Iraqi plants that contain toxicant, or repellent compounds to insects. M.Sc. Thesis, Plant Protection Department, College of Agrriculture, University of Baghdad. 117 pp. (1981).
8. Harborne, J.B. Phytochemical methods. London Publish, (1973).
9. Stahl, E. Thin Layer Chromotography. Alaboratoty hand book 2 nd. Ed. Translated by M.R. Ashworth, springer verlag. New York 421-pp. (1969).
10. McCay, C. M. and R.M. Melampy, care. and rearing of B. germanica in the caltssoff and other culture comstock pub. Co. 283 pp. (1937).
11. Gergeous, S.G. Amen., A.H. The Medical and Veterinary of the insects and Acaros Univeristy of Mousal. Dar Alkutub for printing and publishing. 240 pp (1987).

Inhibition of Colony Growth of Some Dermatophytes by Some Plant Extracts

IHSAN S. DAMIRDAGH AND ALI A.H. AL-JANABI

Department of Biology, College of Science, Al-Mustansiriya University, Baghdad-Iraq.

(Received May 11, 1999; Accepted Nov. 2, 1999)

الخلاصة

عزلت وشخصت اربع انواع من الفطريات المسببة لامراض جلدية في الانسان وهي: *Trichophyton mentagrophytes*, *T. tonsurans*, *T. rubrum*, *Epidermophyton floccosum*. جرى اختبار تأثير مستخلصات مائية وكحولية لعشر انواع من النباتات على نمو هذه الفطريات في اكار السابرويد. هذه النباتات كانت الحرمل *Peganum* *harnala* L. والياس *Myrtus communis* L. والزمان *Punica granatam* L. والحلبة *Trigonella foenum graceum* L. والتوت *Morus alba* L. والكزبرة *Corinadrum sativum* L. والكمون *Cuminum cyminum* L. والنعناع *Mentha virids* L. والمطاط الديني (المقدس) *Ficus religiosa* L. والرشاد *Lepidium sativum* L. تم انماء هذه الفطريات في اكار السابرويد الحاوي على تراكيز مختلفة (غم/لتر) من المستخلصات النباتية المجففة. وتم تقدير نمو الفطر عن طريق قياس قطر مستعمرة الفطر فوجد ان هذه المستخلصات تمنع بدرجات (متفاوتة حسب التركيز وحسب نوع الفطر) مقدار نمو الفطر. ولكن كان مستخلصات نبات الحرمل ثم الياس ثم الزمان هي الاكثر منعاً لنمو الفطريات. وباستخدام المحاليل الكاشفة تبين ان المستخلصات المائية والكحولية للحرمل والمستخلص الكحولي للزمان تحتوي على المركبات القلويدية والكلايكوسيدية ولا تحتوي المواد الفينولية. في حين احتوت مستخلصات الياس المائية والكحولية والمستخلص المائي للزمان على المركبات الفينولية والكلايكوسيدية ولم تحتو على المركبات القلويدية.

ABSTRACT

The aqueous and ethanolic extracts of ten plant species were tested for their antifungal activity against the following dermatophytes:- *Trichophyton mentagrophytes*, *T. Rubrum*, *T. Tonsurans* and *Epidermophyton floccosum*. The plants used in this study were, Harmala seeds (*Paganum harmala* L-Zygophyllaceae), Myrtle leaves (*Myrtus communis* L.-Martaceae), Pomegranate (*Punica granatum* L.) Fenugreek fruit (*Trigonella foenum graecum* L- leguminosae), Mullberry leaves (*Morus alba* L- Moraceae), Criander fruit (*Coriandrum sativum* L. Umbellefear), mint leaves (*mentha viridis* L. labiatae), ficus plant leaves (*Ficus religiosa* L. Moraceae), Garden cress leaves (*Lepidium sativum* L. Cruciferae) and Cunmin leaves (*Cuminum cyminum* L. Umbelleferae). The dried extracts were added at 4.0 mg or 8.0 mg per ml concentration to the Sabourand agar and the growing colony diameter was measured as indication for the antifungal activity in the growth medium. The extracts differed in their inhibitory effect against different fungi, the most effective were extracts of harmala seeds (*peganum harmala* L.); *Myrtus* leaves (*Myrtua comnus* L.) and pomegranates fruit rind (*punica granatum* L.).Ethanolic and aqueos extract of harmala at conc. of 1 mg/ml of Sobouraud medium completely inhibited colony growth of *T. mentagrophytes* and *T. rubrum* and at 3 or 4 mg/ml concentration it completely inhibited the growth of the other two fungi as well.

INTRODUCTION

Dermatophytes are ubiquitous fungi, they have been recorded from all over the world^(1,2,3,4) once a dermatophyte cause an infection it persist for a long time if not for ever in the infected person⁽²⁾, and so it needs continued treatment.

In the hope of obtaining new and more effective drugs for dermatophytes, researchers all over the world are screening extracts of local plants for their antifungal properties^(5,6,7), such test often begin with tests on nutrient agar media⁽⁵⁾ then in animal then in volunteers.

In some countries⁽⁸⁾ villagers use pomades prepared from local plants in preference to the prepared commercial drugs. An article⁽⁸⁾ showed that such locally prepared pomade for treating tinea pedis was better than some commercial ointments in being more effective and prevented recurrent infection for a longer time.

There is a large number of plant species in Iraq grown naturally as weeds or cultivated, some of which have been studied for their antimicrobial activities^(9,10,11).

The purpose of the present work was to test the extracts of some local plants and some imported plant products for their antifungal activity against some locally isolated dermatophytes on nutrient medium as a first step for further studies.

MATERIALS AND METHODS

Test Fungi

The following fungi were clinical isolates of patients suffering from fungal infections in Iraq.

1. *Trichophyton mentagrophytes* from Tinea pedis
2. *T. rubrum* from Tinea cruris
3. *T. tonsurans* from Tinea corporis
4. *Epidermophyton floccosum* from Tinea cruris.

The fungi were isolated and maintained at 25°C on sabourands chloramphenicol-cycloheximide agar (per liter of distilled water dissolve: 10g. peptone, 20g. glucose, 15g. agar and after sterilization at 121°C for 15min. chloramphenicol 0.05g. and cycloheximide 0.4g. were added). The cultures were renewed every four-weeks.

Plant Materials and Extractions

The following plant parts were obtained from the local market or from surrounding gardens;

Inhibition of Colony Growth of Some Dermatophytes by Some Plant Extracts
I. S. Damirdagh And A. A.H. Al-Janabi

1. The rind of pomegranate fruits (*Punica granatum* L. - punicaceae).
2. Harmala (*Peganum harmala* L. - Zygophyllaceae) seeds.
3. Myrtle leave (*Myrtus communis* L. - Myrtaceae).
4. Fruit of fenugreek (*Trigonella foenum* L. - leguminosae)
5. Mulberry leaves (*Morus alba* L. - Moraceae).
6. Coriander fruit (*Coriandrum sativum* L. - Umbellefera).
Imported for culinary uses.
7. Mint leaves (*Mentha viridis* L. - labiatae (lamiaceae).
8. Ficus plant leaves (*Ficus religiosa* L. - Moraceae).
9. Garden cress leaves (*Lepidium sativum* L. -Cruciferae).
10. Cumin leaves (*Cuminum cyminum* L. - Umbellifera)
imported for culinary uses.

All specimens were cleaned and air dried at 25-30°C then ground by mortar and pestle then sieved one gram of the sieved material was soaked in five ml of distilled water or in 70% ethanol for one day at 35°C with shaking, then filtered through filter paper Whatman No. 1. The filtrate was centrifuged and the supernatant liquid was coined as crude liquid aqueous extract or as crude liquid ethanolic extract.

For dried preparations the crude liquid extracts were evaporated under vacuum "Rotary evaporator" at 40°C until dry or a thick syrup was obtained, then this syrup was left in a drying oven at 45°C until dry, this was coined as "dried aqueous extract" or dried ethanolic extract of the plant which was dissolved at specific quantities in sabourauds agar to assay its inhibitory effect on the dermatophytes. In the control plates the agar medium did not contain any addition of plant extracts. For further comparison Nystatin was added to the growth media at concentration of 1mg/ml in another set of plates.

Antifungal Assays

In order to test the effects of the plant extracts we tried several methods.

A. Disc Diffusion Method

Filter paper disc were soaked in solutions of extracts then placed on the surface of the agar medium and

the inhibition zone around the paper disc was measured. This method did not give reproducible results.

B. Agar Diffusion Test

We tried putting the extract in wells dug in agar medium, then measuring the inhibition zone around such wells⁽⁶⁾. Again this method was not satisfactory.

C. Colony Diameter Test

Better and reproducible results were obtained by the method of Kady et al.⁽⁵⁾ by incorporating the plant extract in the growth medium at concentrations ranged from one to eight mg (dried plant extract) per one ml of sabourauds agar in petridishes.

The agar was inoculated by the test fungus, the inoculum was a disc 7mm in diameter plugged out from a 2-4weeks old culture of the fungus grown on sabouraud agar at 25°C, then the plates were incubated at 25°C and the colony growth was estimated weekly during the period of one month, by measuring (millimeters) two perpendicular diameters of the colony.

Two groups of control plates were used. In one group the sabourand agar contained no additives (no plant extract), in the other group the agar contained 1mg Nystatin per ml of the agar.

For each treatment three plates were used and each test was repeated three times. The reading were then averaged and presented in tabular form the analyzed by analysis of variance to show the statistical significance of the data.

D. Dry Weight Assay

The method of determining the dry weight of the total growth was applied to further estimate the inhibitory effect of three plant extracts proved as most effective by the previous methods on two fungi:- *T. mentagrophytes* and *E. floccosum* for this purpose to 50ml of sobouraud broth in a 200ml sized flask was added 200mg of dried ethanolic plant extract so as to obtain 4mg/ml.

Inhibition of Colony Growth of Some Dermatophytes by Some Plant Extracts
I. S. Damirdagh And A. A.H. Al-Janabi

The extracts from either one of Harmala, Pomegranate or Myrtle was tested in this way. This medium was inoculated by adding to it 0.04ml spore suspension of *T. floccosum mentagraphytes* or *E. floccosum* 1.5×10^5 spores/ml.

The mixture was incubated at 25°C for two weeks (for the first fungus) and four weeks (for the second). The control flasks contained no plant extracts.

After incubation the fungal growth was collected by filtration on a previously weighed filter paper (Whatman No.1), then dried in a drying oven at about 60°C for two hours and the filter paper re-weight to determine the weight of the fungal growth.

RESULTS

A. Colony Growth

Table (1) summarizes the colony growth of dermatophytes on sabourauds agar with and without the plant extracts and a similar medium containing Nystatin.

As is shown the dried ethanolic and dried aqueous extracts of harmala seeds, pomegranate fruit rind and myrtle leaves were more effective, than others, in inhibiting the growth of the fungi, the inoculum disc retained its original diameter of 7mm and no growth at all occurred even after 2-4 weeks of incubation at 25°C, meanwhile the Nystatin was less effective although it reduced significantly the growth of the fungi as compared with controls which contained no addition in the growth medium.

The effect of Nystatin on *T. mentagraphytes* was less than that on the other three fungi i.e. *E. floccosum* *T. tonsurans* and *T. rubrum*.

For the purpose of reduction the following data were omitted from table 1; Dried ethanolic extract of Harmala and of Myrtle at concentration of 4mg/ml completely inhibited the colony growth of the tested fungi. Also dried aqueous or ethanolic extract of Mint at concentration of 8mg/ml completely inhibited the growth of only *T. tonsurans* while at 4mg/ml concentration the

colony diameter reached 17mm. The mint extract did not affect the other tested fungi. Similarly ethanolic and aqueous extracts of Mulberry and of coriander did not affect the growth of the tested fungi.

It is clear from table 1 that the tested fungi varied in their sensitivity to the inhibitory effect of a certain plant extract, also a certain fungus showed different sensitivity to different plant extracts.

In another experiment the most promising plant extracts were added to sabourauds agar at 1mg/ml or 2mg/ml or 3mg/ml and the diameter of growing colonies were measured.

The results shown in table 2 indicate that the fungal colonies in control plates (without additives) grew up to 62mm (in diameter), whereas in the presence of dried ethanolic extract of harmala at 1mg/ml or more colony growth of *T. mentagrophytes* and *T. rubrum* were completely inhibited, whereas the colony growth of *T. tonsurans* and *E. floccosum* were highly reduced, as the colony diameter was about 40% of the control. The other plant extracts were also effective but less than of harmala. It is also observable from table (2) that ethanolic extracts of each plant was more preventive than aqueous extract of the same plant.

Table 1: Average colony diameter in (mm) of the tested fungi in sabouraud agar

Agar media with additives	<i>T. mentagrophytes</i> 2 week old*		<i>T. tonsurans</i> 3 weeks old		<i>T. rubrum</i> 4 weeks old		<i>E. floccosum</i> 4 weeks old	
Control	80 ^a		57.5 ^a		46.5 ^a		78.5 ^a	
Nystatin 1mg/ml	46 ^b		7 ^b		21 ^b		7 ^b	
Plant extract*	4 mg/ml	8 mg/ml	4 mg/ml	8 mg/ml	4 mg/ml	8 mg/ml	4 mg/ml	8 mg/ml
Harmala: aque	7 ^c	7 ^c	7 ^b	7 ^b	7 ^c	7 ^c	7 ^b	7 ^b
Myrtle: aque	8 ^c	7 ^c	14 ^b	13 ^{bc}	23 ^b	9 ^c	26 ^c	12 ^b
Pomegranate: aqu.	8 ^c	14 ^c	9 ^{bc}	7 ^{bc}	19 ^b	7 ^c	22 ^c	7 ^b
Eth.	7 ^c	7 ^c	12 ^b	7 ^{bc}	12 ^c	7 ^c	7 ^b	7 ^{bc}
Fenugreek: aque	29 ^b	26.5 ^b	24 ^c	25 ^c	19 ^b	17 ^b	24 ^c	17 ^c
Eth.	52 ^b	52 ^b	41 ^c	37 ^c	12 ^c	15 ^c	23 ^c	22 ^c
Ficus aque	61 ^b	56 ^b	42 ^{ac}	47 ^a	63	60 ^a	64 ^a	66 ^a
Eth.	62.5 ^b	53 ^b	19 ^c	15 ^c	45 ^a	45 ^a	77 ^a	69 ^a
Lipidium sativum aque	48 ^{bc}	47 ^b	19 ^c	14 ^c	41 ^{ac}	38 ^b	14 ^c	7 ^b
Eth.	47 ^{bc}	52 ^b	24 ^c	46 ^a	46 ^a	44 ^a	56 ^c	48 ^c

Inhibition of Colony Growth of Some Dermatophytes by Some Plant Extracts

I. S. Damirdagh And A. A.H. Al-Janabi

Cumin: aque.	54 ^b	65 ^b	25 ^c	21 ^c	49 ^a	43 ^a	59 ^c	62 ^a
Eth.	23 ^b	7 ^c	12 ^b	7 ^a	23 ^b	12 ^c	31 ^c	16 ^b

* see the text for further details

aque. = dried aqueous extract, eth. = dried ethanolic extract
in one column similar letters mean no difference at $p > 0.05$ and different letters mean significant at $P < 0.05$ diameter of the inoculum was 7 mm.

Table 2: Colony diameter in mm after indicated time of incubation of the indicated fungi in sabouraud agar media containing aqueous (aque.) or dried ethanolic (eth.) plant extracts. Diameter of the inoculum was 7mm.

Plant extract	Concentrated mg/ml	<i>T. mentagrophytes</i> 2 week	<i>T. tonsurans</i> 3 weeks	<i>T. rubrum</i> 4 weeks	<i>E. floccosum</i> 4 weeks
Control		62	41	46	62
Harmala Aque	1	7	16	7	24
	2	7	7	7	24
Eth.	1	7	19	7	12
	2	7	21	7	7
Myrtle: aque	1	48 ^A	25	42 ^A	65 ^A
	2	20	17	36 ^A	50
Eth.	1	24	17	30	41
	2	12	7	26	7
	3	10.2	7	16	7
Pomegranate Aque	1	53 ^A	23	44 ^A	53 ^A
	2	41.5	23	36 ^A	42
	3	26	7	28	14
Eth.	1	34	15.5	43 ^A	52 ^A
	2	17.5	7	38.5 ^A	51 ^A
	3	11.5	7	30	47

A: all values except those with "A" are significantly different from the control at 0.05p.

B. Dry Weight

The growth of two fungi as determined by dry weight was highly reduced by the tested extracts.

In the control sabourauds broth (without plant extracts) the dry weight of *T. mentagrophytes* was 0.51g, whereas the dry weight of the grown fungi in a similar media but containing 4mg/ml of dried ethanolic extract of

either pomegranate fruit rind, Myrtle leaves or harmala seeds were 0.21g, 0.36g, or 0.23g respectively.

The dry weight of *E. floccosum* after four weeks of incubation in control medium was 0.53: and in the presence of 4mg/ml of dried ethanolic extract of pomegranate, Myrtle or harmala were 0.08g, 0.03g, 0.08gm respectively. In this test harmala and pomegranate had similar effects.

DISCUSSION

Dermatophytes have been studied in Iraq^(1,12), and there are previous publications about the effects of some plant extracts on such fungi⁽⁹⁾ and on some bacteria⁽⁷⁾. Such studies, however, did not test the effect of several plant extracts at the same time on different fungi.

A certain dermatophytic fungus can be isolated from different types of tinea, conversely different fungi can be present in the same lesion^(1,13,14,12), so one type of antifungal treatment may not give a good result in curing the lesion. Our results support this notion as the presented results indicated that different plant extracts, be it aqueous or ethanolic, had different inhibitory effects on different species of fungi, if this becomes true *In vivo*, then for a certain tinea we need to know exactly the causing fungal species or we should use a mixture of plant extract for the treatment. This variation also indicates presence of different effective compounds in the tested plants which could be extracted or purified from these plants.

This work showed that harmala, pomegranate and Myrtle are the most effective of the ten plant species used here, therefore we think it is necessary to survey more plants and isolate effective compounds from them. Harmala is commonly used as smoke in the folk medicine and it is known to contain many glycosides⁽¹⁰⁾. Extract of harmala has inhibitory effect upon tumor cells and against influenza virus but not against herpes virus⁽¹⁰⁾.

In this work harmala extract inhibited growth of several fungi with different degrees, this means it is not a general toxicant but there must be specific compounds in

harmala seeds that affect fungi in a specific manner. These compounds and their mode of action against microroganisms should be searched for. Also these results supports the idea that folk medicine may have, sometimes at least a scientific principle.

REFERENCES

1. Al-Yazachi, Moayed and Al-Bassam, Al-Fikar. Dermatormycoses in Iraq. J. Fac. Med. Baghdad Vol. 32(4): 431-447 (1990).
2. Nielsen, P.G. An epidemiologic investigation of dermatological fungus infections in the Norhternmost country of Sweden (Norrbotten) 1977-1981. Mykosen 27(4): 203-210 (1984).
3. Soyinka, Femi. Epdemiologic Study of dermatophyte infections in Nigeria (clinical survey and laboratory investigations). Mycopath. 63(2): 99-103 (1978).
4. Todaro, F. Germano, D. and Criseo, G. An outbreak of tinea pedis and tinea cruris in a tire factory in messina, Italy, Mycopath 83(2): 25-27 (1983).
5. Kady, I.A.; El-Maraghy, S.S.S. M.; Mohamed,E.M. Antibacterial and antidermtophyte activities of some essential oils from spices; Qatar Univ. Sci. j. 13: 63-69 (1993).
6. Muir, A.D.; Cole, A.L., and Walker, J.R.L. Antibiotic compound from New Zealand plants. Planta medica, Vol. 44: 129-133 (1982).
7. Twaij, H.M.S. and Al-Zohyri, A.M. Pharmacological, phytochemical and antimicrobial studies on *Myrtus communis*. J. Bio. Sci. Res. 19(1): 24-52 (1988).
8. Lozoya, Y.; Navasso, V.; Garcia, M. and Zurita M. *Solanum chrysotrichum* (Schldl.) a plant used in Mexico for the treatment of skin mycosis. J. Ethnopharmacology. 36: 127-132 (1992).
9. Ghani, H.M.; Yahya, M.M. and Ayoub, M.T. Crude extracts from *Lawsonia inermis* with antidermatophyte activity. Iraq medical. J. Vol. 35(1): 39-43. (1987).

10. Rashaan, L.J.; Adaay, M.H. and Al-Khazraji, A.L.T. In vitro antiviral activity of the aqueous extract from the seed of *peganium harmala*. *Fitoterapia*. Vol. LX(4): 365-366 (1989).
11. Al-Assady et al. Some antifungal activities of *myrtus communis*; Clinical implications on superficial skin infection. *J. Fac. Med. Baghdad* 4: 393-397 (1997).
12. Gumar, Abdu-Wahhab, S. and Guirges S.Y. Survey of aetiological agents of fungal infections of skin. *J. Fac. Med. Baghdad* 20(1): 19-29 (1978).
13. Cabrita, J.; Esteres, J. and Sequeira H. Dermatophytes in Portugal (1972-1981). *Mycopath*, 84(2/3): 159-164 (1983).
14. Caretta, G.; Delfrate, G.; Picco, A.M. and Mangiarotti A.M. Superficial mycoses in Italy, *Mycopath*. 76(1): 27-32 (1981).

A Modified *Salomonella typhi* Ty21a Strain which Encoded to Colonization Factor Antigen

SHAYMA J. AHMED

Department of Pathology, College of Medicine, Baghdad

University - Iraq

(Received - Sept. 6, 1999 ; Accepted May 14, 2000)

الخلاصة

تم الحصول على سلالة من سالمونيلا التيفويد Ty21a المستخدمة كلقاح فموي والمطفرة تلقائياً للمقاومة للمضاد الحيوي الريفاميسين (لأستخدامه كمؤشر وراثي انتخابي) وقد عوملت السلالة مختبرياً لكي تصبح مهياةً (competent) وحولت وراثياً (transformed) ببلازميد من بكتيريا *Klebsiella pneumoniae* والذي يشفر لعامل الاكتصاق الهديبي من النوع الأول (Colonization Factor /I) وللمقاومة لاثنتين من المضادات الحيوية وقد اظهرت المستعمرات المشتقة من هذه السلالة ان لها القابلية على التلازن مع كريات الدم الحمراء للإنسان من فصيلة (A) وانها مقاومة لأحد المضادات الحيوية المكتسبة وقد كان البلازميد المنقول ثابتاً لأكثر من (٥٠٠) جيل من سلالة السالمونيلا المتحولة.

ABSTRACT

It was obtained of an oral vaccine strain of *Salmonella typhi* Ty21a which was spontaneously mutated for Rifampicin resistance (to be used as selective antibiotic marker) treated to be rendered competent then transformed with plasmid from *Klebsiella pneumoniae* which coded for Colonization Factor type I and resistance for two antibiotics. The derived colonies of this strain indicated the ability to agglutination with Human Red Blood cells group (A) as well as resistance for two acquired antibiotic. The

*A Modified Salmonella typhi Ty21a Strain which Encoded to
Colonization Factor Antigen* S. J. AHMED
transfer plasmid was stabled for up 500 generations with in
the transformed *Salmonella* strain.

INTRODUCTION

Genetic recombination techniques are being used to generate various attenuated strains as a candidate vaccines against more than one disease after transferred of the coded genes such as somatic bacterial antigens, adherence factors,... etc. or viral and parasite antigens and expressed these antigens into the new generation⁽¹⁾, the candidate strain can be used to immunize human and animals by eliciting mucosal, humoral and cellular immune responses⁽²⁾.

The *S. typhi* Ty21a has the ability to protect against typhoid fever, the strain was found to be safe and effective in field trials: In Egypt the vaccine gave a protection of 95% following single dose⁽³⁾.

Ty12a was derived from *S. typhi* Ty21a by chemical mutagenesis with a mutation in the *galE* gene⁽⁴⁾.

This strain was used to expresses an enterotoxigenic *Escherichia coli* plasmid encoding Colonization Factor Antigen type I (CFA/I) and heat-stable toxin (ST)⁽⁵⁾, as well as it was used for expressing fragment C of tetanus toxin by stimulated the mucosal IgA cell-mediated immune responses⁽⁶⁾.

The genes which encoded CFA/I in the *Kl. pneumoniae* found on the plasmid or chromosomal DNA which give the bacteria the ability to adhesion on the intestinal epithelium and agglutination with Human Red Blood Cells group (A).^(7,8)

The goal of this research is: transfer of DNA plasmid (pMA2) from *Kl.pneumoniae* into Ty21a, the derived strain has the ability to agglutination with the human red blood cells group A, this mean coded for CFA/I and acquired resistance for two antibiotic which would be important as tags for the strain in future clinical trials. Immunological testing constructed strain against colonizing *Kl. pneumoniae* as well as *S. typhi* infections in under way.

At last study the stability of this plasmid in the new host.

MATERIALS AND METHODS

A- Bacterial strains :

The bacterial strains used in the study are listed in table (1), Ty21a was spontaneously mutant by continuous sub culturing on the high increasing concentrations of antibiotic (10, 25, 50, 75, 100) µg/ml. (unpublished observation). They were minded on Brain Heart Infusion Agar (Oxoid) with selection.

B- Isolation of DNA plasmid

Kl. pneumoniae⁽²⁾ was grown on CFA-agar and tested for mannose-resistant hemagglutination (MRHA) with human Red Blood cells group A⁽⁹⁾, then plasmid was isolated by according to alkaline lysis method⁽¹⁰⁾.

C- Transtormation

CFA/I plasmid was transformed to the competent *S. typhi* Ty21a according to Tasi et al.⁽¹¹⁾.

D- Stability of CFA/I

The stability of CFA/I plasmid was tested in new host was according to standard procedures⁽¹²⁾.

Table -1- Bacterial strain used in this study

Strains	Phenontype & Genotype	References
<i>S. typhi</i> : Ty21a	<i>galE</i> ⁻ , Rif ^r	Genetic engineering & Biotechnology Institute graduate studies, Baghdad university
<i>Kl. pneumoniae</i> (2) (pMA2)	(wild typr) Ap ^r , Cm ^r , CFA/I	Genetic engineering & Biotechnology Institute graduate studies, Baghdad university.
<i>S. typhi</i> : Ty21a GEB122	<i>galE</i> ⁻ , Rif ^r , Ap ^r , CFA/I	This study.

-*galE*⁻: galactose mutation

-, Rif^r, Ap^r, Cm^r : resistance to the antibiotics Rifampicin, Ampicillin and Chloramphenicol sequence.

-CFA/I : Colonization Factor Antigen type I.

RESULTS & DISCUSSION :

The plasmid (PMA2) is about 60 megadaltons coded for AP, Cm resistance and Coloization Factor Antigen (CFA/I). The competent *S.typhi* Ty21a was prepared by using cold CaCl₂ (0.1M) in to (4°C) and the heat shock was in the water bath (40°C) for (30) second.

This plasmid was transferred in high frequency of transformation (1.5×10^{-4}), (the toal count to transformants in 1ml is 150 and the total count of recipient in 1ml is 2×10^7 in other hand the concentration of DNA was 0.05 microgram) one of transformed GEB122 was resistance to Rif (selective marker) and Ap (plasmid marker), *galE*⁻ mutation was also stable in this transforming according to standard procedure⁽¹³⁾ and it had the CFA/I after test⁽⁹⁾.



Figure (1): Agarose gel electrophoretic profiles of CFA/I plasmid DNA obtained from:

- 1- *S. typhi*: Ty21a which has no plasmid
- 2- The donor strain *K1. Pneumoniae* (2) which has CFA/I plasmid
- 3- CFA/I plasmid DNA from *S. typhi* GEB 122.

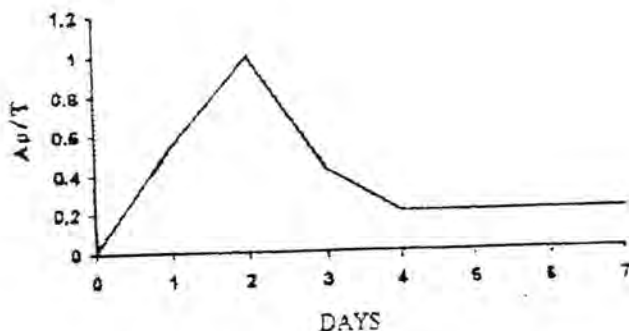


Figure 2: The stability of CFA/I plasmid in *S. typhi* GEB 122. Ap: Ampicilline resistance (100 µg/ml, plasmid marker) T: Total count

Plasmid DNA was prepared from donor, recipient and transformed strains and profile was obtained after agarose gel electrophoresis as shown in Fig-1-

Stability of pMA2 in *S. typhi* GEB 122 was monitored by continuous sub culturing without selection, results have indicated that plasmid loss was observed only after 500 generation, Fig(2) indicating a fairly stable nature.

However, sub culturing with selection for one of the antibiotic markers (Ap) CFA ensures longer stability.

The two markers (Ap. Rif) are seem to be importance for isolating in future *in vivo* studies.

Acknowledgement

I would like to express my deepest gratitude to Dr. Ali Al-Zaag for his kind help and supervision, and thank Dr. M.A., Al-Said for his cooperation.

REFERENCES

1. Roitt, I.M. "Essential Immunology," fifth edition. Black well scientific publications, (1984).
2. Curtiss III, R. ; Kelly, S.M. ; Tingo, S.A. ; Tacket, C.O. ; Levine, M.M, Srinivason, J. and Koopman, M." recombinant *Salmonella* vectors in vaccine development" Dev. Bio. Stand. Basel, Karger. (1994).
3. Silva, B.A., Gonzalez, c. Mora, G.C. and Cabello, F. "Genetic characteristics of *Salmonella typhi* strain Ty21a Vaccine." J. Infect. Dis-155 (5): 1077-1078 . (1987).
4. Germanier, R. and Furer, E. "Isolation and Characterization of galE mutant Ty21a of *Salmonella typhi* a candidate strain for a live Oral typhoid". J. Infect. Dis. 131 : 553-558 (1975).
5. Yamamoto, T.; Tamura, Y. and Yokota, T. "Enteroadhesion fimbriae and enterotoxin of *Escherichia coli* : Genetic transfer to a streptomycin-resistant of gal

- E' Oral-route live-Vaccine *Salmonella typhi* : Ty21a.
"Infect. Immun. 50(3) : 925-928.(1985).
6. Levine, M.M; Galan, J., Barry, E. ; Noriega, F.; Chatfield, S.; Sztein, M.; Dougan, G. and tacket, C.
"Attenuated *Salmonella* as live Oral Vaccine against typhoid fever as live vectors. "Biotechnology, 44 : 193-196. (1996).
7. Brubaker, R. "Mechanisms of bacterial virulence". Ann. Rev : Microbiol. 39 : 21-50. (1985).
8. Schurtz, T., ; Hornick, D.; Korhonen, T. and clegg, S.
"The type 3 fimbrial adhesion gene (mrk D) of *Kelbsiella pneumoniae* is not conserred among all fimbriate strains". Infect Immun. 62 (10): 4186-4191. (1994).
9. Heuzenroeder, M.; Elliot, T. ; Thomas, c. ; Halter, R. and Manning, P. "A new fimbrial type (PCFO0) on enterotoxigenic *Escherichia coli* O0 : HLT⁺, isolated from a case infant diarrhea in central Avatralia". FEMS Microbiol Lett. 66 : 55-60. (1990).
10. Birnboim, H.C. and Doly, J. "A rapid alkaline extraction procedure for screening recombinat plasmid DNA." Nucleic Acid Res. 7 : 1513-1523. (1979).
11. Tasi, S.P., hartin, R.J. and Ryu, J. "Transformation restriction-deficient *Salmonella typhimurium* LT2." J. Gen Microbiol. 135: 2561-2567. (1989).
12. Ali, N.A. "Expression and screetion of OXA-2 Beta-Lactomase by *Streptomyces lividans*". Ph.D. thesis- University of surrey. U.K. (1986).
13. WHO. "The thrity fourth Report". Series of technic reportes. number 700. WHO. Geneva (1984).

Study on Fruit Scab Disease of Cucumber (*Cucumis Sativus*. L.) Caused by *Cladosporium* *Cladosporioides* and its Control

ABDULAZEEZ M. NOKHALAN

Biology Department, College of Science, Al-Mustansiriya
University

(Received July 22, 1999; Accepted Nov. 8, 1999)

الخلاصة

اشتملت الدراسة على دراسة تأثير تراكيز مختلفة من مادة البنليت تحت درجات حرارة مختلفة في مقاومته الفطر *Cladosporium cladosporioides* الذي يسبب جرب ثمار الخيار على الوسط الغذائي PDA وعلى نباتات الخيار وثمارها في البيت الزجاجي، وقد اظهرت نتائج الدراسة ان مادة البنليت تمنع نمو الفطر *Cladosporium sp.* على الوسط الغذائي PDA وعلى نباتات الخيار وثمارها في البيت الزجاجي وباستخدام تراكيز قليلة نسبيا (٠,٢٥ غم/ لتر) وفي مختلف درجات الحرارة (٥، ١٠، ٢٠، ٢٥ درجة مئوية).

ABSTRACT

The aim of the present investigation is to study the effect of different concentrations of Benlate under different temperatures on the fungus *Cladosporium cladosporioides* the causal agent of fruit scab of cucumber on PDA and cucumber fruits and on cucumber plants in greenhouse. The results indicate that Benlate can prevent the growth of the fungus *Cladosporium sp.* on the PDA media on cucumber fruits and cucumber plants in greenhouse in low concentration (0.25g/L) and at different temperatures (5, 10, 15, 20, 25°C).

INTRODUCTION

Cucumber (*Cucumis sativus* L.) crop is considered as one of the important vegetable crops worldwide. In Iraq it is widely cultivated particularly in the middle of country. Cucumber fruits and plants liable to attack by many fungi causing serious diseases^(4,10,15)

Cladosporium sp. considered to be a most serious fungus⁽¹⁴⁾. In many parts of Iraq *Cladosporium cladosporioides* was isolated from cucumber^(10,11), isolates this fungus from cucumber fruits in the markets and from cucumber plants in the covered cultivation⁽⁷⁾ isolated this fungus from tomato in the North of Iraq.

Benlate as systemic fungicide has been used widely during the last five decades to control the post harvested diseases of fruits and plants in the greenhouse^(3,5).

The goal of the present study is to evaluate the effect of Benlate at different temperature on the scab of *Cladosporium* infection in cucumber plants and fruits.

MATERIALS AND METHODS

Isolation and Identification

Diseased fruits and plants of cucumber were collected from markets and greenhouses. Slides were made to examine the fungus and pure culture was prepared. Identification of the fungus was made depending on color and shape of conidia and conidiophores according to (2,6) and confirmed by CMI.

Pathogenicity test was carried out in laboratory by inoculating surface sterilized cucumber fruit with the fungus (small disc, 5mm in diameter, from 10 days of PDA fungal culture). Inoculated fruits were incubated 20-25°C. Control fruits were sprayed with sterilized distill water (SDW).

The effect of Benlate and Temperatur

On the Fungus on Culture Media: Different amounts of Benlate (1/4 g, 1/2g and 1 gram) were added to one liter of potato dextrose agar (PDA), and poured in petri-dishes (10cm in diameter) 1 petri-dishes for each treatment were inoculated with the fungus inoculum (5mm disc of 10 days old of fungus culture). 10 inoculated PDA petri-dishes without Benlate were served as control. The inoculated petri-dishes were incubated at (5,10,15,20 and 25°C).

On Inoculated Cucumber Fruits: Middle size cucumber fruits were sunk in different concentrations of Benlate (1/4g, 1/2g and 1 gram per liter of water) for one minute, then the fruits were sprayed with fungus spore suspension (250,000 spores/ml), 10 ml each. Inoculated fruits were incubated at different temperatures (5,10,15,20,25°C). Ten fruits were used for each treatment. Control fruits were sprayed with SDW.

On Cucumbers Plants: In greenhouse 40 plants of cucumbers (7 leaves stage) were divided in to four groups, each group were treated by one of the Benlate concentrations studied (1/4g, 1/2g or 1 gram of Benlate per liter of water or with DSW as control). 10ml were used for each plant. After that the plants were inoculated with fungus spore-suspension as mentioned in (2.2) and were maintained in greenhouse at 20-25°C.

RESULTS AND DISCUSSIONS

The results presented in table 1,2 and 3 indicate the effect of Benlate *Cladosporium cladosporioides* on growth medium and on the fungus on cucumber plants and fruits.

The growth of the fungus on PDA was completely arrested as no fungus colony appeared even after 10 days of incubation at temperatures ranged between 5 to 25°C, these

*Study on Fruit Scab Disease of Cucumber (Cucumis Sativus. L.)
Caused by Cladosporium Cladosporioides and its Control*

A. M. NOKHALAN

results come in accordance with previous published data on the effect of benlate on the growth of the fungus^(11,8,12)

Similarly benlate prevented fruit infection by the fungus. As shown in table (2) not a single fruit out of 10 at any of incubated temperatures became infected by the inoculated fungus. Apparently these was complete protection of the fruits by the benlate. The protective effect of benlate for the cucumber plant was also clear as shown in table (3). Only 2 plants out of 10 were infected after protection by 0.25g/liter of benlate whereas 9 plants out of 10 were infected after spray by distilled water. These results are in agreement with other published data^(5,9,13)

Depending on the presented results it may be possible to use spray cucumber plants by benlate as a protective measure against the fungus *Cladosporium cladosporioides* infection.

Some further field works may be needed for better judgment of the results and wording of the final recommendation.

Table 1: the effect of Benlate and temperature on the fungus growth on the PDA

Treatment	Growth of fungus on PDA+Benlate after 10 days in different temp.				
	5 °C	10°C	15°C	20°C	25°C
SDW as control	1cm	5cm	10cm	10cm	10cm
1/4 g/liter	Nil	Nil	Nil	Nil	Nil
1/2 g/liter	Nil	Nil	Nil	Nil	Nil
1 g/liter	Nil	Nil	Nil	Nil	Nil

g. Gram Benlate per one liter of PDA

SWD: Sterilized Distill Water

Nil: No Growth

Table 2: The effect of Benlate at different temperature on cucumber fruits infection

Treatment	Percentage of infected fruits by fungus after 10 days				
SDW as control	5 °C	10°C	15°C	20°C	25°C
	10%	30%	60%	100%	100%
1/4 g/liter	Nil	Nil	Nil	Nil	Nil
1/2 g/liter	Nil	Nil	Nil	Nil	Nil
1 g/liter	Nil	Nil	Nil	Nil	Nil

Table 3: The effect of Benlate on the fungus growth on the cucumber plants in the greenhouse

Treatment	The number of used plant	Infected Plants
SDW as control	10	9
1/4 g/liter	10	2
1/2 g/liter	10	Nil
1 g/liter	10	Nil

REFERENCES

1. Agrios G.N. Plant pathology. Academic press New York, (1979).
2. Barnt H.L. and B.B. Hunter. Illustrated genera of imperfect fungi. Burgess publishing companies Minnesota (1972).
3. Borisor, Y.M. Diseases of cucumber plants and effectiveness of some methods of control, Review of plants pathology 55: 528 (1976).
4. Chap and Sherf. Vegetable disease and their control 1st. ed. Ronald press company (1966).
5. Coyier, D.L. and Corey. Control of storage decay in Danjan pear fruit by preharvest application Review of plant pathology 55: 528 (1976).

*Study on Fruit Scab Disease of Cucumber (Cucumis Sativus. L.)
Caused by Cladosporium Cladosporioides and its Control*

A. M. NOKHALAN

6. Clement F.E. and Shear C.L. The Genera of fungi H. W. Wilson Company, New York USA (1931).
7. Damirdagh I.S., Hameed K.M. and Khan A.S. Fungi and plants disease of Northern Iraq. Zanco 8:3 (1983).
8. El-Fahl A.A., Ibrahim A.N. and Abdeal H.R. Control of fruits rot disease of groups in the field and storage (1978).
9. Macornak. Experimental post harvest Citrus fungicide with activity against fungi. Plants disease reporter 61: 788 (1977).
10. Nokhlan A.M. Fungi associated with fruit of cucumbers Basrah City Markets. Basrah J. Agri. Sci. 3(1990).
11. Nokhlan A.M. A study of some storage diseases of cucumber and grape caused by fungi Msc. thesis, College of Sci. Sulaimaniya Univ. (1979).
12. Ogawa, J.M., Manji B.T. and El-Behadli. Chemical control of post-harvest diseases proceeding of third international conference Kingston, Rhode Island 8/17-23 (1975).
13. Osnits Kaya. Benomyl against the disease of cucumber Review of plant pathology. 55: 963(1976).
14. Walker, J.G. Environment and host resistance in relation of cucumber sash phytopathology 40: 1094-1102 (1980).
15. Wasfy E.H. Study on certain diseases of cucurbits Ph.D. Thesis. Agric. Alex, Univ. (1967).

Isolation and Detection of *Clostridium* *Perfringens* and Study of its Physiological Characteristics and Sporulation with Comparison of the Sensory Quality of Beef

ZAID K. KAMOUNA AND HAMEED M. AL-OBAIDY

Department of Food and Science, College of Agriculture,
University of Baghdad, Baghdad, Iraq.

(Received Feb. 3, 2000; Accepted May 15, 2000)

الخلاصة

درست الخصائص الفسلجية والكيموحيوية لبكتريا *Clostridium perfringens* المعزولة محليا من عينات اخذت من التربة، وعند قياس القوة السمية وتحديد المجموعة المصلية التي تنتمي لها السلالة باستعمال ذيفانات سلالات قياسية تعود للانماط A و C و D، وجد ان للسلالة قوة سمية قدرت بحوالي (٤٠٠ ml/MLD) وانها تعود الى المجموعة المصلية A. وقدر النمو الخضري وتكوين الابواغ لسلالة *Cl. perfringens* المعزولة باستخدام لقاح يحوي 10×10^4 خلية خضرية/مل او غم في وسطين مختبريين هما Fluid Thioglycollate (FTG) و Modified Duncan Strong (MDS) فضلا عن وسط لحم الابقار المثلوم المعقم Autoclaved Ground Beef (AGB) المحضونة في الدرجات الحرارية ٣٧ و ٤٢ و ٤٧ م، وقد اظهر وسط AGB بانه الوسط الاكثر تشجيعا للبكتريا على النمو وهو الافضل لسرعة تحفيزه للخلايا الخضرية على تكوين الابواغ مقارنة مع الوسطين الآخرين، وسجل اسرع زمن جيل للبكتريا في الاوساط الثلاثة عند درجة ٤٢ م مما يؤكد ان هذه الدرجة هي الدرجة الحرارية المثلى لنمو البكتريا المعزولة حيث كان زمن الجيل المسجل في وسط AGB هو الاقصر وبلغ (٩,٩٢ دقيقة). وعند تلقيح وسط AGB بـ 10×10^4 خلية خضرية / غم من بكتريا *Cl. perfringens* وحضن في ٤٥ م لمدة ١,٥ ساعة، ثم في ٣٧ م ولحد ١٤ ساعة، لوحظ

Isolation and Detection of Clostridium Perfringens and Study of its Physiological Characteristics and Sporulation with Comparison of the Sensory Quality of Beef Z. K. Kamouna And Ham. M. Al-Obaidy

حصول نمو سريع للخلايا وصل الى 10×10^7 خلية خضرية / غم بعد ٦ ساعات من الحضان، وبقيت اعداد الخلايا ثابتة تقريبا خلال ١٤ ساعة من النمو، وكشف عن وجود عدد قليل من الابواغ (10×10^4) بوغ/غم بعد مرور ٤ ساعات، واستمر العدد بالزيادة ليصل الى (10×10^5) بوغ/غم خلال ١٤ ساعة من النمو. وعند تقويم النوعية الحسية (الرائحة واللون والنسيجية) اثناء نمو وتكوين الابواغ في وسط لحم البقر المثرور المعقم الملقح ببكتريا *Cl. perfringens* خلال فترات حضان مختلفة، حيث وجد ان كل من الرائحة واللون والنسيجية هي مقاييس جيدة جدا لتقويم لحم البقر الملوث ببكتريا *Cl. perfringens* وتبني انه في الوقت الذي يتم فيه تكوين ابواغ البكتريا فان لحم البقر المثرور المطبوخ يصبح غير مقبول حسيا.

ABSTRACT

The physiological and biochemical characteristics of *Clostridium perfringens* bacteria which isolated from samples collected from soil were studied. At measuring the minimal lethal dose and the seriological type of the isolated strain by using standard toxins which belongs to A, C, and D types, it appears that the isolated strain has 400 MLD/ml and it belongs to type A. The growth and sporulation of *Cl. perfringens* was examined in two laboratory media, fluid Thiglycollate (FTG) and Modified Duncan Strong Medium (MDS) in addition to Autoclaved Ground Beef (AGB) at 37, 42 and 47°C by use of 1.0×10^4 cell/ml or g as an initial inoculum. The most encouragement media was AGB for the bacterial growth and the sporulation. The shortest generation times that had recorded in the three media was at 42°C, which indicates that this temperature represent the optimum temperature for the growth of the isolated strain, and the generation time that had recorded in AGB medium was the shortest (9.92min.). When AGB medium was

inoculated with an inoculum 1.0×10^6 cell/g of *Cl. perfringens* and incubated at 45°C for 1.5 hr and at 37°C for up to 14hr, the vegetative cells counts rapidly reached 7.07×10^8 cell/g after 6 hrs of growth. Few numbers of spores (4.46×10^2 spore/g) were first detected at 4hrs, and the number continued to increase to 2.45×10^5 spore/g after 14 hrs of growth. The organoleptic quality (odor, color, and texture) during growth, sporulation of *Cl. Perfringens* cells was evaluated after different incubation periods. The results indicated that the odor, color, and texture are very good indicators of the evaluation of the ground beef which contaminated by *Cl. perfringens* and it has been appeared that the time that the cells are sporulate in ground beef, if will not be acceptable organoleptically.

INTRODUCTION

Clostridium perfringens is the micro aero-tolerant which is responsible of one of the most dispersion food poisoning in the world. It is commonly found in the soil, marine and fresh water sediments and in the intestinal tract of man and animal⁽¹⁾. It is gram-positive, non-motile, straight rod with oval subterminal spores when present.

The occurrence of *Cl. perfringens* food poisoning is associated is with cooked meat (frequently beef) that has remained at room temperature for several hours, or have been permitted to pass slowly through the temperature danger zone ($7.2-60^\circ\text{C}$) as a result of gradual heating or cooling⁽²⁾.

Many researches have been done on the relationship among growth, spore formation, and spoilage of food^(3,4,5).

The aim of this study was to evaluate the organoleptic quality (odor, color and texture) of cooked beef inoculated with *Cl. perfringens* during growth and sporulation.

MATERIALS AND METHODS

Culture

Isolates of *Cl. perfringens* were isolated from soil and spoiled ground beef, and maintained in Cooked Meat Medium (CMM) (Difco) at 4°C.

Biochemical Reactions

- Stormy Fermentation Test: This test was carried out in litmus milk as mentioned in (6).
- Lactose-Gelatin Medium Test: This test was carried out by stab method as mentioned in (6)
- Sulphate and Motility Test: Sulphate medium was inoculated by stab method and layer of liquid parafin was added and incubated anaerobically at 40°C for 24hrs.
- Starch Agar Test: Starch Medium was inoculated by streaking and incubated anaerobically at 40°C for (24-48)hrs, and then 1ugols Iodine was added as mentioned in (7).
- Lecithinase Test: This test was carried out in Egg Yolk Medium and incubated under anaerobic conditions as mentioned in (8).
- Catalase Test: This test was performed according to Collins and Lyne, 1989⁽⁹⁾.
- Hemolysis Test: Blood Agar and Glucose was incubated by streaking and incubated anaerobically at 40°C for 48hrs.

Typing of Isolated Strain

The minimal lethal dose and the toxin identification of the isolated strain were measured by using standard toxins which belongs to A, C and D types as carried by Alani (1997)⁽¹⁰⁾.

Autoclaved Ground Beef (AGB) Samples

Fresh beef were purchased from Department of Animal Production, College of Agriculture, and stored at -22°C until used. The meat was thawed at 4°C for 24hrs

prior to subsequent used. After thawing, skin, fats, and bones were removed from the meat, which was then grounded with the meat grinder. Fifty grams samples of the ground beef were weighed in 100-ml beakers and covered with double layers of aluminum foil. These samples were sterilized in autoclave at 121°C for 15 min and cooled to (45°C) before inoculation (30min).

Determination of Growth and Spores

The growth and sporulation of *Cl. perfringens* were examined in two laboratory media, Fluid Thioglycollate (FTG) and Modified Duncan Strong (MDS), in addition to Autoclaved Ground Beef (AGB) at 37, 42 and 47°C by use of 1.0×10^4 cell/ml or g of the medium as an initial inoculum.

Five mls portion of the AGB was heated at 75°C for 20 min to kill the vegetative cells and activate heat resistant spores⁽¹¹⁾. Vegetative cell counts were determined from unheated portions. From serial dilutions in peptone water, pour plates of Thioglycollate Agar Medium were prepared. The plates were incubated in anaerobic jars at 40°C for 24hrs. The black colonies were counted as *Cl. perfringens* cells, and number of cells per ml or gm was calculated by multiplying number of colonies (30-300) by dilution factor.

Generation Time Determination

Generation time of *Cl. perfringens* was calculated in FTG and MDS in addition to AGB as in the following⁽¹²⁾:

$$n = (\log N_1 - \log N_0) / 0.301$$

n: number of generation

N_0 : Initial number of cells

N_1 : Final number of cells

Mean Generation Time = t/n (t: time)

The Organoleptic Quality of AGB

AGB was inoculated with an inoculum of 1.0×10^6 cell/g of *Cl. perfringens* and incubated at 45°C for 1.5 hrs and at 37°C for up to 14 hrs. After the appropriate

Isolation and Detection of Clostridium Perfringens and Study of its Physiological Characteristics and Sporulation with Comparison of the Sensory Quality of Beef Z. K. Kamouna And Ham. M. Al-Obaidy
incubation periods, each meat sample was placed in a sterile polyethylene bag with sterile distilled water to give a 1:1 (w/v) slurry and macerated for 1 min with a Colowirth Stomacher 400.

The inoculated AGB medium was evaluated for odor, color and texture independently, after a given incubation period and/ compared with the autoclaved control samples incubated under the same conditions. The periods of incubation were 2,4,6,8,10,12 and 14 hrs.

Selection of the individuals for training as sensory panel members was done on the basis of their ability to detect known changes in the product through preliminary evaluation session. A 8-9 member of trained taste panel of graduate students in Food Science Department evaluated the AGB samples.

Evaluations were made in a sensory laboratory with partitioned booths and samples were coded with random numbers, so that the treatments were not identified⁽¹³⁾.

For odor determination, covered beakers containing AGB samples were served to the panelists at 50°C to develop the odor⁽¹⁴⁾. To eliminate the effect of color on the panelists, evaluations were made with out light.

Evaluations of color were made in a prtitioned booth under fluorescent lights, and the panelists were asked to evaluate the color of the AGB sample in the covered beakers without removing the cover to eliminate the effect of odor.

Evaluation of the texture of AGB samples were made without light in order to eliminate the effect of color by using a spatula, the panelists were asked to rate the texture of each sample.

The score sheet was prepared and used in the evaluation for each quality factor (odor, color and texture). Mean scores for each quality factor of each sample were calculated from scores of the individual panelists and subjected to analysis of variance. The 1% level of significance was selected for determination of significant

differences between the samples (inoculated beaker) and the controls (uninoculated beakers)⁽¹⁵⁾.

RESULTS AND DISCUSSION

Biochemical Test Results

All suspected *Cl. perfringens* colonies were subjected to the following biochemical tests after their cells were microscopically examined and gave G+ rods.

Litmus milk tubes which inoculated by the isolated strain of *Cl. perfringens* showed curd and the color of litmus was changed and the stormy fermentation was showed after 5hrs. The organism is distinctively characterized by its stormy fermentation of milk during which gas is evolved followed by coagulation of the casein by the acid formed⁽⁶⁾.

The color of lactose-gelatins was changed from red to yellow indicated that the isolated strain fermented lactose and produced acid. Also, the gelatin was liquified due to the gelatinase production⁽⁶⁾.

The isolated strain showed black line when motility sulfate medium was stabbed because of the production of hydrogen disulfide⁽¹⁶⁾.

When inoculated starch agar plate filled with Lugol's Iodine, it showed clear zone around the colonies as indication of Amylase production.

The isolated strain showed capability of fermentation of a number of mono and disaccharides tested (Cellobiose, Dextrose, Fructose, Galactose, Glucose, Inositol, Lactose, Maltose, Mannose, Raffinose, Salicine, Starch, Sucrose and Trehalose) but not fermenting (Xylose, Sorbitol, Rhamanose, Melibiose, Manitol, Esculin, and Arabinose). These results were coincided with those mentioned by Buchanan et al., 1974⁽¹⁷⁾.

The strain showed positive test for production of the Lecithinase enzyme when the egg yolk was inoculated. There were clear zones around the colonies. These results were coincided with that found by Oka et al., 1989⁽¹⁶⁾. It showed negative taste for catalase production.

Isolation and Detection of Clostridium Perfringens and Study of its Physiological Characteristics and Sporulation with Comparison of the Sensory Quality of Beef Z. K. Kamouna And Ham. M. Al-Obaidy

When Glucose-Blood Agar base was used for the bacteria isolation, the isolated strain showed capability of hemolysis of the human red blood cells.

Typing of the Isolated Strain

Toxic intensities for the A, C, and D standard strains of *Cl. perfringens* were 800, 3200 and 3200 MLD/ml respectively, while that for the isolated strain 400 MLD/ml as shown in table 1.

Table 1: Toxicity of the standard strains and the isolated strain to mouse

The strain	Incubated time (hrs)	Toxin without dilution	Dilution							
			1/5	1/10	1/20	1/40	1/80	1/160	1/320	1/640
The standard strain A	4	+++	+++	+++	+++	+++	++	-	-	-
The standard strain C	6	+++	+++	+++	+++	+++	+++	+++	++	-
The standard strain D	16	+++	+++	+++	+++	+++	+++	+++	+	-
The isolated strain	4	+++	+++	+++	+++	+	-	-	-	-

+ No. of dead mice

Growth and Spore Determinations in the Three Media

The three media used showed differences in the time that cells needed for the logarithmic phase, and the temperature was affected in the limitation of that time.

The results showed that 42°C was the optimum temperature for the growth of the bacteria in the three media. The logarithmic phase was 2hrs. At 37°C the log phase was 3hrs in the media AGB and MDS, while the medium FTG required 4hrs. At 47°C, the log phase was 3hrs in the medium AGB while it was 4hrs in the other two media.

The vegetative cell counts showed differences in the three media after 6hrs of incubation. The medium AGB had the most vegetative cell counts in the three temperatures compared to FTG and MDS. At 37°C, the counts were 1.77×10^8 CFU/g, 7.41×10^7 CFU/ml and 2.94×10^7 CFU/ml respectively. At 42°C, the counts were 7.94×10^8 CFU/g, 2.63×10^8 CFU/ml and 5.75×10^7 CFU/ml respectively, while at 47°C, the counts were 1.25×10^8 CFU/g, 1.0×10^8 CFU/ml and 3.71×10^7 CFU/ml respectively.

Few heat resistant spores were first detected (7.94×10^2 spores/g) after 5 hrs in the AGB medium, then the number continued to increased to 3.16×10^5 spores/g after 24hrs of incubation.

The results showed that the most encouragement medium was AGB for the bacterial growth and for the sporulation. These results were coincidences with the results of Craven, 1980⁽¹⁸⁾. Also, the results showed that the temperature 37°C was the optimum temperature for the spore production in the AGB and MDS media and that was the same as found by Labbe and Duncan, 1974⁽¹⁹⁾, Rey et al., 1975⁽²⁰⁾ and Craven et al, 1981⁽⁴⁾.

Generation Time Calculations

Table 2 showed the generation time of the isolated *Cl. perfringens* in AGB compared to MDS and FTG at all the temperatures applied. The generation time was 9.92 min at 42°C in AGB, while it was 15.34 min and 15.62 min at 37°C and 47°C, respectively. FTG medium comes second recording 12.59min while MDS medium comes third recording 14.09min at 42°C.

As conclusion, the AGB was the optimum medium for growth of *Cl. perfringens* which may be related to its nutritive contents encouraging the bacterial growth⁽²¹⁾ who found that the AGB was a better medium than FTG for the bacterial growth. Anderson et al., 1995⁽²²⁾ mentioned that the generation time for *Cl. perfringens* bacteria could reach to 8 minutes under the optimum conditions.

Table 2: Generation time of the isolated *Cl. perfringens* type A in three media incubated at different temperatures

Medium	Temperature (°C)	Generation Time (min)*
FTG	37	17.19
MDS	37	18.26
AGB	37	15.34
FTG	42	12.59
MDS	42	14.09
AGB	42	9.92
FTG	47	20.30
MDS	47	22.03
AGB	47	15.62

* Mean of four trials

Growth and Spore Determination in AGB

With an inoculum of 10^6 vegetative cells of the isolated *Cl. perfringens* per g of AGB, the vegetative cell counts rapidly reached mean 7.07×10^3 CFU/g after 6hrs of incubation (1.5hrs at 45°C and 4.5hrs at 37°C) (Table 3). After that, the total viable counts increased through 12hrs of growth (6.30×10^3 CFU/g) and then decreased slightly at 14hrs (2.82×10^3 CFU/g).

A few heat resistant spores (4.46×10^2 spores/g) were first detected at 4hrs and the number continued to increase to 2.45×10^5 spores/g after 14hrs of incubation (Table 3).

The times and the temperatures used in this study (preincubation at 45°C for 1.5hrs followed by incubation at 37°C) are similar to the temperature profile that may be expected in typical foodservice systems. That is a cooked meat product, upon cooling, passes through a temperature range ($40-49^\circ\text{C}$) that would allow rapid vegetative cell growth⁽²¹⁾, cooling to a temperature of around 37°C would then be optimum for sporulation and enterotoxin synthesis.

Table 3: Growth and Sporulation of the Isolated *Cl. perfringens* in AGB Inoculated at 45°C and 37°C (Inoculum of 10^6 CFU/g)

Time of Incubation (hrs)	Mean Vegetative Cells (\log_{10}/g)*	Mean Heat-Resistance Spores (\log_{10}/g)
2	6.26	<2.00
4	8.20	2.65
6	8.85	3.41
8	8.67	4.59
10	8.71	4.66
12	8.80	4.63
14	8.45	5.39

* Mean of four trials

The Organoleptic Quality Odor Evaluation

Figure 1 shows the comparison between mean odor determination scores for inoculated and uninoculated samples. The data for odor scores indicated that inoculated AGB samples with *Cl. perfringens* cells were significantly less desirable ($P < 0.01$) than uninoculated controls for all incubation periods starting from 2hrs of incubation (1.5 hrs at 45°C and 0.5hr at 37°C) until 14hrs of incubation. There were no significant differences in the scores between the samples and the control at 0 hr incubation.

The mean odor scores of inoculated AGB reached the highest value (4.55) which corresponded to a rating of slightly undesirable to undesirable (definite off odor) after incubation for 14 hrs. However, the panelists gave scores for the control between 2.17 and 2.58 (desirable to slightly desirable). This finding indicated that the odor is a good indicator for evaluation of AGB quality.

Isolation and Detection of Clostridium Perfringens and Study of its Physiological Characteristics and Sporulation with Comparison of the Sensory Quality of Beef Z. K. Kamouna And Ham. M. Al-Obaidy

Color Evaluation

Figure 2 shows the comparison between mean color determination scores for inoculated and uninoculated AGB samples. The data for color scores indicated that the panelists can identify the inoculated samples from the control starting after 2 hrs of incubation (1.5hrs at 45°C and 0.5hrs at 37°C) by its color only. The inoculated AGB samples were significantly different ($P<0.01$) from controls for all incubation periods. There were no significant differences in scores between the sample and the control at 0hr incubation.

While the controls received lower scores for all incubation periods which were between 1.55 and 2.0 (the color of cooked meat), the incubation samples started from 1.64 (the color of cooked meat), and the value jumped to 3.94 (slightly pink) after 14 hrs of incubation. This finding indicates that the color is a good indicator for evaluation of AGB quality.

Texture Evaluation

Figure 3 shows the comparison between mean texture determination scores for inoculated and uninoculated AGB samples. The data for texture scores indicated that the panelists can identify the inoculated samples from the control starting after 2 hrs of incubation (1.5hrs at 45°C and 0.5hr at 37°C) by rating the texture. The inoculated AGB samples were significantly different ($P<0.01$) from controls for all incubation periods. There were no significant differences in scores between the sample and the control at 0 hr incubation.

The controls received scores between 1.88 (firm) and 2.08 (moderately firm) and the samples received high scores starting from 2.05 (moderately firm) at 0hr of incubation to 4.50 (mushy) after 12hrs of incubation. This result showed that the texture is a reliable indicator for evaluation of AGB quality. These results are in agreement with the results obtained by Craven et al. (1981)⁽⁴⁾ and Al-Obaidy et al. (1985)⁽⁵⁾.

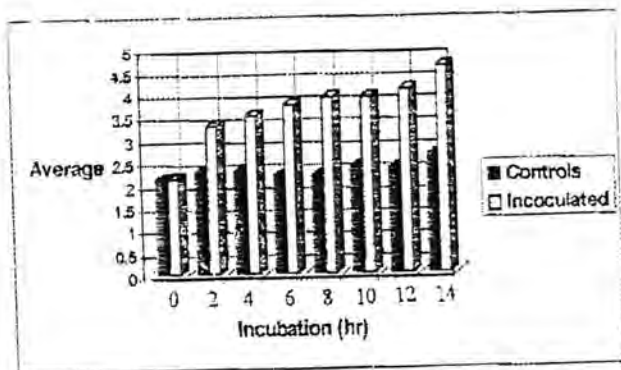


Fig.1. The histogram of the comparison between mean odor determination scores for inoculated and uninoculated samples by Clostridium perfringens bacteria

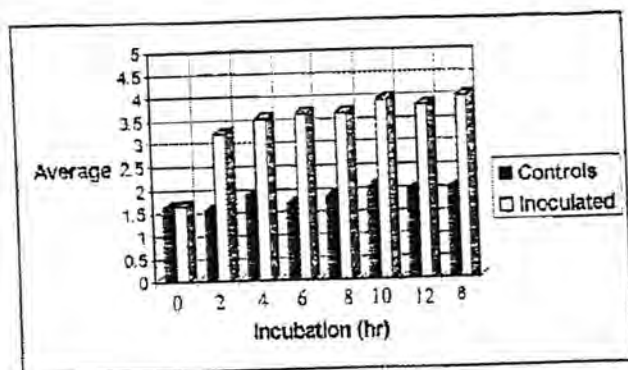


Fig.2. The histogram of the comparison between mean color determination scores for inoculated and uninoculated samples by Clostridium perfringens bacteria

Isolation and Detection of Clostridium Perfringens and Study of its Physiological Characteristics and Sporulation with Comparison of the Sensory Quality of Beef Z. K. Kamouna And Ham. M. Al-Obaidy

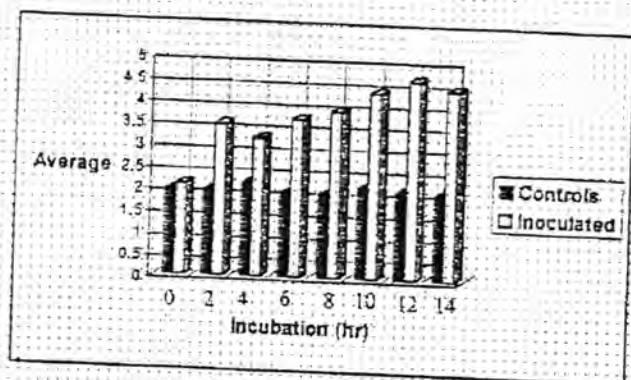


Fig 3 The histogram of the comparison between mean texture determination scores for inoculated and uninoculated samples by *Clostridium perfringens* bacteria.

REFERENCES

1. Taylor, A.W. and Gordon, W.S. A survey of the type of *Clostridium perfringens* present in soil and in intestinal contents of animal and man. J. Pathol. Bacteriol. 50: 271-277 (1940).
2. National Institute for the Food service Industry. Applied Food service sanitation. 2nd ed., Published by D.C. Health and Company, Chicago, Illinois (1978).
3. Hauschild, A.H.W. and Hilsheimer, R. Enumeration of foodborne *Clostridium perfringens* in egg yolk free tryptose sulfite cycloserine agar Appl. Microbiol., 27: 521-526 (1974).
4. Craven, S.E., Blankenshi, L.C. and McDonel, J.L. Relationship of sporulation, enterotoxin formation and spoilage during growth of *Clostridium perfringens* type A in cooked chicken. Appl. Environ. Microbiol. 41: 1184-1191 (1981).
5. Al-Obaidy, H.M., Khan, M.A., Blascheck, H.P. and Klein, B.P. Early detection of *Clostridium perfringens*

- enterotoxin and its relationship to sensory quality of cooked chicken. J. Food Safety. 7: 43-55 (1985).
6. Food and Drug Administration. Bacteriological Analytical Manual. (BAM), 7th ed. Assoc. Off. Anal. Chem., Washington, D.C. (1992).
 7. Harrigan, W.F. and McCance, E.M. Laboratory Methods Analytical in Food and Dairy Microbiology, 7th ed. Acad. Pr. (London) Ltd. (1987).
 8. Gillies, R.R. and Dadds, T.C. Clostridia, In Bacteriology Illustrate (3rd ed.), Longman Group Ltd. (1973).
 9. Collins, M. an Lyne, A. Microbiology Methods, 6th ed., London, Boston, Butterworth (1989).
 10. Alani, M.T.A. Isolation and concentration of *Clostridium perfringens* toxin, M.Sc. thesis, College of Veterinary Medicine, University of Baghdad (1997).
 11. Uemura, T. Incidence of enterotoxigenic *Clostridium perfringens* in healthy humans in relation to the enhancement of enterotoxins production by heat treatment. J. Appl. Bacteriol. 44: 411-419 (1978).
 12. Willardson, R., Busta, F. and Allen C. Growth of *Clostridium perfringens* in the different beef media and fluid thioglycollate medium at a static and constantly rising temperature. J. Food Protect. 42: 144-148 (1979).
 13. IFT Sensory Evaluation Division. Guidelines for preparation and review of papers reporting sensory evaluation data. Food Technol. 35: 16 (1981).
 14. Evans, C.D. Flavor evaluation of fats and oil. J. Amer. Oil Chem. Soc. 32: 596-604 (1955).
 15. Al-Sahoky, M. and Wahaib, K.M. Applications of Design and Analysis of Experiments. Al-Hikma Press, Baghdad (1990).
 16. Oka, S. Ando, Y. and Oishi, K. Distribution of enterotoxigenic *Clostridium perfringens* in water and soil in the southern part of Hokkaido Nippon Suissan Gakkaishi, 55(1) 71-78 (1989).
 17. Buchanan, R.E. and Gibbons, N.E. Bergey's Manual of Determinative Bacteriology, 8th ed. Williams and Wilkins, Baltimor. (1974).

Isolation and Detection of Clostridium Perfringens and Study of its Physiological Characteristics and Sporulation with Comparison of the Sensory Quality of Beef Z. K. Kamouna And Ham. M. Al-Obaidy

18. Craven, S.E. Growth and sporulation of *Clostridium perfringens* in foods, Food Technol., 34: 80-87 (1980).
19. Labbe, R. and Duncan, C.L. Sporulation and Enterotoxin production by *Clostridium perfringens* type A under conditions of control pH and temperature. Can. J. Microbiol. 20: 1493-1501 (1974).
20. Rey, C., Walker, H. and Rohrbach, P. The influence of temperature on growth, sporulation and heat resistance of spores of six strains of *Clostridium perfringens*. J. Milk and Food Technol. 38: 461. (1975).
21. Willardson, R., Busta, F. and Allen C. Growth and survival of *Clostridium perfringens* during constantly rising temperatures. J. Food Sci. 43: 470-475 (1978).
22. Anderson, A., Ronner, U. and Granum, P.E. What problems does the food industry have with the spore-forming pathogens *Bacillus cereus* and *Clostridium perfringens* Int. J. Food Microbiol. 28: 145-155 (1995).

Coherent States and the Classical Limit of the Hydrogen Atom

MOHAMMED A. Z. HABEEB*
ZIYAD A. ABDEL-KADER* AND
KHALID A. AHMAD**

* Department of Physics, College of Science, Baghdad University

**Department of Physics, College of Science, Al-Mustansiriya University

(Received Oct. 6, 1998; Accepted Jan. 24, 1999)

الخلاصة

تم سابقا بناء حالات متشابهة لذرة الهيدروجين بتحويل هذه المسألة الى مسألة متذبذب توافقي في اربعة ابعاد يخضع لشرط محدد. في العمل الحالي تم استعمال هذه الحالات المتشابهة لبحث مسألة الغاية الكلاسيكية لذرة الهيدروجين كمثال لمنظومة كمية. تمت البرهنة على ان هذه الغاية تقابل مجموعة احصائية محكومة بدالة احتمالية توزيع تخضع لمعادلة (ليوفيل) المعروفة في الميكانيك الاحصائي الكلاسيكي للمنظومات المحافظة. كما تمت دراسة العلاقة بين دالة احتمالية التوزيع هذه وتلك التي تم الحصول عليها لنفس المسألة على اساس فرضية "المجموعة الاحصائية المتجانسة". ان دراسة مسألة الغاية الكلاسيكية لذرة الهيدروجين في العمل الحالي باستخدام الحالات المتشابهة تعتبر مثالا اضافيا يسلط الضوء على مسألة طبيعة الغاية الكلاسيكية للمنظومات الكمية بشكل عام.

ABSTRACT

Coherent states for the H-atom problem were previously constructed by transforming this problem to that of a four-dimensional harmonic oscillator with a constraint. In the present work, these coherent states are utilized to investigate the classical limit of the H-atom as an example of a quantum system. It is shown that this limit corresponds to a statistical ensemble governed by a probability distribution

function(PDF), satisfying the well-known Liouville equation of classical statistical mechanics for conservative systems. The connection of this PDF with that obtained for the same problem from a "homogeneous ensemble" assumption, is also investigated. The investigation of the H-atom problem in the present work using coherent states represents an additional example that sheds light on the question of the nature of the classical limit of quantum systems in general.

INTRODUCTION

It is well-known that, essentially, quantization of a physical system starts from a classical model for such a system and relies upon a certain quantization procedure⁽¹⁾. However, quantization procedures are not unique and therefore, may not be equivalent, in the sense that the resulting quantum models obtained by applying different quantization procedures to a certain classical model may not be equivalent. For this reason, quantization ambiguities usually arise⁽¹⁾. Such ambiguities also surround the quantization of dissipative classical models⁽²⁾. This has led to increasing interest in the inverse problem to quantization, which is the problem of obtaining the classical limit of a certain quantum model⁽¹⁻⁸⁾. It is believed that such a limit may shed light on these ambiguities and uncover the nature of the classical limit of the quantum model concerned^(2,3,8).

Originally, coherent states for quantum systems were introduced in this spirit^(9,10). Later on, such coherent states were used to facilitate the approach to the classical limit of some quantum models^(2,7,8) and, hence, have helped to resolve some quantization ambiguities⁽²⁾. They have also been used to investigate the nature of the classical limit of certain quantum systems⁽⁷⁻⁹⁾. Their applications in other areas have also become widespread recently⁽¹⁰⁻¹³⁾.

As far as the last point mentioned above is concerned, investigations have relied on other approaches as well^(3,4-6). One of the most striking conclusions of these approaches is that: the classical limit of quantum mechanics

is always statistical in nature^(3,4-6) and may correspond to a PDF governed by the Liouville equation, well-known in the classical statistical mechanics of conservative systems⁽³⁾. However, the last conclusion, concerning the emergence of the Liouville equation in the classical limit, has been reached on the basis of simple quantum models, such as the simple harmonic oscillator(SHO)⁽³⁾. The investigation of the possibility of reaching the same conclusion on the basis of more complicated quantum models is, therefore, highly motivated.

In this spirit, the aim of the present work is to investigate this point for the H-atom as a model of a quantum system, which is more complicated than the SHO. Although conclusions of statistical nature have been reached for this system in a stationary state⁽⁵⁾, no Liouville equation has been recovered in the classical limit yet. It is expected that the approach used by Ajanapon⁽³⁾ for the SHO would be hindered by mathematical difficulties if applied directly to the H-atom problem. However, the construction of coherent states for the H-atom by Gerry⁽¹⁶⁾ motivates the utilization of these coherent states to investigate the problem of the classical limit for this system. These coherent states were obtained by utilization of the Kustaanheimo-Stiefel (KS) transformation⁽¹⁷⁾, long used in celestial mechanics for regularizing the Kepler problem⁽¹⁸⁾. The KS transformation is a surjection from the R^3 -space to the R^4 -space such that the Kepler problem and, hence, the H-atom problem appear as constrained four-dimensional (4D) oscillators evolving in a fictitious time⁽¹⁶⁾. It may also appear that the KS transformation would facilitate the approach to the classical limit of the H-atom along the lines of Ajanapon⁽³⁾. The details of this are outside the scope of the present work, which is devoted to the utilization of the coherent states constructed by Gerry⁽¹⁶⁾ to investigate the nature of the classical limit of the H-atom.

To this end, the rest of the paper is organized as follows. In Sec (2), a review of coherent states for the N-dimensional SHO quantum problem, and their utilization to

approach the classical limit for this problem via the P-representation⁽¹⁵⁾, is given. This is considered as a case study which lays the background for the latter discussion of the H-atom problem. Then, in Sec. (3) the KS transformation and its use to construct coherent states for the H-atom by Gerry⁽¹⁶⁾ are given along with some of the properties of these coherent states relevant to the present work. Sec. (4) is devoted to the main part of the present work, which utilizes the coherent states of Sec.(3) and some of their properties to approach the classical limit of the H-atom via the P-representation along the lines of Sec.(2). Finally, Sec.(5) gives a discussion and conclusions from which it appears that the Liouville equation again emerges in the classical limit of the H-atom and, therefore, this limit is statistical in nature.

Coherent States and the Classical Limit of the N-Dimensional SHO

A. Coherent States

Consider the N-dimensional isotropic SHO Hamiltonian.

$$\hat{H}_N = \sum_{k=1}^N \left(\frac{\hat{p}_k^2}{2m} + \frac{1}{2} m \omega^2 x_k^2 \right), \quad (1)$$

where ω is the oscillator frequency. Defining annihilation and creation operators by

$$\left. \begin{aligned} \hat{a}_k &= (2m\hbar\omega)^{-\frac{1}{2}} (m\omega x_k + i\hat{p}_k) \\ \hat{a}_k^+ &= (2m\hbar\omega)^{-\frac{1}{2}} (m\omega x_k - i\hat{p}_k) \end{aligned} \right\} \quad (2)$$

which satisfy the commutation relation $[\hat{a}_k, \hat{a}_{k'}^+] = \delta_{kk'}$, we may write \hat{H}_N of eq. (1) as

$$\hat{H}_N = \hbar\omega \sum_{k=1}^N \left(\hat{a}_k^+ \hat{a}_k + \frac{1}{2} \right) \quad (3)$$

For the one-dimensional case, $N=1$, a state manifesting the oscillatory character of the amplitude of the classical oscillator can be defined in various ways^(15,16). This state, denoted by $|\alpha\rangle$, is called a coherent state.

It can be shown that

$$|\alpha\rangle = \exp(-|\alpha|^2/2) \sum_{n=0}^{\infty} \frac{\alpha^n}{(n!)^{1/2}} |n\rangle, \quad (4)$$

where $|n\rangle$ is the conventional number state for the oscillator and $\alpha = \alpha^R + i\alpha^I$ is an arbitrary complex number. The coherent state, $|\alpha\rangle$, is an eigenfunction of \hat{a} with eigenvalue α or $\hat{a}|\alpha\rangle = \alpha|\alpha\rangle$.

The time dependent coherent state is given by

$$|\alpha; t\rangle = \exp(-iH_1 t/\hbar) |\alpha\rangle \\ = \exp(-i\omega t/2) |\alpha(t)\rangle \quad (5)$$

where H_1 is the one-dimensional oscillator Hamiltonian and the fact that $H_1|n\rangle = \hbar\omega(n+1/2)|n\rangle$ has been used. It can be shown that $\alpha(t)$ is given by^(15,16)

$$\alpha(t) = \alpha_0 e^{-i\omega t} \quad (6)$$

For the N-dimensional Hamiltonian H_N of eq (3), one may define an N-dimensional coherent state $|\{\alpha\}\rangle = |\alpha_1, \alpha_2, \dots, \alpha_N\rangle$. From the structure of eq. (3), it can be shown that

$$|\{\alpha\}\rangle = |\alpha_1\rangle |\alpha_2\rangle \dots |\alpha_N\rangle \quad (7)$$

The time dependent counterpart of $|\{\alpha\}\rangle$ can also be defined and it is given by

$$|\{\alpha\}; t\rangle = |\alpha_1; t\rangle |\alpha_2; t\rangle \dots |\alpha_N; t\rangle \quad (8)$$

where the $|\alpha_k\rangle$'s and $|\alpha_k; t\rangle$'s are given by eqs. (4) and (5), respectively. It can be shown that, as for the one-dimensional case^(15,16)

$$\langle\{\alpha\}; t|\{\alpha\}; t\rangle = \langle\{\alpha\}|\{\alpha\rangle = 1 \quad (9)$$

Using eqs. (3), (5), (7) and (8) we obtain

$$\langle\{\alpha\}; t|H_N|\{\alpha\}; t\rangle = \langle\{\alpha\}|H_N|\{\alpha\rangle = \hbar\omega \sum_{k=1}^N (\alpha_k^* \alpha_k + 1/2) \quad (10)$$

Also, since from eqs. (2) one may write

$$x_k = (\hbar/2m\omega)^{1/2} (\hat{a}_k + \hat{a}_k^\dagger), \quad (11a)$$

$$p_k = (m\hbar\omega/2)^{1/2} (1/i) (\hat{a}_k - \hat{a}_k^\dagger) \quad (11b)$$

then, from the fact that $\hat{a}|\alpha\rangle = \alpha|\alpha\rangle$ and using eqs. (5), (7) and (8) we obtain

$$\langle x_k \rangle = \langle\{\alpha\}; t|x_k|\{\alpha\}; t\rangle = (2\hbar/\omega)^{1/2} \alpha_k^R(t), \quad (12a)$$

$$\langle p_k \rangle = \langle \{ \alpha \} | p_k | \{ \alpha \} \rangle = (2\hbar/\omega)^{1/2} \alpha_k^i(t), \quad (12b)$$

where $\alpha_k^R(t)$ and $\alpha_k^I(t)$ are the real and imaginary parts of $\alpha_k(t)$, respectively.

Classical Limit Via the P-Representation

Glauber⁽¹⁵⁾ has defined what is called the P-representation for the density operator $\hat{\rho}$ of a system represented by a certain Hamiltonian for which coherent states are defined in the usual manner. For the system described by H_N of eq.(1), this definition is

$$\hat{\rho}_N = \int P_N(\{a\}; t) |\{a\}\rangle \langle \{a\}| \prod_{k=1}^N d^2 a \quad (13)$$

where $|\{a\}\rangle$ is the coherent state described by eqs.(4) and (7). To obtain the Heisenberg equation of motion for the density operator, one needs the commutators of $\hat{\rho}_N$ with \hat{a}_k and \hat{a}_k^\dagger . These are given by^(7,8)

$$\left. \begin{aligned} \hat{a}_k \hat{\rho}_N &= \int |\{a\}\rangle \langle \{a\}| a_k P_N(\{a\}; t) \prod_{k=1}^N d^2 a_k \\ \hat{a}_k^\dagger \hat{\rho}_N &= \int |\{a\}\rangle \langle \{a\}| (a_k^* - \frac{\partial}{\partial a_k}) P_N(\{a\}; t) \prod_{k=1}^N d^2 a_k \\ \hat{\rho}_N \hat{a}_k &= \int |\{a\}\rangle \langle \{a\}| (a_k - \frac{\partial}{\partial a_k^*}) P_N(\{a\}; t) \prod_{k=1}^N d^2 a_k \\ \hat{\rho}_N \hat{a}_k^\dagger &= \int |\{a\}\rangle \langle \{a\}| a_k^* P_N(\{a\}; t) \prod_{k=1}^N d^2 a_k \end{aligned} \right\} \quad (14)$$

It can be shown that the Heisenberg equation of motion for the density operator is then^(7,8)

$$\frac{\partial}{\partial t} P_N(\{a\}; t) = -i\omega \sum_k k = 1 \left[(a_k^* \frac{\partial}{\partial a_k^*} - a_k \frac{\partial}{\partial a_k}) P_N(\{a\}; t) \right] \quad (15)$$

The classical limit corresponds to $\hbar \rightarrow \{\infty\}$, such that $\{\hbar |a|^2\} \rightarrow \{\text{finite}\}$ ⁽¹⁵⁾.

In this limit, quantal correlations vanish and the expectation values $\langle \{ \alpha \} | x_k | \{ \alpha \} \rangle$ and $\langle \{ \alpha \} | p_k | \{ \alpha \} \rangle$; ($k=1, 2, \dots, N$) remain finite, as can be seen from eqs.(12).

These expectation values become the classical position coordinates x_k^{cl} and momenta p_k^{cl} ($k=1, 2, \dots, N$),

respectively (the superscript cl will be dropped from now on). We may also assume in this limit $P_N(\{\alpha\};t) \rightarrow p_N(\{x\},\{p\};t)$ giving the PDF in phase space. Using these ideas, together with eqs.(12), then eq.(15), after some length manipulations, becomes in this limit

$$\frac{\partial p_N(\{x\},\{p\};t)}{\partial t} = \sum_{k=1}^N \left[(m\omega^2 x_k) \frac{\partial p_N(\{x\},\{p\};t)}{\partial p_k} - \left(\frac{p_k}{m} \right) \frac{\partial p_N(\{x\},\{p\};t)}{\partial x_k} \right] \quad (16)$$

Observing from eq.(1) in its classical form that

$$\frac{\partial H_N}{\partial x_k} = m\omega^2 x_k \quad (17a)$$

$$\frac{\partial H_N}{\partial p_k} = \frac{p_k}{m} \quad (17b)$$

we can write eq.(16) in the form

$$\frac{\partial p_N(\{x\},\{p\};t)}{\partial t} = \sum_{k=1}^N \left[\left(\frac{\partial H_N}{\partial x_k} \right) \left(\frac{\partial p_N}{\partial p_k} \right) - \left(\frac{\partial H_N}{\partial p_k} \right) \left(\frac{\partial p_N}{\partial x_k} \right) \right] = -\{\rho_N, H_N\} \quad (18)$$

where $\{A,B\}$ stand for the Poisson bracket of the dynamical quantities A and B⁽¹⁹⁾.

Review of Coherent States for the H-Atom

The time-independent Schrödinger equation for the H-atom is

$$\left[-\frac{\hbar^2}{2\mu} \sum_{i=1}^3 \frac{\partial^2}{\partial x_i^2} - \frac{e^2}{r} \right] \psi = E\psi \quad (19)$$

where μ is the reduced mass, the x_i 's are Cartesian coordinates of the physical space and $r = (x_1^2 + x_2^2 + x_3^2)^{1/2}$. We now introduce a four-dimensional non-physical space R^4 via the KS transformation, which in terms of the variables u_1, u_2, u_3 and u_4 of R^4 is⁽¹⁶⁻¹⁸⁾

$$\left. \begin{aligned} x_1 &= 2(u_1 u_3 - u_2 u_4) \\ x_2 &= 2(u_1 u_4 + u_2 u_3) \\ x_3 &= u_1^2 + u_2^2 - u_3^2 - u_4^2 \end{aligned} \right\} \quad (20)$$

subject to the constraint

$$0 = u_2 du_1 - u_1 du_2 - u_4 du_3 + u_3 du_4 \quad (21)$$

It is easy to show that

$$R = u_1^2 + u_2^2 + u_3^2 + u_4^2 = u^2 \quad (22)$$

Hence, using eqs. (20), and (22) in eq.(19) we obtain

$$-\frac{\hbar^2}{2\mu} \left[\frac{1}{4} \sum_{j=1}^4 \frac{\partial^2}{\partial u_j^2} - \frac{1}{4r} X^2 \right] \psi - \frac{e^2}{r} \psi = E\psi \quad (23)$$

where

$$X = u_2 \frac{\partial}{\partial u_1} - u_1 \frac{\partial}{\partial u_2} - u_4 \frac{\partial}{\partial u_3} + u_3 \frac{\partial}{\partial u_4} \quad (24)$$

Imposing the constraint condition on ψ such that

$$X\psi = 0 \quad (25)$$

It can be shown that eq. (23) can be written as⁽¹⁶⁾

$$\left[-\frac{\hbar^2}{8\mu} \sum_{j=1}^4 \frac{\partial^2}{\partial u_j^2} - Eu^2 \right] \psi = e^2 \psi \quad (26)$$

where eq. (22) was used

Observing that for bound states of the H-atom, $E < 0$, eq. (26) may be cast in the form of a Schrödinger equation for a four-dimensional oscillator, or

$$\hat{H}_0 \psi = \epsilon \psi \quad (27)$$

Where

$$\hat{H}_0 = -\frac{\hbar^2}{2m} \sum_{j=1}^4 \frac{\partial^2}{\partial u_j^2} + \frac{1}{2} m \omega^2 u^2, \quad (28)$$

$$M = 4\mu, \omega = \left(-\frac{E}{2m}\right)^{1/2} \text{ and } \epsilon = e^2$$

If one now defines the momentum operators canonically conjugate to the u 's in the usual way as $p_i = -i\hbar (\partial/\partial u_i)$, so that

$$\hat{p}^2 = \sum_{j=1}^4 \hat{p}_j^2 = -\hbar^2 \sum_{j=1}^4 \frac{\partial^2}{\partial u_j^2} \quad (29)$$

then eq. (28) may be written in the form

$$\hat{H}_0 = \frac{\hat{p}^2}{2m} + \frac{1}{2} m \omega^2 u^2 \quad (30)$$

Coherent states for the problem represented by eq.(27) can now be introduced as a special case of those given in sec.(2) by considering the special case $N=4$ and taking the constraint condition of eq.(25) into account.

Hence, we first define a set of four annihilation and creation operators⁽¹⁶⁾

$$\left. \begin{aligned} \hat{a}_j &= \left(\frac{m\omega}{2\hbar} \right)^{1/2} u_j + (2m\omega\hbar)^{-1/2} \hat{p}_j \\ \hat{a}_j^+ &= \left(\frac{m\omega}{2\hbar} \right)^{1/2} u_j - (2m\omega\hbar)^{-1/2} \hat{p}_j \end{aligned} \right\} j=1,2,3,4 \quad (31)$$

where $[\hat{a}_j, \hat{a}_j^+] = \delta_{jj}$. Then, \hat{H}_0 of eq.(30) becomes

$$H_0 = \hbar\omega \sum_{j=1}^4 \left[\hat{a}_j^+ \hat{a}_j + \frac{1}{2} \right] \quad (32)$$

Obviously, \hat{H}_0 is a kind of pseudo-Hamiltonian and ε is its corresponding pseudo-energy. Therefore, the variable conjugate to H_0 is not the usual time t but rather a sort of fictitious time variable σ ⁽¹⁶⁾. Taking this into account, one may introduce the coherent states.

$|\{\alpha_j\}; \sigma\rangle = |\alpha_1, \alpha_2, \alpha_3, \alpha_4; \sigma\rangle = |\alpha_1; \sigma\rangle |\alpha_2; \sigma\rangle |\alpha_3; \sigma\rangle |\alpha_4; \sigma\rangle$ where $|\alpha_j; \sigma\rangle$, $j=1,2,3,4$ are one-dimensional oscillator coherent states propagating in the fictitious time $|\alpha_1; \sigma\rangle$ (see sec(2)). Observing that, as in sec.(2) from eqs. (31)

$$\left. \begin{aligned} u_j &= \left(\frac{\hbar}{2m\omega} \right)^{1/2} (\hat{a}_j + \hat{a}_j^+) \\ \hat{p}_j &= \left(\frac{m\hbar\omega}{2} \right)^{1/2} \left(\frac{1}{i} \right) (\hat{a}_j - \hat{a}_j^+) \end{aligned} \right\} j=1,2,3,4 \quad (33)$$

we obtain the analogs of eqs.(12) as

$$\langle u_j \rangle = \langle \{\alpha_j\}; \sigma | u_j | \{\alpha_j\}; \sigma \rangle = \left(\frac{2\hbar}{\omega} \right)^{1/2} a_j^R(\sigma), j=1,2,3,4 \quad (34a)$$

$$\langle p_j \rangle = \langle \{\alpha_j\}; \sigma | p_j | \{\alpha_j\}; \sigma \rangle = (2\hbar\omega)^{1/2} a_j^R(\sigma), j=1,2,3,4 \quad (34b)$$

setting $\langle p_j \rangle = m \frac{d \langle u_j \rangle}{d\sigma}$, it can be shown that⁽¹⁶⁾

$$\langle \ddot{u}_j \rangle + \omega^2 \langle u_j \rangle = 0, \quad (35)$$

where the dot indicates differentiation with respect to σ .

Equivalently⁽¹¹⁾

$$\ddot{a}_j + \omega^2 a_j = 0, \quad (36)$$

which shows that the parameters a_j are periodic in the fictitious time σ . Using these ideas, and taking account of the constraint condition, Gerry⁽¹⁶⁾ obtained a relation between physical time t and fictitious time σ in the form.

$$\frac{d\sigma}{dt} = \frac{1}{\langle \vec{r} \rangle} = \frac{1}{\langle u \rangle^2} \quad (37)$$

where

$$|\langle \vec{r} \rangle| = (\langle x_1 \rangle^2 + \langle x_2 \rangle^2 + \langle x_3 \rangle^2)^{1/2} = \langle u_1 \rangle^2 + \langle u_2 \rangle^2 + \langle u_3 \rangle^2 + \langle u_4 \rangle^2 = \langle u \rangle^2 \quad (38)$$

More details of the properties of the coherent states $|\{a\}; \sigma\rangle$ for the H-atom can be found in ref.⁽¹⁶⁾

Classical Limit of the H-Atom

Based on the presentation given in Sec.(3) it is now clear that with the aid of the KS transformation, the H-atom problem is equivalent to that of a four-dimensional SHO with a constraint. Coherent states for this problem were then defined accordingly as given in Sec.(3) and their properties are fully understood⁽¹⁶⁾. The approach to the classical limit of the H-atom can then be facilitated via the P-representation using these coherent states in analogy to what has been done for the N-dimensional oscillator in Sec.(2), considering $N=4$ and taking account of the constraint condition.

Considering the transformed H-atom problem as given by eq.(32) and the coherent states propagating in the fictitious time σ , one may write.

$$\frac{\partial P_H(\{a\}; \sigma)}{\partial \sigma} = i \left\{ \sum_{j=1}^4 \left[\omega \left(a_j^* \frac{\partial}{\partial a_j^*} - a_j \frac{\partial}{\partial a_j} \right) P_H(\{a\}; \sigma) \right] \right\} \quad (39)$$

This equation is a special case of eq.(15) for $N=4$ with t replaced by σ and subject to the definition $\{a\} = \{a_1 a_2 a_3 a_4\}$ and the constraint condition of Sec.(3).

A classical limit can now be defined as in Sec.(3) but in the R^4 -space. This corresponds to $\{h|\alpha\} \rightarrow \{\text{finite}\}$, $\langle \{\alpha\} | u_j \rangle \rightarrow u_j$, $\langle \{\alpha\} | p_j \rangle \rightarrow p_j$ and $P_H(\{a\}; \sigma)$. In analogy to the derivation of eq.(16), these ideas lead to the equation

governing $\rho_H(\{u\}, \{p\}; \sigma)$ which is the PDF in the $\{u\}-\{p\}$ phase space as

$$\frac{\partial \rho_H(\{u\}, \{p\}; \sigma)}{\partial \sigma} = \sum_{j=1}^4 \left[m\omega^2 u_j \frac{\partial \rho_H(\{u\}, \{p\}; \sigma)}{\partial p_j} - \left(\frac{p_j}{m} \right) \frac{\partial \rho_H(\{u\}, \{p\}; \sigma)}{\partial u_j} \right] \quad (40)$$

where $\{u\} = \{u_1, u_2, u_3, u_4\}$ and $\{p\} = \{p_1, p_2, p_3, p_4\}$. Now, from eqs.(20), their derivatives with respect to t , and with the aid of eq.(37), one may express the u_j and $p_j (j=1,2,3,4)$ in R^4 , as functions of the x_i and $p_i (i=1,2,3)$ in R^3 . Then,

$$\left(\frac{\partial}{\partial u_j} \right) = \sum_{i=1}^3 \left[\left(\frac{\partial x_i}{\partial u_j} \right) \left(\frac{\partial}{\partial x_i} \right) + \left(\frac{\partial p_i}{\partial u_j} \right) \left(\frac{\partial}{\partial p_i} \right) \right] \quad j=1,2,3,4 \quad (41a)$$

$$\left(\frac{\partial}{\partial p_j} \right) = \sum_{i=1}^3 \left[\left(\frac{\partial x_i}{\partial p_j} \right) \left(\frac{\partial}{\partial x_i} \right) + \left(\frac{\partial p_i}{\partial p_j} \right) \left(\frac{\partial}{\partial p_i} \right) \right] \quad (41b)$$

Using eqs. (41) in eq.(40) we obtain

$$\left(\frac{\partial \rho_H}{\partial \sigma} \right) = \sum_{i=1}^3 \left[I_i \left(\frac{\partial \rho_H}{\partial x_i} \right) + J_i \left(\frac{\partial \rho_H}{\partial p_i} \right) \right] \quad (42)$$

where

$$I_i = \sum_{j=1}^4 \left[(m\omega^2 u_j) \left(\frac{\partial x_i}{\partial p_j} \right) - \left(\frac{p_j}{m} \right) \left(\frac{\partial x_i}{\partial u_j} \right) \right] \quad (43a)$$

$$J_i = \sum_{j=1}^4 \left[(m\omega^2 u_j) \left(\frac{\partial p_i}{\partial p_j} \right) - \left(\frac{p_j}{m} \right) \left(\frac{\partial p_i}{\partial u_j} \right) \right] \quad (43b)$$

Also, we have from eq.(35) and the definition $\langle p_j \rangle = m \frac{d\langle u_j \rangle}{d\sigma}$

in the classical limit

$$\left. \begin{array}{l} P_j/m = u_j \\ m\omega^2 u_j = -p_j \end{array} \right\} \quad j=1,2,3,4 \quad (45)$$

Using eqs.(45) in eqs.(44) and considering, as before, the x_i and p_i as functions of the u_j and p_j , which are in turn functions of σ , we obtain

$$I_i = - \sum_{j=1}^4 \left[\left(\frac{\partial p_i}{\partial p_j} \right) \left(\frac{\partial p_j}{\partial \sigma} \right) + \left(\frac{\partial p_i}{\partial u_j} \right) \left(\frac{\partial u_j}{\partial \sigma} \right) \right] = - \left(\frac{\partial x_i}{\partial \sigma} \right) \quad (46)$$

and

$$J_i = -\sum_{j=1}^3 \left[\left(\frac{\partial p_i}{\partial p_j} \right) \left(\frac{\partial p_j}{\partial \sigma} \right) + \left(\frac{\partial p_i}{\partial u_j} \right) \left(\frac{\partial u_j}{\partial \sigma} \right) \right] = \left(\frac{\partial p_i}{\partial \sigma} \right) \quad (47)$$

With the help of eq.(37) in the classical limit, eqs.(46) and (47) may now be written in the form.

$$I_i = -\left(\frac{dx_i}{di} \right) \left(\frac{dt}{d\sigma} \right) = -u^2 \left(\frac{dx_i}{dt} \right) \quad (48)$$

and

$$J_i = -\left(\frac{dp_i}{dt} \right) \left(\frac{dt}{d\sigma} \right) = -u^2 \left(\frac{dp_i}{dt} \right) \quad (49)$$

But since⁽¹⁹⁾

$$\left. \begin{aligned} \left(\frac{dx_i}{dt} \right) &= \left(\frac{\partial H_H}{\partial x_i} \right) \\ \left(\frac{dp_i}{dt} \right) &= -\left(\frac{\partial H_H}{\partial x_i} \right) \end{aligned} \right\} i=1,2,3, \quad (50)$$

where H_H is the classical Hamiltonian for the H-atom,

$H_H = \sum_{i=1}^3 \frac{p_i^2}{2\mu} - \frac{e^2}{r}$, then eq.(24), with the aid of eqs.(48) and

(49), becomes

$$\left(\frac{\partial \rho_H}{\partial \sigma} \right) = -u^2 \sum_{i=1}^3 \left[\left(\frac{\partial H_H}{\partial p_i} \right) \left(\frac{\partial \rho_H}{\partial x_i} \right) - \left(\frac{\partial H_H}{\partial x_i} \right) \left(\frac{\partial \rho_H}{\partial p_i} \right) \right] \quad (51)$$

Remembering the definition of the Poisson bracket⁽¹⁹⁾, this equation may be written as

$$\frac{1}{u^2} \left(\frac{\partial \rho_H}{\partial \sigma} \right) = -\{\rho_H, H_H\} \quad (52)$$

which, with the aid of eq.(37), may be written as

$$\left(\frac{\partial \rho_H}{\partial t} \right) = -\{\rho_H, H_H\} \quad (53)$$

DISCUSSION AND CONCLUSIONS

The main result of the present work is embodied in eq. (53). It is first noticed that this equation is similar to that obtained for the N-dimensional SHO problem, i.e., eq.(18). In both cases, the PDF in the classical limit is seen to be governed by a Liouville equation, which is well-known in classical statistical mechanics⁽²⁰⁾. It should be recalled here, however, that for the special case of the one-dimensional SHO, a Liouville equation has already been obtained by Ajanapon⁽³⁾ using the Feynman path integral approach. As interpreted by Ajanapon⁽³⁾, the emergence of the Liouville equation in the present work signifies again that there is simply no deterministic classical limit of quantum mechanics. Rather, this classical limit is always statistical in nature and not as it is usually thought by some authors⁽¹⁹⁾. Although the result for the N-dimensional SHO problem could have been obtained by a generalization of the procedure followed in ref.(3), its appearance on the basis of coherent states in the present work adds independent support for the main point of view embodied here. However, the result obtained for the H-atom problem in the present work represents the main result which consolidates this point of view since it has not been obtained by other methods previously.

A link between the results obtained in the present work and those obtained by Qian and Huang⁽⁴⁻⁶⁾ can also be made here. It can be seen that in general for any classical PDF we have

$$\begin{aligned}
 \left(\frac{d\rho}{dt} \right) &= \left(\frac{\partial \rho}{\partial t} \right) + \sum_k \left[\left(\frac{\partial p_k}{\partial t} \right) \left(\frac{\partial \rho}{\partial p_k} \right) + \left(\frac{\partial q_k}{\partial t} \right) \left(\frac{\partial \rho}{\partial q_k} \right) \right] \\
 &= \left(\frac{\partial \rho}{\partial t} \right) + \sum_k \left[\left(\frac{\partial H}{\partial q_k} \right) \left(\frac{\partial \rho}{\partial p_k} \right) + \left(\frac{\partial H}{\partial p_k} \right) \left(\frac{\partial \rho}{\partial q_k} \right) \right] \\
 &= \left(\frac{\partial \rho}{\partial t} \right) + \{\rho, H\}
 \end{aligned} \tag{54}$$

where q_k and p_k are the generalized coordinates and their corresponding canonically conjugate momenta, respectively. Then if ρ satisfies a Liouville equation, as for the case of the N-dimensional oscillator or the H-atom, we have from eqs.(18), (53) and (54)

$$\frac{d\rho}{dt} = 0 \quad (55)$$

which implies that

$$\rho(t) = A = (\text{const.}) \quad (56)$$

This result can be contrasted with that obtained by Qian and Huang⁽⁴⁻⁶⁾ in the classical limit using a different approach. For the special case of the H-atom problem treated here, it can be seen that this result is again connected with the conservative nature of this system which leads to a PDF corresponding to a homogeneous ensemble in the classical limit.

In conclusion, we may say that the approach to the classical limit of the H-atom performed in the present work using the coherent states constructed by Gerry⁽¹⁶⁾ adds weight to the point of view that the classical limit of conservative systems is governed by a Liouville equation corresponding to a classical PDF. Finally, it may be considered that the present work represents a good example where the coherent states constructed by Gerry⁽¹⁶⁾ for the H-atom using the KS transformation have found application. This use of the KS transformation also motivates its utilization to study the classical limit of the H-atom using the Feynman path integral approach along the lines of Ajanapon⁽³⁾ for the one-dimensional SHO problem. This will be published elsewhere⁽²²⁾.

REFERENCES

1. Kovner, A. and Rosenstein, B., On quantization ambiguity, J. Phys. A: Math. Gen. 20, 2709 (1978).

2. Habeeb, M.A.Z., Fluid-dynamical interpretation of quantum damped oscillators, *J. Phys. A: Math. Gen.* 20: 5929 (1987).
3. Ajanapon, P., Classical limit of the path-integral formulation of quantum mechanics in terms of the density matrix, *Am. J. Phys.* 55: 159 (1987).
4. Qian, S.W. and Huang, X.Y., On the classical limit of the hydrogen atom wave function, *Phys. Lett. A* 115: 319 (1986).
5. _____, On the classical limit of the stationary state wave function, *Phys. Lett. A* 117: 166 (1986).
6. _____, On the classical limit of the quantum mechanical wave packet, *Phys. Lett. A* 121: 211 (1987).
7. Ghosh, G., Dutta-Roy, B. and Dy, M., On the single-particle Schrödinger fluid, *J. Phys. G: Nucl. Phys.* 3: 1077 (1977).
8. Habeeb, M.A.Z., Coherent states for the cranked harmonic oscillator, *J. Phys. G: Nucl. Phys.* 13: 651 (1987).
9. Arefe'va, I.Y., Parthasarathy, R., Viswanathan, K.S., and Volovich, I.V., Coherent states, dynamics and semiclassical limit on quantum groups, *Mod. Phys. Lett. A* 9: 689 (1994).
10. Huttner, B., Imoto, N., Gisin, N. and Mor, T., Quantum cryptography with coherent states, *Phys. Rev. A* 51: 1863 (1995).
11. Jansky, J., Domokos, P., Szabo, S. and Adam, P., Quantum-state engineering via discrete coherent-state superpositions, *Phys. Rev. A* 51: 4191 (1995).
12. Vieiran, V.R. and Sacramato, P.D., Quantum Monte Carlo algorithms using coherent states, *Physica A* 207: 584 (1994).
13. Matacz, A.L., Coherent state representation of quantum fluctuations in the early universe, *Phys. Rev. D* 49: 788 (1994).
14. Schrödinger, E., Der stetige ubergang von der mikro-zur makromechanik, *Naturwiss.* 14: 664 (1926).

15. Glauber, R.J., Coherent and incoherent states of the radiation field, *Phys. Rev.* 131: 2766 (1963).
16. Gerry, C.C., Coherent states and the Kepler-Coulomb problem, *Phys. Rev.* A33: 6 (1986).
17. Kustaanheimo, P. and Stiefel, E., Perturbation theory of Kepler motion based on spinor regularization, *J. Rein. Angew. Math.* 218: 204 (1965).
18. Stiefel, E.L. and Scheifele, G., "Linear and regular Celestial Mechanics" Springer, Berlin (1971).
19. Goldstein, H., "Classical Mechanics" Addison-Wesley, Reading, Massachusetts, (1980) p.252.
20. Toda, M., Kubo, R. and Saito, N., "Statistical Physics I, Springer series in solid-state science" Springer, Berlin (1995) Vol. 30.
21. Hepp, K., Classical limit for the Q-M correlation-function, *Commun. Math. Phys.* 35: 265 (1974).
22. Habeeb, M.A.Z., Abdel-Kader, Z. Kh. A. and Ahmed, K. A., Classical limit of the path integral formulation of the H-atom, (1998) (to be published).

The $SL(3,R)$ Group and Harmonic Oscillator with Variable Damping

MOHAMMED A. Z. HABEED AND

ZIYAD KH. A. ABDEL-KADER

Department of Physics, College of Science, Baghdad
University

(Received June 1, 1998; Accepted Sept. 30, 1998)

الخلاصة

تمت البرهنة في البحث الحالي على ان التحليل المستند الى نظرية الزمر لمسألة المتذبذب التوافقي ذو الاضمحلال الثابت γ_0 قابل للتعميم لمجموعة من المتذبذبات ذات الاضمحلال المتغير مع الزمن على ان يخضع معامل الاضمحلال المتغير مع الزمن $\gamma(t)$ للشرط (ثابت = $\frac{1}{2} \frac{d\gamma(t)}{dt} + \frac{1}{4} \gamma^2(t)$). وعلى هذا الاساس فقد وجد ان زمرة التناظر لمعادلة الحركة هي الزمرة $SL(3,R)$ وان زمرة التناظر للفعل هي عبارة عن زمر جزئية ذات خمسة بارامترات بينما تكون زمرة التماس لنفس الحالة عبارة عن زمرة (لي) ذات عدد لا متناه من البارامترات. بمعنى اخو ان جميع النتائج المستحصلة سابقا لمسألة المتذبذب التوافقي ذو الاضمحلال الثابت γ_0 تبقى صحيحة في حالة الاضمحلال المتغير مع الزمن تحت الشرط اعلاه لمعامل الاضمحلال $\gamma(t)$.

ABSTRACT

Symmetry group-theoretical analysis for the problem of the harmonic oscillator with constant damping coefficient γ_0 is shown to be still valid for a wider class of oscillators with variable damping coefficient $\gamma(t)$ subject to the condition $(\frac{1}{2} \frac{d\gamma(t)}{dt} + \frac{1}{4} \gamma^2(t) = \text{const.})$. It is found that the point symmetry group for the equation of motion is $SL(3,R)$, and for the action is a five-parameter subgroup, whereas the contact group is an infinite parameter Lie group as for the special case of constant damping.

INTRODUCTION

There has been considerable body of literature devoted to the determination of dynamical symmetries and constants of the motion of classical and quantum particle systems. An example of this is the work of Cervero' and Villarroel⁽¹⁾ on the harmonic oscillator with constant damping term. These authors have found that the global group of point transformations which leave the equation of motion of this system invariant is $SL(3,R)$. They also found that the point symmetry group for the action is a five parameter subgroup of $SL(3,R)$ with five corresponding conserved quantities, only two of which are independent⁽¹⁾. Furthermore, from the same work it turned out that the contact symmetry group for the same problem is an infinite parameter Lie group.

One of the main interests of such kind of work is related to the interpretation problem of dissipation in damped quantum systems. This problem has been dealt with by many authors using different approaches⁽²⁻⁵⁾. The essential conclusion of these approaches is that the main features of the quantum-mechanical problem corresponding to this system are rather those of a simple stationary oscillator with renormalized constant frequency that cannot be at all interpreted as a "dissipative" quantum system as has been claimed by some other authors. Besides, the generalization of the argument of Cervero' and Villarroel⁽¹⁾, as attempted by Habib and Abdel-Kader⁽⁴⁾ and the application of the "homogeneous ensemble" idea by the same authors⁽⁵⁾, have shown the existence of a wider class of harmonic oscillators with variable damping coefficient $\gamma(t)$, satisfying the condition $(\frac{1}{2} \frac{d\gamma(t)}{dt} + \frac{1}{4} \gamma^2(t) = \text{const.})$, which is quantum-mechanically conservative rather than dissipative. This situation has motivated the present work which attempts to investigate whether the work of Cervero' and Villarroel⁽¹⁾ is generalizable to this wider class of oscillators. This is considered to be the first step of the application of the group-theoretical approach to the

interpretation of the problem of dissipation in the harmonic oscillator with variable damping, which will be published elsewhere. Another motivation for the present work is that the group-theoretical analysis of the problem of the harmonic oscillator with variable damping is interesting in its own right to complete previous work on dynamical symmetries^(1,6-10).

To this end, the rest of the paper is organized as follows. In Sec.(2), the complete symmetry group for the problem under consideration is dealt with and in Sec.(3) the point symmetry group for the action is determined together with the constants of the motion. Sec.(4) is devoted to the subject of contact transformations. Finally, Sec. (5) ends up with a discussion and conclusions. Throughout, close analogies with the method applied by Cervero' and Villarroel⁽¹⁾ will be followed.

The Complete Symmetry Group

Consider the system described by the Bateman Lagrangian⁽¹¹⁻¹³⁾

$$L = \frac{1}{2} m_0 e^{\Gamma(t)} (\dot{x}^2 - \omega_0^2 x^2) \quad (1)$$

In terms of the dimensionless variable $\tau = \omega_0 t$, the equation of motion

$$\ddot{x} + \gamma(t) \dot{x} + \omega_0^2 x = 0 \quad (2)$$

Becomes

$$\ddot{x} + \bar{\gamma}(\tau) \dot{x} + x = 0; \quad \left(x \equiv \frac{dx}{d\tau} \right) \quad (3)$$

where $\bar{\gamma}(\tau) = \gamma(\tau)/\omega_0$.

To find the group of transformations that leave the differential eq.(3) invariant, we use the method of Lie^(1,6,14). Defining the general form of the generator of the transformation by⁽⁶⁾

$$\hat{G} = \zeta(x, \tau) (\partial/\partial \tau) + \eta(x, \tau) (\partial/\partial x) \quad (4)$$

we end up with the following set of coupled differential equations:

$$\left. \begin{aligned} \zeta_{xx} &= 0, \\ 2\bar{\gamma}\zeta_x - 2\zeta_{xt} + \eta_{xx} &= 0, \\ \gamma\zeta - \zeta_{tt} + 2\eta_{xt} + 3\zeta_{xx} + \bar{\gamma}\zeta_t &= 0 \\ \text{and } 2\zeta_{tx} - \eta_{xx} + \eta_{tt} + \gamma\eta_t + \eta &= 0 \end{aligned} \right\} \quad (5)$$

After some lengthy manipulations, it can be shown that if the condition

$$\frac{1}{2} \frac{d\gamma(t)}{dt} + \frac{1}{4} \gamma^2(t) = \text{const.} = \delta^2, \quad (6)$$

is satisfied, then the solution of eqs.(5) possesses eight free parameters. Calling these parameters A_1, A_2, \dots, A_8 , the solution becomes^(1,6)

$$\zeta(x, \tau) = A_1 \sinh(\bar{\omega} \tau) + A_2 \cosh(2\bar{\omega} \tau) + A_5 + [A_7 \sinh(\bar{\omega} \tau)] e^{1/2\tau(t)} x \quad (7)$$

$$\eta(x, \tau) = [(\bar{\omega} A_1 - 1/2 \gamma(\tau) A_2) \sinh(2\bar{\omega} \tau) + (\bar{\omega} A_2 - 1/2 \gamma(\tau) A_1) \cosh(2\bar{\omega} \tau)] x + [A_3 \cosh(\bar{\omega} \tau) + A_4 \sinh(\bar{\omega} \tau)] e^{1/2\tau(t)} + A_6 x + [\bar{\omega} A_7 - 1/2 \gamma(\tau) A_8] \cosh(\bar{\omega} \tau) + (\bar{\omega} A_8 - 1/2 \gamma(\tau) A_7) \sinh(\bar{\omega} \tau) e^{1/2\tau(t)} x^2, \quad (8)$$

where,

$$\bar{\omega} = (\omega_0^2 - \delta^2)^{1/2} / \omega_0 \quad (9)$$

With the eight parameter set of solutions of eqs.(7) and (8), we can construct eight linearly independent group generators using eq.(4), as

$$G_1 = (1/\bar{\omega}) [\sinh(2\bar{\omega} \tau) (\partial/\partial \tau) - (\bar{\omega} \cosh(2\bar{\omega} \tau) - 1/2 \gamma(\tau) \sinh(2\bar{\omega} \tau)) x (\partial/\partial x)]$$

$$G_2 = (i/\bar{\omega}) [\cosh(2\bar{\omega} \tau) (\partial/\partial \tau) - (\bar{\omega} \sinh(2\bar{\omega} \tau) - 1/2 \gamma(\tau) \cosh(2\bar{\omega} \tau)) x (\partial/\partial x)]$$

$$G_3 = (i/\bar{\omega}) e^{1/2\tau(t)} \cosh(\bar{\omega} \tau) (\partial/\partial x)$$

$$G_4 = (1/\bar{\omega}) e^{1/2\tau(t)} \sinh(\bar{\omega} \tau) (\partial/\partial x)$$

$$G_5 = (i/\bar{\omega}) (\partial/\partial \tau - 1/2 \gamma(\tau) x \partial/\partial x)$$

$$G_6 = x (\partial/\partial x)$$

$$G_7 = -ie^{1/2\tau(t)} [x \sinh(\bar{\omega} \tau) (\partial/\partial \tau) + (\bar{\omega} \cosh(\bar{\omega} \tau) - 1/2 \gamma(\tau) \sinh(\bar{\omega} \tau)) x^2 (\partial/\partial x)]$$

and

$$G_8 = e^{1/2\tau(t)} [x \cosh(\bar{\omega} t) (\partial/\partial t) + (\bar{\omega} \sinh(\bar{\omega} t) - 1/2\gamma(\tau) \cosh(\bar{\omega} \tau)) x^2 (\partial/\partial x)] \quad (10)$$

In the limit $\delta(t) = \gamma_0 = \text{const.}$, the generators given by eq.(10) go over into those found by Cervero' and Villarroel⁽¹⁾. It can also be shown easily that the generators of eq.(10), subject to the condition of eq.(6) have the same commutation relations as those of formulae (24) and (25) of Lutzky⁽⁷⁾, and formulae (10) and (11) of Cervero' and Villarroel⁽¹⁾. Hence, they generate the Lie algebra of the group $SL(3, \mathbf{R})$ as in those two special cases.

Point Symmetry Group for the Action

To determine the generators of the point symmetry group that leave the action corresponding to the Lagrangian of eq.(1) invariant and their corresponding conserved quantities, we shall apply the well-known Noether theorem^(1,7,15). If the generator is given by eq.(4) then the corresponding conserved quantity is given as

$$\Phi = (\zeta(x, \tau)x - \eta(x, \tau)) \partial L / \partial x - \zeta(x, \tau)L + f \quad (11)$$

where f is a function of x and τ . Then, Noether's method applied to the Lagrangian of eq.(1) leads to the four coupled differential equations

$$\zeta_x = 0, \quad 1/2\gamma(\tau)\zeta - 1/2\zeta_t + \eta_x = 0,$$

$$\eta_\tau - (f_x/m_0)e^{-\Gamma(\tau)} = 0,$$

and

$$((f_t/m_0)\omega_0^2) + 1/2 \gamma(t)x^2 \zeta + \eta_x + 1/2\zeta_\tau x^2 = 0 \quad (12)$$

After some length manipulations, it can be shown that if the condition of eq.(6) is satisfied, then eqs.(12) admit the five parameter set of solutions

$$\zeta(x, \tau) = [B_1 \cosh(2\omega\tau) + B_2 \sinh(2\omega\tau)] + B_5, \quad (13a)$$

$$\eta(x, \tau) = [(\omega B_1 - (\gamma/2)B_2) \sinh(2\omega\tau) + (\omega B_2 - (\gamma/2)B_1) \cosh(2\omega\tau)x + [B_3 \cosh(\omega\tau) + B_4 \sinh(\omega\tau)]e^{-1/2\Gamma(\tau)}]x \quad (13b)$$

and

$$f(x, \tau) = [\cosh(2\bar{\omega} \tau)(m_0 \bar{\omega}^2 B_1 - (1/2)m_0(\gamma/2)B_1 - m_0(\gamma/2)B_2) + \sinh(2\bar{\omega} \tau)(m_0 \bar{\omega} B_2 - (1/2)m_0(\gamma/2)B_2 - m_0(\gamma/2)B_1) - (1/2)m_0(\gamma/2)B_5]x^2 + e^{-1/2\Gamma(t)} [\cosh(\bar{\omega} \tau)(-m_0(\gamma/2)B_3 + \bar{\omega} B_4) + \sinh(\bar{\omega} \tau)(-m_0(\gamma/2)B_4 + \bar{\omega} B_3)]x \quad (13c)$$

where B_1, B_2, \dots, B_5 are arbitrary integration constants. Hence, by eq.(4), one has five generators leaving the action invariant, which are exactly G_1, G_2, \dots, G_5 of eqs.(10). The corresponding conserved quantities then follow from eq.(11) and (13) as

$$I_1 = e^{\Gamma(\tau)} \{ (x^2 + \dot{x}^2) \sinh(2\bar{\omega}\tau) - 2x\dot{x}(\bar{\omega} \cosh(2\bar{\omega}\tau) - (\gamma/2) \sinh(2\bar{\omega}\tau)) - 2x^2[(\bar{\omega}^2 - \gamma/4) \sinh(2\bar{\omega}\tau) - \bar{\omega}(\gamma/2) \cosh(2\bar{\omega}\tau)] \},$$

$$I_2 = e^{\Gamma(\tau)} \{ (x^2 + \dot{x}^2) \cosh(2\bar{\omega}\tau) - 2x\dot{x}(\bar{\omega} \sinh(2\bar{\omega}\tau) - (\gamma/2) \cosh(2\bar{\omega}\tau)) - 2x^2[(\bar{\omega}^2 - \gamma/4) \cosh(2\bar{\omega}\tau) - \bar{\omega}(\gamma/2) \sinh(2\bar{\omega}\tau)] \},$$

$$I_3 = e^{1/2\Gamma(\tau)-\omega t} \{ x + (\gamma/2 - \bar{\omega})x \},$$

$$I_4 = e^{1/2\Gamma(\tau)-\omega t} \{ x + (\gamma/2 + \bar{\omega})x \},$$

And

$$I_5 = e^{\Gamma(\tau)} \{ x^2 + (1 - \gamma/2)x^2 + \gamma x\dot{x} \} \quad (14)$$

As in the constant damping case studied by Cervero' and Villarroel⁽¹⁾, it is easy to show that

$$I_1 = 1/2(I_3^2 - I_4^2),$$

$$I_2 = 1/2(I_3^2 + I_4^2),$$

And

$$I_5 = I_3 I_4 \quad (15)$$

Hence, again there are only two independent constants of the motion. As expected, the constants of the motion of eqs.(14) reduce to those of eqs.(19) of Cervero' and Villarroel⁽¹⁾ for the case $\gamma(\tau) = \text{const}$. We also observe that time translation is not a symmetry of the action for the class of harmonic oscillators with variable damping defined by eq.(6).

Contact Transformations

The interest in the determination of contact transformations for differential equations has increased in recent years. Some of the applications of these contact transformations are also known (see, for example, refs(16,17)). The original technique was first developed by Lie⁽¹⁴⁾ and then by Campbell⁽¹⁸⁾. For the undamped harmonic oscillator the contact group has already been found by Schwarz⁽¹⁹⁾ and turned out to be an infinite

parameter Lie group. For the harmonic oscillator with constant damping coefficient the contact group has also been found by Martini and Kersten⁽²⁰⁾ using the method of mapping among differential equations. It has been indicated by Cervero' and Villarroel⁽¹⁾ that this method is unnecessary and cumbersome compared with their direct application of Lie's original method following the steps of Schwarz⁽¹⁹⁾ with some differences. It turned out that the contact Lie group, as for the undamped case, again has an infinite number of parameters.

In this section we shall show that present problem of the harmonic oscillator with variable damping coefficient, subject to condition of eq. (6), also admits an infinite parameter contact group. Our method is a direct extension of that of Cervero' and Villarroel⁽¹⁾ guided by the results of the previous sections. Therefore, our starting point is to assume the infinitesimal contact transformation operator⁽¹⁾

$$S_c = (\partial W / \partial p)(\partial / \partial \tau) + (p \partial W / \partial p - W)(\partial / \partial x) - (\partial W / \partial \tau + p \partial W / \partial x)(\partial / \partial p) - (\partial^2 W / \partial \tau^2 + 2p \partial^2 W / \partial \tau \partial x + p^2 \partial^2 W / \partial x^2 + \partial x^2 + 2q \partial^2 W / \partial x \partial p + q^2 \partial^2 W / \partial p^2 + q \partial W / \partial x)(\partial / \partial q) \quad (16)$$

where $p = \dot{x}$, $q = \ddot{x}$ and $W = W(x, p)$ is the characteristic generating function of the contact transformation. Then, applying eq. (16) to eq. (2), we obtain

$$S_c(q + \gamma(\tau)p + x) = 0 \quad (17)$$

This yields a partial differential equation for W of the form:

$$\partial^2 W / \partial \tau^2 + p^2 \partial^2 W / \partial x^2 + (\gamma(\tau)p + x)^2 \partial^2 W / \partial p^2 + 2p \partial^2 W / \partial x \partial \tau - 2(\gamma(\tau)p + x) \partial^2 W / \partial p \partial \tau - 2(\gamma(\tau)p + x)p \partial^2 W / \partial x \partial p + Wp(1 + \gamma(\tau)) \partial W / \partial p - x \partial W / \partial x + \gamma(\tau) \partial W / \partial \tau = 0 \quad (18)$$

We also observe that the u and v variables, defining the characteristic curves of Cervero' and Villarroel⁽¹⁾, are in fact their constants of the motion I_3 and I_4 (cf., Schwarz⁽¹⁹⁾). Therefore, we expect the characteristic curves of our hyperbolic-type eq. (18) to be determined by our I_3 and I_4 of eqs. (14), or

$$\begin{aligned} u &= e^{1/2r(t) + \omega t} \{x(1/2 \gamma(\tau) - \bar{\omega}) + p\} \\ v &= e^{1/2r(t) - \omega t} \{x(1/2 \gamma(\tau) - \bar{\omega}) + p\} \end{aligned} \quad (19)$$

Using (u, v, τ) as new coordinates, eq.(18) is transformed into

$$\partial^2 W / \partial t^2 + \gamma(\tau) \partial W / \partial \tau + W = 0 \quad (20)$$

where the condition of eq.(6) has been used. It can be shown that, subject to eq.(6), eq.(20) has the general solution

$$W = e^{1/2\gamma(\tau)} \{ \Delta_1(u, v) e^{\omega t} + \Delta_2(u, v) e^{-\omega t} \} \quad (21)$$

Where Δ_1 and Δ_2 are two arbitrary functions of u and v . It follows that, as for the constant damping case, W depends upon arbitrary functions and, hence, the contact Lie group has an infinite number of parameters. Using eqs.(16) and (21), the general form of the operator S_c becomes

$$S_c = \{ (\partial \Delta_1 / \partial u) e^{2\omega t} + (\partial \Delta_2 / \partial v) e^{-2\omega t} + (\partial \Delta_2 / \partial u) + (\partial \Delta_1 / \partial v) \} (\partial / \partial t) \\ + \{ p [(\partial \Delta_1 / \partial u) e^{2\omega t} + (\partial \Delta_2 / \partial v) e^{-2\omega t} + (\partial \Delta_2 / \partial u) + (\partial \Delta_1 / \partial v)] \\ - (\Delta_1 e^{\omega t} + \Delta_2 e^{-\omega t}) e^{-(1/2)\gamma(\tau)} \} (\partial / \partial x) + \{ (1/2\gamma(\tau) - \omega) \Delta_1 e^{2\omega t} \\ + (1/2\gamma(\tau) + \omega) \Delta_2 e^{-2\omega t} + (\partial \Delta_1 / \partial v) \} (\partial / \partial p) \quad (22)$$

It can be shown that specific choices for Δ_1 and Δ_2 similar to those given by Cervero' and Villarroel⁽¹⁾ for the constant damping case reproduce the point Lie group already discussed in sec.(2), or

	G_1	G_2	G_3	G_4	G_5	G_6	G_7	G_8
Δ_1	$\frac{1}{2\omega} u$	$\frac{i}{2\omega} u$	$-\frac{i}{2\omega}$	$\frac{1}{2\omega}$	$\frac{i}{2\omega} v$	$-\frac{1}{2\omega} v$	$\frac{1}{4\omega} (uv-v)^2$	$\frac{i}{4\omega} (uv+v)^2$
Δ_2	$-\frac{1}{2\omega} u$	$\frac{i}{2\omega} v$	$-\frac{i}{2\omega}$	$-\frac{1}{2\omega}$	$\frac{i}{2\omega} u$	$-\frac{1}{2\omega} u$	$\frac{1}{4\omega} (uv-v)^2$	$-\frac{i}{4\omega} (uv+v)^2$

DISCUSSION AND CONCLUSIONS

The study of dynamical symmetries and constants of the motion for classical and quantum particle problems has extended the number of systems for which the symmetry is known and has also enlarged the known symmetries for particular systems. As a result of such investigations, there has been an increase in the number of systems for which the complete symmetry group is known.

The work of Cervero' and Villarroel⁽¹⁾ has shown that the harmonic oscillator with constant damping coefficient possesses the group $SL(3, R)$ as its complete symmetry group. Since this kind of oscillator has many

applications as a model in widely separated fields such as nuclear physics⁽²¹⁾, quantum optics⁽²²⁻²⁴⁾ and plasma physics⁽²⁵⁻²⁷⁾ among others, the group-theoretical results gain a special kind of importance when dealing with interpretation problems of models of quantum dissipative systems.

Following the line of work of Cervero' and Villarroel⁽¹⁾, and assuming the condition $(\frac{1}{2} \frac{d\gamma(t)}{dt} + \frac{1}{4} \gamma^2(t) = \text{const.})$ obtained from earlier work^(4,5), we have been able in the present work to show that all the group-theoretical results obtained for the harmonic oscillator with constant damping coefficient are extendible to the variable damping case. In particular, it can be concluded that the class of systems, which has $SL(3, \mathbf{R})$ as its complete symmetry group, is now enlarged to include those variable damping oscillators whose damping coefficient $\gamma(t)$ satisfies the condition $((\frac{1}{2} \frac{d\gamma(t)}{dt} + \frac{1}{4} \gamma^2(t) = \text{const.})$, of which there are special cases that have been used in actual applications^(23,28-30).

The results obtained here also motivate the extension of the line of reasoning used by Cervero' and Villarroel⁽³¹⁾ to study the quantum mechanics of the harmonic oscillator with variable damping coefficient and the question of interpretation in this quantum model of dissipation. This will be published elsewhere⁽³²⁾.

REFERENCES

1. Cervero', J.M. and Villarroel, J., $SL(3, \mathbf{R})$ realizations and the damped harmonic oscillator, J.Phys. A.: Math. Gen. 17:1777(1984).
2. Habeeb, M.A.Z., Fluid-dynamical interpretation of quantum damped oscillators, J.Phys.A: Math. Gen. 20: 5929(1987).
3. Habeeb, M.A.Z. and Abdel-Kader, Z.Kh.A., Classical limit of the path integral formulation of a quantum damped harmonic oscillator, Submitted for publication

- The $SL(3,R)$ Group and Harmonic Oscillator with Variable Damping*
M. A. Z. Habeeb And Z. Kh. A. Abdel-Kader
 in Ibn Al-Haitham J. of Pure and Applied Science(1998).
4. Habeeb, M.A.Z. and Abdel-Kader, Z.Kh.A., On energy dissipation in the quantum oscillator with variable mass, Accepted for publication in Al-Mustansiriya J. of Science(1998).
 5. Habeeb, M.A.Z. and Abdel-Kader, Z.Kh.A., Classical limit of the damped harmonic oscillator wave function, Accepted for publication in Al-Mustansiriya J. of Science(1998).
 6. Wulfman C.E. and Wybourne, B.G., Lie groups of Newton's and Lagrange's equations for the harmonic-oscillator, J.Phys.A: Math Gen. 9:507(1976).
 7. Lutzky, M., Symmetry group and conserved quantities for the harmonic oscillator, J. Phys. A:Math Gen. 11:249(1978).
 8. Leach, P.G., Complete symmetry group of the one-dimensional time-dependent harmonic-oscillator, J. Phys. A: Math. Gen. 21:300 (1980).
 9. Leach, P.G., $SL(3,R)$ and the repulsive oscillator, J. Phys. A: Math. Gen. 13:1991 (1980).
 10. Prince, G.E. and Eleizer, C.J., Symmetries of the time-dependent N-dimensional oscillator, J. Phys. A: Math. Gen. 13: 815(1980).
 11. Bateman, H., On dissipative systems and related variational principles, Phys. Rev. 38: 815(1931).
 12. Dodonov, V.V., and Man'ko V.I., Coherent states and the resonance of a quantum damped oscillator, Phys. Rev. A20: 550(1979).
 13. Abdalla, M.S. and Colegrave, R.K., A model for a modulated damping or growth of a harmonic oscillator in classical or quantum mechanics, Lett. Nuovo Cimento 39: 373(1984).
 14. Lie, S., "Geometric der Beruehrungstrans formationen", Chelsea, New York(1977).
 15. Noether, E., Nacher. Ges. Wiss. Gottingen, 235: 57 (1918), as cited by reference⁽⁷⁾

- 16.Boya, L.J. and Cervero', J.M., Contact transformations and conformal group II. Relativistic theory, *Int. J. Theor. Phys.* 12:47 (1975).
17. _____, Contact transformations and conformal group III. Nonrelativistic theory, *Int. J. Theor. Phys.* 12:55 (1975).
- 18.Cervero', J.M., Contact transformations and conformal group III. Finite non-relativistic transformations, *Int. J. Theor. Phys.* 16:333 (1977).
19. _____, Contact transformations and conformal group IV. Contraction of contact Lie algebras, *Int. J. theor. Phys.* 16: 339(1977).
- 20.Campbell, J.E., "Introductory Treatise of Lie's Theory of Finite Continuous Transformations", Chelsea, New York (1966).
- 21.Schwarz, F., Contact symmetries of the harmonic-oscillator, *J. Phys. A: math Gen.* 16: L133 (1983).
- 22.Martini, R. and Kersten, P.H.M., Contact symmetries of general linear 2nd-order ordinary differential-equations, *J. Phys. A: Math Gen.* 16: L455 (1983).
- 23.Kan, K. and Griffin, J., Quantized friction and the correspondence principle, *Phys. Lett.* B50: 241 (1974).
- 24.Colegrave, R.K. and Abdalla, M.S., A canonical description of the Fabry-Perot cavity, *Opt. Acta* 28: 495(1981).
25. _____, Field fluctuation in a Fabry-Perot cavity in resonance with a reservoir of 2-level atoms: 1. Adiabatic fluctuations, *Opt. Acta* 30: 489 (1983) and _____, Field fluctuation in a Fabry-Perot cavity in resonance with a reservoir of 2-level atoms: 2. Non-adiabatic periodic fluctuations, *Opt. Acta* 30: 861(1983).
- 26.Ligare, M. and Becker, S., Simple soluble models of quantum damping applied to cavity electrodynamics, *Am. J. Phys.* 63: 788(1995).
- 27.Ben-Aryeh, Y. and Mann, A., Squeezed states and the interaction of electromagnetic waves with plasma, *Phys. Rev.* A32: 552 (1985).

28. _____, Production of squeezed states in the interaction between electromagnetic-radiation and an electron-gas, Phys. Rev. Lett. 54: 1020 (1985).
29. Sagan, D., On the physics of Landau damping, Am. J. Phys. 62: 450 (1994).
30. Ray, J.R., Lagrangians and systems they describe-how not to treat dissipation I quantum mechanics, Am. J. Phys. 47: 626 (1979).
31. Negro, F. and Tartaglia, A., Quantization of motion in a velocity-dependent field: the v^2 case, Phys., Rev. A23: 1591 (1984).
32. Negro, F. and Tartaglia, A., The quantization of quadratic friction, Phys. Lett. A77: 1 (1980).
33. Cervero', J.M. and Villarroel, J., On the quantum theory of the damped harmonic oscillator, J. Phys. A: Math Gen. 17: 2963 (1984).
34. Habib, M.A.Z. and Abdel-Kader, Z.Kh.A., On the quantum mechanics of the harmonic oscillator with variable damping, (to be published).

Comparison Between Normal Metal, Low and High Temperature Suprconductors

D.N. Rouf*, W.A. Latif,** and K.A. Ahmed**

* Department of Applied Science, Technology University

** Department of Physics College of Science, Al-Mustansiriyah University

(Recieved Oct. 6, 1998 ; Accepted May 16 1999)

الخلاصة

العمل يعرض حساب المعلومات المتعددة والمؤثرة على تصغير خطوط النقل الدقيقة من مادة $YBa_2Cu_3O_7$ فائقة التوصيل في درجات الحرارة العالية لصفحة بعرض 1 مايكرون وطبقة عازلة تمتد من - 0.2 (200 مايكرون. النتائج قورنت مع النحاس في درجة حرارة الغرفة Nb في 4.2k، وذلك باستخدام نظرية ماتي - ياردين. بينت النتائج ان مادة $YBa_2Cu_3O_7$ فائقة التوصيل في الحرارة العالية تمتلك شقوق على النحاس ومقارب بالخصائص الى Nb في درجات الحرارة الواطنة مع الميزة بكونه يعمل في حوالي 100k وهذا يختزل تعقيدات التقنية بشكل فعال.

ABSTRACT

This work presents calculations of the various parameters affecting the miniaturization of the high temperature superconducting $Ba_2Cu_3O_7$ microstrip line, for strip width of $1\mu m$ and dielectric layer ranging from $200\mu m$ - $0.2\mu m$. These results are compared with Cu at room temperature and Nb at $4.2k^{[1]}$, using Mattis-Bardeen Theory. The results show that the high temperature superconductor $Ba_2Cu_3O_7$ is superior to Cu and has close characteristics to Nb at low temperature, but with an advantage of being operated at $\sim 100k$ which reduces the technical complications drastically.

INTRODUCTION

Low temperature superconductors have been thoroughly studied theoretically and experimentally and extensively used in industry ever since the superconductivity was first discovered by Onnes in 1911. Since the discovery of new ceramic materials that become superconductors at more than 77k^[1] a huge publication appeared in literature concerning both the study and application of high temperature superconductors.

In this paper we present a detail calculations comparing the properties of three example conductors ; Cu at room temperature, Nb at 4.2k^[2], and Ba₂Cu₃O₇ at 77k examining the attenuation, dipersion, and characterisitic impedance of microstrip lines as a function of frequency and dielectric thickness to find out the benfits and limitation of such industrial materials. Also a simulation of the pulse transmission is used to evaluate the utility of the example strip lines for high speed digital applications. The microstrip line geometry to be considered is shown in figure 1. To simplify the calculation, only the transverse electromagnetic (TEM) mode is considered and the strip line width w is taken to be much greater than the dielectric thickness, s , so that fringing fields can be neglected. These assumptions eliminate dispersion associated with the discontinuity in dielectric constant at the air / dielectric interface, which is an important source of dispersion for w comparable or less than s ^[3].

Under the above assumptions the properties of a strip line follow almost immediately once the surface impedance of the conductor is calculated.

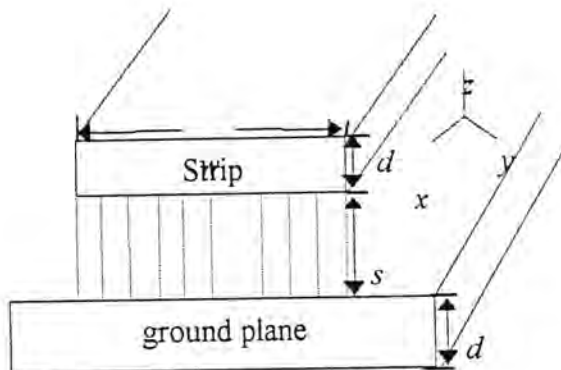


Fig. 1 Strip line geometry in cross - section

Surface Impedance

Since the mean free path ℓ_m for the normal electrons is short compared to all other dimensions in the problem, a local equation for the current density J and the electric field E is applicable.

$$J = \sigma E \quad (2.1)$$

where σ is complex conductivity. The surface impedance, for an infinite conducting slab of thickness d and a boundary condition that the magnetic field is zero at the surface of the strip line i.e. at $z = d$, is given by^[11]:

$$Z_s = (i\omega\mu_0 / \sigma)^{1/2} \coth [(i\omega\mu_0\sigma)^{1/2}d] \quad (2.2)$$

where it is assumed that $\mu = \mu_0$, the permeability of free space, which is true for most metals. Where the real part of Z_s , called the surface resistance, accounts for the system losses and the imaginary part, called the surface reactance, contributes to the system inductance. For copper σ is a real constant, while for superconductors σ is a complex,

frequency dependent quantity. The two-fluid model has been used to characterize superconductors at low frequencies^[4], but the Mattis-bardeen Theory^[5] was found to be essential for frequencies approaching the energy-gap frequency^[6].

For normal metals, the classical skin depth δ_c is applicable

$$\delta_c = \sqrt{\frac{2}{\omega \mu_0 \sigma}} \quad (2.3)$$

Since δ_c decreases with increasing frequency there exists a frequency above which $\delta_c < \ell_m$ and a local relation between J and E can no longer be assumed. For superconductors, the decay length into the conductor at frequencies less than the gap frequency is the penetration length λ ^[2].

$$\lambda = [\hbar \coth (\Delta/2k_B T) / \pi \mu \Delta \sigma_n]^{1/2} \quad (2.4)$$

which, in contrast to δ_c , is frequency independent.

The material parameters of copper, niobium and $Ba_2Cu_3O_7$ are presented in table 1. The parameters for copper are taken Kautz^[2], those for niobium are based on the thin-film measurements of Henkels and Kircher^[7], while those for $Ba_2Cu_3O_7$ are as follows; the normal conductivity σ_n is based on the measurements of Heise et al.^[8], the gap parameter Δ and the transition temperature T_c are based on the measurements of Van Benthum et al.^[9], and the mean free path ℓ_m is based on the measurements of Hagen et al.^[10].

Table 1 Material parameters

material	Cu	Bn	$Ba_2Cu_3O_7$
$T_c(K)$	---	9.2	92.0
$\Delta(meV)$	---	1.48	14.27
$\sigma_n (\Omega m)^{-1}$	$\sigma = 5.88 \times 10^7$	1.59×10^7	6.25×10^5
$\lambda(0) (m)$	---	8.6×10^{-8}	1.5×10^{-7}
ℓ_m	3.82×10^{-9}	1.1×10^{-8}	0.67×10^{-8}

At frequencies less than 3×10^{12} Hz, the mean free path ℓ_m is much shorter than the conductor thickness, at such frequencies the surface impedance of copper at 295K is given by equation (2.2), above this frequency $\delta_c < \ell_m$ and the skin effect is anomalous. At frequencies less than 4×10^9 Hz, $\delta_c \gg d$ and equation (2.2) reduces to

$$Z_s = \frac{1}{\sigma d} + \frac{i}{3} \omega \mu_0 d \quad \delta_c \gg d \gg \ell_m \quad (2.5)$$

at higher frequencies, δ_c becomes small compared to d and equation (2.2) reduces to

$$Z_s = (1 + i) \sqrt{\frac{\omega \mu_0}{2\sigma}} \quad d \gg \delta_c \gg \ell_m \quad (2.6)$$

For a conductor thickness of $d = \ell \mu\text{m}$, the real and imaginary parts of the surface impedance of the three example materials are shown in figure 2. The surface resistance of the superconductors, at frequencies below the gap frequency, is many orders of magnitude smaller than that of normal metal. For $\text{Ba}_2\text{Cu}_3\text{O}_7$ the surface resistance and reactance are double that of Nb. In a strip line the smaller surface resistance resulting in lower attenuation. Also the surface reactance below the gap frequency varies as ω , making it appear exactly as an inductance. this property gives a strip line with a very low dispersion. Above the gap frequency, a superconductor behaves like a normal metal with conductivity $\sigma_n^{[2]}$.

Propagation Constant and Characteristic Impedance

The propagation constant γ and the characteristic impedance Z_0 of a strip line can be expressed, in terms of the series impedance Z and the shunt admittance Y of a unit length of line, as

$$\gamma = \sqrt{ZY} \quad (3.1)$$

$$Z_0 = \sqrt{Z/Y} \quad (3.2)$$

where, for $w \gg s$, Z and Y are, in turn

$$Z = i\omega\mu_0 \frac{s}{w} + \frac{2}{w} Z_s \quad (3.3)$$

$$Y = i\omega\epsilon\epsilon_0 \frac{w}{s} \quad (3.4)$$

Where w is the stripline width the first term of Z is the inductive impedance associated with the magnetic field in the dielectric region and the second term accounts for penetration of fields into the conductor. Y is the capacitive admittance between the strip and the ground plane. The power attenuation in decibels per length α_{dB} and the phase velocity v_ϕ can be obtained directly from the real and imaginary parts of the propagation constant. then,

$$\alpha_{dB} = C_{dB} \alpha \quad (3.5)$$

$$v_\phi = \frac{\omega}{\beta} \quad (3.6)$$

where α , β are the real and imaginary parts of the propagation constant, respectively, and $C_{dB} = 20 \log e$, and e is the base of the natural logarithm.

The phase vlocity, attenuation, and characteristic impedance of a room temperature copper strip line are obtained by reviewing approximate expressions for γ and Z_0 applicable in the following limits^[2] for ascending order of frequency.

(I) For

$$\delta_s \gg d, \sqrt{sd}$$

$$v_{\phi} = \sqrt{\frac{\omega s d \sigma}{s d \sigma}} \left[1 - \frac{d^2}{3\delta_c^2} - \frac{s d}{2\delta_c^2} \right]$$

$$\alpha_{dB} = C_{dB} \sqrt{\frac{\omega \epsilon \epsilon_0}{s d \sigma}} \left[1 - \frac{d^2}{3\delta_c^2} - \frac{s d}{2\delta_c^2} \right]$$

$$Z_0 = \frac{1}{w} \sqrt{\frac{s}{\omega \epsilon \epsilon_0 \sigma d}} \left\{ \left[1 + \frac{d^2}{3\delta_c^2} + \frac{s d}{2\delta_c^2} \right] - i \left[1 - \frac{d}{3s} - \frac{s d}{2\delta_c^2} \right] \right\}$$

(II) for

$$d \ll \delta_c \ll \sqrt{s d}$$

$$v_{\phi} = \frac{1}{\sqrt{\mu_0 \epsilon \epsilon_0}} \left[1 - \frac{d}{3s} - \frac{\delta_c^4}{8s^2 d^2} \right]$$

$$\alpha_{dB} = \frac{C_{dB}}{\sigma s d} \sqrt{\frac{\epsilon \epsilon_0}{\mu_0}} \left[1 - \frac{d}{3s} - \frac{4d^4}{45\delta_c^4} \right]$$

$$Z_0 = \frac{s}{w} \sqrt{\frac{\mu_0}{\epsilon \epsilon_0}} \left\{ \left[1 + \frac{d}{3s} + \frac{\delta_c^4}{8s^2 d^2} \right] - i \frac{\delta_c^2}{2s d} \left[1 - \frac{d}{3s} + \frac{4d^4}{45\delta_c^4} \right] \right\}$$

(III) for

$$\delta_c \ll s, d$$

$$v_{\phi} = \frac{1}{\sqrt{\mu_0 \epsilon \epsilon_0}} \left[1 - \frac{\delta_c}{2s} \right]$$

$$\alpha_{dB} = \frac{C_{dB}}{s} \sqrt{\frac{\omega \epsilon \epsilon_0}{2\sigma}} \left[1 - \frac{\delta_c}{2s} \right]$$

$$Z_0 = \frac{s}{w} \sqrt{\frac{\mu_0}{\epsilon \epsilon_0}} \left\{ \left[1 + \frac{\delta_c}{2s} \right] - i \frac{\delta_c}{2s} \left[1 - \frac{\delta_c}{2s} \right] \right\}$$

For the parameters of a superconducting strip line, the following approximations are applicable for frequencies less than the gap frequencies (7.2×10^{11} Hz for Nb and 6.9×10^{12} Hz for $\text{Ba}_2\text{Cu}_3\text{O}_7$);

$$v_{\phi} = \frac{1}{\sqrt{\mu_0 \epsilon_0}} \left(1 + \frac{2\lambda}{s} \coth \frac{d}{\lambda} \right)^{-1/2}$$

$$\alpha_{\text{dB}} = C_{\text{dB}} \mu_0^{3/2} \lambda^3 \frac{\sigma_1 \omega^2}{2s} \left[\frac{\epsilon_0}{1 + \frac{2\lambda}{s} \coth \frac{d}{\lambda}} \right]^{1/2} \left(\coth \frac{d}{\lambda} + \frac{d/\lambda}{\sinh^2(d/\lambda)} \right)$$

$$Z_0 = \frac{s}{w} \sqrt{\frac{\mu_0}{\epsilon_0}} \left(1 + \frac{2\lambda}{s} \coth \frac{d}{\lambda} \right)^{1/2}$$

Graphs for the phase velocity, attenuation and the real and imaginary of characteristic impedance, as a function of frequency, of the three example strip lines with conductor thickness $d = 1 \mu\text{m}$, and dielectric thickness, s , ranging from $200 \mu\text{m}$ to $0.2 \mu\text{m}$, are shown in figures (3), (4), (5), and (6) respectively. In these calculations the dielectric constant ϵ is assumed to be 4. The various parameters affected by the frequency and dielectric thickness can be described as follows :

A. Phase Velocity : In the lowest frequency range v_{ϕ} for vopper is proportional to $\sqrt{\omega}$ and goes to zero at zero frequency. However, if we consider the phase shift that results because of the velocity of the low frequency being less than the high frequency asymptotic velocity, then for a fixed length of line l this shift.

$$\Delta\phi = \omega l \left(\frac{1}{v_{\phi}(\omega)} - \frac{1}{v_{\phi}(\infty)} \right)$$

also goes to zero at zero frequency as $\sqrt{\omega}$, thus, dispersion at low frequencies is not the problem that figure 3 suggests. At somewhat higher frequencies limit II applies, in which v_{ϕ} approaches the asymptotic value $(1 - d/2s) / \sqrt{\mu_0 \epsilon_0}$ with a correction term proportional to $\ell \omega^2$. As δ_c becomes less than d as well as s , limit III applies and v_{ϕ} approaches $1/$

$\sqrt{\mu_0 \epsilon \epsilon_0}$ with a correction term of $\delta_0/2s$. Because this term varies as $1/\sqrt{\omega}$, $\Delta\phi$ varies as $\sqrt{\omega}$ and dispersion effects increase with ω just as at very low frequencies. Also, a thin dielectric enhances dispersion since the correction term is proportional to $1/s$.

v_ϕ , for Nb and $\text{Ba}_2\text{Cu}_3\text{O}_7$, is independent of frequency since λ_s , as opposed to δ_s , is frequency independent. Thus, as s decreases v_ϕ also decreases. This decrease is slightly greater in case of $\text{Ba}_2\text{Cu}_3\text{O}_7$ than in Nb for dielectric thickness $2\text{ }\mu\text{m}$ and $0.2\text{ }\mu\text{m}$.

B. Attenuation: α_{dB} , for copper, increases as $\sqrt{\omega}$ at very low and high frequencies with a frequency plateau in between as shown in figure 4. As a function of dielectric thickness, the attenuation always increases with decreasing s either as $1/\sqrt{s}$ or as $1/s$. For the superconducting strip lines, since σ_1 , the real part of the conductivity

$$\frac{\sigma_1}{\sigma_n} = \frac{2\Delta}{k_B T} \frac{\exp(\Delta/k_B T)}{[1 - \exp(\Delta/k_B T)]^2} \ln(\Delta/h\omega)$$

only weakly depends on frequency (by the natural logarithm factor), hence, α_{dB} is nearly proportional to ω^2 as a function of the dielectric thickness, the attenuation is proportional to $1/s$.

C. The Characteristic impedance: For copper, in the limit of low frequencies the real and imaginary parts of Z_0 both diverge as $1/\sqrt{\omega}$. The significance of this divergence relates to the reduction of the transmission line to a simple resistor at low frequencies. In the limit II the real of Z_0 approaches its high asymptote, $\sqrt{\mu_0 \epsilon \epsilon_0} s/w$, and the imaginary part goes to zero. The correction term to the real part is $\delta_0/2s$ so that the dielectric thickness directly

influences the ability to match impedance over a wide range of frequencies. Z_0 like v_s changes with s but remains frequency independent. The imaginary part of Z_0 is negligible.

IV Pulse Propagation

In this section we consider the propagation of a Gaussian pulse over a strip line of length l using the circuit shown in figure 7. The source impedance Z_s is matched to the asymptotic high frequency value of Z_0 in the case of normal state strip line

$$Z_s = \frac{s}{w} \sqrt{\frac{\mu_0}{\epsilon \epsilon_0}} \quad (4.1)$$

and in the superconducting case is matched to the low frequency impedance

$$Z_s = \frac{s}{w} \sqrt{\frac{\mu_0}{\epsilon \epsilon_0}} \left(1 + \frac{2\lambda}{s} \coth \frac{d}{\lambda} \right)^{1/2} \quad \omega \ll \frac{2\Delta}{h} \quad (4.2)$$

The degree to which a voltage pulse V_s is reproduced across the load is affected both by γ , in the dispersion and attenuation of the line, and by Z_0 , in reflection at the interface between the line and the source or load due to imperfect impedance.

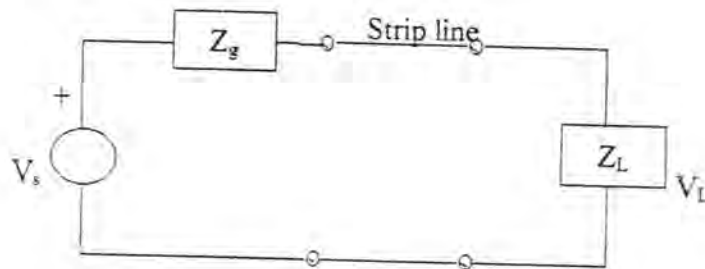


Fig. 7 circuit for analysis of pulse transmission.

The Gaussian pulses considered are of the form

$$V_s(t) = V_0 e^{-t^2/2\tau^2} \quad (4.3)$$

where the standard deviation τ measures the pulse width. Taking the Fourier transform of (4.3) yields.

$$\begin{aligned} V_s &= \int_{-\infty}^{\infty} V_s(t) e^{-i\omega t} dt \\ &= \sqrt{2\pi} \tau V_0 e^{-\omega^2 \tau^2 / 2} \end{aligned} \quad (4.4)$$

so that the frequency spectrum is also Gaussian with a standard deviation $\Delta \omega = 1/\tau$. Solving the circuit of figure 7 for the sinusoidal steady - state yields

$$V_L = \left[\left(1 + \frac{Z_g}{Z_L} \right) \coth v\ell + \left(\frac{Z_0}{Z_L} + \frac{Z_g}{Z_0} \right) \sinh v\ell \right]^{-1} V_s \quad (4.5)$$

Substituting equation (4.4) and taking the Fourier transform yields

$$\begin{aligned} V_L(t) &= \sqrt{\frac{2}{\pi}} \tau V_0 \int_{-\infty}^{\infty} d\omega e^{-\omega^2 \tau^2 / 2} \\ &\times \text{Re} \left\{ e^{i\omega t} / \left[\left(1 + \frac{Z_g}{Z_L} \right) \coth v\ell + \left(\frac{Z_0}{Z_L} + \frac{Z_g}{Z_0} \right) \sinh v\ell \right] \right\} \end{aligned} \quad (4.6)$$

To evaluate the above integral and to determine the shape of a pulse after traversing various length of strip line a program has been developed in which the Mattis - Bardeen results for α and β (i.e. fir γ)^[5] have been used.

Since Z_L and Z_0 are both proportional to $1/w$ the above calculation will not depend upon the strip line width.

The result of such simulation for Cu at 295K, Nb at 4.2K, and $\text{Ba}_2\text{Cu}_3\text{O}_7$ at 77K, for a given dielectric thickness

and an initial pulse width, are shown in figures 8,9,10, respectively. The traces shown are for a pulse after traversing a strip line of length 0, 0.1, 1, and 10 cm, where the time origin for each trace has been shifted by an amount

$$t_1 = \frac{l}{v_p(\infty)} \text{ such that a pulse traveling at the asymptotic}$$

high - frequency phase velocity $v_p(\infty)$ would always be centered at the origin.

To study the reflection at the interface between the line and the load due to impedance miss-matching, two cases were considered for the Ba_2 , Cu_3O_7 strip line. The load impedance was taken, in the first case, to be half the source impedance and in the second case, was taken to be twice. The results are shown in figures 11 and 12, respectively. The results indicate an amplitude reduction, for the case $Z_L = Z_g/2$, by a factor of 30% for a pulse of width 1ps on a line of length 10 cm and dielectric thickness ranging from $20\mu m$ to $0.2\mu m$, which is a drastic attenuation. However, the attenuation for the same pulse on a line of length 1 cm is only about 0.1% which indicates that such length can be used to connect the electronic components even with mismatched impedance. On the other hand, when $Z_L = 2Z_g$, the 1ps pluse on a line of 10cm long the attenuation is about 0.3% which is although a little higher than the case of $Z_L < Z_g$, but still negligible. Thus, both cases can be used for interconnection of electronic devices. Comparing the two cases with the case of matched impedance ($Z_L = Z_g$), when the load impedance is higher than the source impedance the results shows an increase in amplitude of the reflected wave due to a constructive interference with the incident wave, whereas when a $Z_L < Z_g$ reduction in amplitude is noticed and believed to be caused by destructive interference. The same conclusion can be drawn for a pluse of width 0.5 ps launched through a line of the same length and range of dielectric thickness.

Studies for a pulse of $\tau = 50ps$ launched through the microstripline has been carried out. If such a pluse is ever to

be useful in digital applications, then the attenuation in amplitude should be less than 20%, then it is obvious from figure 8 (for $s = 20 \mu\text{m}$) for a dielectric thickness $s = 20 \mu\text{m}$, $2 \mu\text{m}$, and $0.2 \mu\text{m}$, the useful strip line length are less than 10 cm, 1 cm, and 0.1 cm, respectively. Thus with $s \leq 2 \mu\text{m}$, the performance of a room temperature copper strip line can be a limiting factor even for lengths typical of microcircuit dimension^[2]. Theoretical arguments indicate that it may be possible to generate pulses with widths as short as 1 ps using a Josephson junction pulser^[11]. The propagation of such a pulse on a normal - state strip line is shown in figure 8b, using a $\tau = 0.5 \text{ ps}$ to give a full width of $\sim 1 \text{ ps}$. In going from 50 to 0.5 widths, it is evident that the distortion of the shorter pulse is much the same as that of the longer one after propagating only 1/10 of the distance. The propagation of these pulses can be explained in terms of the dispersion and attenuation shown in figures 4 and 5, respectively. For $\tau = 50 \text{ ps}$ and 0.5 , $\Delta\omega = 2 \times 10^{10}$ and $2 \times 10^{12} \text{ rad/s}$ which give $\Delta\nu = 3.2 \times 10^9$ and $3.2 \times 10^{11} \text{ Hz}$, respectively. the relevant form of v_ϕ and α_{dB} for this range of frequencies are approximately those given by limit III. In this region $\alpha_{dB} \propto \sqrt{\omega}$, so that going from 3.2×10^9 to $3.2 \times 10^{11} \text{ Hz}$ results in an increase in attenuation by a factor of 10. Also, because $\alpha_{dB} \propto 1/s$, an increase in attenuation of a 50 ps pulse on a $2 \mu\text{m}$ line is comparable to that of a 0.5 ps pulse on a $20 \mu\text{m}$ line. The same conclusion can be drawn for the phase velocity. The deviation of v from its high frequency values is proportional to $1/s \sqrt{\omega}$, the phase shift over a given length of line due to this deviation is thus proportional to $\sqrt{\omega}/s$. Hence, broadening of a pulse and displacement of its peak from $t = t'$ change with ω and s just as α_{dB} . Figures 9 and 10 show the results of a pulse propagation for superconducting Nb an $\text{Ba}_2\text{Cu}_3\text{O}_7$, for a pulse with a $\tau = 1 \text{ ps}$ and 0.5 ps , respectively. Attenuation and dispersion become significant at frequencies below the gap frequency, which results in the degradation and distortion of the pulse,

respectively^[6]. However, the 50ps pulse did not show any significant distrtion even after propagationg a distant of 10cm on a line with 0.2 μ m of dielectric.

CONCLUSION

To miniaturize the strip line an attempts were made to reduce the dielectric thickness between the two plates and using the same dielectric constant for all the three examples strip line considered. The superiority of superconductors strip line over the normal conductor is evident. It showed six orders of magnitude less losses. In reducing the dielectric thickness from 200 μ m to 0.2 μ m, the phase velocity, at 10 GHz, has shown 67% decrease for copper, while for Ba₂Cu₃O₇ and Nb the decrease was 35% and 26% respectively. The increase in attenuation with the reduction of dielectric thickness is enormously higher in the case of normal conductor than in the case of superconductors especially at low frequencies. In comparing the characteristic impedance at frequencies below the gap frequency, the superconductors show much higher device density over the normal conductor. However, at large spacing of the plates \sim 200 μ m and the same frequency \sim 10 GHz, we may have the same device densities for the two superconductors, but when the dielectric thickness is reduced to \sim 0.2 μ m, the Nb shows \sim 1/8 better device density than Ba₂Cu₃O₇, figures 5 c, d, but this probably much more cost effective than working at temperatures around 100K compared with the liquid helium temperature 4.2K, at which the Nb operates.

In terms of pluse propagation, figures 8, 9, 10 show the superiority of superconducting strip lines over the normal - state line even for $\tau = 0.5$ ps, because such a pulse can propagate without distrtion for distances of 10 cm on a line with 0.2 μ m of dielectric. Moreover, figures 9 and 10 show negligible difference in pulse propagating on either Nb or Ba₂Cu₃O₇ strip line, which emphasizes the superiority of

$\text{Ba}_2\text{Cu}_3\text{O}_7$ over Nb for its high temperature operating advantage.

REFERENCES

1. M.K. Wu, J.R. Ashburn, C.J. Torng, P.H. Hor, R.L. Meng, L. Gao, Z.J. Huang, Y.Q. Wang, and C.W. Chu, "Superconductivity at 93K in a New Mixed Phase Y-Ba-Cu-O Compound at Ambient Pressure" *Phys. Rev. Lett.* 58, (1987).
2. R.L. Kautz, "Miniaturization of Normal-State and Superconducting Strip lines" *Journal of Research of the National Bureau of Standards* Vol. 84, No. 3, 247-259, (1979).
3. D.G. Corr and J.B. Davies, "Computer Analysis of the Fundamental and Higher order modes in Single and Coupled Microstrip" *IEEE Trans Microwave Theory tech.*, Vol MTT-20, 669-678, (1972).
4. J.C. Swihart, "Field Solution for a thin-films Superconducting Tunneling Transmission line", *J. Appl. Phys.*, 32, 461-469, (1961).
5. D.C. Mattis and J. Bardeen, "Theory of the Anomalous skin effect in Normal and Superconducting Metals" *Phys. Rev.* 111, 412-417, (1958).
6. R.L. Kautz, "Picosecond pulses on Superconducting Strip lines", *J. Appl. Phys.* 49 (1), 308-314, (1978).
7. W.H. Henkel and C.T. Kircher, "Penetration Depth Measurements on Type II Superconducting Films" *IEEE trans. mag*, MAG-13, 63-66, (1977).
8. Heise, P. Gutsmedl, K. Neumaier, Chr. Probst, H. Bermolt, P. Muller, and K. Andress, "On the influence of the Heat Treatments on the Magnetic and Thermodynamic properties of Sintered $\text{YBa}_2\text{Cu}_3\text{O}_7$ " *Physica C*, 153-155, 1507-1508, (1988).
9. P.J.M. van Bentum, H.F.C. Hovers, H. van Kempen, L.E.C. Van De Leemput, M.T.M.F. De Nivelte, L.W.N. Schreurs, R.T.M. Smokers, and P.A.A. Teunissen,

Comparison Between Normal Metal, Low and High Temperature
Suprconductors

D.N. Rouf, et al

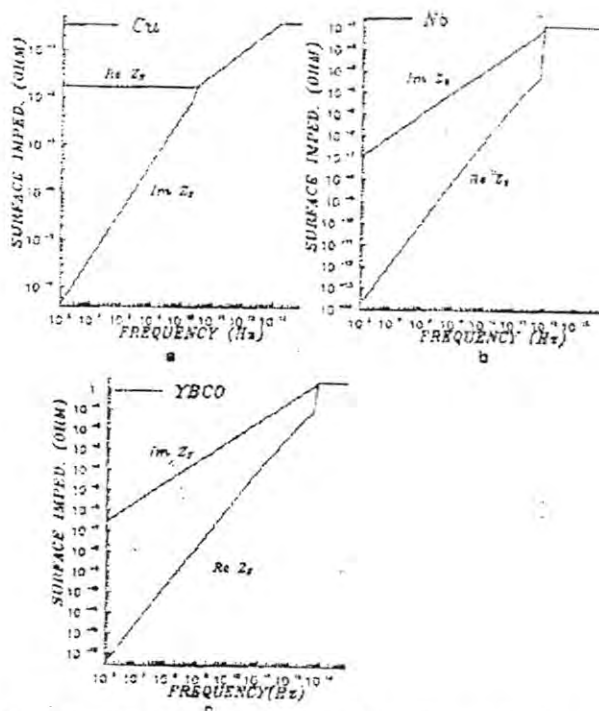


Fig. 2 Surface impedances as a function of frequency

(a) Cu at 295K.

(b) Nb at 4.2K.

(c) $YBa_2Cu_3O_7$ at 77K.

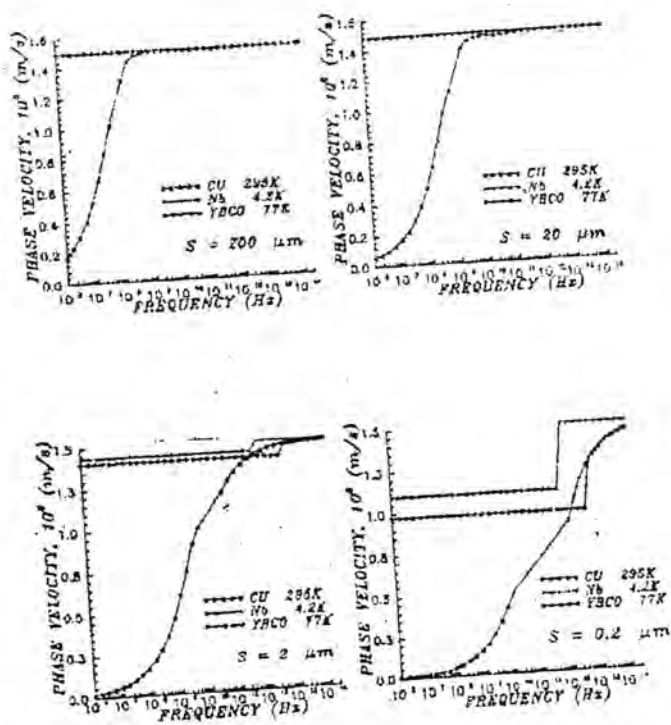


Fig. 3 Phase velocity as a function of frequency for different materials and dielectric thickness.

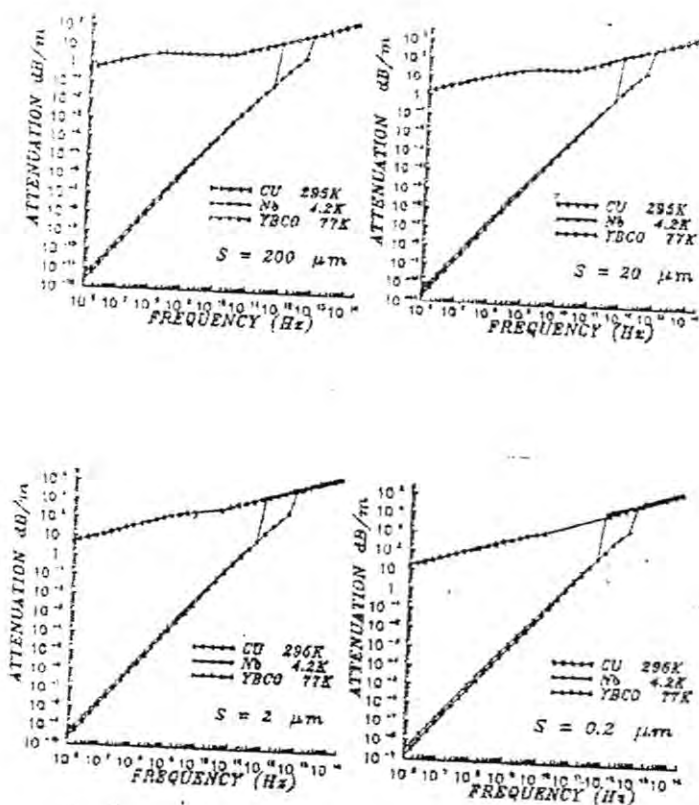


Fig. 4 Attenuation as a function of frequency
for different materials and dielectric thickness.

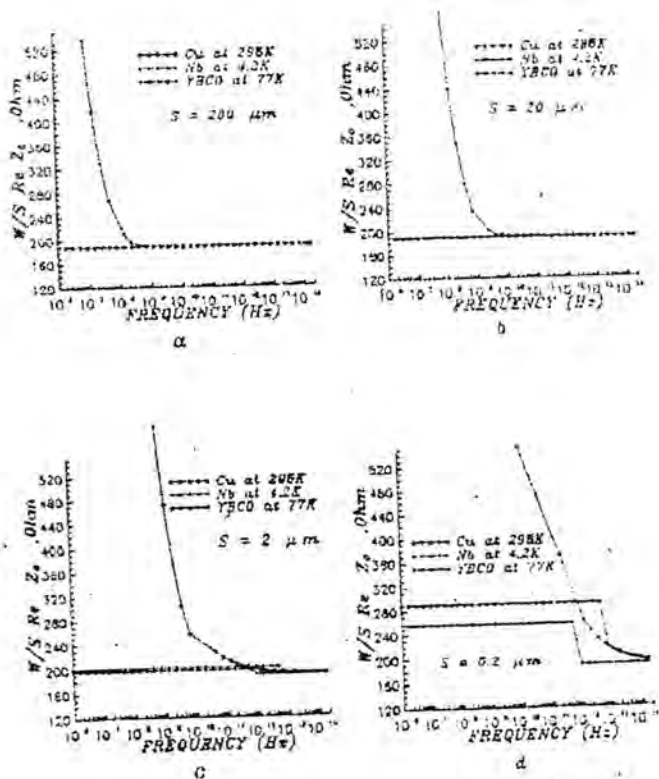
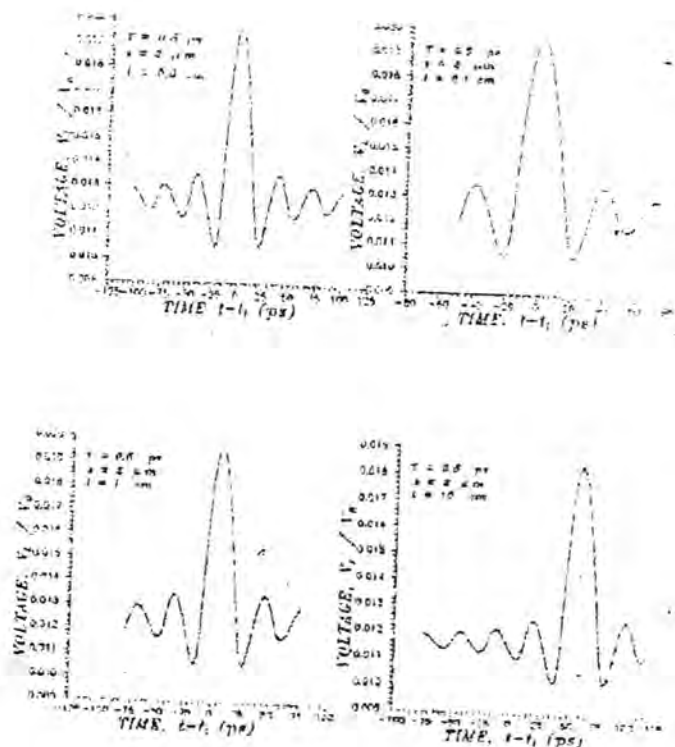


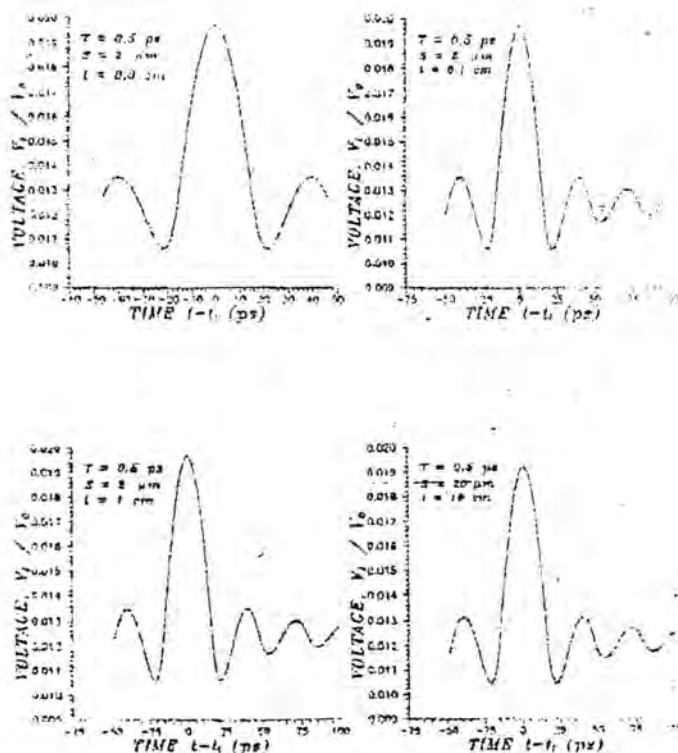
Fig. 5 The real part of the characteristic impedance as a function of frequency for different materials and dielectric thickness.

Comparison Between Normal Metal, Low and High Temperature
Suprconductors
D.N. Rouf, et al



b (ii)

Fig. 9 Propagation of a Gaussian pulse for μ_{HVO} or μ_{2n} .
The time origin has been shifted by an amount
 $t = t_0 (1)$ where the low frequency phase velocity
is 1.44×10^8 m/s.



b(ii)

Fig. 1D Propagation of a Gaussian pulse for Nb at 4.2K
 The time origin has been shifted by an amount
 $t_0 = t/v_p(f)$ where the low frequency phase velocity
 is 1.41×10^8 m/s.

*Comparison Between Normal Metal, Low and High Temperature
Suprconductors*

D.N. Rouf, et al

- "Determination of the Energy gap in $\text{YB}_2\text{Cu}_3\text{O}_{7-\delta}$ by using Far infrared reflection and Andreev reflection", *Physica C*, 153-155, 1718-1723, (1988).
10. S.J. Hagen, T.W. Ting, Z.Z. Wang, J. Horvath and N.P. Ong, "Out of the Plane Conductivity in Single-Crystal $\text{YBa}_2\text{Cu}_3\text{O}_7$ " *Phys. Rev B*, 37(13), 7928-7931, (1988).
11. D.G. McDonald and R.L. Peterson, "Design of Josephson Junction Picosecond Pulser" *J. Appl. Phys.*, 48(12), 5366-5369, (1977).

EO, M1, E2 TRANSITIONS OF COLLECTIVE LEVELS BELOW 1.821 MeV IN Pt-196

IMAN T. AL-ALAWY

College of Science, Physics Department

Al-Mustansiriyah University

(Received Oct. 31, 1998 ; Accepted May 16, 1999)

الخلاصة

ان دراسة طيف انتقالات الاكترون الداخلية والانتقالات الكهربائية EO تؤكد بان نواة pt-196 غير مستقرة مع كما وان مستوياتها تمتلك برم صفري وقطبيه موجب. وهذا ما اكده أيضاً نموذج التشوه الديناميكي. حيث كانت نتائجه متوافقة بشكل جيد جداً مع النتائج العملية. استخدام نموذج IBM-2 في هذا البحث والذي يعطي وصفاً كافياً لنموذج التشوه الديناميكي للمستويات ذات البرم الصفري والقطبيه الموجبة وانتقالاتها الكهربائية E2, EO وكذلك الانتقالات المغناطيسية M1 فكانت النتائج الحالية متوافقة بشكل جيد جداً مع النتائج العملية المتوفرة.

ABSTRACT

Measurements of the internal conversion electron spectrum and the identification of EO transitions provide additional evidence for the gamma-unstable description of Pt-196 and the nature of their 0^+ states. The dynamic deformation model (DDM) predicts that Pt-196 is a well deformed gamma-unstable nucleus and gave excellent agreement with experimental results. The alternative but equivalent $O(6)$ description within IBM-2 provides in general an adequate description of the 0^+ levels and their EO decay and the multipolarity modes.

INTRODUCTION

A description of even-even nuclei in terms of a system of interacting bosons able to occupy two levels, one with angular momentum $L=0$ (s = boson) and another with angular momentum $L=2$ (d -boson). These bosons generate a $U(6)$ symmetry spanned by the $1 + 5$ components of the one-boson states $s^+ |0\rangle$ and $d_M^+ |0\rangle$. The Hamiltonian can be written in terms of the generators of subgroups $SU(5)$, $SU(3)$ and $O(6)$. The group $O(6)$ of orthogonal transformations in six dimensions may be useful in describing nuclear spectra at the end of major shells. The fifteen generators of $O(6)$ are $(d^-, d)^{(1)}$, $(d^+, d)^{(3)}$, $(d^+, s + s^-, d)^{(2)}$. Then the five extra labels are needed to classify the totally symmetric irreducible representations $[N]$ of $U(6)$ when the group chain $U(6) \supset O(6) \supset O(5) \supset O(3) \supset O(2)$ is used. A quantum numbers which describes the totally symmetric irreducible representations of $O(6)$ are labeled $[1], [2]$ by $[N] \sigma \tau \nu_\Delta L M_L$ where :

$\sigma = N, N-2, \dots, 0$ or 1 (for $N = \text{even or odd}$).

$\tau = \sigma, \sigma - 1, \dots, 1, 0$.

ν_Δ = counts boson triplets coupled to zero angular momentum.

L = total angular momentum.

$M_L = Z$ component of L .

The values of L contained in each representation τ of $O(5)$ are obtained by

$\tau = 3 \nu_\Delta + \lambda, \nu_\Delta = 0, 1, \dots$

and $L = 2\lambda, 2\lambda-2, \dots, \lambda + 1, \lambda$

The 0^+ states are important. The $E0$ transitions between 0^+ states other than the ground state are indicates a good interpretation of Pt-196, which is a pure $O(6)$ description [3], [4], [5], [6]. The 0^+ states are investigating by measuring the internal conversion electrons emitted by an excited nucleus produced by thermal neutron capture. In $E0$ transitions between 0^+ states the change of angular momentum is zero, so that gamma-rays cannot compete with the emission of the conversion electrons caused by

penetration of atomic electrons caused by penetration of atomic electrons inside the nucleus. Thus the decay for transition energies $\leq 2m_0 c^2$ occurs only by internal electron conversion^[7]. These electrons not only carry away the energy of the nuclear transition, but their relative intensities provide information on the nuclear wavefunctions. It is this information which makes $0^- - 0^+$ transitions sensitive testes of nuclear models.

Internal conversion is the only decay mode between 0^+ states, but E0 transitions also occur in other cases where the levels have the same spin and parity. An example of the need for systematic E0 studies is provided by Se-78^[8]. Another example is the nucleus Yb-172 which is studied by Cresswell et al. (1981)^[9]. While Subber et al.^[10] studied the nuclear structure of Yb-172 in (1988). The measurements of the internal conversion electron spectrum provide additional information about the nature of the excited 0^+ states in Hg-200^[11]. While in Te-124 nucleus^[6], the inter 0^+ level transitions played an important role in establishing the character of 0_3^+ and 0_2^+ states. The Pt-196 nucleus is an example of the $0(6)$ limit of the ${}^2\text{IBM}^{[4]}$. The results of measurement by Kane et al. (1982)^[12] indicated that the E0 transitions in Pt-196 supported the $0(6)$ interpretation. The forbidden $0_3^+ - 0_2^+$ gamma-transition has been studied^[13] in Pt-196 with the $0(6)$ symmetry. The $0_3^+ - 0_2^+$ transition is very important and cannot be neglected, the E0 selection rules $\Delta\sigma = 2$, $\Delta\tau = 0$. This transition has been studied by Harder et al. (1988)^[14] for Pt-196, the measurements show that the $B(E0; 0_3^+ - 0_2^+) / B(E0; 0_3^+ - 0_1^+) = 0.20$ and $X(E0/E_2) = 0.68$ while $\rho^2 > 0.0008$.

Data Analysis and Discussion

Parameters and the Multipolarity

Several parameters may be used in the analysis of E0 transitions. The most appropriate one is the square of the E0, E2 mixing ratio as in the following equation [15], [16]:

$$q^2 [(E0/E2); I_i \rightarrow I_f] = \frac{B(E0; I_i \rightarrow I_f)}{\alpha_k (E2) B(E2; I_i \rightarrow I_f)} \quad (1)$$

where $B(E0)$, $B(E2)$ are transition probabilities of $E0$ and $E2$; and α_k is the total conversion coefficient,

Therefore q^2 could be written, in term of ρ (the nuclear strength parameter) and Ω_k (the electronic factor tabulated by Bell et al. (1970)[17], as [6], [16]:

$$q^2 = 2.8 \times 10^{-14} (2I_i + 1) \frac{(\Omega_k \text{ in sec}^{-1})}{\alpha_k (E2) (E_\gamma \text{ in MeV})^5} \frac{\rho^2 (E0; I_i \rightarrow I_f)}{\langle I_f || M(E2) || I_i \rangle^2} \quad (2)$$

Hence, the dimensionless ratio which is defined by Rasmussen (1960) [18], [19] could be written as :

$$X(E0/E2; I_i \rightarrow I_f) = \frac{\rho^2 (E0; I_i \rightarrow I_f) e^2 R^2}{B(E2; I_i \rightarrow I_f)} \quad (3)$$

where $R = 1.2A^{1/3}$ fm and $B(E2)$ is measured in $e^2 b^2$ units. $I_i = I_f$ when $I_i = I_f \neq 0$ but $I_f = 2^-$ when $I_i = I_f = 0$. Thus X -values may be used in all cases or decays involving $E0$ transitions while q^2 is only useful when γ -ray components are also present in the transition. The evaluation of the strength of $E0$ matrix elements is $X(E0/E2)$ a dimensionless ratio which may be obtained from equation (3). The $q(E0/E2)$, $\rho(E0)$ and $X(E0/E2)$ values for a number of transitions are shown in table-1.

Table -1: Experimental and theoretical data on E0 transitions in Pt-196 nucleus

Type of transition	$E\gamma$ (MeV)	$q(E0/E2)$	$\rho(E0)$	$N(E0/E2)$	Reference
$2\gamma^-2\gamma^+$	0.333	0.56 ± 0.10	-0.039 ± 0.007	$(1.27\pm0.25)*10^{-3}$	[20]
		0.43 ± 0.05	0.016 ± 0.002	$(7.50\pm0.80)*10^{-4}$	[20]
		or	or	or	
		$^{145}_{-0.110\pm0.110}$	$^{0005}_{-0.004\pm0.004}$	$^{6.5}_{(4.9\pm4.9)*10^{-5}}$	[20]
		0.39 ± 0.05	0.056 ± 0.007	$(6.1\pm0.8)*10^{-4}$	[20]
		or	or	or	
		0.22 ± 0.07	-0.032 ± 0.011	$(1.9\pm0.6)*10^{-4}$	
		-----	-----	$^{10}_{3.6\pm8 * 10^{-4}}$	[16]
				$3*10^{-4}$ (Theo.)	[16]
			0.056 ± 0.007	-----	[21]
			or		
			-0.032 ± 0.011		
			-0.02 (Theo.)		[21]
			-----	$(-0.014\pm0.005)^2$	[19]
				$(-0.018)^2$ (Theo.)	[19]
		$^{16}_{-0.23\pm20}$	-----	$^{18}_{0.00056\pm14}$	[22]
		or		or	
		$^{009}_{0.44\pm0.10}$		$^{25}_{0.00071\pm20}$	[20]
$0^+_{02}-0^+_{01}$	0.267	-----	$\rho^2 > 0.0008$	0.68	[14]

Comparisons of Results With Nuclear Models

One of the aims of any nuclear model is to explain the level structure of Pt-196 and the observed transitions provide to test the applicability of the model to a nucleus for which there is a strong evidence that it is gamma-unstable.

Dynamic Deformation Model (DDM)

The (DDM) has been developed over many years starting from the Pairing-Plus-Quadrupole (PPQ) model of Kumar and Baranger (1968)^[23] and Kumar (1975)^[19]. This model is attempt to describe the collective-spherical-transitional-deformed transitions and to span from the s-shell to heavy nuclei using microscopic theory of collective motion. The results of (DDM)^[6] based on shape parameters

(the magnitude of the nuclear deformation vector and the asymmetry angle) will be discussed latter in this paper.

2-2-2 The interacting Boson Model IBM-2

The proton neutron interacting boson Hamiltonian may be written as [1], [2]:

$$\hat{H} = \epsilon_{\pi} (d^+ \times d)_{\pi} + \epsilon_{\nu} (d^+ \times d)_{\nu} + V_{\pi\nu} + k Q_{\pi} Q_{\nu} + M_{\pi\nu} \quad (4)$$

where the quadrupole operator is :

$$Q_p = (s^+ \times d + d^+ \times s)_p^{(2)} + X_p (d^+ \times d)_p^{(2)} ; p = \pi \text{ or } \nu \quad (5)$$

and

$$V_{pp} = \sum_{L=0,2,4} (1/2) C_{LP} (2L+1)^{(1/2)} [(d^+ \times d)_p^{(L)} (d \times d)_p^{(L)}]^{[0]} \quad (6)$$

and the Majorana term may be written as :

$$M_{\pi\nu} = \xi_2 (s_{\nu}^+ \times d_{\pi}^+ - s_{\pi}^+ \times d_{\nu}^+)^{(2)} (s_{\nu} \times d_{\pi} - s_{\pi} \times d_{\nu})^{(2)} \\ - \sum_{k=1,3} 2 \xi_k (d_{\pi}^+ \times d_{\nu}) (d_{\pi} \times d_{\nu})^{(k)} \quad (7)$$

$\epsilon_{\pi} = \epsilon_{\nu} = \epsilon$ are the proton and neutron energies respectively. In the present work we used the IBM-2 by using the NPBOS Code [24]. The parameters obtained for Pt-196 with $N_{\pi} = 2$ and $N_{\nu} = 4$, in MeV, are:

$$\begin{array}{lll} \epsilon = 0.580 & C_{0\nu} = 0.600 & \xi_2 = 0.040 \\ k = -0.180 & C_{2\nu} = 0.020 & \xi_1 = \xi_3 = -0.100 \\ X_{\nu} = 1.050 & C_{4\nu} = 0.000 & \\ X_{\pi} = -0.800 & C_{L\pi} = 0.000 & \end{array}$$

The Majorana term $M_{\pi\nu}$ parameters have a strong influence on the magnitude and sign of the reduced matrix element $\langle ||E2|| \rangle$ and $\langle ||M1|| \rangle$ of many transitions. In order

to explain this dependence we introduce the transition operators given by [1], [2] :

$$T^{(E0)} = \alpha_{\pi} N_{\pi} + \alpha_{\nu} N_{\nu} + \beta_{\pi} [d_{\pi}^{-} \times d_{\pi}]_0^{(0)} + \beta_{\nu} [d_{\nu}^{-} \times d_{\nu}]_0^{(0)} \quad (8)$$

where α and β are constants and does not give rise to transitions.

$$T^{(E2)} = e_{\pi} Q_{\pi} + e_{\nu} Q_{\nu} \quad (9)$$

$$T^{(M1)} = (3/4\pi)^{1/2} [g_{\pi}(d_{\pi}^{+} \cdot d)_{\pi}^{(1)} + g_{\nu}(d_{\nu}^{+} \cdot d)_{\nu}^{(1)}] \quad (10)$$

where e_{π} and e_{ν} are effective boson charges, g_{π} and g_{ν} are the boson g factors. The effective boson charges e_{π} and e_{ν} are obtained in the present work by using the IBM-2 program NPBTRN code^[24]. Thus $e_{\pi} = e_{\nu} = 1.0$ for Pt-196.

The matrix elements could be deduced from IBM-2 used in this work. Therefore we can calculate the electromagnetic transition rates and quadrupole moments. The electromagnetic transition rates are governed by $B(E2)$ values. They are defined as [1], [2] :

$$B(E2; L \rightarrow L') = \frac{1}{2L+1} \langle L' || T^{(E2)} || L \rangle^2 \quad (11)$$

and the quadrupole moments

$$Q_L = (16\pi/5)^{1/2} \begin{pmatrix} L & 2 & L \\ -L & 0 & L \end{pmatrix} \langle L || T^{(E2)} || L \rangle \quad (12)$$

The $B(E2)$ values are listed in (table -2) for both experimental and IBM-2 calculated in the present work. A comparison of the parameters (energy ratios, branching ratios, and the quadrupole moment ratio) are given in (table-3). The agreement of (DDM) values with the experiment [29] are good. Also the results of the calculations, the IBM-2 values, show a good agreement with experiment for both

calculated from the present work and that predicted from [28].

2-3 Conversion Electron and Multipolarity

The additional data on E0 transitions, using data taken at ILL, Institute Laue-Langevin (Grenoble, France) [29] is a powerful tool for investigating 0^+ states as it measures the internal conversion electrons emitted by an excited nucleus produced by thermal neutron capture [13]. These E0 transitions allows the IBM-2 to be further tested while the (DDM) of Kumar has the same feature for a gamma-unstable Pt-196 nucleus.

The internal conversion coefficients α_k were evaluated from the ratio of measured electron intensity to gamma-ray intensity. These intensities are measured by Kane et al. (1982) [12] and Harder et al. (1988) [14].

A number of lines corresponding to E0 transitions were observed^[13] relative to k-shell. Decay from the 0_4^+ to 0_3^+ , 0_2^+ , 0_1^+ states were studied. Although the decays from 0_3^+ to 0_2^+ , 0_1^+ and from 0_2^+ to 0_1^+ states are possible transitions, the M1 and E2 transitions were observed and studied. The results are very sensitive to these multipolarity for the transitions from states other than 0^+ states. These calculations shown in table -4 could be deduced a useful information from the analysis of Pt-196 spectrum.

Table -2 : Transition rates $B(E2) (eb)^2$ of Pt - 196

$B(E2)(eb)^2$	Experimental				IBM-2		
	[25]	[26]	[27]	[28]	[28]	[27]	[PW]
$2_1^- - 0_1^-$	0.276 ± 0.001	1.27	1.30 ± 0.05	0.264 ± 0.011	0.289	3.007	1.1894
$2_2^- - 0_1^-$	$< 2 \times 10^{-3}$	< 1.3	—	—	—	0.002	1.3391
$2_2^- - 2_1^-$	0.34 ± 0.03	—	0.318 ± 0.023	0.318 ± 0.023	0.400	0.791	1.9622
$0_2^+ - 2_1^-$	0.021 ± 0.01	—	—	—	—	—	—
$0_2^+ - 2_2^-$	0.14 ± 0.07	—	0.142 ± 0.077	—	—	0.541	—

Table -3 : Comparison of parameters of Pt-196 (Exp. , DDM, and IBM-2)

Parameters	Dynamical symmetry [1], [2]			EXP. [29]	DDM [6]	IBM-2 [28]	IBM-2 [PW]
	SU(5) Vib.	SU(3) Rot.	O(6) γ -unstable				
$E(4_1^+) / E(2_1^+)$	2.0	3.33	2.5	2.47	2.6	2.6	2.5
$E(2_2^+) / E(4_1^+)$	1.0	$\gg 1$	1.0	0.78	0.76	0.85	0.85
$E(0_2^+) / E(2_1^+)$	2.0	$\gg 2$	4.5	3.19	3.39	3.7	3.56
$B(E2: 2_2^+ \rightarrow 0_1^+)$ $B(E2: 2_1^+ \rightarrow 0_1^+)$	0.0	0.0	0.0	1×10^{-6}	0.015	3×10^{-6}	0.285
$B(E2: 2_1^+ \rightarrow 0_1^+)$ $B(E0: 0_2^+ \rightarrow 0_1^+)$	β^{2*}	$4\beta^{2*}$	---	< 0.005	0.047	---	---
$B(E2: 0_2^+ \rightarrow 0_1^+)$ $B(E2: 2_2^+ \rightarrow 2_1^+)$	2.0	0.0	1.43	1.23 [25]	---	---	1.465
$B(E2: 2_2^+ \rightarrow 0_1^+)$ $B(E2: 0_2^+ \rightarrow 2_1^+)$	--	--	0.0	0.16 [1] 0.15 [25]	---	---	---
$B(E2: 0_2^+ \rightarrow 2_2^+)$ $B(E2: 0_2^+ \rightarrow 2_1^+)$	2.0	0.0	0.0	0.08 [25]	---	---	---
$B(E2: 2_1^+ \rightarrow 0_1^+)$ Q_2^+ / Q_2^+	0.0	1.0	0.0	-0.51	0.10	-0.25	-1.324

* $\beta = 0 \rightarrow 0.625$

Table -4 : The conversion electron relative intensities with the deduced conversion coefficients, using ICC [30], and the transition multipolarities for transitions in Pt-196

$I_i^-(\sigma, \tau)$	$I_f^-(\sigma, \tau)$	$E_\gamma(\text{MeV})$ [14], [31]	$I_\gamma[14]$	$I_e[14]$	α_{exp} [PW]	$\alpha_{\text{theo. [pw]}}$			Multipolarity	
						E1	E2	M1	[31]	[pw]
$2_1^+(96.1)$	$0_1^-(6.0)$	0.365	1000	40.97	0.041	0.014	0.067	0.156	E2	E2
$2_2^+(6.2)$	$0_1^-(6.0)$	0.689	<0.6	<0.09	0.150	0.004	0.006	0.022	E2	E2+M1
$2_2^+(6.2)$	$2_1^+(6.1)$	0.333	411	22.90	0.056	0.013	0.035	0.165	E2+M1 +E0	E2+M1 +E0
$0_2^+(6.3)$	$0_1^-(6.0)$	1.135	—	{<0.80}	—	—	—	—	—	—
$0_2^+(6.3)$	$2_1^-(6.1)$	0.780	{39}	{0.28}	0.007	0.003	0.007	0.021	—	E2
$0_2^+(6.3)$	$2_2^-(6.2)$	0.447	15.3	0.38	0.025	0.011	0.030	0.123	—	M1+E2
$2_3^+(6.4)$	$0_1^+(6.0)$	1.362	< 0.6	(a)	—	—	—	—	—	—
$2_3^+(6.4)$	$2_1^-(6.1)$	1.006	{24}	{0.09}	0.004	0.002	0.004	0.088	M1+E2	M1+E2
$2_3^+(6.4)$	$2_2^-(6.2)$	0.673	{30}	{0.86}	0.029	0.005	0.012	0.044	—	M1+E2
$2_3^+(6.4)$	$0_2^-(6.3)$	0.226	1.3	(a)	—	—	—	—	—	E2
$0_3^+(4.0)$	$0_1^+(6.0)$	1.403	—	35.68 ^(b)	—	—	—	—	—	E0
$0_3^+(4.0)$	$2_1^-(6.1)$	1.047	{30}	(a)	—	—	—	—	—	—
$0_3^+(4.0)$	$2_2^-(6.2)$	0.689	< 0.6	< 0.09	0.150	0.003	0.008	0.024	—	M1+E2
$0_3^+(4.0)$	$0_2^-(6.3)$	1.135	—	{1.92}	—	—	—	—	—	—
$0_3^+(4.0)$	$2_3^-(6.4)$	1.362	(a)	(a)	—	—	—	—	—	—
$2_4^+(4.1)$	$0_1^+(6.0)$	1.605	{3.3}	(a)	—	—	—	—	—	—
$2_4^+(4.1)$	$2_1^-(6.1)$	1.249	{16.3}	0.95 ^(b)	0.058	0.077	0.003	0.005	—	E0+E2 +M1
$2_4^+(4.1)$	$2_2^-(6.2)$	0.916	{6.5}	{(0.04)}	0.006	0.0024	0.006	0.018	—	E2

Continued (2/2)

$I_j^+(\sigma, \tau)$	$I_i^+(\sigma, \tau)$	$E\gamma(\text{MeV})$ [14],[13]	$I\gamma[14]$	$I_e[14]$	α_{exp} [PW]	$\alpha_{\text{theo. [pw]}}$			Multipolarity	
						E1	E2	M1	[31]	[pw]
$2_4^+(4,1)$	$0_2^+(6,3)$	0.469	< 0.6	< 0.09	0.150	0.007	0.036	0.064	---	M1+E2
$2_4^+(4,1)$	$2_3^+(6,4)$	0.243	< 0.6	{(0.13)}	0.217	0.033	0.952	0.424	---	E2+M1
$2_4^+(4,1)$	$0_3^+(4,0)$	0.202	0.7	(a)	---	---	---	---	---	---
$2_5^+(6,5)$	$0_1^+(6,0)$	1.677	{15}	(a)	---	---	---	---	---	---
$2_5^+(6,5)$	$2_1^+(6,1)$	1.322	{13,8 ^(b) }	(a)	---	---	---	---	---	---
$2_5^+(6,5)$	$2_2^+(6,2)$	0.989	{3.1}	{0.30}	0.097	0.002	0.006	0.016	---	M1+E2
$2_5^+(6,5)$	$0_2^+(6,3)$	0.542	{0.7}	< 0.09	0.129	0.006	0.007	0.055	---	M1+E2
$2_5^+(6,5)$	$2_3^+(6,4)$	0.316	0.5	< 0.09	0.180	0.026	0.73	0.328	---	M1+E2
$2_5^+(6,5)$	$0_3^+(4,0)$	0.275	< 0.6	< 0.09	0.150	0.029	0.084	0.377	---	---
$2_5^+(6,5)$	$2_4^+(4,1)$	0.073	(a)	(a)	---	---	---	---	---	---
$0_4^+(2,0)$	$0_1^+(6,0)$	1.823	---	{<80 ^(b) }	---	---	---	---	---	---
$0_4^+(2,0)$	$2_1^+(6,0)$	1.468	{8.4}	(a)	---	---	---	---	---	---
$0_4^+(2,0)$	$2_2^+(6,2)$	1.135	< 0.6	(a)	---	---	---	---	---	---
$0_4^+(2,0)$	$0_2^+(6,3)$	0.688	< 0.6	< 0.09	0.150	0.003	0.0064	0.024	---	M1+E2
$0_4^+(2,0)$	$2_3^+(6,4)$	0.462	< 0.6	< 0.09	0.150	0.001	0.0023	0.007	---	M1+E2
$0_4^+(2,0)$	$0_3^+(4,0)$	0.421	---	< 0.09	---	---	---	---	---	---
$0_4^+(2,0)$	$2_4^+(4,1)$	0.219	< 0.6	(a)	---	---	---	---	---	---
$0_4^+(2,0)$	$2_5^+(6,5)$	0.146	< 0.6	(a)	---	---	---	---	---	---

(a) : Out side the energy range of experiment.

(b) : Ref. No. [12]

() : The placing of this transition is not confirmed.

{ } : The transition violates either the E2 or E0 selection rules

E2 : $\Delta\sigma = 0$, $\Delta\tau = 1$;E0 : $\Delta\sigma = 2$, $\Delta\tau = 0$.

REFERENCES

1. Iachello F. and Arima A. : The interacting boson model. Ed. Landshoff P.V., McCrea W.H., Sciama D.W., and Weinberg S., Pub. Cambridge University. PP. 19-63 (1987).
2. Bonatsos D.: Interacting boson models of nuclear structure. Ed. Hodgson P.E. . Pub. Oxford University. PP. 14-34 (1988).
3. Cizewski J.A., Casten R.F., Smith G.J., Stelts M.L., Kane W.R., Börner H.G., and Davidson W.F. : Evidence for a new symmetry in nuclei. The structure of Pt-196 and the $O(6)$ limit. Phys. Rev. Letters, 40, 167 (1978).
4. Arima A. and Iachello F. : Phys. Rev. Lett., 40, 385 (1978).
5. Köppel Th. J. and Faessler A. : Description of the even-mass Hg and Pt isotopes by a microscopic collective Hamiltonian Nucl. Phys. A403, 263 (1983).
6. Subber A.R.H., Park P., Hamilton W.D., Kumar K., Schreckenbach K., and Colvin G. : E0 transitions in the γ -unstable nucleus Te-124 J. Phys. G: Nucl. Phys. 12, 881 (1986).
7. Krane K.S. : Introductory nuclear physics. Ed. Krane K.S. . Pub. John Wiley and Sons, Inc. . PP. 341 348 (1988).
8. Subber A.R.H. : Ph.D. Thesis Sussex University (1987).
9. Cresswell J. R., Forsyth P.D., Martin D.G.E., and Morgan R.C. : Nuclear structure studies of Yb-172. J. Phys. G: Nucl. Phys., 7, 235 (1981).
10. Subber A.R.H., Hamilton W.D., Van Isacker P., Scheckenbach K., and Colvin G. : J. Phys. G: Nucl. Phys., 14, 87 (1988).
11. Subber A.R.H., Hamilton W.D. and Colvin G.: Excited 0^+ states and E0 transitions in Hg-200. J. Phys. G: Nucl. Phys., 13, 1299 (1987).

12. Kane W.R., Casten R.F., Warner D.D., Scheckenbach K., Faust H.R., and Blakeway S. : *Phys. Letts.*, B117, 15 (1982).
13. Cizewski J.A., Casten R.F., Smith J.H., Macphail M.R., Stelts M.L., Kane W.R., Borner H.G., and Davidson W.F. : *Nucl. Phys.*, A323, 349 (1979).
14. Harder M., Veskovic M., Hamilton W.D., and Krusche B. : Nuclear characterisation by measuring E0-transition Pt-196. *Inst. Phys. Conf. Ser. No. 88; Capture gamma-ray spectroscopy*. Ed. Abrahams K. and Van Assche P.. Pub. Institute of Physics, Bristol and Philadelphia. PP. S529-S531 (1988).
15. Church E.L., and Weneser J. : *Phys. Rev.* 104, 1382 (1958).
16. Lang J., Kumar K., and Hamilton J. : E0, E2, M1 multipole admixtures of transitions in even-even nuclei. *Rev. Mod. Phys.*, 54, 119 (1982).
17. Bell A.D., Avelo C.E., Davidson M.G., and Davidson J.P. : *Can J. Phys.*, 48, 2542 (1970).
18. Rasmussen J.O. : *Nucl. Phys.*, A19, 85 (1960).
19. Kumar K. : In the electromagnetic interaction in nuclear spectroscopy. Ed. Hamilton W.D.; Pub. North-Holand. P.55 (1975).
20. Aldushchenko Voinava N.A. : E0 transitions in atomic nuclei. *NDT* 11, 299 (1973).
21. Pauli H.C., Alder K., and Steffen R.M. : In the electromagnetic interaction in nuclear spectroscopy. Ed. Hamilton W.D.; Pub. North-Holand. P. 341 (1975).
22. Doubt D. (1971): Written in Lange J. et al. *Rev. Mod. Phys.*, 54, 119 (1982).
23. Kumar K. and Baranger M. : *Nucl. Phys.*, A122, 273 (1968).
24. Otsuka T. : Program Package NPBOS, NPBTRN. KVI report No. 63.
25. Casten R.F. and Warner D.D. : The interacting boson approximation. *Rev. Mod. Phys.*, 60, 389 (1988).

E₀, M1, E2 Transitions Of Collective Levels Below 1.821 Mev In Pt-196

J. T. Al-Awady

26. Siegbahn K.: Alpha, Beta and Gamma-Ray Spectroscopy, Pub. North-Holland Co., Amsterdam, Vol. 2 P. 1613 (1968).
27. Hess P.O., Maruhn J., and Greiner W. : J. Phys. G.: Nucl. Phys. 7, 737 (1981).
28. Bijker R., Dieperink A.E.L., Scholten O., and Spanhoff R.: Nucl. Phys. A344, 207 (1980).
29. Mampe W., Schreckenbach K., Jeuch P., Maier B.P.R., Braumandle F., Larysz J., and Von Egidy T. : Nuclear Instruments and Methods, 154, 127 (1978).
30. Rosel F., Fries H.M., Alder K., and Pauli H.C.; ICC values for Z=68-104. : Atomic Data and Nuclear Data Tables, 21, 291 (1978).
31. Lederer C.M., and Shirley V.S. : Table of Isotopes 7th Edn (New York : Wiley), (1978).

The Variation of Probability Distributions with Atomic Number

KHALIL H. AL-BAYATI AND MOHAMMED I. SANDUK

Department of Physics, College of Science, University of Baghdad,
Al-Jadriya, P.O. Box: 47036, Baghdad-Iraq

ABSTRACT

In addition to the product $\Delta X \Delta P$, the moments calculations (Skewness and Kurtosis) are used to study the behavior of the probability distributions curves. This concept is applied on the ground state wave function of lithium like atoms where $3 \leq Z \leq 8$. Weiss's wave function is used to find ΔX and ΔP and other parameters. The results show that the uncertainty product is not enough to characterize the deviation from Gaussian distribution. So, the moments calculations are necessary.

INTRODUCTION

Far from the quantum mechanics interpretation of the uncertainty principal, the uncertainty relation is a well known relation in signal analysis. Where the product of variances of two signals one of them is the Fourier transform of the other can not be less than a certain minimum value. "This is essential a mathematical phenomenon bound in with the interdependence of time and frequency"⁽¹⁾. This phenomenon is based in dealing with:

- 1- Signal analysis of two signals bounded by Fourier transformation.
- 2- The statistical distributions of the probabilities.

Returning to quantum mechanics, the two signals may have the form like $\psi(x)$ and $\phi(p)$, and the statistical distributions are the probability densities. If the standard deviations of the probability densities of both signals are ΔX and ΔP respectively, the uncertainty relation is:

$$\Delta X \Delta P \geq \hbar / 2 \quad (1)$$

The statistical distribution can be in many forms. The standard one is the Gaussian distribution. In Gaussian case the product is:

$$\Delta X \Delta P = \hbar / 2 \quad (2)$$

and it is called the minimum level of uncertainty. Far from the physical meaning of \hbar , this is a mathematical property of the product of the standard deviations (of two Gaussian wave functions one of them is the Fourier transform of the other⁽¹⁾). An example for this case is the linear harmonic oscillator (LHO) in the ground state ($n=0$).

The other allowed case, is that of

$$\Delta X \Delta P > \hbar / 2 \quad (3)$$

in which the product exceeds the minimum level (equation 2). In this case the envelope is skewed (Non-Gaussian). So the uncertainty product may be used to distinguish the distribution type (Gaussian or non-Gaussian).

The effect of distribution shape on the product is quite obvious. But this shape depends on the potential that controls the motion.

In this work we study the variation of uncertainty product due to the variation of the atomic number. The shape of probability distribution or its deviation from Gaussian will be refereed to that variation. The used data are extracted from application of a Hartree-Fock wavefunction on lithium like atoms.

Potential Effect

There is no meaning of localization of free particles (zero potential energy), where in this case we have a monochromatic wavefunction. The problem of localizability is associated with bounded particle states. In other word, there will be a certain distribution of probability density, i.e. the wavefunction is multichromatic.

The shape of wavefunction depends on the potential part (of the Hamiltonian) in the Schrödinger equation. As a pedagogical example, Schrödinger's equation of LHO is:

$$i \hbar \partial \psi / \partial t = - \hbar^2 / 2m \partial^2 \psi / \partial X^2 + (kX^2/2) \psi \quad (4)$$

where k is the force constant. The potential energy for ground state ($n=0$) is of type $kX_0^2/2$, and the distributions of this state are of Gaussian type, like:

$$\psi(X)\psi^*(X) = \delta(2\pi)^{-1/2} \exp(-X^2/2\delta^2)$$

where δ is the variance $(\Delta X)^2$. So the uncertainty product will have the minimum value.

System like atoms have a more complicated potential type. For hydrogen atom, the potential is of type $1/r$. The wavefunction for $1s$ is:

$$\psi(r) = A \exp -r/n r_b$$

where r_b is Bohr radius. So there are not any expected Gaussian form for the probability densities, and the uncertainty product exceed the minimum value.

Li-Like Atoms

The potential will take more complicated form in case of high atomic number (Z). In this case potential energy terms arising from the mutual repulsion between any two electrons will be present. The Hamiltonian of such a system is of the form⁽²⁾:

$$H = \sum_i H_i + \frac{1}{2} \sum_{ki} V_{ki} \quad (5)$$

Where H_i is the Hamiltonian of the i -th electron in the field of a nucleus of charge Ze and $V_{ki} = e^2/r_{ki}$ is the potential of interaction of two electrons.

In this case there is no simple solution of Schrödinger's wave equation. There were many attempts to simplify the problem. The most important attempt is that so called Hartree-Fock (HF) approximation⁽³⁾.

Weiss⁽⁴⁾ computed the wavefunction by expansion method for the $2s$, $2p$, $3s$, $3p$, and $3d$ states of the lithium atom and its isoelectronic ions through $Z=10$. In a previous work⁽⁵⁾ this method was adopted in addition to the electron correlation⁽⁶⁾ method.

By using this method one can get the following results⁽⁵⁾:

First, HF functions in position and momentum space: 1- the one particle radial distribution functions for $K\alpha K\beta$ shell ($D(r_1)$ and $D(p_1)$). 2- the interparticle distribution for $K\alpha K\beta$

shells ($f(r_{12})$ and $f(p_{12})$). The distributions are for Li, Be⁺, B²⁺, C³⁺, N⁴⁺, and O⁵⁺. Note Figure 1.

Second, the expectation values in position and momentum space for: 1- one electron nucleus separation distances ($\langle r_1 \rangle$ and $\langle p_1 \rangle$). 2- The inter-particle separation distances ($\langle r_{12} \rangle$ and $\langle p_{12} \rangle$). Note Figure 2.

Third: The standard deviations in position and momentum space Δr_1 , Δp_1 , Δr_{12} and Δp_{12} . Note Figure 3.

It found that there is an error in Weiss's wavefunction for the 2s-state of the C³⁺ ion ($Z=6$)⁽⁵⁾. Consequently this function has not been used in the present work.

The Probability Distribution

The distributions of probability ($f(r_{12})$ and $f(p_{12})$) for the ground state of Li, B²⁺, C³⁺, N⁴⁺ and O⁵⁺ are shown in Figure 1. The radius (r_M mode) at which the probability of finding the electron is greatest can be calculated by:

$$\frac{d}{dr} (f^* f d\tau) = 0 \quad (6)$$

Figure 2 (as an example the calculations has been done for two electron system only) shows r_{M12} , p_{M12} and the difference between the expected value $\langle r_{12} \rangle$ (mean value) and the mode (r_{M12}) where

$$\langle r \rangle - r_M = D(r) \quad (7)$$

This difference is a sort of representation of how much is the deviation from a symmetrical distribution (where $D=0$). For position calculations, the reduction in $D(r)$ (with Z) is owing to the increases of the distribution height (with Z), which makes the distribution more narrow, and more symmetric. For momentum calculation, $D(p)$ has an opposite behavior.

The departures of the one point distribution from a Gaussian form can be characterized by the Skewness (S) and Kurtosis (K), which are respectively the appropriately normalized third and fourth moments⁽⁷⁾.

$$S = \langle r^3 \rangle / \sigma^3 \equiv a_3 \quad (8)$$

$$K = \langle r^4 \rangle / \sigma^4 \equiv a_4 \quad (9)$$

Where σ is the standard deviation. For a Gaussian distribution, $S \equiv 0$ and $K \equiv 3$.

The calculated S and K for $f(r_{12})$ and $f(P_{12})$ are shown in Figure 4 as varied with Z . These distributions are leptokurtics ($K > 3$) and positively skewed ($S > 0$) for $f(r_{12})$. For $f(P_{12})$ the distributions are platykurtics ($K < 3$) and positively skewed ($S > 0$). The deviations from Gaussian are clear and varying with Z . the behavior of S_r and K_r is opposite to the behavior of S_p and K_p with Z . This is owing to reciprocity relation between the position and the momentum.

It is possible to refer the uncertainty product to both parameters S and K for r and P , by using eqs. (8 and 9) as:

$$\Delta X \Delta P = \frac{\langle P^4 \rangle \langle r^4 \rangle}{\langle P^3 \rangle \langle r^3 \rangle} \frac{S_r S_p}{K_r K_p} \quad (10)$$

The Uncertainty Product

Figure 3 shows, first that the position is more certain (well-defined) as Z increases, whereas the momentum has an opposite feature. Second, single electron measurements are more accurate than those of two electrons measurements, where $\Delta r_1 < \Delta r_{12}$ and $\Delta P_1 < \Delta P_{12}$.

The product $\Delta r_1 \Delta P_1$ (Figure 5) decreases with Z . This is owing to Coulomb force, which makes a shrinkage in $\langle r_1 \rangle$. The values of the product $\Delta r_1 \Delta P_1$ are around 0.5 and exceed this lower limit as Z increases. These unexpected values may be attributed to the approximation feature of the functions!

The product $\Delta r_{12} \Delta P_{12}$ has a small different behavior with Z . It decreases until $Z=6$ then increases. This behavior is owing to the fact that the standard deviation increases with Z becoming larger than the expected values for the case of $Z > 6$. The values of $\Delta r_{12} \Delta P_{12}$ are greater than 0.5 (around 0.75).

CONCLUSION AND REMARKS

For the case of the complicated systems we find that:

- 1- As in the ordinary relation between r and P , the reciprocity between r and P is quite clear in S and K of the distributions.
- 2- The distributions are non-Gaussian according to S and K calculations. So the uncertainty products are greater than the minimum level.
- 3- As the uncertainty product decreases towards the minimum level, the values of S_r and K_r show more deviation from Gaussian values. Whereas for such behavior we have to expect an approach to Gaussian. So we say that the uncertainty product is not sufficient to characterize the deviation from Gaussian distribution, and the moments calculations are necessary for that purpose.

Acknowledgement

Many thanks to Dr. R.A. Radhi of department of Physics university of Baghdad for his comments and stimulating notes.

REFERENCES

- 1- Bracewell R.N. The Fourier Transform and its Applications. Tokyo; McGraw-Hill Kogakusha, P 160 (1978).
- 2- Davydov A.S. Quantum Mechanics. Oxford; Pergamon, P 297 (1985).
- 3- Hartree D.R. The calculation of atomic structures. New York; Wiley (1957).
- 4- Weiss A.W. Configuration interaction in simple atomic system. Phys. Rev. 122: 1826-1836 (1961).
- 5- Al-Bayati K.H. PhD. Thesis. Leicester, U.K., (1984). Banyard K.E. and K.H. Al-Bayati: Intra-and inter-shell correlation effects in Li-like ions: Coulomb holes and

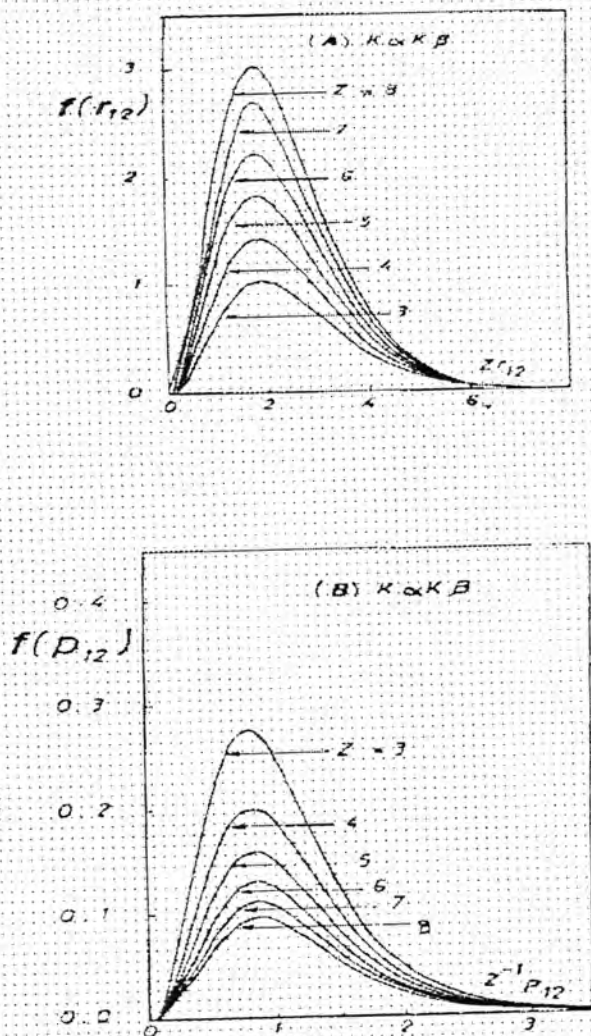


Figure 1: The HF function A- $f(r_{12})$ and B- $f(p_{12})$, plotted against the scaled distance Zr_{12} for position and $Z^{-1}p_{12}$ for momentum (in atomic units)

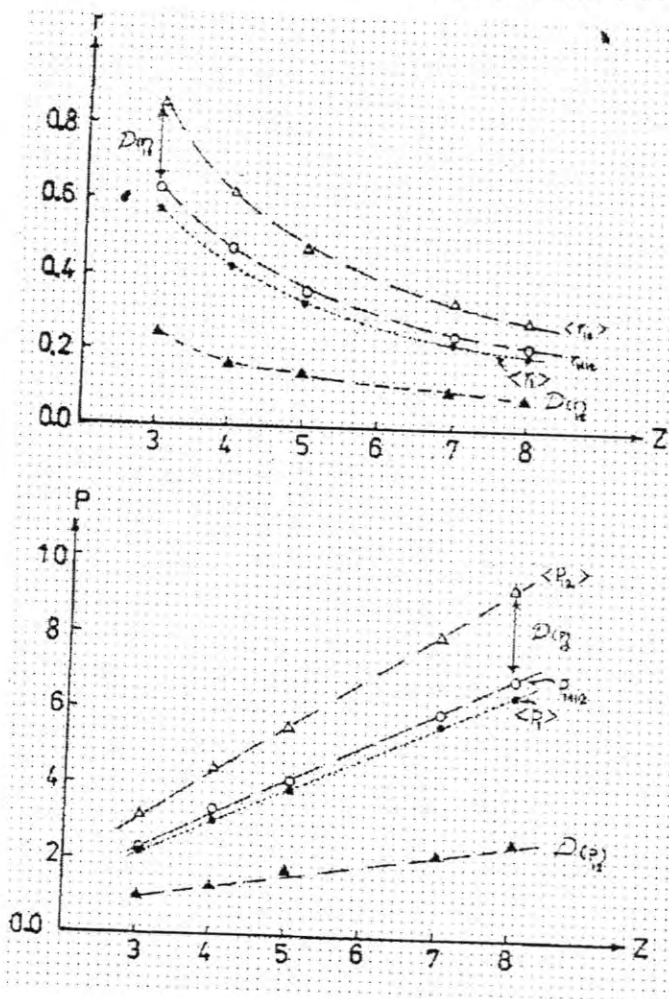


Figure 2: The expectation values (for A-position and B-momentum). The position and momentum of highest probability and the difference between them. Plotted against Z .

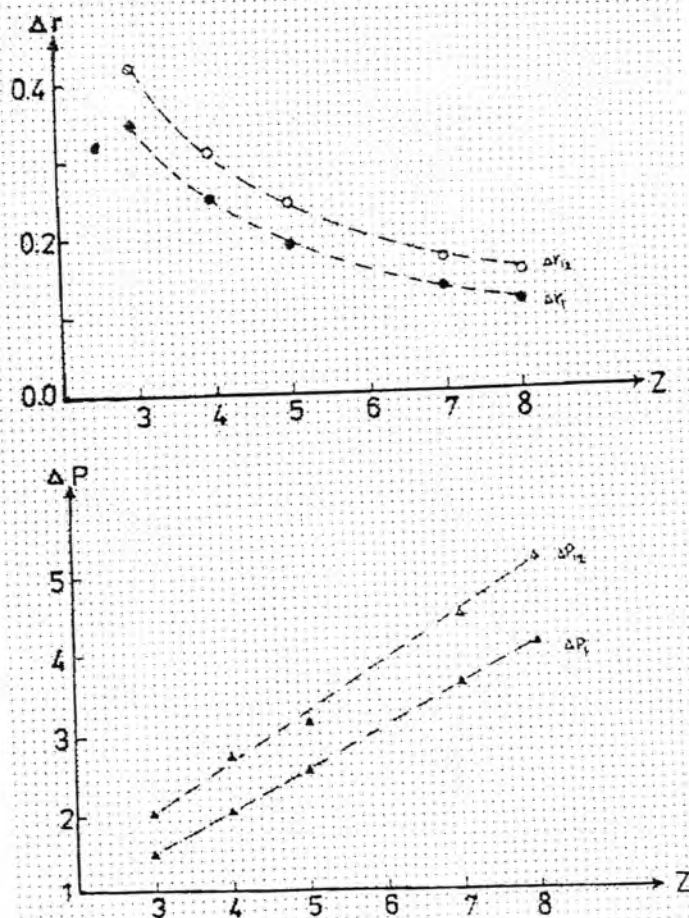


Figure 3: The standard deviations for: A-position and B-momentum plotted against Z

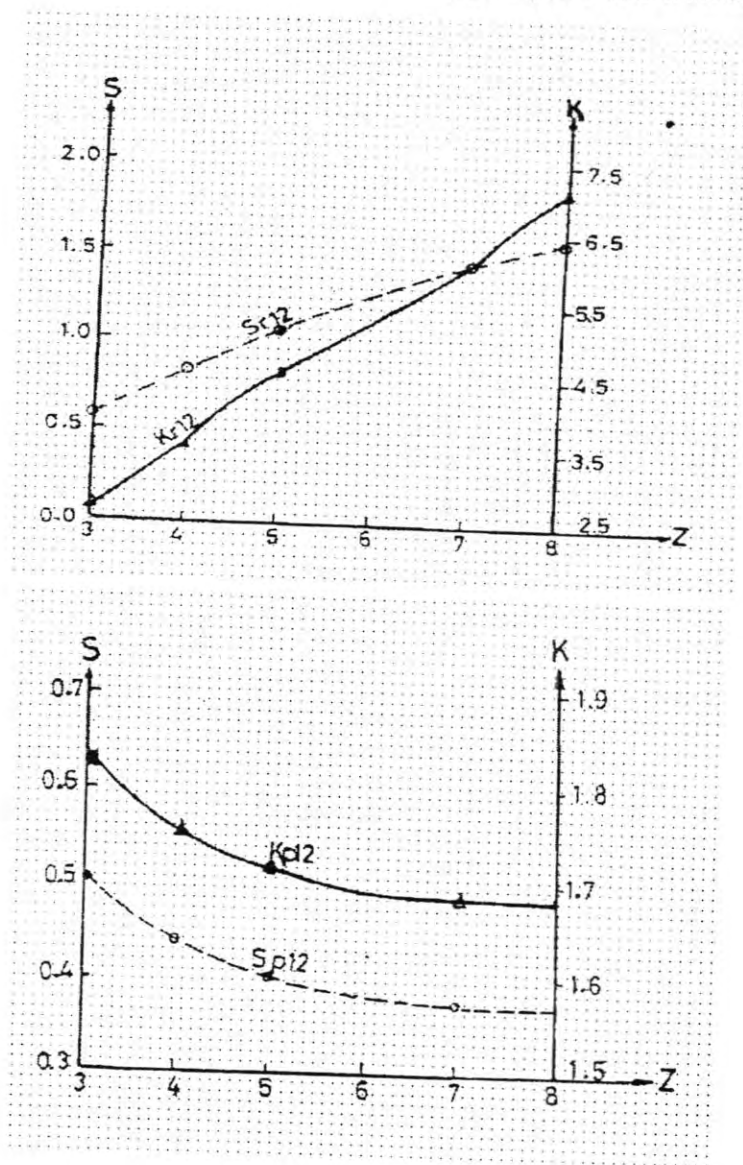


Figure 4: The Kurtosis and the Skewness coefficients for the functions are shown in figure 1. Plotted against Z.

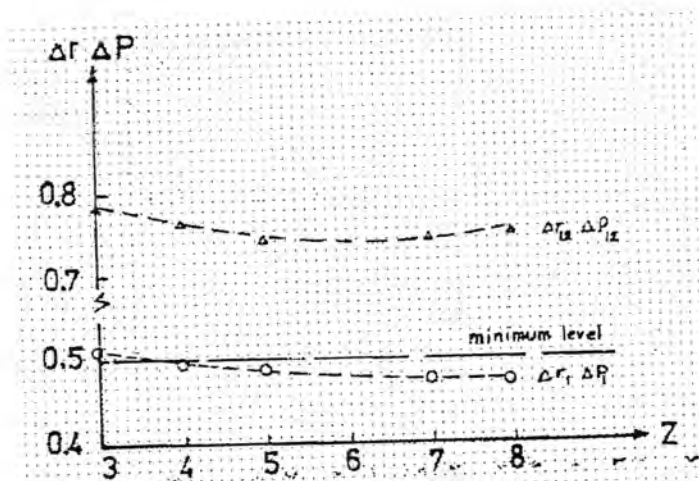


Figure 5: The product $\Delta r \Delta p$ from the data of figure 3, plotted against Z .

- their interpretation. J. Phys. 19: 2211-2225, (1986).
 Banyard K.E., K.H. Al-Bayati and P.K. Youngman:
 Electron correlation in momentum space: Z-dependent
 variations throughout a series of Li-like ions. J. Phys. B:
 At. Mol. Opt. Phys. 21: 3177-3189 (1988).
 6- Banyard K.E. Electron correlation in atoms and
 molecules J. Chem. Educ. 47: 668-671 (1970).
 7- Hahn G.J. and S.S. Shapiro. Statistical models in
 engineering, John Wiley & Sons, Inc., New York, 45-
 47 (1967).

Photostabilization of Polystyrene by Hindered Amines

F.M. AL-SALAMI

Chemistry Department, College of Science, University of Al-Mustansiriya, Baghdad

(Received Sept. 25, 1998; Accepted May 16, 1999)

الخلاصة

حضر وشخص في هذا البحث سبعة مركبات امينية معاقة فراغيا وتم استخدامها في عملية التثبيت الضوئي للبولي ستايرين. وتم تشخيص هذه الامينات بواسطة مطيافية الاشعة تحت الحمراء وبواسطة تحليل العناصر. وتمت دراسة الصفات الفيزيائية لها وهذه الامينات هي:

١. ن،ن'-ثنائي ايزوبوتيل ٥،٢،٥،٢-رباعي مثيل بنزيدين
٢. ن،ن'-ثنائي اثيل ٥،٢،٥،٢-رباعي مثيل بنزيدين
٣. ن،ن'-ثنائي سايكلو هكسيل ٥،٢،٥،٢-رباعي مثيل بنزيدين
٤. ن،ن'-ثنائي بروبييل بنزيدين
٥. ن،ن'-ثنائي سايكلو هكسيل بنزيدين
٦. ن،ن'-ثنائي اثيل بنزيدين
٧. ن،ن'-ثنائي مثيل بنزيدين

واستخدم الضوء الاحادي الموجة بطول ٣٢٠ نانومتر ودرجة حرارة ٦٠°م. وتمت متابعة عملية التجزئة الضوئية لرقائق البولي ستايرين بسمك ٣٠٠ مايكرون بوجود وعدم وجود مقاومات مطيافية واستخدمت الاشعة تحت الحمراء في المنطقة ١٧٠٠-١٨٠٠ سم^{-١} لحساب نسبة تكوين مجاميع الكربونيل خلال عملية التجزئة وحصول الاكسدة الضوئية. وقد وجد من خلال التجارب العملية ان نسبة كفاءة الامينات المحضرة كمثبتات ضوئية وكمانعات للاكسدة للبولي ستايرين كانت حسب الترتيب الاتي:

٧>٦-٥-٤>٣-٢-١

ABSTRACT

In this paper new hindered amine compounds were synthesized and identified by (infrared spectroscopy and by C.H.N. analysis). These compounds are

1. N,N'-diisobutyl 2,5,2,5-tetramethyl benzidine
2. N,N'-diethyl 2,5,2,5-tetramethyl benzidine
3. N,N'-dicyclohexyl 2,5,2,5-teramethyl benzidine
4. N,N'-dipropyl benzidine
5. N,N'-dicyclohexyl benzidine
6. N,N'-diethyl benzidine
7. N,N'-dimethyl benzidine

Irradiation was affected by fluorescent lamps at wavelength at 320nm about 60 C. The photodegradation process of for polystyrene films (thickness 300 u) without additives (control) and with hindered amines additives was followed by infrared spectroscopy, experimental results generally show that the additives as photostabilizers are decreasing in the following order:

1-2-3>4-5-6>7

INTRODUCTION

Antioxidants⁽¹⁾ are of major importance to the polymer industry because they extend the polymers useful temperature range and service life. The variety of antioxidants available and their specific uses have grown concomitantly with volume of polymers produced and the increase in types of synthetic polymers on the market.

An antioxidant is defined⁽²⁾ as a substance that opposes oxidation or inhibits reactions promoted by oxygen or peroxides. In the specific case of antioxidants for polymers, they are substances that retard atmospheric oxidation or the degradative effects of oxidation when added in small proportions, for this reason they are also known as aging retardants. Oxidative degradation by ozone, however, is controlled by antiozonants.

Two major areas of polymer deterioration protection are of concern. In the manufacture of synthetic polymers deterioration protection is needed during processing and storage. These protecting agents are often referred to as "stabilizers"⁽³⁾.

The generally accepted mechanics^(4,5) will be presented, with some of the differences of opinion briefly indicated.

Oxidation of polymers can lead to chain scission cross linking, or formation of oxygen-containing functional groups in the polymer or its degradation products. The object here is to summarize the role that antioxidants play in avoiding minimizing or slowing these adverse oxidative processes.

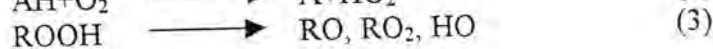
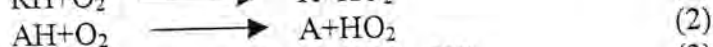
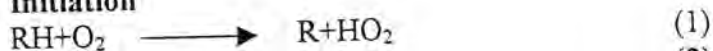
RH=polymer molecule, AH = antioxidants,

A= antioxidant radical, RO₂ = polymer peroxyradical and

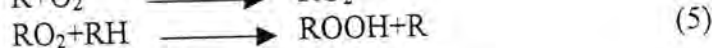
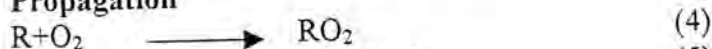
ROOH=polymer peroxide.

Initiation reactions are shown in equation 1-3, propagation I nequations 4 and 5, chain-transfer reactions in equations, and 7, and termination reactions in equations 8-10.

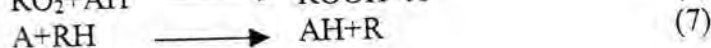
Initiation



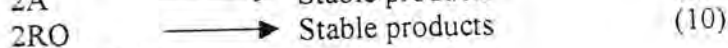
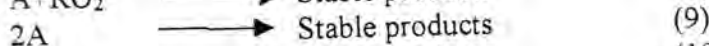
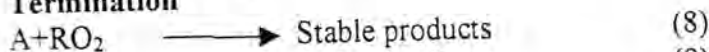
Propagation



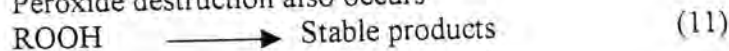
Chain transfer



Termination



Peroxide destruction also occurs



In addition to initiation reactions 1,2 and 3 other kinds of activation reactions can occur as represented by equation 12. In absence of initiators such as

Activation



The radical R may come from heat, light, or ionizing radiation⁽³⁾.

Antioxidants may retard oxidation by one or more of the proposed mechanisms, the phenolic and amine type antioxidants⁽⁴⁾ operates mainly through chain transfer and termination mechanisms. As represented by reaction 6 followed by reactions 8 and 9.

The compounds which are usually used to retard or inhibit these processes have traditionally been referred to as ((stabilisers)) in plastics technology and ((antioxidants)) in rubber technology⁽⁵⁾.

The first systematic attempt at developing efficient stabilisers resulted in the (uv-absorbers)). These were followed by the energy transfer agents or energy quenchers⁽⁶⁾.

The development of uv-stabilisers and their mode of action has received widespread interest in the field of research, all stabilisers are believed to owe their mode of action to some or all of the following mechanisms:

- 1- Ultraviolet screening
- 2- Ultraviolet absorption
- 3- Excited state deactivation or quenching
- 4- Freeradical scavenging and hydroperoxide decomposition

It is generally believed that 3 and 4 are the most effective^(6,7).

Studies of antioxidant action have provided indirect evidence for the importance of the same process in the thermal oxidative degradation of polymers.

It has been shown⁽⁸⁻¹³⁾ that the decomposition of hydroperoxides by non-radical reactions provides a powerful preventive antioxidant mechanism which is complementary to the kinetic chain breaking process

originally studied in detail by Bolland⁽¹⁴⁾ and elaborated by subsequent workers⁽¹⁵⁻¹⁷⁾.

Also photostabilizatic by hindered amines was studied⁽¹⁸⁾.

In this paper a new hindered amines of N,N-disubstituted benzidine compounds were synthesized and their effectiveness as photostabilizers for polystyrene films was investigated.

EXPERIMENTAL

Materials

All hindered amines were prepared by adding 1 mole of the propriate diamine and 2 mole of the halide in presence of sodium acetate, refluxed in acetone for 45 mins., while to yellow precipitate, was obtained, separated and recrystilized from T.H.F., dried under reduced pressure at room temperature. Table 1 shows some physical properties of the prepared hindered amines.

Technique

Polystyrene films of thickness =300 microns were made by mixing 0.5% by weight of different additive materials with polystyrene by using chloroform as a solvent as a solvent. The films were made in 5*5 cm pieces and mounted by wrapping them around an aluminium blank panel.

The panel holder is resting it in a slot on the accelerated weathering tester type (Q,UV).

Irradiation was performed by uv, 320nm, 10 watt, 1 amp and the temperature at 60°C during the irradiation experiments.

The degree of photodegradation process was determined by measuring the percent carbonyl group (%CO) generated during the photolysis process following the equation

$$\%CO = A/a. 1 \times 100$$

where

A= carbonyl absorbance at 1700 cm⁻¹

a= absorbitivity of polystyrene

I = thickness of sample in mils

1000 mils = 1.0 inch

Carbonyl index (CI) is determined by dividing the absorbance at 1700 cm^{-1} and the absorbance of the reference peak at 1800 cm^{-1}

$$\text{CI} = A_{1700} / A_{1800}$$

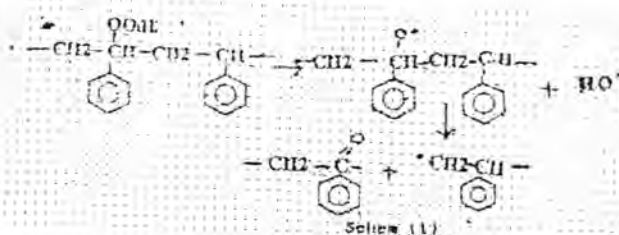
Infrared spectra were recorded by Perkin Elmer 1300 spectrophotometer. UV visible spectra were recorded by Hitachi U. 2000 spectrophotometer.

RESULTS AND DISCUSSION

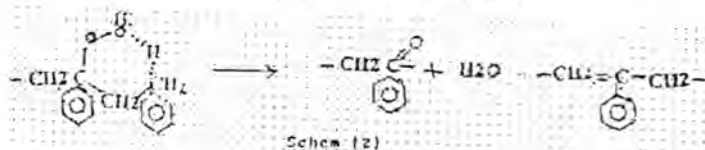
During the photo-oxidation of polystyrene two characteristic IR-absorption bands are formed:

At $3600 - 3400\text{ cm}^{-1}$ (attributed to the formation of the hydroxyl groups) and $1800 - 1700\text{ cm}^{-1}$ (attributed to carbonyl groups)⁽¹⁾.

Irradiation of polystyrene film at 60°C (fig.1) show the formation of IR peaks at 1685 cm^{-1} and 1725 cm^{-1} . The absorption at 1685 cm^{-1} was attributed to the carbonyl-group-stretching frequency of acetophenone⁽⁵⁾, which is due to from the polymer hydroperoxides can decompose according to the following reactions.



Another possible reaction for the formation of acetophenone from polymerhydroperoxide.



The rate of photodegradation of polystyrene films were followed by measuring the increase in carbonyl concentration (%CO) created during exposure to uv light with irradiation time. Figure 2 shows the variation of percent carbonyl (%CO) with irradiation time at 60°C for all types of polystyrene films.

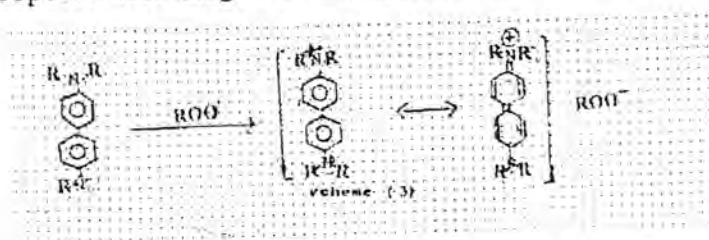
From figure 2 that all hindered amine compound 1,2,3 were the more effective in photostabilization of polystyrene films.

One additional method of radical interception involved with aromatic amines is through electron-transfer complexes.

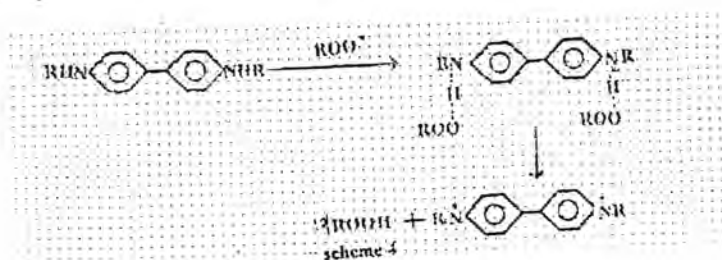
These are especially important where the nitrogens atoms are completely substituted such as N,N-disubstituted benzidine compounds where more active stabilizer.

The electronic effects of substituents in aromatic hindered amines leads to increased activity, attributed to more conjugation of biphenyl in benzidine compounds.

According to the experimental results obtained mechanisms of photostabilization of PS films were proposed according to uv absorption as in scheme 3.



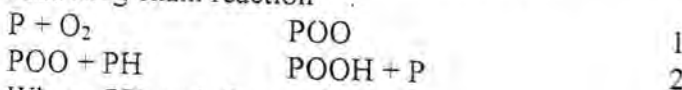
Also chain breaking acceptors (CB-A) antioxidants were proposed according to uv absorption as in scheme 4⁽¹⁹⁾.



The photodegradation rate determining step which is found to be directly proportional to the square root of carbonyl index $(CI)^{1/2}$.

The relationship between $(CI)^{1/2}$ and irradiation time for some of the stabilized and nonstabilized polystyrene films, is illustrate the straight line as in fig(3). This straight line relationship indicates that the photodecomposition of the additives is first order reaction.

The photodegradation of polystyrene involves the following chain reaction⁽²⁰⁾



Where PH and P are the polystyrene molecules and its macroradical respectively. Reaction (2) is the photodegradation rate determining step which is found to be directly proportional to the square root of carbonyl index $(CI)^{1/2}$.

The induction period (t_{in}) which is the period of retarded antioxidation of polymer, shown in fig. 2, also illustrate that the additive used as uv absorber radical scavenger is longer than the induction period shown I nPS film without additive (control).

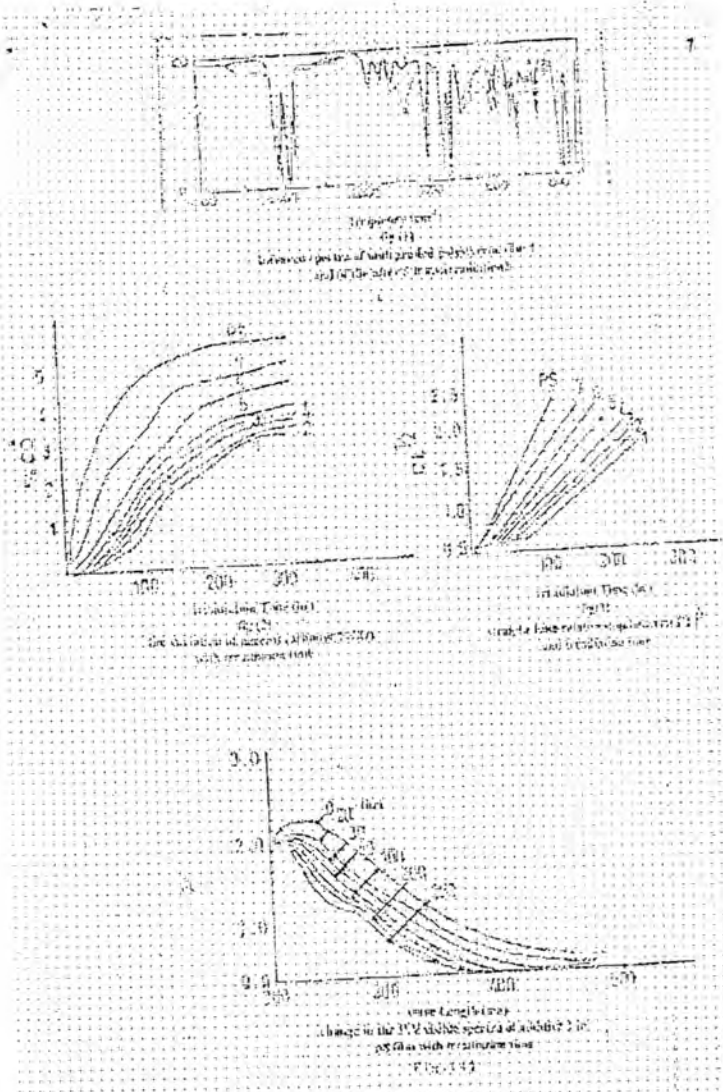
Fig. (4) shows the change in the uv visible spectra of additive 1 in polystyrene film with irradiation time, shows fair stability against photo decomposition.

Experimental results generally show that the hindered amines as photostabilizers are decreasing in the following order

1-2-3>4-5-6>7

Table 1: Some physical properties of the prepared new hindered amines

	Compound	Chemical formula	Mol. Wt gm/mol	Melting point C	-IR absorption cm ⁻¹	C.H. Analysis					
						C		H		N	
						Exp	Theo	Exp.	Theo	Exp.	Theo
1	N,N-di isobutyl 2,5,2,5 tetramethyl benzidine		324	>370	NH= 3350	80.7	81.48	10.1	9.87	9.2	8.6
2	N,N-diethyl 2,5,2,5 tetra methyl benzidine		286	>360	NH = 3360	82.1	83.91	10.2	9.79	9.5	9.7
3	N,N-dicyclo hexyl 2,5,2,5 tetra methyl benzidine		404	> 360	NH = 3360	81.1	83.58	9.31	9.9	8.1	6.9
4	N,N-dipropyl benzidine		272	340	NH = 3350	80.0	79.41	9.51	10.29	9.2	10.2
5	N,N-dicyclo hexyl benzidine		348	355	NH = 3350	81.5	82.75	9.72	9.14	8.5	8.04
6	N,N-diethyl benzidine		240	350	NH = 3350	81.2	80.0	9.5	8.33	10.1	11.6
7	N,N-dimethyl benzidine		212	375	NH = 3340	80.8	79.24	8.2	7.54	10.8	11.2



REFERENCES

1. C.C. Davis and J.T. Blak, eds Chemistry and Technology of Rubber, Reinhold Publishing Corp. New York (1937).
2. W.O. Landberg, ed., Autoxidation and Antioxidants, Vols. 1 and 11, Interscience Publishers, a division of John Wiley and Sons, Inc., New York (1961).

3. K.U. Ingold, (Inhibition of the Autoxidation of Organic Substances in the Liquid Phase) *Chem. Res.* 61, 563, 589 (1961).
4. J.R. Shelton, *Rubber Chem. Technol.* 30, 1251-1200 (1956).
5. B. Ranby and J.F. Rabek *Photodegradation, Photooxidation and Photostabilisation of polymers.* Wiley, New York (1975).
6. O. Cicchetti, *Adv. Polym. Sci.* 7, 70 (1970).
7. G. Scott, in *Developments in polymer degradation*. 1(N. Irrassie ed.) Applied Science Publishers, London, 205 (1977).
8. G. Scott, *Atmospheric Oxidation and Antioxidants*, Chapter 5, London and New York, Elsevier, (1965).
9. J.D. Holds Worth, G. Scott and J. *Appl. Polym. Sci.* 13P. 1329 (1969).
10. G. Scott and P.A. Shearn, *J. Appl. Poly. Sci.* 13 P1329 (1969)
11. C. Armstrong, M.A. Plant and G. Scott, *Eur. Polym. J.* 11 P. 161 (1975).
12. G. Scott. *Eur. Polym. J. Suppl. P.* 189 (1969).
13. K.J. Humphris, and G. Scott, *pure Appl., Chem.* 36 p16 (1973).
14. J.L. Bolland and P. Have, *discuss Faraday Soc.* 2p 252 (1974).
15. C.E. Boozer, G.S. Hammond, C.E. Hamilton and J.N. Sen, *J. Am. Chem. Soc.* 77 p3233, 3238 (1955).
16. A.F. Bickel and F.C. Kooyman. *J. Chem. Soc.* P321 (1953), P2215 (1956) p2217 (1957). P2415 (1957).
17. D.S. Davies. H.L. Goldsmith. A.K. Gupta and G.R. Lester, *J. Chem. Soc.* 4926 (1956).
18. N.C. Billingham, *Polym. Comm.* Vol. 25, 235 (1984).
19. M.A.J. Al-Moudaris M.Sc. thesis, Mustansiriah University College of Science Chemistry Dept., Baghdad (1996).
20. C.E. Boozer and G.S. Hammond. *J. Am. Chem. Soc.* 76, 3861-3862 (1954).

Preparation of New Acetylenic Amines of Expected Pharmacological Activity

ABDUL-HUSSAIN KHUTHEIR AND ADIL O. ABDEL BAGI

Department of Chemistry, College of Science, University of Al-Mustanisiya, Baghdad-Iraq

(Received Dec. 7, 1999; Accepted May 14, 2000)

الخلاصة

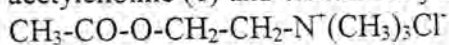
تم تحضير وتخصيص عدد من مركبات الامينات الاسيتيلينية ذات
الاهمية الدوائية والمستقاة من الحوامض الامينية والامينات الثانوية الحلقية.

ABSTRACT

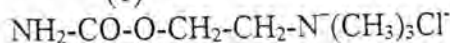
A number of expected pharmacologically important acetylenic amines derived from amino acids and a secondary cyclic amines have been synthesized and characterized.

INTRODUCTION

Acetylenic amines constitutes a class of chemical compounds, that have received little attention despite the fact that a number of them are pharmacologically active compounds⁽¹⁾, which resemble in some cases that of acetylcholine (1) and carbaminolcholine (2).

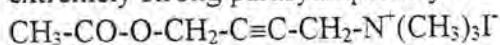


(1)



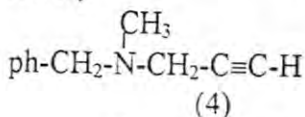
(2)

Compounds (1) & (2) are known to have a parasympathomimetic activity⁽²⁾. It has been found that the introduction of acetylenic function enhances the parasympatholytic effect as in 4-acetoxy-2-butynyltrimethyl ammonium iodide⁽³⁾ which has an extremely strong parasympatholytic activity⁽³⁾.



(3)

Moreover, a noticeable example is pargyline (N-benzyl-N-methyl pro-2-ynyl amine (4), an inhibitor of mono amine oxidase and is effective also as anti hypertensive drug but its use is limited because of its toxicity⁽³⁾.

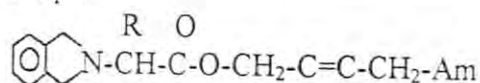


Also acetylenic moiety was found to be of great importance in other acetylenic amines such as N-(4-morpholino)-2-butyne acetate, which showed a moderate activity against leukemia⁽⁴⁾.

RESULTS AND DISCUSSION

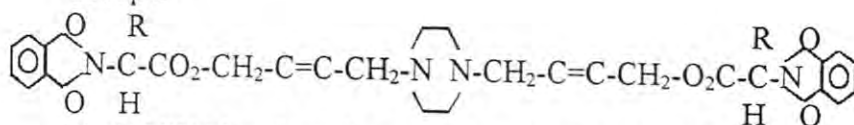
Two categories of acetylenic amines group (1 and 2) that are expected to show pharmacological activity as oxotremorine antagonists have been synthesized through the Mannich reaction in basic medium by the following route (Scheme)

Group 1



4(N-tert-amino)-2-butyne-2-phthalimido acetate or propionate

Group 2

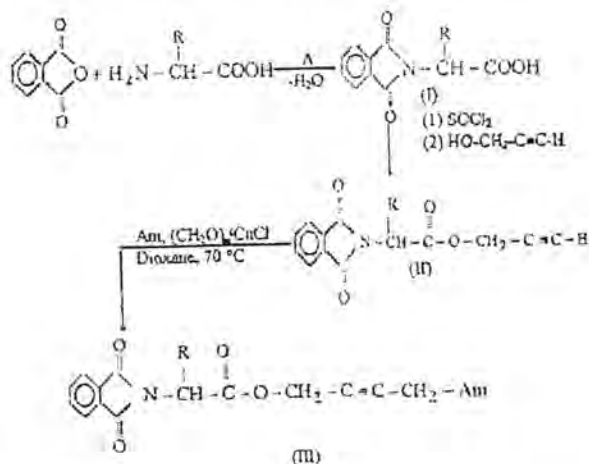


Bis-N,N'[(4-but-2-ynyl,2-phthalimido acetate) piperazine.

In the synthesis of these new compounds we used three amino acids namely, glycine, DL-alanine and L-Asparagine; hoping to prepare new biologically active compounds.

Moreover, in group (2) we selected piperazine as the secondary amine in order to obtain compounds with two phthalimido groups and two 2-butyne chains, so as to increase the known biological activity of piperazine itself. Such modifications may enhance the pharmacological properties of phthalimido compounds originally prepared by Dalhborg⁽⁵⁾.

Scheme



Group 1			Group 2		
	R	Am		R	Am
a	-H	Piperidine	g	-H	piperazine
b	-CH ₃	piperidine	h	-CH ₃	piperazine
c	-CH ₂ -CO-NH ₂	Piperidine	i	-CH ₂ -CONH ₂	Piperazine
d	-H	Morpholine			
e	-CH ₃	Morpholine			
f	-CH ₂ CO-NH ₂	Morpholine			

The synthesized products were collected as solid compounds, purified by recrystallization and column chromatography using chloroform as eluent. These compounds were characterized via spectroscopic data. Elemental analysis (C.H.N.) agrees well with the proposed formula. Tables (3&4) show the properties of the acetylenic amines of groups 1&2 respectively.

In propargyl esters (II) the I.R. spectrum shows the presence of $\nu_{C\equiv C-H}$ bond stretch, at $3300-3280\text{cm}^{-1}$ and $\nu_{C\equiv C}$ bond stretch in the range of $2125-2110\text{cm}^{-1}$.

Upon conversion to the Mannich product (III), the band at $3300-3280\text{cm}^{-1}$ ($\nu_{C\equiv C-H}$ disappeared as expected, while the band which is responsible for $(C=C)$ stretching appeared as a weak band in range $(2260-2160\text{cm}^{-1})$ in the I.R. spectrum of the Mannich product of group 1. But it did

Preparation of New Acetylenic Amines of Expected Pharmacological Activity

A. H. Khutheir And A. O. Abdel Bagi

not appear in the I.R. spectrum of the Mannich product of group 2. This is understandable in terms of the highly symmetrical molecules of group 2, so the vibrational stretching of $C\equiv C$ will not cause a change in dipole moment & thus this band will be I.R. inactive.

The 1H Nuclear Magnetic Resonance spectrum, compound (IIIId) as a representative example of group 1 and compounds IIIg & IIIh from group 2 (tables 3&4) respectively, gave the expected signals according to the proposed structures. The CH_2 protons on both sides of $C=C$ bond appear as two triplets due to long range coupling.

The Ultraviolet spectrum of the acetylenic amines of groups 1&2 showed bands due to $\pi-\pi$ transitions. The λ_{max} values are found in tables 3&4.

EXPERIMENTAL

General Procedure for Preparation of N-Phthalyl Amino Acids⁽⁶⁾

A mixture of amino acid (0.05mole) and phthalic anhydride, 0.05 mole (7.4g) was placed in a pyrex test tube, the tube was placed in an oil-bath preheated to 180-185°C for 15 min. The mixture was stirred occasionally for the first 10 min. the phthalic anhydride which sublimed and deposited on the walls of the test tube was pushed down into the reaction mixture by means of a glass rod.

The mixture was left undisturbed during the remaining five min. The test tube was then inverted and the walls were scraped out. The residue was recrystallized from water. Table 1 shows the properties of these derivatives.

Table 1 some properties of N-phthalyl amino acids (I)

cpd	-R	yield	M.P.	Formula	Elemental analysis Cal. % (found %)		
No.		%	°C		C	H	N
1	-H	90	190-92	C ₁₀ H ₇ NO ₄	58.51 (57.80)	3.41 (3.12)	6.83 (6.39)
2	-CH ₃	88	157	C ₁₁ H ₉ NO ₄	60.27 (59.51)	4.11 (3.92)	6.39 (6.20)
3	-CH ₂ CONH ₂	78	185-88	C ₁₂ H ₁₀ N ₂ O ₅	54.96 (54.95)	3.81 (3.80)	10.68 (9.54)

General Procedure for Preparation of N-Phthalyl Amino Acid Propargyl Esters⁽⁷⁾ (II, Scheme)

A mixture of N-phthalyl amino acid (I) 0.01 mole and excess of thionyl chloride was refluxed gently on a water bath in a hood for 30 mins. using a drying tube filled with anhydrous CaCl₂. The excess thionyl chloride was evaporated from the reaction mixture under reduced pressure, and then an excess propargyl alcohol was added. The flask was allowed to stand on the water bath for further 30 mins, then transferred to a separatory funnel, washed with (3x20)ml of 10% sodium carbonate and dried over magnesium sulfate, filtered and evaporated under reduced pressure to give the product. The properties are listed in table 2 below.

Table 2: Some properties of N-phthalyl amino acids propargyl esters (II, scheme)

cpd	-R	yield	M.P.	Formula	Elemental analysis Cal. % (Found %)		
No.		%	°C		C	H	N
1	-H	66	95-96	C ₁₃ H ₉ NO ₄	64.19 (64.40)	3.70 (4.10)	5.76 (5.32)
2	-CH ₃	70	75	C ₁₄ H ₁₁ NO ₄	65.36 (64.40)	4.28 (4.10)	5.44 (5.03)
3	-CH ₂ CONH ₂	50	oily	C ₁₅ H ₁₂ N ₂ O ₅	64.19 (64.40)	4.01 (3.70)	9.36 (8.90)

General Procedure for Preparation of Acetylenic Amines Through Mannich Reaction in Basic Medium^(8,9)

A mixture of the acetylenic compound, (N-phthalyl amino acid propargyl ester II), 0.003 mole, paraformaldehyde (0.0033 mole) and appropriate secondary amine (0.033mole) and catalytic amount of cuprous chloride (25mg) in 10 ml peroxide free of dioxane was heated at 70°C for 3 hours with continuous stirring. The mixture was cooled down, filtered and 25ml of water was added to the filtrate. The crude product was collected and recrystallized from a mixture of chloroform and ether or purified by neutral alumina column using chloroform as eluent to produce pure solid compounds. The properties of new acetylenic amines are shown in tables (3&4).

Table 3: Properties of Acetylenic amines of group (1) IIIa-f) 4-(N-tert-amino)-2-butynyl, 2-phthalimido acetate or substituted propionate

cpd. No.	yield %	M.P. C°	I.R. cm ⁻¹		UV λ_{\max}^a	Elemental analysis Cal. % (found %)			¹ HNMR (δ)ppm. of some of the prepared cpds
						C	H	N	
IIIa	45	160	1730	2160	231.0, 292.0	67.05 (66.97)	5.88 (5.95)	8.23 (7.30)	
IIIb	55	179-80 (dec.)	1730	-	229.5, 292.0	67.79 (67.74)	6.21 (6.02)	7.91 (6.94)	
IIIc	35	174-6	1730	2210	233.0, 291.5	65.96 (66.10)	5.75 (4.98)	7.32 (7.20)	
IIId	50	170-1	1720	2260	232.0, 257.0	63.16 (63.67)	5.26 (4.94)	8.19 (8.10)	(7.7)[m,Ar-H];(4.0)[t,O-CH ₂ C=C]; (3.55)[m,O(CH ₂) ₂];(3.25)[S,N-CH ₂]; (2.95)[t,=C-CH ₂ -Am]; (2.65)[m,N(CH ₂) ₂]
III e	65	183-4 (dec)	1720	2190	238.5, 292.0	64.04 (64.84)	5.61 (5.21)	7.86 (6.79)	
III f	50	168-9	1720	2200	236.0, 293.0	60.15 (60.31)	5.26 (5.04)	10.50 (9.88)	

a = Solvent methanol

Table 4: Properties of Acetylenic amines of group (2) (IIIg-i) Bis-N,N'[4-but-2-ynyl, 2-phthalimido acetate] piperazine

cpd. No.	yield %	M.P. C°	I.R. cm ⁻¹		UV λ_{\max}^a	Elemental analysis Cal. % (found %)			¹ HNMR (δ)ppm. of some of the prepared compounds
			$\nu_{C=O}$	$\nu_{C\equiv C}$ C-N		C	H	N	
IIIg	80	172-3	1720	- 1200	238.5, 292.5	64.49 (63.93)	4.79 (5.20)	9.30 (8.19)	(7.7)[m,Ar-H]; (4.7)[t,O-CH ₂ -C \equiv C]; (4.35)[T, \equiv C-CH ₂ -Am]; (3.3)[S,N-CH ₂] (2.5)[S,CH ₂ piperazine]
III h	75	152 (dec.)	1755 1720	- 1220	238, 292	65.12 (65.18)	5.12 (4.91)	8.97 (8.50)	(7.75)[m,Ar-H]; (4.8)[t,O-CH ₂ -C \equiv]; (4.45)[t, \equiv C-CH ₂ -Am]; (3.2)[2,N-CH] (2.49)[S,CH ₂ piperazine]; (1.5)[d,C-CH ₃]
III i	48	165-6	1730	- 1200	236, 291	63.34 (62.84)	4.98 (4.81)	8.21 (7.96)	

a= solvent methanol

b= These compounds did not give acetylenic stretching band (see Results & Discussion)

REFERENCES

1. R.B. Barlow, "Introduction to Chemical Pharmacology" 2nd. Ed. Methuen and Co., London, p. 221 (1964).
2. Richard Dahlbom, Birgitta Erbing & K. Olsson. Acta Pharmaceutica Suecia-Acetylene Compof Potential Pharmacological value 6, 349-358(1969).
3. R. Pirisino, G.B. Ciottoli, F. Buffoni, B. Anselmi and C. currach, BR. J. Clin. Pharmacol., N- Oxidation of Pargyline 7, 595, (1979).
4. A.H. Khutheir, F.T. Abachi, Iraqi, طريقة تحضير وفعالية المركب (٤-مورفولينو-٢-بيوتيل) الخلات Patent 2511 (1993).
5. U. Svensson, R. Dahlbom, and M.R. Blair, Acta pharm. suecica, Acetylenic compounds of potential pharmacological value XIX, 12, 290 (1975).
6. J.H. Billman, W.F. Harting. Amino acids V. Phthalyl Derivatives J. Am. Chem. Soc. 70, 1473, (1948).
7. J. Baldwin "Experimental Organic Chemistry" 2nd. Ed. Mc. Graw-Hill Book Company, Kogakusha Company, TOKYO p 120, (1970).
8. A.H. Kutheir and F.T. Abachi, N-Oxidation of pharmacological important acetetylenic amines, J Iraqi Chem. Soc., 12, No. 2, (1987).
9. J. H. Abdulwahid, Preparation of some acetylenic amines derived from piperazine (M.Sc. thesis), Univ. of Al-Mustansiriya, (1993).

Synthesis of N-(2,4-Dinitrophenyl)-N'-(Substituted)-1,4-Diamino-2-Butynes

MAZIN J. HABIB

Department of Chemistry, College of Science, Al-Mustansiriyah University, Baghdad-Iraq.

(Received Feb. 22, 1999; Accepted Nov. 2, 1999)

الخلاصة

يتناول البحث تحضير ٤،٢-ثنائي نايتروبنزين بروبيل أمين، وذلك بمفاعلة ٤،٢-ثنائي نايتروكلوروبنزين مع أمين البروبيل، ثم ادخال هذا المركب بتفاعل مانح لغرض تحضير مجموعة من مركبات الامينات الاستيلينية الجديدة، والتي يتوقع لها فعالية بايولوجية مضادة للاستيل كولين والهستامين. شخّصت المركبات المحضرة بالتحليل الدقيق للعناصر وبطييف الاشعة تحت الحمراء.

ABSTRACT

Six new acetylenic amines derived from 2,4-dinitrobenzene propargyl amine have been synthesized. These compounds are characterized by (I.R) spectrometer and elemental analysis.

INTRODUCTION

Acetylenic drugs are frequently more active, less toxic, and more easily absorbed into the body than their olefinic or saturated analogs⁽¹⁾.

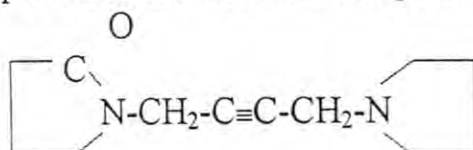
Propargylic amines could be used as anticancer and hypotensive agents⁽²⁾.

According to the basic medicinal theory which states that "making a chemical change on a compound which acts as a cause of the disease may lead to obtaining a compound having an effectiveness that makes it's effect miscarry", therefore, many acetylenic amines similar to oxotremorine⁽¹⁾ were prepared using "Mannich reaction"^(3,4,5), some of these compounds have

biological and pharmacological activities better than those of currently available anticholinergic compounds (having no side effects)⁽⁶⁾.

In this work, a new series of substituted acetylenic amines was synthesized. This involved the reaction of 2,4-dinitrochlorobenzene with propargyl amine in the presence of triethyl amine as a base.

Then followed by "Mannich reaction" on 2,4-Dinitrophenyl propargyl amine. An anticholinergic and antihistaminic activities are expected to the resultant compounds.



[1]

Experimental

Melting points were determined on a capillary Thomas Hoover melting point apparatus model 6427-F10 and are uncorrected. The IR spectra were recorded on a Pye-Unicam model Sp₃-100 spectrophotometer as KBr disc.

Elemental analysis was performed on a CHN analyzer type Heraeus at the chemical Laboratories of the Ministry of Industry and Minerals.

Materials

2,4-Dinitrochlorobenzene (BDH chemicals), propargyl amine (99% Aldrich chemicals), all the secondary amines used in "Mannich reaction"

[Table 1] were of high purity (BDH chemicals) and (Aldrich chemicals).

Preparation of N-(2,4-Dinitrophenyl) Propargyl amine [2]^(7,8)

Propargyl amine (0.006 mol.) was added dropwise with stirring during (15min) into 2,4-dinitrochlorobenzene (0.004 mol), then few drops of triethyl-amine (Et_3N) was added.

The mixture was refluxed on an oil bath at 70°C for 2 hours. Ice water (20ml) was then added to the mixture. The white precipitate which separated, was filtered and recrystallized from acetone (55% yield).

C.H.N. analytical results are given below:

Analysis %					
Calculated			Found		
C	H	N	C	H	N
49.76	1.38	19.35	49.23	1.15	19.26

Preparation of Acetylenic Amines by "Mannich Reaction"-General Procedure⁽⁹⁾

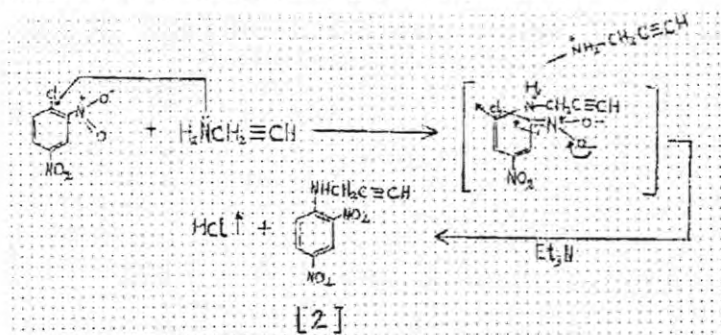
A mixture of N-(2,4-dinitrophenyl) propargyl amine (0.66 gm) (0.003 mol) and formaldehyde (0.07 ml of 37%) (0.003mol) was dissolved in (10ml) of dioxane (free from peroxide). Then a small amount of CuCl was added as a catalyst.

The mixture was heated on a water bath to (70°C) and the secondary amine (0.003mol) was added dropwise. Heating and stirring continued at the above temperature for one hour.

Ice water (15ml) was added to the reaction mixture. The white precipitate which separated was filtered and recrystallized. The physical properties of the synthesized compounds are given in Table 1.

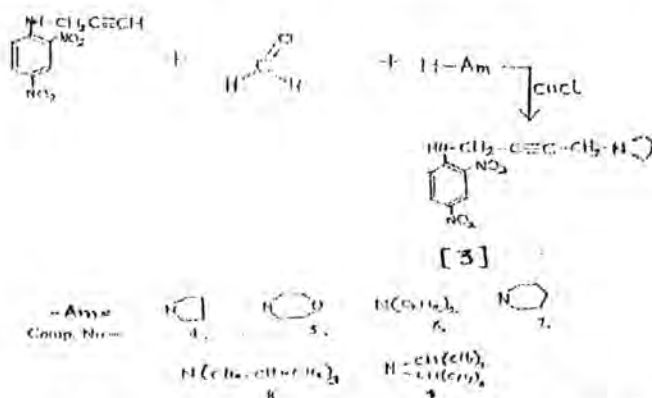
RESULTS AND DISCUSSION

The suggested mechanism of the reaction of propargyl amine with 2,4-dinitrochlorobenzene is addition-elimination⁽¹⁰⁾. The first step involves the attack of the amine on 2,4-dinitrochlorobenzene (an activated aryl halide). This step is followed by the elimination step in which the chloride leaves to give compound (2).



Compound (2) was characterized by its IR spectrum, whereby the symmetrical stretching band of N-H for the secondary amines at 3320cm^{-1} and symmetrical stretching band of C-H at 3280cm^{-1} in addition to the aromatic symmetrical stretching band of C=C at 1590 and 1420cm^{-1} appeared, in addition to the verification of the molecular formulae of the resultant compounds from the theoretical and experimental values of (C.H.N.) analysis.

Reaction of compound (2) with a number of secondary amines and formaldehyde in the presence of Cuprous chloride as catalyst afforded six new acetylenic amines (3) with the following mechanism⁽¹¹⁾.



The structure, physical properties and IR spectral data of the synthesized compounds are given in Table (1), where the absorption band of $\equiv\text{CH}$ group at (3280cm^{-1}) of all the prepared compounds disappeared. This indicates that "Mannich reaction" was successfully conducted.





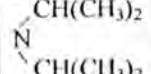
The absorption band ranges of symmetrical stretching band of (aryl-N-II) appeared at $(3320\text{cm}^{-1}-3345\text{cm}^{-1})$ and the symmetrical stretching band of NO_2 appeared at $(1400\text{cm}^{-1}-1520\text{cm}^{-1})$ while the aromatic stretching band of $(\text{C}=\text{C})$ appeared at $(1470\text{cm}^{-1}-1600\text{cm}^{-1})$.

REFERENCES

1. T.F. Ruffledge "Acetylenic Compounds", Reinhold Book Corp., New York, 314(1968).
2. S. Fujiki, "Synthesis of acetylenicamines" Nippon Kagaku Zasshi, 87, 189, (1996); Chem. Abst., 65, 15215 (1996).
3. Mousa, N." Synthesis of series of acetylenic compounds of pyroglutamic acid with potential biological activity", M.Sc. thesis, Baghdad University, Iraq (1976).
4. Dahlbom, R. and Karlen, B. "Acetylene compounds of potential pharmacological value, VIII, studies on N-(4-dialkylamino-2-butylnl)-substituted cyclic imides", J. Med. Chem., 6: 843-6 (1966).

Synthesis of N-(2,4-Dinitrophenyl)-N'-(Substituted)-1,4-Diamino-2-Butynes
M. J. Habib

Table 1: Some properties, IR spectral data and CHN analysis of Acetylenic amines⁽⁴⁻⁹⁾

Comp. No.		Melting point C	Yield %	Solvent used for recrystallization	I.R. spectral data cm ⁻¹				Molecular formula	Analysis % (Calculated) found		
					V _{asy} arom C=C	V _{asy} arom NO ₂	δ _{NH}	V _{N-H}		C	H	N
4		129 ± 1 dec	47	Acetone	1590 1480	1520	1350	3340	C ₁₄ H ₁₇ N ₄ O ₄	(55.08) 55.10	(5.57) 5.62	(18.36) 18.28
5		213 dec	42	Ethanol-water	1590 1470	1510	1360	3345	C ₁₄ H ₁₇ N ₄ O ₅	(52.33) 52.30	(5.29) 5.11	(17.44) 17.50
6	N(C ₂ H ₅) ₂	112dec	59	Acetone	1600 1470	1510	1355	3325	C ₁₄ H ₁₉ N ₄ O ₄	(54.72) 54.68	(6.18) 6.09	(18.24) 18.20
7		182± 1dec	53	Ethanol-water	1580 1460	1515	1350	3320	C ₁₅ H ₁₉ N ₄ O ₄	(56.42) 56.33	(5.95) 5.89	(17.55) 17.52
8	N(CH ₂ CH=CH ₂) ₂	122± 1dec	62	Ethanol-water	1590 1500	1400	1360	3340	C ₁₆ H ₁₉ N ₄ O ₄	(58.0) 58.1	(5.74) 5.71	(16.91) 16.83
9		126 ± 1dec	49	Acetone	1580 1470	1500	1365	3330	C ₁₆ H ₂₃ N ₄ O ₄	(57.31) 57.26	(6.86) 6.76	(16.71) 16.82

5. Linaquist, A., B. Svensson, J., and Dahlbom, R., "Acetylene compounds of potential pharmacological value, XXI, Some optically active N-(4-tert.-amino-1-methyl-2-butnyl)- substituted succinimides and 2-pyrrolidones and their absolute configurations"; *Acta. Chem. Scand. Ser. B*, 30, (60): 617-20 (1976).
6. Karlen, B., Lindeke, B., and Lindgren, S., "Acetylene compounds of potential pharmacological value, XIV, studies on N-(1-amino alkynyl)-substituted succinimides and maleimides", *J. Med. Chem.*, 14: 651-8 (1970).
7. Meadow, J.R., and Reid, B.E., "Pseudosaccharin chloride, agent for the identification of alcohols", *J. Am. Chem. Soc.* 65: 457-8 (1987).
8. Salman, S.R., Shubber, A.K., Hussein, F.A., Shubber, S.K., "Preparation of some pseudosaccharin allylethers and saccharin anils", *J. Chem. Eng. Data* 32(3): 392-3 (1987).
9. Salvador, R.L., and Simon, D., "A study of the Mannich reaction with propargyl alcohol", *Canadian J. chem.*, 44, 2510-5 (1966).
10. Hettler, "Chapman Mumm rearrangement of pseudosaccharing ethers" *Tetrahedron Letters*, 15, 1793-6 (1968).
11. Reid, W., and Neskelborg, K., "Effect of tert. Amines on O-metalic arylhalides III", *Ann. Chem.*, 635: 97 (1950).

The Role of Tide Modifying Factors in the NW Arabian Gulf

HASSAN H. SALMAN

Department of Meteorology, College of Science, Al-Mustansiriya University

(Received Feb. 28, 2000; Accepted May 21, 2000)

ABSTRACT

This study implies an assessment to the role of the tidal modifying factors in the Iraqi marine waters in terms of energy of the system. These factors include hydraulic energy gradient discharge, channel width and depth these factors were investigated in three sections: Shatt Al-Arab at Fao, Khor Abdallah near Wrbah spit and Khor Al-Zubair. Funneling phenomenon was clear as proved by tidal amplitudes and energy levels. Estuarine effects on the tides are manifested only at Shatt Al-Arab section.

INTRODUCTION

Iraqi marine water, though it is very limited in geographical extent, it is a field where various physical parameters are acting in a way so as to represent a unique physical system. This could take place every time and everywhere as long as these parameters are available. The specificity of this system is the result of modification of the action of these physical parameters. This paper tries to deal with one phenomenon, i.e. the tide, hopefully giving an analysis of tidal features of an area characterized by shallow depths, considerable amount of fresh water input, presence of bays (Khors), besides the interference with meteorological elements. A map showing the location of three sections on the studied area is given in figure 1.

The tidal characteristics of the Arabian Gulf are rather complex. Many varieties of tidal types are encountered. All are mixed ranging from predominately semi-diurnal in the northern and western parts of the gulf to predominately diurnal in the central parts⁽¹⁾.

The Role of Tide Modifying Factors in the NW Arabian Gulf

H. H. Salman

Another feature is the relatively high tidal ranges throughout the Gulf. It exceeds three meters at Shatt Al-Arab and is over one meters everywhere⁽²⁾.

The main distinctive factor that affects the tide in the northern part of the Arabian Gulf is the Shatt Al-Arab river flow.

Shatt Al-Arab length is about 190km and the average width approximates 500m. Downstream Basrah. The depth varies from 8-15m⁽³⁾.

Mean water level of Shatt Al-Arab at Fao (about 10km to the north of the sea coast) ranges from 0-0.41m, being 0.25-1.81m (G.T.S) for wet (1988) and dry (1989) years respectively Fig (2)⁽⁴⁾.

The discharge of Shatt Al-Arab is also varying depending on the hydrometeorological factors in the catchment areas of Tigris, Euphrates and Karun rivers. Hydrographs of Shatt Al-Arab at Fao are given in figure (3)^(3,4).

The flow rate of Shatt Al-Arab water and the tidal regime particularly at the head of the Gulf are the main mutually dependent factors in the estuarine region^(2,3).

The existence of several bays in the Arabian Gulf represents another structural feature, which may complicate the tidal regime particularly in the northern parts of the Gulf. Khor Al-Zubair, Khor Abdallah and Khor Al-Ammayah are only examples. Recently, Khor Al-Zubair is connected to Basrah Canal, which collects the drainage of leaching saline soils of the middle and lower Mesopotamian Plain. This has converted this bay to a new artificial estuary with certain physical and environmental implications, all of which are of vital importance to oceanographers and environmentalists.

Data and Method

Hydrological and oceanographic data were accumulated through the survey of the Iraqi marine water and Shatt Al-Arab during several years of research and routine activities^(5,6,7).

Water depths were recorded for Shat Al-Arab at Fao, Khor Abdallah and Khor Al-Zubair on hourly basis for a complete tidal cycle at each station using echosounder. Alongwith, water velocity measurements were taken by current meter. Both instruments after being calibrated were mounted on a mooring boat in the navigation channels of Shat Al-Arab, Khor Abdallah and Khor Al-Zubair. In each case boat were anchored from front and rear sides to avoid rotation when the tide changes direction.

Data accumulated were representative of tidal phases covering a wide range of hydrological variabilities. These data were suitably adequate for the study of factors affecting the tidal regime in the area.

It is suggested here that a comprehensive treatment to the action of the factors modifying the tides in this area might deal with the energy of the system. Tide at the mouth of river entrance causing height variation to move up through the estuary and even rivers themselves. The tidal wave penetrating up the estuary is modified as a result of change of width and/or depth, friction and of river discharge.

Ignoring friction the wave energy flux will remain constant as the wave advances up the estuary i.e.

$$E = ga^2 \quad (1)$$

Where E is wave group energy in joule. m/kg, g is the acceleration due to gravity in m/sec² and a is the amplitude in m.

$$K = EBC \quad (2)$$

$$C = \sqrt{gd} \quad (3)$$

Where B is the breadth in m, C is the celerity in m/sec, and d is the water depth in m. Substituting 1 and 3 in 2.

$$K = (\rho ga^2 B \sqrt{gd})/2 \quad (4)$$

Where ρ is the density of water in kg/m³

The energy of the tidal wave is faced by river flow energy (kinetic) E_k given in joule

$$E_k = mv^2/2 \quad (5)$$

Where m is the mass in kg and v is the water velocity in m/sec.

Looking to the subject from the angle of tidal current, the small tidal velocities over great depths may increase whenever the cross section narrows, either because of a decrease in depth from the open seawater towards the shallower coastal areas or as a result of lateral constraints in strait⁽⁹⁾. The maximum tidal velocity (U) in such straits or bays can be given as:

$$U = 2\mu A\pi / ST \quad (6)$$

Where U is given in m/sec, 2μ is the tidal range in m, A is the area in m^2 . S is the cross sectional area in m^2 and T is the tidal period in sec.

Frictional forces, especially those resulting from the roughness of the sea or riverbed, might largely influence both tidal oscillations and currents. The dissipation of kinetic energy manifests itself in the modification of the undisturbed tidal wave. In general, the explanation for the modification of the progressive wave in shallow water must be sought in the bottom friction, which is given in the following formula⁽⁹⁾:

$$F_b = \kappa \rho U^2 \quad (7)$$

where F_b is given in Nt/m^2 and κ is the Karman constant.

RESULTS AND DISCUSSION

Hydraulic Gradient

Hydraulic gradient of any river is measure of its energy. For Shatt Al-Arab, this gradient is largely varied depending mainly on the catchments condition, (natural and artificial), and tidal flow (tidal phase and cycle). Since the distance from Basrah to Fao is about 100km so the gradient at Basrah shows a maximum value for dry year (1988-1989) is 1.35×10^{-5} and a minimum of 0.33×10^{-5} . For a wet year (1987-1988), the maximum gradient is 1.8×10^{-5} and a minimum of 0.25×10^{-5} ⁽⁴⁾.

Based on calculation done on average flow of Shatt Al-Arab at Basrah and Fao⁽³⁾, the gradient was estimated as 2.6×10^{-5} and 1.3×10^{-5} respectively. But later work based on recent measurements shows a decrease in the hydraulic

gradient of Shatt Al-Arab at Basrah to $2 \times 10^{-5(10)}$. Latest estimation, also based on field data, was 1×10^{-6} and 2×10^{-6} for ebb and flow respectively for Karun confluence and Fao segment. About half this figure is the gradient of the stretch downstream⁽¹¹⁾. This points out to the increasing works aiming at controlling the flow of water in the tributaries of the river in the catchment area. However, it is thought that a tendency in the climatic data towards drier conditions in the area may exist.

The hydraulic gradient changes its direction during high water tide (flow). The degree to which the gradient changes its direction depends on the tidal levels and fresh water discharge of the river. A tidal wave may block the way against river water flow admitting water level to raise in the river channel sequentially upstream causing corresponding stagnation of the water mass in the river. This slack water condition may last about 30 minutes at maximum at Fao. Maximum reversal of gradient assumed to occur during high water spring tide accompanied with the lowest water level in dry season. The effect is intensified with the blow of southeasterly winds.

For Khor Abdallah, it is not easy to make accurate measurements to the hydraulic gradient the main factor controlling it may be the local instantaneous tidal elevations. This could be true for Khor Al-Zubair despite the drainage water entering it from Shatt Al-Basrah. The maximum discharge of the drainage water is about $200 \text{ m}^3/\text{sec}$, which corresponds to a residual current in Khor Al-Zubair section in the order of 0.01 m/sec . Assuming steady state condition, this according to Manning equation, could create a gradient of about 3×10^{-9} which is negligible.

Water Flow

Shatt Al-Arab water flows through Fao with a rate ranging from -0.6 to 0.1 m/sec depending on tidal condition and whether is a wet or dry year.

Typical velocity curve during complete tidal cycle is given in figure (4). It clearly shows that maximum speed

occurs during ebb, while minimum occurs at flood. Ebb takes about 5 hours while flow takes about 6.5 hours. There is a period of about 30 minutes for slack water condition. Discharges through this section, as calculated for the net flow curves, was $1020\text{m}^3/\text{sec}$.

Insignificant amount neither from Shatt Al-Arab nor Khor Al-Zubair discharge can reach Khor Abdallah, therefore, the tidal action perhaps is the only factor responsible for the discharging water masses through this section.

For Khor Al-Zubair section a discharge of $200\text{m}^3/\text{sec}$ may spread out offshore. This may bear only a local almost limited effect on the environment.

Tide

a: Tidal amplitude

Measurements indicate that the maximum ranges of tide 3.6, 3.4 and 4.8m for Shatt Al-Arab, Khor abdallah and Khor Al-Zubair respectively. These values are similar to those published about this area⁽¹²⁾. However, occasional abnormal records respectively were noticed. Again tidal phase whether neap, spring or intermediate is the main factor which control the range. However, it is evident that tidal amplitudes (half the tidal range) for Khor Al-Zubair exceeds that of Shatt Al-Arab and Khor Abdallah. This can be attributed to the funneling effect. In this context and in the light of eq. 4. It can be concluded that amplitude is more sensitive to narrowing of Khor Abdallah than shoaling i.e.

$$a \propto B^{1/2} d^{1/4}$$

This is confirmed for Khor Al-Zubair tidal amplitudes. They increase from about 1m near Al-Baker Oil Terminal (12 nautical miles offshore) to about 1.7m in Khor Abdallah reaching to 2.4m in Khor Al-Zubair. Depth of the whole region is variable from about 20m (in the navigational channel) to less than 10m elsewhere. However, widths steadily decrease through Khor Al-Zubair.

Funneling effect can also be noticed when tidal waves enter Shatt Al-Arab estuary but it seems that

freshwater input and the frictional forces are among many factors that develop the natural tidal picture.

b: Tidal Current

The tidal stream entering the gulf through the Strait of Hormiz can be predicted by eq. 6 using the well known figures needed as follows:

Area of the Arabian Gulf (A) = 239000 km², mean tidal range (2μ) = 1.2m, cross section area of the strait (S) = 60×10^5 m²⁽¹³⁾. The result is about 2.2m/sec, which is about 4.5 knots. Resolution for tidal stream passing to Khor Al-Zubair by using data of table (1) and an area of about 50 km² gives a value of 0.28m/sec.

c: Tidal Energy

Estimated tidal energy for Shatt Al-Arab, Khor Abdallah and Khor Al-Zubair are given in table (2). For Shatt AL-Arab is about 100000kW as a maximum value. Kinetic energy resulted from Shatt Al-Arab flow is in the order of 735kW pointing out the big difference between the tidal marine and the freshwater flow kinetic energy.

For Khor Abdallah a maximum of 425000kW being completely resulted from marine source. No effect from other sources is expected. Compared to this amount, a slightly lesser maximum of tidal energy (400000kW) is estimated for Khor Al-Zubair. However, in terms of energy flux, energy of Khor Al-Zubair must be greater than that of Khor Abdallah as relatively higher tidal ranges and amplitudes characterized the former. This energy is almost equivalent to the energy of Skjertadt Fjord (Norway) where a power of 600000hp is obtained. The conditions of this bay is reflected by the following numerical values:

$$A=250\text{m}^2, S=100 \times 30\text{m}^2, 2U=2.0\text{m}, U=7.5\text{m/sec}^{(9)}$$

d: Friction

The tidal friction is of special importance with regards to the dissipation of energy especially in shallower seas where high velocities of tidal currents are found.

However, according to eq 7. It seems that the role of friction is very limited in modifying tides of the Iraqi marine water, mainly due to the smooth nature of the seabed in the area as a result of the widespread distribution of fine sediments such as mud and silt⁽¹⁴⁾. On the other hand, it can be stated that the effect of friction for Shatt Al-Arab is many times greater than that of Khor Abdallah or Khor Al-Zubair. This could be attributed to the nature of the bed (almost sand)⁽¹⁴⁾. Shatt Al-Arab water discharge may be considered as obstacles to the marine tidal current. the asymmetrical character of the flow curve is an evidence to this finding.

Effect of Meteorological Factors

Some meteorological factors such as wind velocity and atmospheric pressure where known to influence the tidal elevations and/or tidal currents.

No published work concerning this subject was done. However many observations from which one can make some concluding remarks.

A low barometric pressure at 34mb below the average can cause a difference in height of about 0.30m, since a low pressure will tend to raise sea level and a high pressure will tend to depress it⁽¹²⁾.

It is well known from the investigation of wind speed and direction in the area that the northern and northwestern directions are prevailing (72%), while the southeastern wind constitutes about 22%⁽¹⁵⁾.

Since the later blows onshore it will pile up water and causes high water to be higher than the normal conditions.

CONCLUSION

The field data and the calculation carried out are given for each section leads to an appraisal of the responsibility of many factors that modifies the tidal regime in the Iraqi marine waters. This evaluation was approached

via the energy concept. The following conclusions was reached:

1. Width of channel and its consequent funneling phenomenon is a factor of greater importance than depth and bottom configuration.
2. The effect of freshwater input to the marine water mass is locally confined in the estuarine region where it is temporally modifies the tidal picture, depending on the catchment condition and its management. Considerable amount of tidal energy is dissipated due to Shatt Al-Arab water flow.
3. More detailed research work is needed before any judgement about the role of the meteorological parameters. In the light of the present level of meteorological and oceanographical data of the area such judgment is premature.

Table 1: Characteristics of some hydraulic parameters of sections representing Iraqi marin waters

Section	depth (d) m	width (b) m	C.S area (a) m ²	tidal amplitude (a)m	average depth velocity (V) m/sec
Shatt Al-Arab	14.0	560	4940	1.8	0.40
	11.0	500	3660		-0.70
Khor Abdallah	11.4	3000	18400	1.7	0.20
	8.0	2300	10800		-0.21
Khor Al- Zubair	12.5	2000	12400	2.4	0.23
	8.0	1500	9100		-0.29

Table 2: Energy of Shatt Al-Arab and Iraqi marine water

Section	Energy (E) kW	Source
Shatt Al-Arab	100000	Tidal River flow
	735	
Khor Abdallah	425000	Tidal
Khor Al-Zubair	400000	Tidal

The Role of Tide Modifying Factors in the NW Arabian Gulf
H. H. Salman

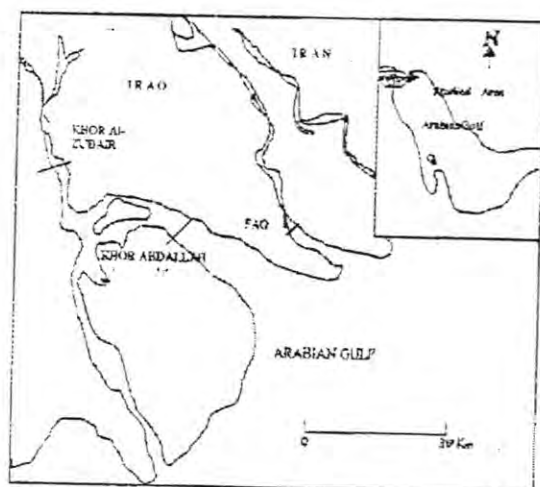


Fig. 1. Map of the north-west of the Arabian Gulf and the location of the studied sections.

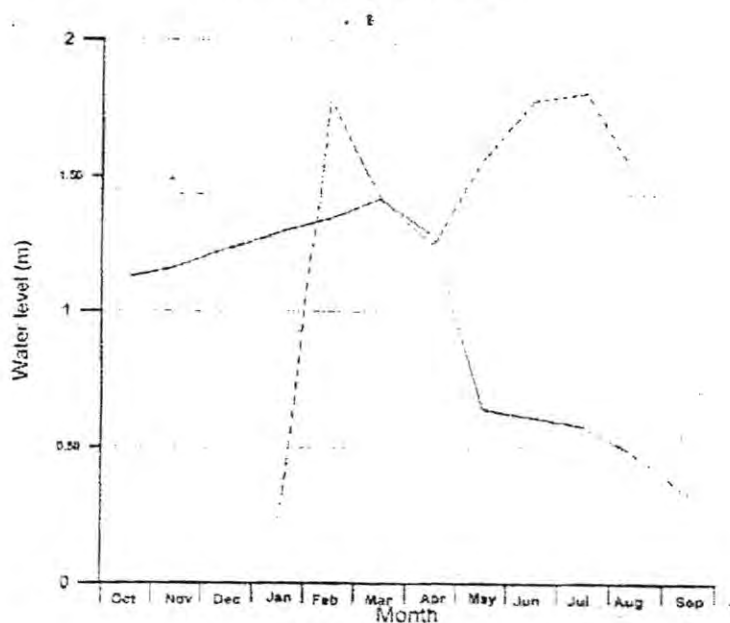


Fig.2 Fluctuation of Shatt Al-Arab water level at Basrah during the water years 1987-1988 (dashed) and 1988-1989 (solid)

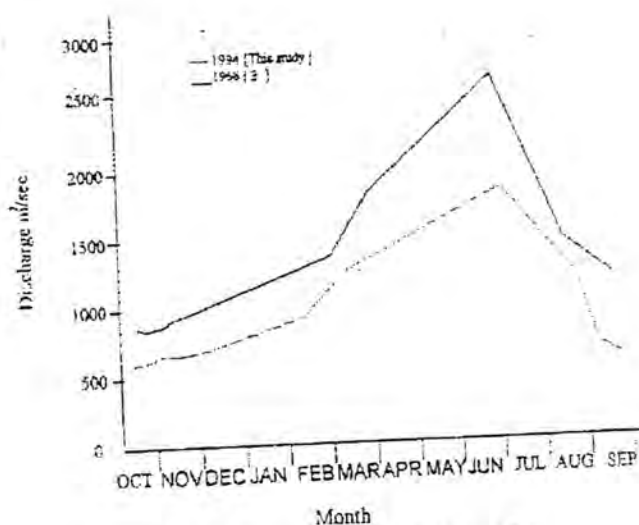


Fig.3 Hydrographs of shatt Al-Arab at Fao

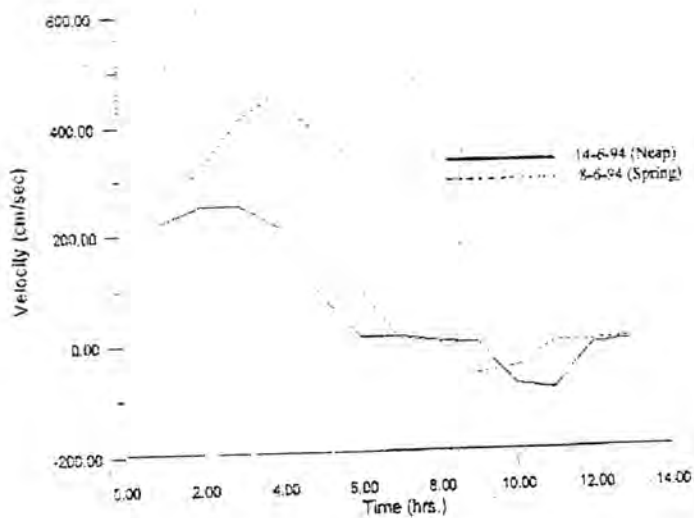


Fig.4- Velocity curves of Shatt Al-Arab at Fao.

REFERENCES

1. El-Sabh, M., Numerical simulation of the movement and dispersion of oil slicks in Kuwait Action Plan (KAP) region. Paper presented at the symposium/workshop on fate and fluxes of oil pollutants in the KAP region. University of Basrah, Basrah, Iraq, (1984).
2. Hunter, J., The physical oceanography of the Arabian Gulf. Conference on environment and pollution, Kuwait University, Kuwait pp1-23, (1986).
3. Karim H., and Salman, H. Estimation of the sediment discharge, sedimentation rate and the fate of hydrocarbon residues of Shatt Al-Arab Sediments, NW Arabian Gulf. *Marina Mesopotamica* Vol. 2 No. 1, pp. 103-115 (1987).
4. Basrah Irrigation Directorate, Unpublished data on level of Shatt Al-Arab in 1988-1989.
5. Al-Mahdi A. and Salman H. Some hydrological characteristics of Shatt Al-Arab. *Marina Mesopotamica* Vol. 12 (1997).
6. Salman, H. and Baker N., Tidal calculation for Umm Qasr by time series analysis. *Marina Mesopotamica* Vol. 5, No. pp 41-54 (1990).
7. Regional Organization of Protection of Marine Environment (ROPME). The final report of the 18 month pollution monitoring and Research Program in Iraq (1986).
8. Pond, S. and Packard, G. Introduction Dynamical Oceanography pp329. Pergamon press (1983).
9. Dietrich G. General oceanography: An Introduction pp588. John Wiley (1967).
10. Marine Consulting Bureau. Shatt Al-Arab Survey Project Phase 1. A report submitted to Al-Furat Center for studies and Design. (1994).
11. Al-Manssory F. Sediment Transport in the lower reach of Shatt Al-Arab, unpublished thesis, Basrah University 119p (1996).

12. Hydrographer of the Navy, Hydrographer Department, Ministry of Defence, UK. Admiralty Tide Tables Vol. 2, 459p. (1998).
13. Karim, H., and Salman H., Geology of the Arabian Gulf. Marine Science Publication No. 6 pp329 (1988).
14. Salman, H., Al-Jiburi, H. and Al-Dabbas, M., Sedimentological and Mineralogical investigation of N.W. Arabian Gulf. Jour. Wat. Res., Vol. 4, No. 2 pp 44-76 (1985).
15. Al-Shammary, F. Tidal phenomenon in Iraqi marine water and the effect of meteorological factors. Unpublished Msc. thesis submitted to the college of science, Al-Mustansiriya University p140 (1999).

On Infinite Dimensional Leslie Matrices in

Sequence Space ℓ_p , $1 < p < \infty$

ABDUL SAMEE ABDUL RAZZAK AL-JANABE* AND
OMER F. MUKHERJI**

* Mathematics Department, College of Science, Al-Mustansiriya University, Baghdad - Iraq

** Mathematics Department, College of Education -Makalla, University of Aden, Hudramout, Yemen.

(Received Sept. 14, 1998; Accepted May 14, 2000)

ABSTRACT

An infinite dimensional generalization of the Leslie matrix is introduced and we assume that the top row $(\{\alpha_n\}_{n=1}^{\infty})$ and the subdiagonal $(\{\omega_n\}_{n=1}^{\infty})$ of such matrix are considered to be elements in the Banach space ℓ_p , $1 < p < \infty$. This paper aims to prove that the multiplication by the infinite-dimensional Leslie matrix determines a compact linear operator from ℓ_p to ℓ_p , $1 < p < \infty$. It shows also such a matrix has an eigenvalue which is positive and real, and the corresponding eigenvector has positive entries.

INTRODUCTION

The matrix proposed by Leslie, 1945⁽¹²⁾ has constant elements and describe the dynamics of an age-structured population. The model in matrix form is,

$$X_{t+1} = LX_t$$

Where X_t is an m -vector giving the number of females of each of m age group at time t , and L is a square matrix of order m . (Leslie matrix).

The first row of L contains m age specific fecundity rates and the subdiagonal immediately below the main diagonal contains $m-1$ age specific survival rates and all other elements are zero^(3,12,14,15).

An eigenvalue of Leslie matrix has been evaluated and it has become an important value for describing the limiting behavior of the population⁽¹⁰⁾. It is well known that Leslie matrices have exactly one positive eigenvalue λ_1

Say, which dominates, the others in modulus. Kirkland⁽¹⁰⁾ constructed a region for the non-positive spectrum of Leslie matrix.

In this paper we assume that the Leslie matrix has an infinite dimension with the top row $\{\alpha_n\}$ and subdiagonal $\{\omega_n\}$ are elements in the Banach space ℓ_p , $1 < p < \infty$.

The space of all sequences $x = \{x_n\}_{n=1}^{\infty}$ such that $\sum_{n=1}^{\infty} |x_n|^p < \infty$ with the norm defined by $\|x\|_p = (\sum_{n=1}^{\infty} |x_n|^p)^{1/p}$ ⁽²⁷⁾.

Our aim is the same as in the work that has been done in paper (1), but here we assume that the components, $\{\alpha_n\}$ and $\{\omega_n\}$ of Leslie matrix are elements in ℓ_p , $1 < p < \infty$, and we prove that the infinite-dimensional Leslie matrix has a real positive eigenvalue and the corresponding eigenvector has positive entries. Also, we prove that such matrix defines a compact linear operator from ℓ_p into ℓ_p , $1 < p < \infty$.

The Infinite-Dimensional Leslie Population Matrix in Banach Space ℓ_p , $1 < p < \infty$

We consider a population divided into an infinite number of age groups. The top row α_j of Leslie matrix considered to denote the number of individuals produced by each individual in age group at time t and the subdiagonal ω_j of Leslie matrix, denotes the probability of survival from age group j to age group $j+1$.

The infinite-dimensional Leslie matrix is a matrix $(a_{ij})_{i,j=1}^{\infty}$ whose elements satisfy

$$a_{ij} = \begin{cases} \alpha_j & , i=1 \text{ and } j=1,2,3,\dots \\ \omega_j & , i=2,3,\dots \text{ and } j=i-1 \\ 0 & , \text{otherwise} \end{cases}$$

where $0 < \omega_j < 1$ and $\alpha_j \in \mathbb{R}_{+0}$, consequently we put $\alpha := \{\alpha_n\}_{n=1}^{\infty}$ and $\omega := \{\omega_n\}_{n=1}^{\infty}$.

In any normed space X , strong convergence implies weak convergence with the same limit but the converse is not generally true. If the dimension of X is finite then weak

convergence implies strong convergence. It should be noted that weak convergence implies strong convergence even if the dimension of X is infinite. This case was shown by I. Schur (1921) to be true through his example in $\ell_1^{(4,8)}$.

The following theorem states a criterion for the compactness of an operator defined on a Banach space whose proof can be found in (13).

Theorem 1

Let X and Y be two Banach spaces and let $T: X \rightarrow Y$ be a linear operator. Then T is compact if and only if T maps every weakly convergent sequence in X into a strongly convergent in Y .

An infinite-dimensional Leslie matrix $(\alpha_{ij})_{i,j=1}^{\infty}$ can be used to define an operator $L: X \rightarrow Y$ where X and Y are taken as spaces of sequence $\ell_p, 1 < p < \infty$. L is given by $Lx = y$ where $x = \{\zeta_j\}_{j=1}^{\infty}$ and $y = \{\eta_i\}_{i=1}^{\infty}$ are related by

$$\eta_i = \sum_{j=1}^{\infty} a_{ij} \zeta_j \quad \forall i = 1, 2, \dots [4]$$

We choose the elements of the infinite-dimensional Leslie matrix $(a_{ij})_{i,j=1}^{\infty}$ be such that the above series converges for each i and the resulting vector y belongs to $Y = \ell_p, 1 < p < \infty$.

Lemma 1:

Let X and Y be two infinite Banach spaces with schauder bases. Then every infinite matrix $(a_{ij})_{i,j=1}^{\infty}$ determines a linear operator U from X into Y and vice versa.

Proof:

Let X and Y be two infinite Banach spaces and let $U: X \rightarrow Y$ be a linear operator. Consider $\{e_j\}_{j=1}^{\infty}$ be a Schauder basis for X and $\{g_i\}_{i=1}^{\infty}$ be analogous bases for Y . If $x \in X$ and $y \in Y$, Thus

$$x = \sum_{j=1}^{\infty} x_j e_j \quad \text{and} \quad y = \sum_{i=1}^{\infty} y_i g_i$$

if $y = Ux$, then we have,

$$y = U\left(\sum_{j=1}^{\infty} x_j e_j\right) = \sum_{j=1}^{\infty} x_j Ue_j$$

we denote the coordinates of the elements Ue_j by $a_{1j}, a_{2j}, a_{3j},$ Therefore,

$$y = \sum_{\alpha=1}^{\infty} y_{\alpha} g_{\alpha} = \sum_{j=1}^{\infty} x_j \sum_{\alpha=1}^{\infty} a_{\alpha j} g_{\alpha} = \sum_{\alpha=1}^{\infty} \left(\sum_{j=1}^{\infty} a_{\alpha j} x_j \right) g_{\alpha}$$

but g_1, g_2, \dots are linearly independent, therefore $y_i = \sum_{j=1}^{\infty} a_{ij} x_j$, $i=1, 2, \dots$

Hence the coordinates of $y=Ux$ are obtained from those of x by an infinite matrix $(a_{ij})_{i,j=1}^{\infty}$.

Conversely, let $(a_{ij})_{i,j=1}^{\infty}$ be an infinite-dimensional matrix. Since X and Y are infinite Banach spaces with schauder bases, then every $x \in X$ and $y \in Y$ can be written respectively as $\sum_{j=1}^{\infty} x_j e_j$ and $\sum_{i=1}^{\infty} y_i e_i$

Consider the system of equations

$$\sum_{j=1}^{\infty} a_{ij} x_j = y_i \quad \forall i = 1, 2, \dots$$

$$\text{Thus } Ux = \sum_{j=1}^{\infty} x_j Ue_j = \sum_{j=1}^{\infty} x_j \sum_{\alpha=1}^{\infty} a_{\alpha j} g_{\alpha} = \sum_{\alpha=1}^{\infty} \left(\sum_{j=1}^{\infty} a_{\alpha j} x_j \right) g_{\alpha} = \sum_{\alpha=1}^{\infty} y_{\alpha} g_{\alpha} =$$

$$y \in Y \Rightarrow Ux = y$$

Hence, $U: X \rightarrow Y$ is a linear operator therefore an infinite dimensional matrix $(a_{ij})_{i,j=1}^{\infty}$ determines a linear operator U from X into Y .

The following theorem shows that in the Banach space $\ell_p, 1 < p < \infty$, The weak convergence is equivalent to coordinate-wise convergence and the norms of the terms of the sequence are bounded.

Theorem 2⁽²⁾

For $1 < p < \infty$ Suppose $x_n = (\alpha_1^{(n)}, \alpha_2^{(n)}, \dots, \alpha_k^{(n)}) \in \ell_p$ and $X = (\alpha_1, \alpha_2, \dots, \alpha_k, \dots) \in \ell_p$. Then $x_n \rightarrow \mu x$ if and only if:

- 1) $\|x_n\| \leq M, \forall n$ where M is a positive constant,
- 2) for every $i, \alpha_i^{(n)} \rightarrow \alpha_i$ as $n \rightarrow \infty$.

Let $L=(a_{ij})$ be an infinite-dimensional Leslie matrix multiplying L by itself n -times we get the following block matrix,

$$L^n = (a_{ij}^{(n)}) = \begin{bmatrix} \overbrace{\hspace{10em}}^Z & & \\ \prod_{i=1}^{n-1} \omega_i : & & V \\ \prod_{i=2}^{n-1} \omega_i : & a_{ij} & \\ \prod_{i=3}^{n+1} \omega_i : & & 0 \\ \vdots & & \\ \vdots & & \\ \vdots & & \end{bmatrix}$$

where Z is $(n-1) \times \infty$ matrix,

V is $1 \times (n-2)$ matrix and

0 is $\infty \times (n-2)$ matrix

Notice that all Leslie matrices have constant elements.

Thus

$$\lim_{n \rightarrow \infty} L^n = a_{ij} \text{ or } \lim_{n \rightarrow \infty} a_{ij}^{(n)} = a_{ij} \quad \forall_{i,j}$$

$$\text{Now, let } a_{ij}^{(k)} \rightarrow a_{ij} \text{ in } \ell_p \text{ as } k \rightarrow \infty \quad (1)$$

And let $x^{(k)} \rightarrow x$ in ℓ_p as $k \rightarrow \infty$. Theorem 2 we have

$$\alpha_j^{(k)} \rightarrow \alpha_j \text{ as } k \rightarrow \infty \quad (2)$$

from (1) and (2) we get

$$a_{ij}^{(k)} \alpha_j^{(k)} \rightarrow a_{ij} \alpha_j \text{ as } k \rightarrow \infty, \quad \forall_{i,j}$$

$$\text{Consequently } \lim_{k \rightarrow \infty} \sum_{j=1}^{\infty} a_{ij}^{(k)} \alpha_j^{(k)} = \sum_{j=1}^{\infty} a_{ij} \alpha_j \quad \forall_i$$

$$\text{And so } \lim_{k \rightarrow \infty} \sum_{i=1}^{\infty} \sum_{j=1}^{\infty} a_{ij}^{(k)} \alpha_j^{(k)} = \sum_{i=1}^{\infty} \sum_{j=1}^{\infty} a_{ij} \alpha_j$$

$$\text{Or } \left\| \sum_{i=1}^{\infty} \sum_{j=1}^{\infty} (a_{ij}^{(k)} \alpha_j^{(k)} - a_{ij} \alpha_j) \right\|^p \rightarrow 0 \text{ as } k \rightarrow \infty$$

Proposition 1

Let $\alpha := \{\alpha_n\}_{n=1}^\infty \in \ell_p$ and $\omega := \{\omega_n\}_{n=1}^\infty \in \ell_p$, $1 < p < \infty$. Then the multiplication by infinite-dimensional Leslie matrix (a_{ij}) Defines a compact linear operator L from ℓ_p into ℓ_p .

Proof: An infinite Leslie matrix (a_{ij}) can be used to define an operator $L: \ell_p \rightarrow \ell_p$, $1 < p < \infty$, which is given by $Lx = y$ where $x = \{\zeta_i\}_{i=1}^\infty \in \ell_p$ and $y = \{\eta_i\}_{i=1}^\infty \in \ell_p$ one related by

$$\eta_i = \sum_{j=1}^{\infty} a_{ij} \zeta_j, \quad \forall i=1, 2, \dots$$

If we take the domain of L is ℓ_p , then the series is convergent for each i and $y \in \ell_p$.

Then the linear operator L is closed and therefore is bounded by "closed graph theorem".

Finally to show that L is compact operator, we show that L maps weakly convergent sequence into strongly ones.

Let w_k as $k \rightarrow \infty$, then $\zeta_j^{(k)} \rightarrow \zeta_j$ as $k \rightarrow \infty$, $a_{ij}^{(k)} \zeta_j^{(k)} \rightarrow a_{ij} \zeta_j$.
 Now,

$$\begin{aligned} \|Lx_k - Lx\|_p^p &= \sum_{i=1}^{\infty} |\eta_i^{(k)} - \eta_i|^p \leq \sum_{i=1}^{\infty} \left| \sum_{j=1}^{\infty} a_{ij}^{(k)} \zeta_j^{(k)} - \sum_{j=1}^{\infty} a_{ij} \zeta_j \right|^p \leq \\ &\sum_{i=1}^{\infty} \sum_{j=1}^{\infty} |a_{ij}^{(k)} \zeta_j^{(k)} - a_{ij} \zeta_j|^p \rightarrow 0 \text{ as } k \rightarrow \infty \end{aligned}$$

Hence $\|Lx_k - Lx\|_p^p \rightarrow 0$ as $k \rightarrow \infty$

Therefore L maps a weakly convergent sequence into a strongly ones; Thus L is a compact linear operator from ℓ_p into ℓ_p , $1 < p < \infty$

If $A = (a_{ij}) \in R_{+0}^{N \times N}$ ($a_{ij} \geq 0 \quad \forall i, j=1, 2, \dots$) then the directed graph $D(A)$ associated with A is given by,
 $D(A) = \{(i, j) \in I \times I \mid a_{ij} > 0\}$ and it is strongly connected if for every pair $(i, j) \in I \times I$, a directed path $(i, k_1), (k_1, k_2), \dots, (k_n, j)$ in $D(A)$

That is, a directed path is strongly connected if for any pair of nodes p_i and p_j there exists a directed path connecting p_i to p_j .

Irreducibility of a matrix is known to be equivalent to strong connectedness of its directed graph since the birth rate in age groups of Leslie matrix are non-zero elements so the directed graph is strongly connected and hence the infinite dimensional Leslie matrix is irreducible⁽⁶⁾.

Lemma 2:

Let $A=(a_{ij}) \in R_{+0}^{IN \times IN}$ be an irreducible matrix then for all $(i,j) \in IN \times IN$ $\exists n \in IN$ such that $a_{ij}^{(n)} > 0$ when $A^n = (a_{ij}^{(n)})$ $\forall i \leq n$.

For the proof see (1)

Our main result is the following:

Theorem 3:

Let $L=(a_{ij})$ be an infinite-dimensional Leslie matrix. Suppose $\alpha, \omega \in \ell_p$, $1 < p < \infty$, and let the set $B = \{(i,j) \in IN \times IN | a_{ij} > 0\}$ is infinite.

Then there exists an eigenvalue $\lambda_1 \in R_+$ of L and a corresponding eigenvector $x^1 \in \ell_p$ with $Lx^1 = \lambda_1 x^1$ and $\zeta_j^1 > 0$ $\forall j \in IN$

The proof of this theorem is based on the following result due to Kreind-Rutman⁽¹¹⁾.

Theorem 4:

Let X be real Banach space and $K \subset X$ be a convex closed cone with $K \cup (-K) = X$ and $K \cap (-K) = \{0\}$. Let $T \in \alpha(X, X)$ be a compact operator leaving the cone K invariant, is $Tx \in K \quad \forall x \in K$

$\exists x^0 \in K - \{0\}$, $\|x^0\| = 1$, $\exists n \in IN$ and $C \in R_+$ such that $T^n x^0 - Cx^0 \in K$

Then the operator T has an eigenvalue $\lambda_1 \in R_+$ and an eigenvector $x^1 \in K$ associated with λ_1

Proof of Theorem 3:

Let $K = \{x = \{\zeta_i\} \in \ell_p \mid \zeta_j \geq 0 \ \forall j \in \mathbb{N}, 1 < p < \infty\}$

It is clear the K is a closed convex cone, see (1)

Let $x \in K$ then $\zeta_j \geq 0 \ \forall j \in \mathbb{N}$, and let $(a_{ij})_{i,j=1}^\infty$ be an infinite dimensional Leslie matrix defines a bounded linear operator $L: \ell_p \rightarrow \ell_p$ $1 < p < \infty$ then $Lx = y$ where $x = \{\zeta_j\}_{j=1}^\infty$ and

$y = \{\eta_i\}_{i=1}^\infty$ are related by $\eta_i = \sum_{j=1}^\infty a_{ij} \zeta_j, \ \forall i = 1, 2, \dots$

But the Leslie matrix has non-negative elements thus $a_{ij} \geq 0 \ \forall i, j$ then $\eta_i \geq 0 \ \forall i \in \mathbb{N}$ this means $y \in K$ and therefore $Lx \in K \ \forall x \in K$.

Hence, (a) of theorem 4, For condition (b) of same theorem, we notice that L is irreducible by the infiniteness of B

For $i=1$ and $j=1 \quad \exists n \in \mathbb{N}$ such that $a_{11}^{(n)} > 0$

$$\text{Let } x^0 = \begin{bmatrix} 1 \\ 0 \\ 0 \\ 0 \\ \vdots \\ \vdots \end{bmatrix} \in K \setminus \{0\} \text{ and } c = a_{11}^{(n)} > 0$$

Now $L^n x = \sum_{j=1}^\infty \zeta_j L^n e_j$, where $\{e_j\}_{j=1}^\infty$ is a bases for the domain

$\ell_p = \sum_{j=1}^\infty \zeta_j \sum_{i=1}^\infty a_{ij}^{(n)} g_i$, where $\{g_i\}_{i=1}^\infty$ is a basis for the range ℓ_p

$$= \sum_{j=1}^\infty \left(\sum_{i=1}^\infty a_{ij}^{(n)} \zeta_j \right) g_i$$

$$\text{Hence } L^n x^0 = \sum_{i=1}^\infty a_{i1}^{(n)} g_i$$

In a matrix from this can be written as $(a_{i1}^{(n)})^T g$ where $(\)^T$ is the transpose and g is the columnvector with components g_1, g_2, \dots

Now, as $g_{i1}^{(n)} > 0$ then $L^n x^0 > 0$, hence, $L^n x^0 - cx^0 = Lx^0 - a_{11}^{(n)} x^0 \in K$, therefore (b). Thus there is an eigenvalue $\lambda_1 \in \mathbb{R}_+$ of L and corresponding eigenractor $x^1 \in \ell_p$.

Finally, we prove that $\zeta_j^1 > 0 \quad \forall j \in \mathbb{N}$. suppose $\zeta_j^1 = 0 \quad \forall j \in \mathbb{N}$. then the j -th coordinate of $L^n x^1 = \lambda_1^n x^1$ is zero.

Since we have $\eta_i = \sum_{j=1}^{\infty} a_{ij} \zeta_j$, $i=1,2,\dots$ then the coordinate of $y=Lx$ are obtained from those of x by the transformation accordign to the matrix (a_{ij}) . Therefore, the j -th coordinate of $L^n x^1$ is zero. Thus $\exists k \in \mathbb{N}$ such that $\zeta_k^1 > 0$ and $\exists n \in \mathbb{N}$ such that $a_{jk}^{(n)} > 0$ by lemma 2.

So we have, $0 = \sum a_{j1}^{(n)} \zeta_1^1 \geq a_{jk}^{(n)} \zeta_k^1 > 0$, contradiction. Hence $\zeta_j^1 > 0 \quad \forall j \in \mathbb{N}$.

Bounds for the Eigenvalues of an Inifinite-Dimensioanl Leslie Matrix in Banach Space ℓ_p , $1 < p < \infty$

The spectrum $\sigma(T)$, of an operator T defined on an infinite dimensional Banach space X is partitioned into three desjoint sets, point spectrum of T , $P\sigma(T)$, continners spectrum of T , $c\sigma(T)$, and residual spectrum of T , $R\sigma(T)$ ⁽¹⁾.

In finite-dimensional space Y with T defined an all Y ten $R\sigma(T) = \emptyset$ and $c\sigma(T) = \emptyset$ ^(2,7).

Definition 1:

Let $(a_{ij})_{i,j=1}^{\infty}$ be an infinite-dimensional Leslie matrix which defines a bounded linear opertor $L: \ell_p \rightarrow \ell_p$, $1 < p < \infty$ then ℓ_p -norm of L is given by

$$\alpha \leq \left(\sum_{i,j=1}^{\infty} |a_{ij}|^q \right)^{1/q} \text{ where } \frac{1}{p} + \frac{1}{q} = 1$$

1. all eigenvalues λ of an infinite-dimensional Leslie matrix $L = (a_{ij})_{i,j=1}^{\infty}$ lie i nth disk $|z| \leq \|L\|_p$. $1 < p < \infty$, $z \in \mathbb{C}$, \mathbb{C} is the complex number.
2. If $\lambda_1 \in \mathbb{R}_+$ is a eigenvalue of an infinite-dimensional Leslie matrix L and λ_i is any other real or complex eigenvalue of L then $|\lambda_i| \leq \lambda_1$.

Theorem 5:

Let $(a_{ij})_{i,j=1}^{\infty}$ be an infinite-dimensional Leslie matrix which defines a bounded linear operator L from ℓ_p into ℓ_p , $1 < p < \infty$.

If 0 and 1 is a limit point of the pint spectrum of, $p\sigma(L)$, of L , then it is in the continuous spectrum $c\sigma(L)$

Proof:

Let $x \in \ell_p$, $1 < p < \infty$, then x can be written as

$X = \sum_{j=1}^{\infty} x_j e_j$, where $\{e_j\}_{j=1}^{\infty}$ is a basis for ℓ_p consider $\{\lambda_n\}$ be a sequence of the eigenvalues of an infinite-dimensional Leslie matrix $(a_{ij})_{i,j=1}^{\infty}$ which defines a bounded linear operator $L: \ell_p \rightarrow \ell_p$, $1 < p < \infty$, be such that $\lambda_n \rightarrow 0$ as $n \rightarrow \infty$ with $\lambda_n \neq 0 \forall n$. Consider also, $L_{\lambda_n} = (\lambda_n - L)$ then $L_0 = -L$.

Suppose $L_0 x = 0$, then $0 = \sum_{j=1}^{\infty} a_{ij} x_j, \forall i$

Since Leslie matrix has $a_{ij} \geq 0 \forall i,j \rightarrow x_j = 0$; hence $x = 0$.

Thus, L_0 is one-to-one, means that L_0^{-1} exist therefore 0 is not an eigenvalue of L .

Also L_0^{-1} is not bounded. Indeed,

$$\|L_0 x\|_p = \|-Lx\|_p = \|Lx\|_p = \|\lambda_n x\|_p \rightarrow 0 \text{ as } n \rightarrow \infty$$

Hence, it is impossible to find a constant k such that $k\|x\| \leq \|L_0 x\|_p, x \in \ell_p$.

Finally, we prove that the range of L_0 is dense in ℓ_p . Since

$$y = Lx = -L_0 x \rightarrow y_i = \sum_{j=1}^{\infty} a_{ij} x_j, \forall i$$

Thus the range is a closed subspace of ℓ_p , and hence the range of L_0 , means that the range of L_0 , $R(L_0)$ is dense in ℓ_p , $1 < p < \infty$.

Therefore 0 is in the continuous spectrum of L , i.e. $0 \in c\sigma(L)$.

Again, suppose $\lambda_n \rightarrow 1$ as $n \rightarrow \infty$, with $\lambda_n \neq 1 \forall n$. Then $L_1 = (1 - L)$

Let $L_1x=0$, $x \in \ell_p$, $1 < p < \infty \rightarrow (1-L)x=0$ or $x=Lx$

Since $\{\lambda_n\} = \Lambda$ be a sequence of the eigenvalues of L , then $Lx = \Lambda x$ or $x = \Lambda x$.

or $\sum_{n=1}^{\infty} x_n e_n = \sum_{n=1}^{\infty} x_n \lambda_n e_n$, or $\sum_{n=1}^{\infty} (1 - \lambda_n) x_n e_n = 0$, or

$$\left(\sum_{n=1}^{\infty} |(1 - \lambda_n) x_n e_n|^p \right)^{1/p} = 0$$

now, for all n , we have

$$0 \leq |(1 - \lambda_n) x_n e_n| = (|(1 - \lambda_n) x_n e_n|^p)^{1/p} \leq \left(\sum_{n=1}^{\infty} |(1 - \lambda_n) x_n e_n|^p \right)^{1/p} = 0$$

$$\rightarrow |(1 - \lambda_n) x_n e_n| = 0 \quad \forall n$$

but $\lambda_n \neq 1 \quad \forall n$, hence $x_n = 0 \quad \forall n$.

Therefore, $x = 0$, means that L_1 is one-to-one, so L_1^{-1} exists, thus 1 is not an eigenvalue of L . The inverse operator L_1^{-1} is not bounded.

Indeed,

$$\|L_1 x\|_p = \|(x - Lx)\|_p = \|x - Lx + \lambda_n x - \lambda_n x\|_p \leq \|(1 - \lambda_n)x\|_p \rightarrow 0 \text{ as } n \rightarrow \infty$$

K such that

$$K\|x\|_p \leq \|L_1 x\|_p, \quad x \in \ell_p, \quad 1 < p < \infty.$$

Finally, we prove that the range of L_1 , $R(L_1)$ is dense in ℓ_p .

Let $y = \{y_i\} \in \ell_p$ then by definition of L $y_i = \sum_{j=1}^{\infty} a_{ij} x_j$, $\forall i$.

Since the Leslie matrix $(a_{ij})_{i,j=1}^{\infty}$ has non negative elements thus $y_i > 0 \quad \forall i$ and hence y .

Let $\varepsilon > 0$ be given, let $x = \{x_j\} \in \ell_p$ be such that

$$\sum_{j=n_0+1}^{\infty} |x_j|^p < \varepsilon^p / 2 \quad \forall n_0 \in \mathbb{N}.$$

without loss of generality, let $a_{ij} = 0 \quad \forall i$ and $j > n_0$, $n_0 \in \mathbb{N}$.

Let $y \in R(L_1)$, the range of L_1 be such that

$$\sum_{j=1}^{n_0} |(e_j - a_{ij}) x_j|^p < \varepsilon^p / 2, \quad n_0 \in \mathbb{N}, \quad i = 1, 2, \dots$$

Now

$$\|y-y\|_p^p = \sum_{j=1}^{\infty} |(e_j - a_{ij})x_j - y_j|^p \leq \sum_{j=1}^{\infty} |(e_j - a_{ij})x_j|^p =$$

$$\sum_{j=1}^{n_0} |(e_j - a_{ij})x_j|^p + \sum_{j=1}^{\infty} |x_j|^p, n_0 \in \mathbb{N} < \frac{\varepsilon^p}{2} + \frac{\varepsilon^p}{2} = \varepsilon^p,$$

$n_0 \in \mathbb{N}$. Hence $\|y-y\|_p^p < \varepsilon$.

Therefore, the range $R(L_1)$, of L_1 is dense in ℓ_p , thus 1 is in the continuous spectrum of L , i.e. $1 \in c\sigma(L)$.

REFERENCES

1. Abdul Samee A. Al-Janabi and Omer F. Mukherij, "One an infinite-dimensionanl Leslie matrix in sequence space ℓ_2 ", to appear.
2. Bachman G. and Narici L. "Functional analysis", Academic Press, Inc., New York and London, (1966).
3. Beddington J.R. and Taylor D.B. "Optimum age hjarvesting of a population", Biometries 29, pp. 801-809 (1973).
4. Choudary B. and Sudarsan. N., "Functional analysis with application", willy eastem Limited, India (1989).
5. Cooke Richard, G., "Infinite matrices and sequence spaces", Macmillan and Co. Ltd. St. Martin's Street, London, (1950).
6. Csetenyi A.I. and Logofet D.O., "Leslie model revisited: Some generalization to block structures", Ecological modeling 48, pp 277-290, (1989).
7. Erwin Kreyszing, "Introductory functional analysis" John Wiley and Son's, Inc. (1978).
8. Kantorovich L.V. and Akilov G.P., "Functional analysis", Program press. Ltd. Heading Hill Hall, Oxford, England, (1982).
9. Kaveh A., "Structural mechanics: Graph and matrix methods", Research studies press Ltd., (1995).
10. Kirkland Steve, "An eigenvalue region for Leslie matrices", SIAM J. Matrix Anal. Appl. Vol. 13, No. 2, pp 507-529 (1992).

11. Krien M.G. and Rutman M.A. "Linear operator leaving invariant a cone in Banach space" *Uspekhi Matem Nouk* (n.s) Vol. 3, No. 1 (23) pp 3-95, (1948).
12. Leslie P.H., "On the use of matrices in certain population mathematics", *Biometrika* 33, pp 183-212 (1945).
13. Liusternik L.A. and Sobolev V.J. "Element of functional analysis", Fredrick Ungar publishing Co., New York (1961).
14. Pollard J.H., "Mathemmmatical modeles for the growth of human population" Cambridge University Press, Cambridge, UK., (1973).
15. Rorres Charis, "Application of linear algebra", John Wiley and Son's, Inc. (1977).
16. Varga Richard S., "Matrix iterative analysis", Prentice-Hall, Inc., Englood Cliffs, N.J. (1962).

Finiteness of Fully Stable Modules

MAHDY S. ABBAS

Mathematics Department, College of Science, University of Al-Mustansiriya

(Received Apr. 18, 1999; Accepted July 22, 1999)

الخلاصة

في هذا البحث قمنا بدراسة شروط الانتهاء على موديلات تامة الاستقرارية حيث شخصنا تركيب بنية الموديلات الجزئية لهذا الصنف من الموديلات. درسنا العلاقة بين الاستقرار التامة وشبه الاغمارية للموديلات ذات الشروط المنتهية. الاسلوب الذي استخدم لهذه النتائج هو التوضع.

INTRODUCTION

Throughout R represents a commutative ring with identity, and M a unital left R -module. A submodule N of M is said to be stable if $\theta(N) \subseteq N$ for each R -homomorphism θ from N to M . In case each submodule of M is stable. M is called fully stable. The ring R is called fully stable if it is fully stable R -module⁽¹⁾. An R -module M is fully stable if and only if each cyclic submodule of M satisfies the double annihilator condition that is $\text{ann}_M(\text{ann}_R(x)) = (x)$ for each x in M ⁽¹⁾. In this paper we give the structure of submodules of fully stable module with finiteness conditions. The relationship between fully stability and quasi-injectivity through finiteness of modules is examined. The tools used here for this purpose is localization.

Localization of Full Stability

In this section we investigate the behaviour of a fully stable module under the operation of localization of modules. We show that if M is a fully stable R -module and p is a prime ideal of R then M_p is a fully stable R_p -module provided that R is a Noetherian ring. However, example (2.4) shows that the answer of . First we have the following

Proposition

Let M be an R -module, if for each prime ideal p of R . The localization M_p is fully stable R_p -module, then M is a fully stable R -module.

Proof: For any R -submodule N of M and R -homomorphism $\theta: N \rightarrow M$, define $\theta_p: N_p \rightarrow M_p$ by $\theta_p(ns) = \theta(n)/s$ for each $n \in N$ and $s \in R_p$. It is a matter of checking that θ_p is an R_p -homomorphism, then $(\theta(N))_p = \theta_p(N_p) \subseteq N_p$ for each prime ideal p of R , hence $\theta(N) \subseteq N$. Therefore M is a fully stable R -module.

An R -module M is said to be a multiplication module if each submodule of M is of the form IM for some ideal I of R ⁽⁶⁾. A finitely generated R -module M is multiplication if and only if M_p is a cyclic R_p -module for each prime ideal p of R ⁽⁹⁾. A commutative ring R is called regular (Von Neumann) if for each $x \in R$, there exists an element $y \in R$ such that $x = xyx$. It is known that every regular ring is fully stable. A generalization of this for modules is the following.

Corollary: Every multiplication (hence locally cyclic) module over a regular ring is full stable

Proof: Let M be a multiplication R -module for each prime ideal p of R . the R_p -module M_p is cyclic. Hence, $M_p = R_p \text{ann}_{R_p}(M_p)$ but R is regular ring. Then so is $R \text{ann}_R(M)$. Hence, $(R \text{ann}_R(M))_p = R_p \text{ann}_{R_p}(M_p)$ which is a field. Thus, it is fully stable as R_p -module therefore, M_p is a fully stable R_p -module, by proposition (2.1), M is a fully stable R -module

Proposition: Let R be a Noetherian ring, if M is a fully stable R -module, then so for M_s for every multiplicatively closed subset S of R .

Proof: It is enough to show that $\text{ann}_{M_s}(\text{ann}_{R_s}(x_s)) = (x_s)$ for each x_s in M_s by using proposition (3.14) in (5) we have $\text{ann}_{M_s}(\text{ann}_{R_s}(x_s)) = \text{ann}_{M_s}(\text{ann}_R(x))_s = (\text{ann}_M(\text{ann}_R(x)))_s = (X)_s = (x_s)$.

Example⁽¹⁰⁾

Let $F = \mathbb{Z}_2$ set $F_n = F$ for $n=1, 2, \dots$. $M = \prod_{n=1}^{\infty} F_n$ and R be the F -subAlgebra of M generated by $\bigotimes_{n=1}^{\infty} F_n$ and the unity of M . Let p denote the prime ideal F_n of R . For each $K \geq 1$. Let e_k denote the element of p which has 1 in the k th place and zero elsewhere. For each $g \in M$, $e_k \in \text{ann}_R(g)$ if and only if g has zero in the k th place, it follows that $g \in \text{ann}_M(\text{ann}_R(g))$, thus $\text{ann}_M(\text{ann}_R(g)) = (g)$, thus M is a fully stable R -module, it is easy to check that R_p is isomorphic to F . Thus, M_p is exactly a vector space over F . Whose dimension is greater than 1. Therefore, M_p is not a fully stable R_p -module⁽¹⁾.

Finite length fully stable modules

It is known that an R -module M is fully stable if and only if $N = \sum_{\theta \in \text{Hom}_R(N, M)} \theta(N)$ for each submodule N of M , that is there exists a finite family $\{\phi_i\}$ of elements from $\text{Hom}_R(N, M)$ such that $N = \sum \phi_i(N)$. In the following proposition we prove Fitting's lemma in terms of fully stable module.

Proposition: Let M be a fully stable R -module satisfying the d.c.c. on submodules of M . Then for each submodule N of M and each R -homomorphism $f \in \text{Hom}_R(N, M)$, there exists a positive integer n such that $N = f^n(N) + \text{Ker}(f^n)$.

Proof: Full stability of M gives the following chain of submodules of M

$$N \supseteq f(N) \supseteq f^2(N) \supseteq \dots$$

There exists an integer n_0 such that for all $n > n_0$, $f^n(N) = f^{n_0}(N)$.

Let $x \in N$, then $\alpha f^n(x) \in f^n(N)$, then there is $y \in N$ such that $f^n(x) = f^{2n}(y)$, hence $f^n(x - f^n(y)) = 0$, thus $k = x - f^n(y) \in \text{Ker}(f^n)$ therefore

$$X = f^n(y) - k \in f^n(N) + \text{ker}(f^n)$$

A submodule N of an R -module M is said to be pseudo-stable if $\theta(N) \subseteq N$ for each R -monomorphism $\theta \in \text{Hom}_R(N, M)$, if each submodule of M is pseudo-stable, M is called pseudo fully stable module⁽²⁾. The following corollary is immediate.

Corollary: Let M be a pseudo-fully stable R -module satisfying the d.c.c. on submodules of M . Then for each submodule N of M and each R -monomorphism $f \in \text{Hom}_R(N, M)$, there exists a positive integer n such that $N = f^n(N)$.

Proposition: Let M be a fully stable R -module of finite length. Then for each submodule N of M and R -homomorphism $f \in \text{Hom}_R(N, M)$, there exists a positive integer n such that $N = f^n(N) \oplus \text{Ker}(f^n)$.

Proof: By proposition (3.1), $N = f^t(N) + \text{Ker}(f^t)$ for some positive integer t . Consider the following chain

$$\text{Ker}(f) \subseteq \text{Ker}(f^2) \subseteq \text{Ker}(f^3) \subseteq \dots$$

There is a positive integer m such that $\text{Ker}(f^s) = \text{Ker}(f^{2s})$ for all $s > m$. Put n the maximum of s and t , then $N = f^n(N) + \text{Ker}(f^n)$. Let $x \in f^n(N) \cap \text{Ker}(f^n)$ then there is an element $y \in N$ such that $x = f^n(y)$ and $f^n(x) = 0$. Now $0 = f^n(x) = f^{2n}(y)$, hence $y \in \text{Ker}(f^{2n})$ thus $x = f^n(y) = 0$. Therefore $N = f^n(N) \oplus \text{Ker}(f^n)$.

Recall that an element x in R is π -regular if there exists an element y in R and a positive integer n such that $x^n y x^n = x^{n(7)}$. R is called π -regular ring if each element of R is π -regular. An R -module M is fully stable if and only if each cyclic submodule is stable⁽¹⁾. In (3) we introduced the concept of semi-fully stable module as a generalization of fully stable module. An R -module M is said to be semi-fully stable if for each cyclic submodule N of M and R -homomorphism $f: N \rightarrow M$, there exists $g \in \text{End}_R(M)$ such that $f(n) = g \cdot n$ for each $n \in N$. This is equivalent to saying that each R -homomorphism of the cyclic submodule of M into M is extendable to an R -endomorphism of M ⁽³⁾.

Theorem: Let M be a fully stable R -module. Then for each cyclic submodule N of M the following statements are equivalent:

1. $\text{Hom}_R(N, M)$ is π -regular ring.
2. For each $f \in \text{Hom}_R(N, M)$, there exists a positive integer n such that $N = f^n(N) \oplus \text{Ker}(f^n)$.

Proof: Full stability of M implies that $\text{End}_R(M)$ is a commutative ring⁽¹⁾, and by the above argument $\text{Hom}_R(N, M) \subseteq \text{End}_R(M)$, thus $\text{Hom}_R(N, M)$ is a commutative ring (In fact $\text{Hom}_R(N, M)$ is a sub ring of $\text{End}_R(M)$).

(1)=(2) for each $f \in \text{Hom}_R(N, M)$, there exists $g \in \text{Hom}_R(N, M)$ and a positive integer n such that $f^n g f^n = f^n$, put $h = f^n g$, then $h^2 = h$, $f^n(N) = h(f^n(N)) \subseteq h(N)$, and $h(N) = f^n g(N) \subseteq f^n(N)$, then $f^n(N) = h(N)$. Further, $\text{Ker}(f^n) = (1-h)(N)$ but $N = h(N) \oplus (1-h)(N)$, then $N = f^n(N) \oplus \text{Ker}(f^n)$.

(2)=(1) for each $f \in \text{Hom}_R(N, M)$, there exists a positive integer n such that $N = f^n(N) \oplus \text{Ker}(f^n)$. For each $x \in N$, $x = f^n(y) + k$ for some $y \in N$ and $k \in \text{Ker}(f^n)$, $y = f^n(y_1) + k_1$ where $y_1 \in N$ and $k_1 \in \text{Ker}(f^n)$.

$f^n(x) = f^n[f^n(y_1) + k_1] = f^{2n}(f^n(y_1))$, put $u_x = f^n(y_1) \in f^n(N)$ where $f^n(x) = f^{2n}(u_x)$. Define $g: N \rightarrow M$ by $g(x) = u_x$ where $f^n(x) = f^{2n}(u_x)$ for each x in N , we claim that u_x is a unique element in $f^n(N)$ such that $f^n(x) = f^{2n}(u_x)$. For if $t \in f^n(N)$ such that $f^n(x) = f^{2n}(t)$, then $f^n(x) = f^{2n}(t - u_x) = 0$, hence $f^n(t - u_x) \in f^n(N) \cap \text{Ker}(f^n)$, thus $f^n(t - u_x) = 0$. And $t - u_x \in f^n(N) \cap \text{Ker}(f^n)$

therefore $t = u_x$. Using this uniqueness we can show that $u_{x+x_1} = u_x + u_{x_1}$ and $u_{rx} = r u_x$ for each $x, x_1 \in N$ and $r \in R$, furthermore, $u_{g(x)} = g(u_x)$, hence $g \in \text{Hom}_R(N, M)$ for each $x \in N$.

$$f^n g f^n(x) = f^n(g(f^n(x))) = f^n(u_{f^n(x)}) = f^n(f^n(u_x)) = f^{2n}(u_x) = f^n(x),$$

therefore, $\text{Hom}_R(N, M)$ is π -regular ring.

The following corollary follows from theorem (3.4) and proposition (3.3)

Corollary: Let M be a fully stable R -module of finite length, then $\text{Hom}_R(N, M)$ is π -regular ring for each cyclic submodule N of M .

Example:

Let R be any field, set $R_i = R$ for $i=1,2,3$. Consider the R -module $M = \bigoplus_{i=1}^3 R_i$, since $\text{End}_R(M)$ is isomorphic to the ring of all 3×3 matrices over R . Hence, it is non-commutative, thus M is not fully stable R -module⁽¹⁾. For the submodule of $N = R \oplus O \oplus O$ of M , we define $f, g: N \rightarrow M$ by $f(r, 0, 0) = (0, r, 0)$ and $g(r, 0, 0) = (0, 0, r)$ for each $r \in R$. Note that $f, g \in \text{Hom}_R(N, M)$ and $\text{Hom}_R(N, M) \subseteq \text{End}_R(M)$, but $g \circ f$ will not give the structure of ring. Therefore full stability of the module M in theorem (3.5) is essential to let $\text{Hom}_R(N, M)$ is a subring of $\text{End}_R(M)$.

Recall that an R -module M is uniform if every non-zero submodule of M has non-zero intersection with every other non-zero submodule of M . It is well known that if an R -module M is uniform (resp. of finite length), then M_p is uniform (resp. of finite length) R_p -module for each prime ideal p of R ⁽⁵⁾.

Remark: If each submodule N of an R -module is of the form $\text{ann}_R(I)$ for some ideal I of R , then M is a fully stable module⁽¹⁾.

Next we consider the relation between full stability and finiteness condition of modules.

Theorem: Every uniform module of finite length is fully stable.

Proof: Let M be a uniform R -module of finite length, then for each prime ideal p of R , the R_p -module M_p is uniform and of finite length⁽⁵⁾, but R_p is a local ring, then each submodule of M_p is of the form $\text{ann}_{M_p}(J)$ for some ideal J of R_p ⁽⁴⁾. By remark (3.7), for each prime ideal p of R , M_p is a fully stable R_p -module. Proposition (2.1) complete the proof.

The converse of theorem (3.8) may not be true in general, for example the \mathbb{Z} -module \mathbb{Z}_p^∞ is a uniform fully stable⁽¹⁾, but it is not of finite length.

An R -module M is said to be quasi-injective if every R -homomorphism of a submodule N of M into M can be extended to an R -endomorphism of M ⁽⁷⁾. In (2) we have shown that every fully stable module over a Dedekind domain is quasi-injective. In the rest of this section we consider the relationship between the following properties of modules, full stability. Finiteness conditions and quasi-injectivity.

Proposition: Every uniform finitely generated stable module over a Noetherian ring is of finite length.

Proof: Let M be a uniform finitely generated fully stable module over a Noetherian ring R . Then M is quasi-injective⁽²⁾, (Corollary (3.3)) finite length of M follows from ((4), proposition (4.1)).

Corollary: Let M be a uniform finitely generated module over a Noetherian ring R . Then the following statements are equivalent:

1. M is fully stable
2. M is of finite length
3. M is quasi-injective

Proof:

(1)-(2) follows from theorem (3.8) and proposition (3.9)

(2)-(3) follows from ((4), proposition (4.1) and corollary (4.3)).

In the following example we give a non-trivial uniform finitely generated fully stable module over a Noetherian ring.

Example

Let K be any field and $R=K[x]$ where $x^2=0$. For any non-zero element y in R , then $y=a+bx$ for some $a,b \in K$. Note that y is unit if and only if $a \neq 0$, thus, Rx is the only non-zero ideal of R , hence R is a uniform Noetherian ring.

Furthermore, $\text{ann}_R(\text{ann}_R(x))=(x)$ implies that R is fully stable ring.

REFERENCES

1. Abbas M.S. and Naoum A.G.; On fully stable modules, To appear.
2. Abbas M.S. and Naoum A.G.: Full stability and injectivity, To appar.
3. Abbas M.S.: Semi-fully stable modules, Al-Mustansiriya J. of Sci. (To appear).
4. Alamelu S.: On quasi-injective modules over Noetherian rings, J. of Indian Math. Soc., 39(1975) 121-130.
5. Atiyah M.F. and Moeckel I.G.: Introduction to commutative Algebra, Addison-Wesley publishing Company, Inc. (1969).
6. Barnard A.: Multiplication modules, J. Algebra, 71(1981) 174-178.
7. Johnson R.E., Wong E.T.: Quasi-injective modules and irreducible rings, J. London Math. Soc., 39(1961) 260-268.
8. McCoy N.H.: Generalized regular rings. Bull AMS. 45(1939).
9. Naoum A.G., and Hasan M.A.: The residual of finitely generated multiplication modules. Arch. Math. (Basel) 46 (1986), 225-230.
10. Weakley W.D.: Modules whose distinct submodules are not isomorphic, comm. Algebra, 15(1987) 1569-1587.

Direct Reduction of Some Nonlinear Evolution Equations

INAAM A. MLLOKI AND AMAL K. AL-TAMIMI

Department of Mathematics, College of Science, University of Al-Mustansiriya

(Received Sept. 10, 1999; Accepted Nov. 10, 1999)

الخلاصة

في بحثنا هذا قمنا بمناقشة طريقة مباشرة جديدة لاختزال المعادلة التفاضلية الجزئية الى معادلة تفاضلية اعتيادية باستخدام التحويل:

$$u(x,t) = \alpha(x,t) + \beta(x,t)w(z), \quad z = \zeta(x,t)$$

تستند هذه الطريقة الى الافتراض بان المعادلة التفاضلية الاعتيادية الناتجة يمكن تكاملها مباشرة لغرض الحصول على معادلة تفاضلية اعتيادية خالية من النقاط الحرجة المتحركة ولذا فان شروطا معينة تؤدي الى تحديد الاختزال وقد حصلنا على نتائج مشابهة لما حصل عليها في المصدر (٢).

ABSTRACT

In this paper we discuss a new procedure of reducing nonlinear partial differential equation to a single ordinary differential equation. The procedure is applied to Burgers', KdV and Boussinesq equations. Some similarity reductions of these equations to the first and second Painleve' equations are obtained.

INTRODUCTION

There is much current interest in the mathematically and physically significant determination of direct reductions of a given partial differential equation (PDE) to a single ordinary differential equation (ODE) (see(5)). This purpose can be achieved in several ways in the literatures. The most familiar way is the classical method of similarity using Lie group of infinitesimal transformation originally

developed by Lie⁽⁴⁾. Clarkson and Kruskal^(2,3), introduced, in 1989, a direct method that involves no group theoretical techniques for reducing a PDE to an ODE, some new similarity reductions of some evolution equations were obtained.

It has been noted⁽¹⁾ that there is a connection between these nonlinear PDEs solvable by inverse scattering transform (IST) and nonlinear ODEs without movable critical points. By a movable we mean, its location in the complex plane depends on the constants of integration of the ODE. A family of solutions of the ODEs without movable critical points is said to have the P-property: P stands for Painleve⁽⁴⁾. The ODE is of P-type if all its solutions have this property.

In this paper, we propose a direct method of determining reduction of a given n th order PDE (with the dependent variable u and the independent variables x and t), to a single ODE of Painleve' type using the ansatz

$$u(x,t) = \alpha(x,t) + \beta(x,t)w(z), \quad z = \zeta(x,t) \quad (1.1)$$

where α, β and z are assumed to be sufficiently differentiable functions and $w(z)$ is n times differentiable.

Outline of the Procedure

To illustrate the steps of our procedure of direct reduction we see first that substituting (1.1) into the given PDE leads to rather complicated polynomial expression involving various monomial products of derivatives of w whose coefficients depend on the partial derivatives of α, β and z . We assume that this expression is an ODE for $w(z)$ which can be integrated to an ODE of P-type. Hence, three kinds of conditions (or assumptions) are used to specify the direct reduction (1.1), i.e., to specify α, β, z and the equation for $w(z)$. These conditions are:

- i) The coefficients of different monomials are functions of z only.
- ii) Integrability conditions for direct integration.
- iii) Conditions of P-type equations.

In the next section we apply the above procedure to Boussinesq equation

$$u_{tt} + \frac{1}{2}(u^2)_{xx} + u_{xxxx} = 0 \quad (2.1)$$

to the KdV equation

$$u_t + \delta u u_x + \mu u_{xxx} = 0 \quad (2.2)$$

and to the Burgers equation

$$u_t + \delta u u_x + \mu u_{xx} = 0 \quad (2.3)$$

Application of the Method

A. Boussinesq Equation

In this section we shall apply the procedure discussed in section 2 to the Boussinesq equation (2.1). Substituting (1.1) into equation (2.1) and collecting coefficients of the same terms of $w(z)$ and its derivatives we get

$$w^{(4)} = Ew^{(3)} + Fw^{(2)} + Gw' + Hw + Iww'' + Iw'^2 + Rww' + Sw^2 + T \quad (3.1)$$

where

$$E = (6\beta z_x^2 z_{xx} + 4z_x^3 \beta_x) / (-\beta z_x^4), \quad (3.1a)$$

$$F = (\beta z_t^2 + \alpha \beta z_x^2 + 4z_{xxx} z_x \beta + 12\beta_x z_x z_{xx} + 3\beta z_{xx}^2 + 6\beta_{xx} z_x^2) / (-\beta z_x^4), \quad (3.1b)$$

$$G = (\beta z_{xxxx} + 4\beta_x z_{xxx} + 6\beta_{xx} z_{xx} + 4\beta_{xxx} z_x + 2\alpha_x \beta z_x + 2\alpha \beta_x z_x + \alpha \beta z_{xx} + 2\beta_t z_t + \beta z_{tt}) / (-\beta z_x^4), \quad (3.1c)$$

$$H = (\beta_{xxxx} + 2\alpha_x \beta_x + \alpha \beta_{xx} + \alpha_{xx} \beta + \beta_{tt}) / (-\beta z_x^4), \quad (3.1d)$$

$$I = (\beta^2 z_x^2) / (-\beta z_x^4) = -\beta / z_x^2, \quad (3.1e)$$

$$R = (4\beta \beta_x z_x + \beta^2 z_{xx}) / (-\beta z_x^4), \quad (3.1f)$$

$$S = (\beta_x^2 + \beta \beta_{xx}) / (-\beta z_x^4), \quad (3.1g)$$

and

$$T = (\alpha_{tt} + \alpha \alpha_{xx} + \alpha_x^2 + \alpha_{xxx}) / (-\beta z_x^4), \quad (3.1h)$$

We assume that E, F, G, H, I, R, S and T are functions of z only so that equation (3.1) will be an ODE for $w(z)$.

Lemma

If the two sets of relations (integrability conditions for direct integration),

$$F'' - E''' - G' + H = 0, \quad S + \frac{1}{2} I'' - \frac{1}{2} R' = 0 \quad (3.2)$$

and

$$3F'' - 2F' + G = 0, R - 2I' = 0 \quad (3.3)$$

are satisfied then equation (3.1) is integrable to the second order ODE

$$w'' = Ew' + (F - 2E')w + \frac{1}{2}Iw^2 + T_2, T_2 = \int T_1 dz, T_1 = ST dz \quad (3.4)$$

Proof: If we integrate equation (3.1) once we get

$$w''' = Ew'' + (F - E')w' + (E'' - F' + G)w - Iww' + \frac{1}{2}(R - I')w^2 + \int T dz + \int (F'' + E''' - G' + H)w dz + \int (S + \frac{1}{2}I' - R'/2)w^2 dz \quad (3.5)$$

By the first set of relations (3.2), equation (3.5) becomes

$$w''' = Ew'' + (F - E')w' + (E'' - F' + G)w - Iww' + \frac{1}{2}(R - I')w^2 + T_1, T_1 = \int T dz \quad (3.6)$$

If we integrate equation (3.6) second we obtain

$$w'' = Ew' + (F - 2E')w + \frac{1}{2}Iw^2 + T_2 + \int (3E'' - 2F' + G)w dz + \frac{1}{2} \int (R - 2I')w^2 dz, T_2 = \int T_1 dz \quad (3.7)$$

Then, the relations defined by (2.3) imply that (3.7) gives (3.4).

P-Type conditions of Equation (3.4)

By comparing equation (3.4) with the general form of the absence of movable critical points (see (4)):

$$w'' = L(z, w)w'^2 + M(z, w)w' + N(z, w) \quad (*)$$

we have $L=0$ therefore, equation (3.4) will take the form of equation

$$w'' = (A_0(z) + A_1(z)w)w' + B_0(z) + B_1(z)w + B_2(z)w^2 + B_3(z)w^3 \quad (**)$$

Then

$$A_0 = E,$$

$$A_1 = 0,$$

$$B_0 = T_2$$

$$B_1 = F - 2E'$$

$$B_2 = \frac{1}{2}$$

$$B_3 = 0$$

$$(3.8)$$

Since $A_1 = B_3 = 0$ implies that the equation (2.2) leads to the equation

$$w'' = 6w^2 + pz + q \quad (3.9)$$

this gives that $T = T_2$

$$A_0 = E = 0, B_0 = pz + q \text{ i.e. } T(z) = 0, B_1 = F - 2E' = 0$$

$$\text{i.e. } F = 0, B_2 = I/2 = 6 \text{ i.e. } I = 12 \quad (3.10)$$

and from (3.2), (3.3) we find

$$G=0, H=0, R=0 \text{ and } S=0 \quad (3.11)$$

Combining these conditions (P-type conditions) with the relations (3.1a) to (3.1h) gives the following system of eight PDEs with unknown functions α, β and z

$$3\beta z_{xx} + 2\beta_x z_x = 0 \quad (3.12a)$$

$$3\beta z_{xx}^2 + 4\beta z_x z_{xxx} + 12\beta_x z_x z_{xx} + 6\beta_{xx} z_x^2 + \alpha \beta z_x^2 + \beta z_t^2 = 0 \quad (3.12b)$$

$$\beta z_{xxxx} + 4\beta_x z_{xxx} + 6\beta_{xx} z_{xx} + 4\beta_{xxx} z_x + 2\alpha_x \beta z_x + 2\alpha \beta_x z + \alpha \beta z_{xx} + 2\beta_t z_t + \beta z_{tt} = 0 \quad (3.12c)$$

$$\beta_{xxxx} + 2\alpha_x \beta_x + \alpha \beta_{xx} + \beta_{tt} = 0 \quad (3.12d)$$

$$\beta = -12z_x^2 \quad (3.12e)$$

$$4\beta_x z_x + \beta z_{xx} = 0 \quad (3.12f)$$

$$\beta_x^2 + \beta \beta_{xx} = 0 \quad (3.12g)$$

$$\alpha_{tt} + \alpha \alpha_{xx} + \alpha_x^2 + \alpha_{xxxx} = 0 \quad (3.12h)$$

substituting (3.12e) in (3.12a) we get

$$z(x,t) = \theta(t)x + \sigma(t) \quad (3.13)$$

where θ and σ are arbitrary functions of t . Then

$$\beta(x,t) = -12\theta^2(t) \quad (3.14)$$

from equation (3.12b) and by using (3.13) we obtain

$$\alpha(x,t) = \frac{(\theta'x + \sigma')^2}{\theta^2} \quad (3.15)$$

from equation (3.12c) and by using (3.13), (3.14) and (3.15) we get

$$\beta z_{tt} + 2\beta_t z_t + 2\beta \alpha_x z_x = 0 \quad (3.16)$$

which gives

$$\theta'' = 0 \text{ and consequently } \sigma'' = 0$$

i.e.

$$\theta(t) = c_1 t + c_2 \quad (3.17)$$

and

$$\sigma(t) = c_3 t + c_4 \quad (3.18)$$

where c_1, c_2, c_3 and c_4 are arbitrary constants. Then the transformation becomes

$$\begin{aligned} u(x,t) &= -(\theta'x + \sigma')^2 / \theta^2 - 12\theta^2 w(\theta x + \sigma) \\ &= -(c_1 x + c_3)^2 (c_1 t + c_2)^{-2} - 12(c_1 t + c_2)^2 w(z), \\ z &= (c_1 t + c_2)x + c_3 t + c_4 \end{aligned} \quad (3.19)$$

we can set $c_1 = 1, c_2 = c_3 = c_4 = 0$ then (3.20) becomes

$$u(x,t) = -12t^2 w(z) - x^2 t^{-2}, \quad z = tx \quad (3.20)$$

where $w(z)$ satisfies (3.9) and it is known, by trivial changes in the variables, this equation may be brought into one or other of the three standard forms:

- i) $w''=6w^2$ (when $p=q=0$)
- ii) $w''=6w^2 + \frac{1}{2}$ (when $p=0, q \neq 0$)
- iii) $w''=6w^2 + z$ (when $p \neq 0, q=0$)

(3.21)

Note: by rescaling $w(z)$ in (3.20) we get one of the new reduction of the Boussinesq equation to PI which was found by Clarkson and Kruskal⁽²⁾.

KdV Equation

Now, we apply the procedure to the KdV equation (2.3). Substituting (1.1) into (2.3) and collecting coefficients of the same terms of $w(z)$ and its derivatives we get

$$w'''' = Fw'' + Gw' + Hw + Rww' + Sw^2 + T \quad (3.22)$$

where

$$F = 3\beta z_x z_{xx} + 3\beta z_x^2 / (-\beta z_x^3) \quad (3.22a)$$

$$G = (\beta z_t + \delta \alpha \beta z_x + 3\mu \beta z_x z_{xx} + 3\mu \beta z_{xx} z_x + \mu \beta z_{xxx}) / (-\mu \beta z_x^3) \quad (3.22b)$$

$$H = (\beta_t + \delta \alpha \beta_x + \delta \beta \alpha_x) / (-\mu \beta z_x^3), \quad (3.22c)$$

$$R = (\delta \beta^2 z_x) / (-\mu \beta z_x^3) = -\delta \beta / \mu z_x^2 \quad (3.22d)$$

$$S = \delta \beta \beta_x / (-\mu \beta z_x^3) = -\delta \beta_x / \mu z_x^3 \quad (3.22e)$$

and

$$T = (\alpha_t + \delta \alpha \alpha_x + \mu \alpha_{xxx}) / (-\mu \beta z_x^3) \quad (3.22f)$$

We assume that F, G, H, R, S and T are functions of z only so that equation (3.22) will be an ODE for $w(z)$.

Lemma:

If we have the set of two relations (integrability conditions for direct integration

$$F'' - G' + H = 0, S = -\frac{1}{2} R' = 0 \quad (3.23)$$

Then equation (3.22) is integrable to the second order ODE

$$w'' = Fw' + (G - F')w + \frac{1}{2} R w^2 + T_1, T_1 = \int T dz \quad (3.24)$$

Proof: Since the direct integration of equation (3.22) yields the second ODE

$$w'' = Fw' + (G - F')w + \frac{1}{2} R w^2 + \int T dz + \int (F'' - G' + H) w dz + \int (S - R'/2) w^2 dz \quad (3.25)$$

then it is clear that by (3.23) we get the required ODE (3.24)

P-Type Conditions of Equation (3.24)

Now comparing equation (3.24) with the general form of second order. ODE of the absence of movable critical points (*), we have $L=0$. Consequently, equation (3.24) will take the form (**)

Hence,

$$A_0=F, A_1=0, \\ B_0=T_1, B_1=G-F', B_2=\frac{1}{2}R, B_3=0 \quad (3.26)$$

Since $A_1=B_3=0$ and $B_2 \neq 0$ then the equation (3.24) takes the form of equation (3.9), this gives that

$$A_0=F=0, T_1 p z_{\eta} + (\text{i.e. } T=p), B_1=G-F'=0, \\ B_2=\frac{1}{2}R=6 \text{ (i.e. } R=12) \quad (3.27)$$

From (3.23) we get

$$G=0 \text{ and then } H=0 \text{ and } S=0 \quad (3.28)$$

Combining these conditions (P-type conditions) with the relations (3.22a) to (3.22f) gives the following system of six PDEs with unknown α, β and z

$$3\beta z_{xx} + 3\beta_x z_x = 0 \quad (3.29a)$$

$$\beta z_t + \delta \alpha \beta z_x + \mu \beta z_{xxx} + 3\mu \beta_x z_{xx} + 3\mu z_x \beta_{xx} = 0 \quad (3.29b)$$

$$\beta_t + \delta \alpha \beta_x + \delta \beta \alpha_x + \mu \beta_{xxx} = 0 \quad (3.29c)$$

$$\delta \beta = -12\mu z_x^2 \quad (3.29d)$$

$$\beta_x = 0 \quad (3.29e)$$

$$\alpha_t + \delta \alpha \alpha_x + \mu \alpha_{xxx} = -\mu p z_x^3 \beta \quad (3.29f)$$

To get the transformation (1.1) we must solve the above system. From the equation (3.29e) we get

$$\beta(x,t) = \theta(t)$$

where $\theta(t)$ is an arbitrary function of t . Equation (3.29d) gives

$$z_x = \sqrt{\frac{\delta}{-12\mu}} \theta^{1/2}$$

therefore

$$z(x,t) = \sqrt{\frac{\delta}{-12\mu}} \theta^{1/2} x + \sigma(t) \quad (3.30)$$

where $\sigma(t)$ is an arbitrary function of t . Substituting β and z in equation (3.29b) we get

$$\theta(\sigma' + \frac{1}{2} \sqrt{\frac{\delta}{-12\mu}} \theta^{-1/2} \theta' x) + \delta \theta \sqrt{\frac{\delta}{-12\mu}} \theta^{1/2} = 0$$

which gives

$$\alpha(x,t) = -\frac{1}{\delta} \sqrt{\frac{-12\mu}{\delta}} \theta^{-\frac{1}{2}} - \frac{1}{2\delta} \theta' \theta^{-1} x \quad (3.31)$$

substituting α, β and z in equation (3.29c) gives

$$\theta' = 0 \text{ i.e. } \beta(x,t) = \theta(t) = a \quad (3.32)$$

where a is a constant. Therefore

$$z(x,t) = \sqrt{\frac{\delta a}{-12\mu}} x + \sigma(t) \quad (3.33)$$

and

$$\alpha(x,t) = -\frac{1}{\delta} \sqrt{\frac{-12\mu}{\delta a}} \sigma' \quad (3.34)$$

By substituting (3.34) in equation (3.29f) we get

$$\sigma'' = -\delta^3 a^3 p / 144\mu \quad (3.35)$$

then

$$\sigma(t) = -\frac{\delta^3 a^3 p}{288\mu} t^2 + c_1 t + c_2 \quad (3.36)$$

and

$$\alpha = \frac{\delta^3 a^3 p}{144\mu} \sqrt{\frac{-12\mu}{\delta a}} t - \frac{c_1}{\delta} \sqrt{\frac{-12\mu}{\delta a}} \quad (3.37)$$

then

$$u(x,t) = \frac{\delta^2 a^3 p}{144\mu} \sqrt{\frac{-12\mu}{\delta a}} t - \frac{c_1}{\delta} \sqrt{\frac{-12\mu}{\delta a}} + aw(z) \quad (3.38)$$

$$z = \sqrt{\frac{\delta a}{-12\mu}} x - \frac{\delta^3 a^3 p}{288\mu} t + c_1 t + c_2$$

where c_1 and c_2 are arbitrary constants. Since we can set $a=12$, $\delta=\mu=1$, $c_2=0$ then the direct reduction (3.38) becomes

$$u(x,t) = -12w(z) - 12pt - c_1, \quad z = x + 6pt^2 + c_1 t \quad (3.39)$$

where $w(z)$ satisfies (3.9)

Note: By rescaling $w(z)$ in (3.39) we get the same direct reduction which was found by Clarkson and Kruskal⁽²⁾.

Burgers' Equation

We illustrate our procedure of direct reduction of Burgers' equation (2.4). First, we substitute (1.1) into equation (2.4) and collecting the coefficients of the same terms of $w(z)$ and its derivatives we get.

$$w'' = Fw' + Gw + Rww' + Sw^2 + T \quad (3.40)$$

where

$$F = (\beta z_t + \delta \alpha \beta z_x + \mu \beta z_{xx} + 2\mu z_x \beta_x) / (-\mu \beta z_x^2) \quad (3.40a)$$

$$G = (\beta_t + \delta \alpha \beta_x + \delta \beta \alpha_x + \mu \beta_{xx}) / (-\mu \beta z_x^2) \quad (3.40b)$$

$$R = \delta \beta / (-\mu z_x) \quad (3.40c)$$

$$S = \delta \beta_x / (-\mu z_x^2) \quad (3.40d)$$

And

$$T = (\alpha_t + \delta \alpha \alpha_x + \mu \alpha_{xx}) / (-\mu \beta z_x^2) \quad (3.40e)$$

We assume that F, G, R, S and T are functions of z only so that equation (3.40) will be an ODE for $w(z)$.

It can be easily seen that, if we assume the set of two conditions

$$G - F' = 0 \quad (3.41a)$$

$$S - \frac{1}{2} R' = 0 \quad (3.41b)$$

Are satisfied then (3.40) can be integrated and reduced to the generalized Riccati equation

$$w' = \frac{1}{2} R w^2 + F w + T_1, \quad T_1 = \int T dz \quad (3.42)$$

which has considerable theoretical interest since its solution free from movable critical points, it has only movable poles. We shall use (3.41) to specify β and z .

Lemma:

For the direct reduction (1.1)

- i) $\beta(x, t)$ is a function of t only
- ii) $z(x, t)$ is a linear function in x

Proof: The integrability condition (3.41b) can be written using (3.40d) as

$$\beta_x = R' z_x (\mu z_x) / 12 \delta \quad (3.43)$$

and from (3.40c) we have

$$\mu z_x = \delta \beta / R \quad (3.44)$$

hence,

$$\frac{\beta_x}{\beta} = \frac{1}{2} \frac{R' z_x}{R} \quad (3.45)$$

and by integrating with respect to x we have

$$\beta(x,t) = \theta(t) \sqrt{R(z)}, \quad (3.46)$$

where $\theta(t)$ is arbitrary function of t . Substituting (3.46) in (1.1) gives that we can choose $R(z)=1$. Consequently,

$$z_x = \frac{\delta}{\mu} \beta, \quad \beta = \theta(t)$$

which gives,

$$z(x,t) = \frac{\delta}{\mu} \theta(t)x + \sigma(t) \quad (3.47)$$

where θ and σ are arbitrary functions of t .

According to this lemma and the relations (3.41a) and (3.41b) we can rewrite the system (3.40) as follows:

$$\delta \theta' x + \mu \sigma' + \delta^2 \theta \alpha = -\delta^2 \theta^2 F, \quad (3.48a)$$

$$\mu \theta' + \mu \delta \theta \alpha_x = -\delta^2 \theta^3 F' \quad (3.38b)$$

and

$$\mu \alpha_t + \mu \delta \alpha \alpha_x + \mu^2 \alpha_{xx} = -\delta^2 \theta^3 T. \quad (3.48c)$$

from equation (3.48a) we have

$$\alpha(x,t) = -\frac{1}{\theta} \left(\frac{x}{\delta} \theta' + \frac{\mu}{\delta^2} \sigma' \right) - \theta F \quad (3.49)$$

then we can take $F=0$ i.e.

$$\alpha(x,t) = -\frac{1}{\theta} \left(\frac{x}{\delta} \theta' + \frac{\mu}{\delta^2} \sigma' \right) \quad (3.50)$$

then we get the direct reduction

$$u(x,t) = -\frac{1}{\theta} \left(\frac{x}{\delta} \theta' + \frac{\mu}{\delta^2} \sigma' \right) + \theta w(z), \quad z = \frac{\delta}{\mu} \theta(t)x + \sigma(t) \quad (3.51)$$

by substituting (3.50) in (3.48c) we have the two following equations

$$\theta \theta'' - 2\theta'^2 = a \frac{\delta^4}{\mu^2} \sigma^6 \theta \theta'' - \theta'^2 = a \frac{\delta^4}{\mu^2} \theta^6 \quad (3.52a)$$

$$\theta\sigma'' - 2\sigma'\theta' = \frac{\delta^4}{\mu^2} \theta^5 (a\sigma + b) \quad (3.52b)$$

This is the same result with $\delta=\mu=1$, which was found by Clarkson and Kruskal in 1989, i.e. by the use of integrability conditions of equation (3.40) to the generalized Riccati equation we can get Clarkson and Kruskals results.

P-Type Conditions of Equation (3.40)

Now, since equation (3.40) is second order ODE we can directly compare it with the general form of second order ODE of the absence of movable critical points, we note that $L=0$ and consequently equation (3.40) must take the form since $A_1=R \neq 0$, $B_3=0$, then equation (3.40) will take the form (see (14) p. 331):

$$w'' = q(z)w' + q'(z)w - 2ww' \quad (3.53)$$

i.e. we get the following relations

$$F = q(z)$$

$$G = q'(z)$$

$$R = -2$$

And

$$S = T = 0$$

Which gives the following system of five PDEs

$$(\beta z_t + \delta \alpha \beta z_{xx} + \mu \beta z_{xx} + 2\mu z_x \beta_x) = \mu \beta z_x^2 q(z) \quad (3.55a)$$

$$(\beta_t + \delta \alpha \beta_x + \delta \beta \alpha_x + \mu \beta_{xx}) = -\mu \beta z_x^2 q'(z) \quad (3.55b)$$

$$\delta \beta = 2\mu z_x \quad (3.55c)$$

$$\beta_x = 0 \quad (3.55d)$$

$$\alpha_t + \delta \alpha \alpha_x + \mu \alpha_{xx} = 0 \quad (3.55e)$$

From equation (3.55b) we have

$$\beta(x,t) = \theta(t) \quad (3.56)$$

Equation (3.55c) gives that

$$z(x,t) = \frac{\delta}{2\mu} \theta(t)x + \sigma(t) \quad (3.57)$$

Substituting $\beta(x,t)$ and $z(x,t)$ in equation (3.55a) we have

$$\alpha(x,t) = -\frac{\theta}{2} q - \frac{\mu}{\delta^2 \theta} \left(\frac{\delta}{\mu} \theta' x + 2\sigma' \right)$$

and since we can set $q(z)=0$ then

$$\alpha(x,t) = -\frac{1}{\theta} \left(\frac{1}{\delta} \theta' x + 2 \frac{\mu}{\delta^2} \sigma' \right) \quad (3.58)$$

which gives that

$$\theta \theta'' - 2\theta'^2 = 0, \quad (3.60)$$

and

$$\theta \sigma'' - 2\theta' \sigma' = 0 \quad (3.61)$$

equation (3.60) can be integrated to

$$\theta' = c\theta^2 \quad (3.62)$$

Now, we have two cases

Case (i) $c=0$, then we have $\theta=\theta_0$, $\sigma(t)=at+b$, then we get the direct reduction

$$u(x,t) = \frac{-2\mu}{\delta^2} \frac{a}{\theta_0} + \theta_0 w(z), \quad z = \frac{\delta}{2\mu} \theta_0 x + at + b \quad (3.63)$$

where $\theta_0 \neq 0$, a and b are arbitrary constants. We set (i.e. without loss of generality) $\theta_0=1$, $\mu=1/2$, $\delta=1$ then we have the direct reduction

$$u(x,t) = w(z) - a, \quad z = x + at + b \quad (3.64)$$

Case (ii): $c \neq 0$, then by solving equations (3.60) and (3.61) respectively we have

$$\theta(t) = (-ct - t_0)^{-1}, \quad (3.65)$$

and

$$\sigma(t) = \frac{a}{c} (-ct - t_0)^{-1} + b \quad (3.66)$$

then we get

$$u(x,t) = \frac{-c}{\delta} (-ct - t_0)^{-1} x - \frac{2a\mu}{\delta^2} (-ct - t_0)^{-1} + (-ct - t_0)^{-1} w(z) \\ z = \frac{\delta}{2\mu} (-ct - t_0)^{-1} x + \frac{a}{c} (-ct - t_0)^{-1} + b \quad (3.67)$$

where t_0, a and b are arbitrary constants. Since we can set $\delta=1$, $\mu=1/2$, $c=-1$, $t_0=0$, $a=0$ and $b=0$, then we have the direct reduction

$$u(x,t) = \frac{x}{t} + \frac{1}{t} w(z), \quad z = \frac{x}{t} \quad (3.68)$$

Note: These two results are special cases from the results obtained from (3.51) and (3.52).

REFERENCES

1. Ablowitz, M.J., Ramani A., and Sequer, H., A connection between nonlinear evaluation equations and ordinary differential equations of P-type *J. Math. Phys.*, 21(4), 715-721 (1980).
2. Clarkson, P.A., and Kruscal, M.D., New similarity reductions of the Boussinesq equation. *J. Math. Phys.* 30(10): 2201-2213 (1989).
3. Clarkson, P.A., and Kruscal, M.D., New similarity solutions for the modified Boussinesq equation. *J. Phys. A. Math. Gen.* 22: 2355-2367 (1989).
4. Ince, E.L., Ordinary differential equations, Dover Publ. Ince., New York, (1956).
5. Olver, P.J., Direct reduction and differential constraints. *Proc. R. Soc. Lond. A.*, 444: 509-523 (1994).

Scheduling Job Classes on a Single Machine with batches to Minimize the Sum of the Weighted Completion Times

TARIK S. ABDUL-RAZAQ AND KAWA A. ABDULLAH

Mathematical Department, College of Science, University of Al-Mustansiriya

(Received Sept. 10, 1999; Accepted Nov. 2, 1999)

الخلاصة

تناولنا في هذا لبحث دراسة n من النتائج (Jobs) على ماكينة واحدة وان هذه النتائج مقسمة الى F من المجموعات (Families) كل مجموعة f ($f=1, \dots, F$) تحتوي على n_f من النتائج. الغرض من هذه الدراسة هو ايجاد الترتيب الامثل للنتائج لتصغير المجموع الوزني لاقوات الاتمام (Total weighted completion time)، وقد استعملت خوارزمية التفرع والتقييد (Branch and bound algorithm) وهي تعتمد على القيد الاعلى (Upper bound) والقيد الادنى (Lower bound) وطريقة لاتفرع (Branching method)، هذه الخوارزمية تعتمد ايضا على قواعد الهيمنة (Dominance rules) لتقليل عدد التفرعات في شجرة البحث (Search tree)، ومن الجدير بالذكر هنا ان للمسالة قيد البحث تطبيقات عملية كثيرة في العديد من الدراسات والبحوث توجد تطبيقات مختلفة لمسائل الجدولة والتي تكون فيها النتائج مصنفة الى مجموعات ومثال على تطبيق هذه المسالة في مجال صناعة الانابيب الفولاذية (steel pipes)، عملية صنع الانابيب تعتمد على استعمال الاسطوانة، حيث ان الاسطوانة تعتمد على القطر الخارجي للانبوب، تغيير الاسطوانة يمثل وقت الانتقال من صنع انبوب ذي قطر معين الى صنع انبوب ذي قطر اخر، لذا فان الانابيب التي لها نفس القطر الخارجي تقع في نفس المجموعة.

ABSTRACT

In this paper a new branch and bound algorithm for a single machine scheduling problem with batching is given. Jobs are partitioned into families, and a set-up time is necessary when there is a switch from processing jobs of one family to jobs of another family. The objective is to minimize the total weighted completion time. A new lower bound based on relaxation of set-ups is derived. Computational experience with instances having up to 50 jobs shows that the lower bound is effective in restricting the search.

INTRODUCTION

The problem may be stated as follows. Consider the set of jobs $N = \{1, \dots, n\}$ and one machine. The machine can not process more than one job at a time, the jobs are divided into F families. Each family f , for $1 \leq f \leq F$, contains n_f jobs. The jobs are numbered $1, \dots, n$. Sometimes it is more convenient to refer to job (i, f) , which is the i th job in family f , for $1 \leq i \leq n_f$. All jobs are available for processing at time zero, and are to be scheduled on a single machine. We let p_{if} denote the processing time of job (i, f) , and w_{if} is its weight. A sequence-independent set-up time s_f is incurred whenever a job in family f is processed immediately after a job in a different family. Also, an initial set-up time s_f is required if a job from family f is the first to be processed. The machine cannot perform any processing whilst under going a set-up. The objective is to find a schedule, with an associated completion time C_{if} for each job (i, f) ($i=1, \dots, n_f$, $f=1, \dots, F$) which minimizes the sum of weighted completion times

$$\sum_{(i,f) \in N} w_{if} C_{if}$$

In this section we shall give a brief review of the algorithms for scheduling that deal with job grouping. Our review consolidates results from the single-machine scheduling literature and presents them within a general framework.

For $1/s_f/L_{\max}$ problem, Monma and Potts⁽¹¹⁾, show that jobs within each family are sequenced in EDD (Earliest Due Date) order. Thus, the problem requires the merging of ordered lists of jobs, where lists contains all jobs of a family in EDD order.

Hariri and Potts⁽⁹⁾ gave a BAB algorithm to solve the $1/s_f/L_{\max}$ problem. A partitioning of the n jobs into F families is given. A set-up time is required at the start of each batch, where a batch is a largest set of contiguously scheduled algorithm. Their computational results indicate that instances with up to 50 jobs can be solved.

The $1/s_f/\Sigma C_i$ problem of scheduling n jobs on a single machine is considered by Gupta⁽⁸⁾, where the jobs are partitioned into two classes and a set-up time is necessary between jobs of different classes.

Gupta proposes an algorithm which requires $O(n \log n)$ times, which, he claims that it generates an optimal schedule for minimizes the sum of completion times. However, Potts⁽¹²⁾ shows using a counter-example that it can fail to generate an optimal schedule. Ahn and Hyun⁽¹⁾ derive a DP algorithm for the sum of completion times problem which generates an optimal solution in $O(n^2)$ time. Also, Monma and Potts⁽¹¹⁾ use DP to show that the sum of weighted completion times problem is solvable in $O(n^4)$ time. A variant of the DP algorithm for Monma and Potts is proposed by Potts⁽¹²⁾ to solve the sum of weighted completion times problem in $O(n^3)$ time. Although the algorithms of Ahn and Hyun, and Monma and Potts solve problems with more than two job classes, they are of little practical use unless the number of classes is small.

Potts⁽¹²⁾ proposes some interesting research problems for the case of several job classes. One of the important research area include the derivation of branch and bound algorithms (which we propose in this paper), and worst-case analysis of heuristics for the $1/s_f/\Sigma w_i C_i$ problem.

For $1/s_f/\Sigma C_i$ problem, Mason and Anderson⁽¹⁰⁾ drive a BAB algorithm which relies mainly on dominance rules to restrict the search tree. Their computational results for

Scheduling Job Classes on a Single Machine with batches to Minimize the Sum of the Weighted Completion Times

T. S. Abdul-Razaq And K. A. Abdullah

$1/s_f/\Sigma C_i$ problem indicate that instances with up to 30 jobs can be solved. Anderson et al.⁽²⁾ show that the $1/s_f/\Sigma C_i$ problem indicate that instances with up to 30 jobs can be solved. Anderson et al.⁽²⁾ show that $1/s_f/\Sigma w_i C_i$ problem, in which families of jobs with associated sequence independent set-up times are to be scheduled on a single machine to minimize the total weighted completion time, can be viewed as a sequencing problem. Since jobs within each family must be sequenced in SWPT order (Monma and Potts⁽¹¹⁾), it can also be regarded as a problem of merging ordered lists of jobs, where each ordered list contains all the jobs in one family. In 1998 Crauwels et al.⁽⁷⁾ presents several BAB algorithms for the $1/s_f/\Sigma w_i C_i$ problem, their computational results with instances having up to 50 jobs shows that the lower bounds are effective in restricting the search tree. Also Baker⁽³⁾ in 1998 examines optimal and heuristic solution procedures for the same problem, his computational experiments with a basic BAB procedure shows how problem parameters affect run times.

Local search heuristic are developed by Crauwels et al.⁽⁶⁾ for the $1/s_f/\Sigma w_i C_i$ problem.

The $1/s_f/\Sigma U_i$ problem, for an arbitrary number of families is shown to be NP-hard by Bruno and Downey⁽⁴⁾. Various attempts by Crauwels et al.⁽⁵⁾ to solve problem instances of a reasonable size using BAB approach indicate its challenging nature. Therefore, they propose local search heuristics to solve the problem.

Problem Structure

To state our problem of scheduling more precisely, we are given a set N containing n jobs that are divided into F families. Each family f , for $f=1, \dots, F$ contains n_f jobs. We assume that the jobs within each family are indexed in SWPT order. Thus, $p_{1f}/w_{1f} \leq \dots \leq p_{n_f f}/w_{n_f f}$ for $f=1, \dots, F$

A sequence independent set-up time $s_f \geq 0$ is incurred whenever a job in family f is processed immediately after a job in a different family. Also, an initial set-up time s_f is

required if a job from family f is processed first on the machine.

Suppose the processing order $\sigma=(\sigma(1),\dots,\sigma(n))$, a vector $(s_{\sigma(1)},\dots,s_{\sigma(n)})$ of corresponding set-up times is easily constructed: the set-up time required immediately before the processing of job $\sigma(i)$ ($i=1,\dots,n$) is given by:

$s_{\sigma(1)}$ is the set-up time of the first job (positive integer constant),

$$s_{\sigma(i)} = \begin{cases} \alpha_{fg} & \text{if } i > 1, \sigma(i-1) \in f \text{ and } \sigma(i) \in g, f \neq g \\ 0 & \text{otherwise} \end{cases}$$

where α_{fg} is a positive integer constant, f and g are families.

Then, the sum of weighted completion times for σ can be expressed as:

$$\sum_{i \in N} w_{\sigma(i)} C_{\sigma(i)} = \sum_{i \in N} (W - \sum_{j=1}^i w_{\sigma(j-1)}) (s_{\sigma(i)} + p_{\sigma(i)}) \quad (1)$$

where $W = \sum_{i \in N} w_i$, $w_{\sigma(0)}=0$

Thus, by scheduling job $\sigma(i)$ in position i of the sequence, its overall contribution to the weighted sum of completion times is observed to be $(W - \sum_{j=1}^i w_{\sigma(j-1)}) (s_{\sigma(i)} +$

$p_{\sigma(i)})$.

Note that equation (1) can also be used for the case of no set-up times. Also it should be noted that this is for the first time the weighted sum of completion times can be written as a simple expression as in (1) (see Potts(1991)⁽¹²⁾).

Our problem can be formally stated as:

$$\text{Minimize } \sum_{(i,f) \in N} w_{if} C_{if} = \sum_f \sum_{i \in f} w_{if} C_{if}$$

Subject to

$$\left. \begin{aligned} C_{if} &= s_f + p_{if} \\ C_{if} &\geq C_{i-1,f} + p_{if}, (i,f) \in N, i > 1 \end{aligned} \right\} \quad (2)$$

Where C_{if} denotes the completion time of job (i,f) . Constraints (2) ensure that the SWPT ordering within families.

We first present two fundamental results on the structure of an optimal schedule.

Theorem (2.1) (Monma and Potts⁽¹¹⁾)

In any optimal schedule jobs within each family are sequenced in SWPT order.

From Theorem (2.1), our problem reduces to one of merging SWPT order lists of jobs for the different families to form a sequence. This insight reduces the number of schedules we have to enumerate to $n!/(n_1!n_2!\dots n_F!)$.

Consider any schedule $S=(B_1,\dots,B_r)$, where each batch $B_i(i=1,\dots,r)$ contains jobs from a particular family $f(f=1,\dots,F)$ and begins with a set-up. We define the weighted processing time (WPT) ratio R for each batch B_i to be

$$R(B_i) = (s_f + \sum_{(i,f) \in B_i} p_{if}) / \sum_{(i,f) \in B_i} w_{if}$$

The following result gives a generalized SWPT rule for batches that uses WPT ratios.

Theorem (2.2) (Mason and Anderson⁽¹⁰⁾)

In any optimal schedule, batches are sequenced in non-decreasing order of WPT ratios.

We wish to find a schedule which minimizes the total weighted completion time of the jobs. We can limit our search for an optimal solution to the class of schedules that satisfies these two theorems above. Furthermore, when we construct heuristic methods, we make use of these two theorems also.

Special Cases Yield Optimal Solution

The following results give an optimal solution to our problem. Suppose that we have n jobs that are divided into F families.

Theorem (3.1)

For the $1/s_f/\sum w_i C_i$ problem there is an optimal solution if the families can be ordered such that $p_{ni,i}/w_{ni,i} \leq p_{1,i+1}/w_{1,i+1}$ and $s_i \leq s_{i+1}$ for $i=1,\dots,F-1$.

Proof: It is clear that if we ordered the jobs in SWPT order, then there is no need to split if the jobs are already grouped into families when arranged in SWPT order. Since $p_{ni,i}/w_{ni,i} \leq p_{1,i+1}/w_{1,i+1}$ and $s_i \leq s_{i+1}$ then the schedule of families obtained by non-decreasing order of s_i gives us an optimal solution.

Theorem (3.2)

If the number of families is equal to the number of jobs (i.e. $F=n$), and suppose that for each job i there is a processing time p_i , a positive w_i and a set-up time s_i for $i=1, \dots, n$, then there is an optimal schedule in which jobs are sequenced in non-decreasing order of $(s_i+p_i)/w_i$, $s_i \geq 0$.

Proof: Let $\sigma ij \sigma'$ be a schedule where σ and σ' are two partial schedules, let i, j two jobs with $s_i+p_i/w_i > s_j+p_j/w_j$. Let T be the time that jobs of σ be completed.

$$w_i C_i + w_j C_j = w_i(T+s_i+p_i) + w_j(T+s_i+p_i+s_j+p_j),$$

Now consider the new schedule $\sigma ij \sigma'$ in which all the completion time for σ and σ' are the same as in $\sigma ij \sigma'$, let C'_i and C'_j are the completion times for jobs i and j in the new schedule, hence

$$w_i C'_j + w_i C'_i = w_j(T+s_j+p_j) + w_i(T+s_j+p_j+s_i+p_j)$$

$$\sum_{i \in N} w_i C_i - \sum_{i \in N} w_i C'_i = w_i C_i + w_j C_j - (w_j C'_j + w_i C'_i).$$

Now since $(s_i+p_i)/w_i > (s_j+p_j)/w_j$ then $w_i C_i + w_j C_j > w_j C'_j + w_i C'_i$ hence $\sum_{i \in N} w_i C_i > \sum_{i \in N} w_i C'_i$. By repeating this procedure we get an optimal schedule in which jobs are sequenced in non-decreasing order of $(s_i+p_i)/w_i$.

It is useful to view some times a family as a single composite job with processing time P_f and weight W_f ($f=1, \dots, F$). For each family f we calculate P_f and W_f as follows:

$$\left. \begin{aligned} P_f &= s_f + \sum_{j \in f} p_j \\ W_f &= \sum_{j \in f} w_j \end{aligned} \right\} \quad (3)$$

Scheduling Job Classes on a Single Machine with batches to Minimize the Sum of the Weighted Completion Times

T. S. Abdul-Razaq And K. A. Abdullah

From these we define the weighted mean processing time of family f as

$$WPT(f) = P_f / W_f, f = 1, \dots, F \quad (4)$$

Theorem (3.3)

If there are only two jobs in each family f , such that $p_{jr} \leq s_g + p_{ig}$, where j is the second job of a family f , and i is the first job of a family $g \neq f$, then there exist an optimal schedule in which the families will be ordered by shortest weight mean processing time rule (SWMPT). That is, f precedes g , if and only if $WPT(f) \leq WPT(g)$.

Proof: It is clear from the condition on the jobs $p_{jr} \leq s_g + p_{ig}$, that each family forms a single composite job. Let $S = (f_1, f_2, \dots, f_i, f_j, \dots, f_F)$ be a sequence in which families f_i and f_j , $1 \leq i < j = i+1 \leq F$ are not in SWMPT order. Consider the change in total weighted completion time if the processing order of f_i and f_j is reversed to get a new sequence S' .

Clearly in the new sequence S' all the completion times of the jobs originally scheduled before family f_j will not be changed as in S . Hence we need only to consider the total weighted completion time of the composite jobs in families f_i and f_j .

Let T be the time that jobs scheduled before family f_i of S be completed. Hence, the difference Δ in the total weighted completion time.

$$\Delta = W_i (T + P_i) + W_j (T + P_i + P_j) - W_i (T + P_j) - W_i (T + P_j + P_i), \text{ where } P_i, P_j, W_i \text{ and } W_j \text{ are defined by (3)}$$

$$\Delta = W_j P_i - W_i P_j \geq 0 \text{ if } P_i / W_i \geq P_j / W_j$$

Hence, there exist an optimal schedule in which the families will be ordered by SWMPT rule.

Heuristic Methods

In this section, we propose heuristic methods which have applied once at the top of the branch and bound BAB search tree to find an upper bound UB. It is well known that the computations can be reduced by using a heuristic

method to find a good solution to act as an upper bound on the sum of the weighted completion times prior to the application of a BAB algorithm.

We apply two heuristic methods, the better of the two heuristic sequences is used to provide an initial upper bound. The first heuristic method UB1 is obtained by using SWPT procedure. However, for the second heuristic method UB2 is obtained as follows:

Step1: Index the jobs within each family in SWPT order.

Step 2: $\text{Set } R_f = (s_f + \sum_{i \in f} p_{if}) / \sum_{i \in f} w_{if}$ for $f=1, \dots, F$

Step 3: Families are sequenced in non-decreasing order of R_f for $f=1, \dots, F$.

Assume the processing of the jobs is $\sigma = (\sigma(1), \dots, \sigma(n))$.

Step 4: The sum of the weighted completion times for σ is computed by

$$UB2 = \sum_{i \in N} (W - \sum_{j=1}^i w_{\sigma(j-1)}) (s_{\sigma(i)} + p_{\sigma(i)}) \quad (5)$$

Where $W = \sum_{i \in N} w_i$, $w_{\sigma(0)} = 0$ and $s_{\sigma(i)}$ is the set-up time of job $\sigma(i)$

Hence, $UB = \text{Min} \{UB1, UB2\}$

Derivation of the Lower Bounds

In this section, we shall be interested in deriving new lower bounds on the total weighted completion time.

Relaxation of Constraints

To construct a lower bound (RCLB), by a relaxation of constraints. We first relax all set-up times for each family f (i.e. $s_f=0$) to give a $1/s_f \sum w_i C_i$ problem. This relaxed problem is solved by SWPT rule⁽¹³⁾; jobs are sequenced in non-decreasing order of p_i/w_i ($i \in N$). Assume the resulting sequence is $(\gamma(1), \dots, \gamma(n))$. Hence, the lower bound RCLB is equal to the weighted sum of completion times in the relaxed problem, i.e.

$$RCLB = \sum_{i \in N} w_{\gamma(i)} C_{\gamma(i)} \quad (6)$$

Scheduling Job Classes on a Single Machine with batches to Minimize the Sum of the Weighted Completion Times

T. S. Abdul-Razaq And K. A. Abdullah

Where the sequence γ is SWPT order.

Modified Lower Bound

In this section the method of improving the lower bound is presented. We aim to modify the lower bound RCLB given in section (5.1). Our new modified lower bound (MOLB) is derived using objective splitting. The total weighted completion time can be partitioned into contributions from processing times and from the set-up times. The SWPT sequence minimizes the first contribution. The total weighted completion time of this sequence gives the RCLB (see section 5.1). The following technique is applied to families with zero processing times and the processing time of a family is replaced by its set-up time. Let for each family f , $f=1, \dots, F$ $W_f = \sum_{i \in f} w_{if}$ and s_f is its set-up time, then the families are sequenced such that s_f in non-decreasing order and W_f in non-increasing order, minimizes the second contribution. Hence, our modified lower bound MOLB can be written as

$$\text{MOLB} = \text{RCLB} + \sum_f W_f s_f + \sum_f (W - \sum_{j=1}^f W_{\gamma(j)}) s_{\pi(f)} \quad (7)$$

Where $W_f = \sum_{i \in f} w_{if}$, $W = \sum_f W_f$ and

$$\begin{aligned} W_{\gamma(1)} &\geq \dots \geq W_{\gamma(F)} \\ s_{\pi(1)} &\leq \dots \leq s_{\pi(F)} \end{aligned} \quad (8)$$

It is clear that the first term ($\sum_f W_f s_f$) of the second contribution is constant. By comparing equation (7) with equation (1), MOLB is a valid lower bound.

New Lower Bound Based on Relaxation of Set-Ups

In this section we shall derive a new lower bound RSLB. Suppose a schedule consists of a sequence of the n jobs, may be defined as a sequence of batches, where each batch contains jobs from a particular family and begins with a set-up.

A simple new lower bound can be calculated by applying the generalized SWPT rule to the problem of minimizing the total weighted completion time, where the fact that the jobs are divided into a number of batches, is ignored and each family has only one set-up time. Thus, no set-up time is required for two or more batches of the same family. In this relaxed problem the completion time for some job (i,f) appear in the other batches of the same family can be decreased with the set-up time $(C'_{if}=C_{if}-s_f)$ because at least one family $f(f=1,\dots,F)$ has more than one batch in the optimal schedule.

The following result describes how batches are identified in the weighted completion time problem⁽¹⁴⁾.

Theorem (5.1) (Webster and Baker⁽¹⁴⁾)

For the $1/s_f/\sum w_i C_i$ problem, if
$$\frac{s_f + \sum_{k=1}^i p_{k,f}}{\sum_{k=1}^i w_{k,f}} \geq \frac{p_{i+1,f}}{w_{i+1,f}}$$

for $f=1,\dots,F$, then there is an optimal schedule in which the jobs $(1,f)$ to $(i+1,f)$ are processed consecutively.

By using theorem (5.1) we construct a batch B_f contains jobs $(1,f)$ to $(i+1,f)$. In order to get all B_f we repeat this process for all families $f(f=1,\dots,F)$. Let the processing time of B_f and its weight defined as

$$P_{Bf} = s_f + \sum_{(i,f) \in B_f} p_{if} \text{ and } W_{Bf} = \sum_{(i,f) \in B_f} w_{if}$$

The remaining jobs (jobs are not in any batch B_f) (i,f) (for $i=1,\dots,n_f$ and $f=1,\dots,F$), will represent batches containing single jobs with processing time p_{if} and weight w_{if} . It is clear that these single batches are relaxed batches because it begins with a set-up time zero.

Now consider any schedule $S=(B_1,\dots,B_r)$, where weighted processing time (WPT) ratio to be.

$$WPT(B_j) = \begin{cases} P_{B_j} / W_{B_j} & \text{if } B_j \text{ containing one or more than one job} \\ \text{with set-up time} & \\ p_{if} / w_{if} & \text{if } B_j \text{ containing one job with no set-up time} \end{cases}$$

Scheduling Job Classes on a Single Machine with batches to Minimize the Sum of the Weighted Completion Times

T. S. Abdul-Razaq And K. A. Abdullah

Now by using the generalized SWPT rule for batches that uses WPT ratios. It is clear that the optimal solution RSLB obtained from Theorem (2.2) is a lower bound for the original problem.

Although we have no proof that $RSLB \geq MOLB$, initial experiment have shown RSLB to compare favorably with MOLB.

The following theorem shows that the lower bound RSLB is equivalent to the lower bound of Baker BALB⁽³⁾ for the total weighted completion time.

Theorem (5.2)

The lower bound RSLB is equivalent to the lower bound BALB.

Proof: By using Theorem (5.1) for each family $f(f=1, \dots, F)$ we have

$$P_{Bj}/W_{Bj} \leq p_{i+2,f}/w_{i+2,f} \leq \dots \leq p_{nj,f}/w_{nj,f}$$

Where $P_{Bf} = \sum_{i \in B_f} p_i$, $W_{Bf} = \sum_{i \in B_f} w_i$ and $i+2$ is the first job that

follows the last job $i+1$ of the batch B_f . The derived problem can be solved by Horn's algorithm and the resulting sequence gives us the lower bound BALB⁽³⁾. This sequence is exactly the sequence obtained by using the generalized SWPT rule for the derived problem which gives us the lower bound RSLB.

Branch and Bound Algorithm

In this section, we describe our branch and bound algorithm which uses forward branching with relaxation of the set-ups (FBRs) and its implementation. The algorithm uses a forward sequencing branching rule for which nodes at level K of the search tree correspond to the initial sequences in which jobs are sequenced in the first K positions. At the root of the search tree heuristic methods of section 4 are applied to generate an initial upper bound UB. Also, at the root node an initial lower bound RSLB on the cost of an optimal schedule which described in section 5.3 is used. At each node of the branch and bound search tree,

the following dominance rules are used, in an attempt to eliminate nodes though these dominance rules.

Rule 1: (Monma and Potts, 1989). There exists an optimal schedule in which the jobs in each family appear in SWPT order, that is, in non-decreasing order of p_{if}/w_{if} .

Rule 2: (Mason and Anderson, 1991). There exists an optimal schedule in which the batches appear in SWPT order; that is, in non-decreasing order of the ratio R_{if} , where $R_{if} = p_{if}/w_{if}$ denote the weighted processing time for the first i jobs of family f , if they formed an initial batch.

Rule 3: (Mason and Anderson 1991). If there is more than one job from the same family f with equal p_{if}/w_{if} ratio then there is an optimal solution in which they appear consecutively.

Also an additional dominance condition is helpful. Let f denote a family that is processed in more than one batch in an optimal schedule, and let u and v denote two consecutive jobs in family f that appear in different batches. In other words, job (u, f) completes a batch, and job (v, f) starts the next batch of family f .

Rule 4: (Mason and Anderson 1991). In an optimal schedule, the first job (i, g) that follows job (u, f) must satisfy $p_{ig}/w_{ig} \leq p_{vf}/w_{vf}$

Rule 5: (Webster and Baker 1995). If
$$\frac{s_f + \sum_{k=1}^i p_{k,f}}{\sum_{k=1}^i w_{k,f}} \geq \frac{p_{i+1,f}}{w_{i+1,f}}$$

then jobs $(1, f)$ through $(i+1, f)$ are processed consecutively.

These rules are also used by Crauwels et al.⁽⁷⁾ in their branch and bound algorithms. In our branch and bound algorithm FBRS, if Rule 5 holds, then jobs 1 through $j+1$ of family f can be considered as a single composite job, thus reducing the effective size of the problem and accelerating the solution.

A dynamic programming dominance rule is also useful. For two initial partial schedules $S_1 = \sigma_{ij}$ and $S_2 = \sigma_{ji}$ which have identical final jobs and which contain the

Scheduling Job Classes on a Single Machine with batches to Minimize the Sum of the Weighted Completion Times

T. S. Abdul-Razaq And K. A. Abdullah

same jobs, if S_2 has a completion time of its last jobs and a total weighted completion time that are no smaller than the corresponding value for S_1 , then S_2 is dominated by S_1 .

It should be noted that in our branch and bound algorithm if the jobs of F-1 families are partial scheduled, then the remaining unscheduled jobs of the last family are sequenced in SWPT order.

Also in our algorithm, when we expand a partial schedule by starting a new batch, the first job in this batch must satisfy Rule 4, otherwise the partial schedule is dominated.

It is clear that in branch and bound algorithms, if the lower bound for any node (partial schedule) is greater than or equal to the total weighted completion time of a given feasible schedule (current upper bound UB), then this node is discarded.

Dominated nodes can be dropped from consideration, thus reducing the size of the search tree.

For all nodes that remain after we apply dominance rules above, we can use the procedure described in section 5.3 to compute a lower bound RSLB on the total weighted completion time. Let S be the set of unsequenced jobs, σ be an initial partial sequence of jobs. In this case a lower bound RSLB can be obtained by

$$RSLB = \sum_{f \in \sigma} \sum_{i \in \sigma} w_{if} C_{if} + \sum_{f \in S} \sum_{i \in S} w_{if} C_{if} \quad (9)$$

Where the first term in (9) is the total weighted completion time for the jobs already sequenced. The second term in (9) is the weighted completion time for the unsequenced jobs obtained by using section 5.3. Having found RSLB, for each immediate successor of the node from which we are branching, the minimum lower bound is then found. If it is not less than the current upper bound UB, this node is eliminated. Otherwise it is selected for our next branching.

The branch and bound method continues in a similar way. Whenever a complete sequence is obtained, this sequence is evaluated and the upper bound UB is altered if the new value is less than the old one.

The procedure is repeated until all nodes have been considered (i.e., lower bounds of all nodes in the scheduling tree are greater than or equal to the UB), a feasible solution with this UB is an optimal solution.

Finally, the search strategy used in our algorithm is the newest active search. This selects a node from which to branch has the smallest lower bound amongst nodes.

Computational Experience

In this section, we report on the results of computational tests to assess the effectiveness of the branch and bound algorithm. The algorithm was coded in FORTRAN 77 and was run on a CUP-PENTIUM 133 mhz, RAM 16MB computer. Computation is abandoned if a limit of 200000 nodes is exceeded.

Test problems with 30, 40 and 50 jobs, and with 4, 6, 8 and 10 families were generated as follows⁽⁷⁾. For each combination of n and F , the jobs are uniformly distributed across families, so that each family contains either $\lfloor n/F \rfloor$ or $\lceil n/F \rceil$ jobs. Processing times and weights are randomly generated integers from the uniform distribution defined on $(1, 10)$. Since the size of set-up times relative to processing times may affect problem 'hardness', we generated problems with small (S), medium (M) and large (L) set-up times. Medium set-up times are randomly generated integers from the uniform distribution defined on $(1, 10)$. Having generated an instance with medium set-up times $s_{if}(i=1, \dots, F)$, corresponding instances with small set-up times $\lfloor s_{if}/2 \rfloor$ and with large set-up times $2s_{if}$ were constructed. For each of the 12 combinations of n and F , 50 test problems with small, medium and with large set-up times were created. This method of data generation follows that given in (Crauwels et al. 1998⁽⁷⁾).

A comparison of the computational results that are obtained by Mason and Anderson⁽¹⁰⁾ for their algorithm and Crauwels et al.⁽⁷⁾ for their algorithms with the results of our algorithm (forward branching with relaxation of the set-up (FBRs)), provides further evidence to support the claim of

*Scheduling Job Classes on a Single Machine with batches to
Minimize the Sum of the Weighted Completion Times*

T. S. Abdul-Razaq And K. A. Abdullah

similarity between problems that differ only in their ranges of processing and set-up times.

As in Crauwels et al.⁽⁷⁾ a variety of the number of jobs per family ranges from 3 (for $n=30$ and $F=10$) to 12 and 13 (when $n=50$ and $F=4$). Also, a variety of set-up time ranges is considered.

Computational Experience with the Lower Bound

The lower bound of Mason and Anderson⁽¹⁰⁾ and our new lower bounds were tested on $n=50$, $F=10$ and set-up times are medium. Mason and Anderson lower bound and our new lower bounds based on objectives splitting MOLB and on the relaxation of set-ups RSLB were computed for each of the 50 problems.

Results comparing the lower bounds are given in table 1. The first column is the number of the problems while the second column gives the value of an optimal solution, found using the branch and bound algorithm FBRS as described in section 6. The value of the better of the two heuristic sequences is used to provide an initial upper bound UB is given in third column. The remaining columns give values of the lower bound of Mason and Anderson (OSLB), the new modified lower bound MOLB and the new lower bound RSLB respectively. Cases for which a problem is solved by the lower bounding procedure, i.e., when UB is equal to initial lower bound are marked. It is clear that from table 1 indicates that 19 problems are solved without using branch and bound algorithm.

Table 1: Comparison of values of lower bounds

Number	Optimum	UB	OSLB	MOLB	RSLB
1	28431	28431	27684	27662	28431*
2	27616	27616	26657	25789	27616*
3	32413	32413	32135	31126	32413*
4	34581	34581	33684	32236	34581*
5	31083	31083	29829	28467	31083*
6	32594	27594	26825	25559	27594*

Continued Table 1: Comparison of values of lower bounds

Number	Optimum	UB	OSLB	MOLB	RSLB
7	31217	31217	29684	28954	31217*
8	29727	29727	29508	28954	31217*
9	28939	28939	24995	24926	27505
10	27916	27916	27565	27565	27916*
11	29913	29913	29436	29436	29913*
12	26340	26340	25626	23214	26340*
13	31681	31681	31588	31105	31681*
14	30288	30288	30128	29493	30288*
15	35952	35952	35679	35454	35952*
16	35793	35793	35396	35150	35793*
17	27259	27259	26772	25648	27259*
18	25654	25654	24914	24477	25654*
19	31172	31172	31046	30578	31172*
20	36108	36108	35687	34644	36108*
21	26902	26902	25553	25517	26768
23	26991	26991	24134	23252	26273
24	22797	22797	18991	18529	21172
25	21711	21711	18318	17260	20054
26	22595	22595	19942	18922	21688
27	30909	30909	28289	28082	29946
28	31165	31165	28775	28486	30460
29	32542	32542	27206	26603	30399
30	28428	28428	23202	23202	26617
31	40222	40222	36744	35736	38235
33	26912	26912	24653	24268	26298
34	22474	22474	19822	19478	21797
35	27999	27999	23692	23418	26983
36	28841	28841	25367	24906	28236
37	37200	37200	32840	32138	35428
38	25440	25440	22224	21904	24061
39	31211	31211	27646	26633	30400
40	28874	28874	25996	25041	27729
41	27869	27869	24726	23824	27525

*Scheduling Job Classes on a Single Machine with batches to
Minimize the Sum of the Weighted Completion Times*

T. S. Abdul-Razaq And K. A. Abdullah

Continued Table 1: Comparison of values of lower bounds

Number	Optimum	UB	OSLB	MOLB	RSLB
42	32996	32996	29441	28892	31869
43	30812	30812	27776	27417	30216
44	36388	36388	31661	31426	35406
45	32260	32260	28619	27847	31145
46	35536	35536	29202	28168	32245
47	26772	26772	24243	23643	25400
48	24505	24505	21084	21084	23285
49	22416	22416	19433	18942	21017
50	23044	23044	20188	19828	21628

UB: initial upper bound

OSLB: a lower bound obtained by objective splitting.

MOLB: a modified lower bound obtained by objective splitting

RSLB: a lower bound obtained by relaxation of the set-ups.

*: indicates that the problem is solved by the lower bounding procedure.

Computational Experience with the Branch and Bound Algorithms

This section describes a comparison of the computational results that are obtained by Crauwels et al.⁽⁷⁾ for their algorithms, with the results of our algorithm FBRS. The first of their algorithm is based on a forward branching with objective splitting (FBOS) and is essentially the algorithm of Mason and Anderson⁽¹⁰⁾. The second branch and bound algorithm employs forward branching and multiplier adjustment (FBMA). A part from the method of computing lower bounds, the first and second algorithm are identical to our algorithm. The third of their branch and bound algorithm uses a binary branching rule and subgradient optimization (BBSO). The lagrangian lower bound is computed at each node of the second and third algorithm. For FBOS, computation is abandoned if a limit of 50000 nodes is exceeded, whereas a time limit of 600

seconds is used for BBSO. No limits are applied for FBMA⁽⁷⁾.

Table (2) gives results for the four branch and bound algorithms. For each combination of n and F , average for the instances with small, medium and large set-up times. When there are unsolved problems, the values listed under ANN is lower bound on the true average.

There is no strong indication from the results of Table (2) that one algorithm is superior to the others. Algorithm FBMA has the advantage that there is no unsolved problems compared with the other algorithms. On the other hand, average number of nodes are slightly smaller for large set-up times for our algorithm.

Table 2: Comparative computational results

Table 2: Comparative computational results										
Set Up times	N	F	FBRs		FBMA	BBSO		FBPS		
			ANN	NU	ANN	ANN	NU	ANN	NU	
S	1	4	4245	-	74	440	-	657	-	
		6	4464	1	92	113	-	1775	-	
		8	5105	1	95	103	-	3732	-	
		10	4805	1	66	53	-	2778	-	
	30	4	15367	3	184	2401	7	2477	-	
		6	39941	7	161	1127	5	9069	-	
		8	5372	-	171	507	1	22167	7	
		10	44979	7	148	277	1	20292	7	
	40	4	23137	2	365	3554	34	5591	-	
		6	40633	6	437	2124	17	29478	9	
		8	15769	2	451	1334	9	44658	35	
		10	11021	2	436	891	7	46818	42	
	M	30	4	831	-	44	108	-	371	-
			6	199	-	53	64	-	757	-
			8	445	-	43	28	-	1199	-
			10	119	-	45	26	-	956	-
40		4	704	-	165	1243	5	1522	-	
		6	2421	-	112	401	1	4082	-	
		8	327	-	143	298	-	8703	1	
		10	1040	-	94	85	-	6992	-	
50		4	6	-	30	69	-	198	-	
		6	4	-	22	19	-	294	-	
		8	5	-	22	16	-	322	-	
		10	6	-	21	14	-	257	-	
30	4	6	-	30	69	-	198	-		
	6	4	-	22	19	-	294	-		

		8	5	-	22	16	-	322	-
		10	6	-	21	14	-	257	-
	40	4	11	-	65	354	1	661	-
	L	50	6	7	-	51	95	-	1292
			8	6	-	49	83	-	1655
			10	8	-	34	29	-	1770
		50	4	12	-	113	845	5	1535
			6	11	-	180	620	3	5215
			8	8	-	118	88	-	8225
			10	9	-	101	105	-	11633

FBRs: algorithm with forward branching and relaxation of set-ups

FBMA: algorithm with forward branching and multiplier adjustment

BBSO: algorithm with binary branching and sub gradient optimization.

FBOS: algorithm with forward branching and objective splitting

ANN: average number of nodes in the branch and bound search tree

NU: number of unsolved problems

FBRs, for instance, among the 600 test problems with large set-up time only 6 requires more than 30 nodes of the search tree of FBRs.

In our experiments with FBRs, summarized in Table (2) 450 test problems contained four families and with small, medium and with large set-up times were only 5 unsolved. Also two facts are clear from table 2 with small and large set-up times. First, the average number of nodes almost rises as the number of jobs per family increases. Second, the average number of nodes rises as the set-up time decreases. Hence, in the limit, of course, as the setup time approaches zero, the optimal solution reduces to the SWPT sequence, and this obtained in $O(n \log n)$ time. However, for positive but small setup times the FBRs algorithm takes a relatively long time to find optimal solution. As expected, the relative size of setup time affects problem hardness. Results in table 2 indicates that all the four algorithms find the test problems with small setup

times to be the hardest, and those with large setup times are the easiest. This computational relationship has also been noticed by Baker⁽³⁾. For the harder problems, the algorithms FBRS and FBMA are clearly superior to both FBOS and BBSO.

Figure (1) shows the frequency histogram of the number of nodes for the 600 problems with $n=50$ for FBRS algorithm. We observe that almost 80.2% of the problems generate a branch and bound algorithm with less than 1000 nodes. As indicated in table 2, 15 of these problems remain unsolved, because of limit of 200000 nodes.

CONCLUSIONS

In this paper, we have developed a solution procedure for the problem of scheduling families of jobs in a single machine to minimize the total weighted completion time, where a setup time is incurred whenever the machine switches from processing a job in one family to a job in another family. A new lower bound based on relaxation of setup times is derived.

It should be kept in mind that the time required to find an optimum will increase as the setup time gets smaller. One possible explanation for the effect of the setup time on run time is that the lower bound we used are less effective for small setup times than for large setup times.

The branch and bound algorithm FBRS using relaxation of setup times is efficient and is able to solve problems with up to 50 jobs. Our branch and bound adopts a forward branching rule and uses various dominance rules. This algorithm is superior to the branch and bound algorithm of Mason and Anderson⁽¹⁰⁾ (algorithm FBOS) which uses objective splitting in its lower bounding procedure. Computational results indicate that our algorithm FBRS is better than the algorithm BBSO which uses a lagrangian subgradient optimization bound and which employs a more flexible branching rule. Also it should be noted that the algorithms FBRS and FBMA

Scheduling Job Classes on a Single Machine with batches to Minimize the Sum of the Weighted Completion Times

T. S. Abdul-Razaq And K. A. Abdullah

which uses forward branching and multiplier adjustment are better than both algorithms FBOS and BBSO.

REFERENCES

1. Ahn, B. and Hyun, J., "Single facility multi-class job scheduling", *comput. Oper. Res.* 17: 265-272 (1990).
2. Anderson, E.J., Class, C.A. and Potts, C.N. Local search in combinatorial Optimization, edited by E.H.L. Aarts and J.K. Lenstra, Wiley, (1997).
3. Baker, K.R., Solving the weighted completion time problem with batch setups, working paper no. 98-811, the Amos Tuck School of Business Administration, Dartmouth College, Hanover, N.H.
4. Bruno, J. and Downey, P., "Complexity of task sequencing with deadlines, setup times and changeover costs, *SIAM Journal on Computing* 7, (1978) 393-404.
5. Crauwels, H.A.J., Potts, C.N. and Van Wassenhove, L.N., Local search heuristic for single-machine scheduling with batching to minimize the number of late jobs, *European J. Oper. Res.* 90: 200-213 (1996).
6. Crauwels H.A.J., Potts, C.N. and Van Wassenhove, L.N., Local search heuristics for single-machine scheduling with batch setup times to minimize total weighted completion time, *Ann. Oper. Res.* 70: 261-279 (1997).
7. Crauwels H.A.J., Hariri, A.M.A., Potts C.N. and Van Wassenhove, L.N., Branch and bound algorithms for single machine scheduling with batch setup times to minimize total weighted completion time, to appear.
8. Gupta, J.N.D., Optimal schedules for single facility with two job classes. *Comput. Oper. Res.* 11:409-413 (1984).
9. Hariri, A.M.A. and Potts, C.N., "Single machine scheduling with batch setup times to minimize maximum lateness", *Ann. Oper. Res.* 70:75-92 (1997).

10. Mason, A.J. and Anderson, E.J., Minimizing flow time on a single machine with job classes and setup times. *Naval Res. Logist.* 38: 333-350 (1991).
11. Monma, C.L., and Potts, C.N., On the complexity of scheduling with batch setup times. *Oper. Res.* 37:798-804 (1989).
12. Potts, C.N., Scheduling two job classes on a single machine, *comput. Oper. Res.* 18: 411-415 (1991).
13. Smith, W.E., Various optimizers for single-stage production, *Naval Res. Logist. Quart* 3:59-66 (1956).
14. Webster, S.W. and Baker, K.R., Scheduling groups of jobs on a single machine, *Oper. Res.* 43:692-703 (1995).



مجلة
علوم الملائكة

السنة ٢٠٠٠

عدد ١

مجلد ١١

تصدرها كلية العلوم بالجامعة المستنصرية - بغداد - العراق

مجلة علوم المستنصرية

رئيس التحرير

الدكتور رشيد حمود النعيمي

استاذ - فيزياء جو

مدير التحرير

الدكتور عبد الواحد باقر

استاذ - احياء مجهرية

هيئة التحرير

الدكتور رضا ابراهيم البياتي

الدكتور احسان شفيق توفيق

الدكتور عبد السميع عبد الرزاق الجنابي

الدكتور قيس جميل لطيف

الدكتور هاشم حميد جواد

الدكتور محمد الشريفي على

استاذ - كيمياء

استاذ - علوم حياة

استاذ مساعد - رياضيات

استاذ مساعد - انواع جوية

استاذ مساعد - فيزياء

استاذ مساعد - حاسبات

- | الموضوع | رقم |
|--|-----|
| تمنيع الابقار الجافة بلباق البروسيل المجهزة س - ١٩
فاروق خالد حسن وفلاح خليل العاني | ١ |
| دراسة تأثير اشعة ليزر النتروجين في حيائية الرؤيسات الأولية
لطفيلي المشوكات الحبيبية <i>Echinococcus granulosus</i>
في الزجاج
امل مصطفى مكي، خليل ابراهيم حاجم، اياد غازي انور | ١٠١ |
| ايجاد طاقة السطح النووي لنظير السلينيوم $^{74}_{34}\text{Se}_{40}$ بأستخدام
نموذج اليوزونات المتفاعلة الأول (IBM-1)
خالد سلمان ابراهيم ، ايمان طارق العلوي وأنعام حاتم خضير | ٢٧ |
| تأثير ظاهرة النينو على التغيرات المطري في العراق
نعمة محسن لفنة | ٣٧ |

تمنيع الابقار الجافة بلقاح البروسيل المجهضة س - ١٩

فاروق خالد حسن* وفلاح خليل العاني**

*كلية طب المستنصرية-بغداد

**كلية الطب البيطري، جامعة العلوم والتكنولوجيا-اربيل

(استلم بتاريخ ١٩٩٩/٣/٢ : وقبل للنشر في ١٩٩٩/١١/٢)

ABSTRACT

Brucellosis poses a serious threat to Iraqi cattle and buffaloes industry as well as to human health. To control the disease local Br. abortus S-19 vaccine was prepared & applied to immunize 557 dry pregnant cows. Immunization was monitored by Rose - Bengal & tube - agglutination tests. Vaccination reduced the incidence of retained placemtae and endometritis.

الخلاصة

الاجهاض الساري احد اهم الامراض التي تصيب الابقار والجاموس وتسبب كثيراً من المشاكل الاقتصادية وتهدد صحة الانسان في العراق. لذا بدأ التفكير بانتاج لقاح محلي فعال أمين للسيطرة على المرض في العجلات. ولأكمال السيطرة على المرض لقحت الابقار الجافة لتمنيوعها وقد ثبت نجاح التلقيح في تجمع حيواني شمل ٦٧٦ بقرة باستخدام لقاح س - ١٩ وتوبعت مناعياً باستخدام فحصي الروزبنكال والتلازن الانبوبي. قلل التلقيح نسب الاصابة باحتباس المشيمة والتهاب بطانة الرحم.

المقدمة

يعتبر مرض الاجهاض الساري (داء البروسيلات) احد اهم الامراض البكتيرية المتوطنة والمعدية في الابقار والجاموس في العراق^(٣,٢٠) تسببه البروسيلا المجهضة (Br. abortus)، يشكو منه مربى الابقار والجاموس ومن اهم اعراضه الاجهاض المفاجئ والذي يحدث غالباً في الاشهر الاخيرة من الحمل. خسائره الاقتصادية كبيرة بسبب فقدان الولادات ونقص في كمية الحليب المنتج وترد في نوعيته اضافة الى المشاكل التناسلية الناجمة عنه كأحتباس المشيمة والتهاب بطانة الرحم في الابقار والتهاب الخصى والقناة المنوية في الثيران. وما قد يرافق ذلك من مداخلات نتيجة الاصابة الثانوية بجراثيم اخرى والتي جميعها او بمفردها تؤدي الى ضعف الاخصاب والعقم^(٤). وللبروسيلا المجهضة تأثير مباشر على الصحة العامة اذ تصيب الانسان مسببة مرضى الحمى المتموجة أو حمى مالطا حيث ينتقل اليه عند التعامل مع اللحوم الملوثة بجراثيم البروسيلا او عن طريق تناول الحليب الطازج ومشتقاته. وعموما فحمى مالطا هي احد الامراض المشتركة المهمة التي تؤثر على فاعلية المصاب ونشاطه ومضاعفاته التي تشمل اجهزة الدم والتناسل والعصبي والتنفسي اضافة الى العظام والمفاصل والحواس^(٥,٦).

اهتمت دول العالم في النصف الثاني من هذا القرن في سبل السيطرة على المرض في مضيفه الرئيسي - الحيوان باستخدام التلقيحات حيث استخدم لقاح ٢٠/٤٥ المقتول لتمنيع الابقار ولقاح س - ١٩ لتمنيع العجلات والاباكير^(٨) وضمن التوجه العام للسيطرة على الامراض الاوسع انتشاراً والاكثر اذى كان لمختبرات كلية الطب البيطري - جامعة بغداد مساهمة في تحضير لقاح س - ١٩ ، وقد تم استخدامه بنجاح في تمنيع العجلات والاباكير. استهدفت هذه الدراسة الى معرفة تأثير فاعلية لقاح س - ١٩ المصنع محلياً على الابقار الجافة ومدى استجابتها مناعياً لهذا اللقاح.

المواد وطرائق العمل

١. استخدمت في الدراسة ٦٧٦ بقرة حامل من نوع فريزن - هولشتاين وباعمار مختلفة تتراوح من ٣ - ٨ سنوات جفت في الشهر السابع بانتظار الولادة. تم تلقيح ٥٥٧ بقرة في بداية جفافها بـ لقاح س - ١٩ الحاوي على 3×10^4 بكتريا / مل في محطة لتربية الابقار قرب بغداد.

٢. حضر لقاح البروسيلا المجهضة س - ١٩ المضعف الحي في مختبرات كلية الطب البيطري - جامعة بغداد في دراسة سابقة، وفق المواصفات العالمية، يعطى تحت الجلد وبجرعة 3×10^4 بكتريا / مل لـ تمنيع العجلات والاباكير، وقد استخدم في هذه الدراسة لـ تمنيع الابقار الجافة^(١٥).

٣. حضرت الاوساط الزرعية والمحاليل والكواشف في هذه الدراسة وفق ما جاء في دليل تقنيات مختبر داء البروسيلات^(١٠)، وقد عُمّت الاوساط الزرعية بالموصدة تحت ضغط ٢١ باوند/انج^٢ وبدرجة حرارة ١٢٠°م ولدة ١٥ دقيقة.

٤. أ - جمعت الاجنة المجهضة، المشيمة، الفلقات والافرازات المهبلية من الابقار واستخرجت محتويات المعدة والزنة بشكل معقم وزرعت على الاوساط الزرعية الآتية : وسط اكار البروسيلا، وسط اكار الترتيك سوى المضاف اليه مصل الدم، وسط اكار الدم، وسط ماكونكي وحفظت هذه الاوساط الزرعية في الحاضنة تحت ظروف هوائية اعتيادية مع طاقم مشابه اخر حفظ في ظروف لاهوائية مستخدمين اكياس مولدات النمو اللاهوائي. حفظت الاوساط الزرعية تحت حرارة ٣٧°م لمدة ٧٢ ساعة.

فاروقى خالد حسن وفلاح خليل العائى

ب- غسلت المشيمة والفلقات بالمحلول الفسيولوجي المعقم مع استخدام ماصة باستور بعد تحريكها يمينا وشمالا لجمع ما لا يقل عن ١-٣ قطرة لغرض الزرع الجرثومي.

أما الافرازات المهبلية فقد عوملت معاملة المشيمة، في حين اخذت مسحات من محتويات الكرش والمشيمة والافرازات المهبلية لغرض صبغة كوام او صبغة كوستر. توبع الزرع بعد مرور ثلاثة ايام في جميعها ويوميا بعد ذلك لمدة اسبوعين.

٥. توبع نوع البروسيلا باستخدام المصل الاحادي بعد استكمال الفحوص الكيمياحيوية الموصوفة^(١٢) تم اجراء الفحوص المصلية قبل وبعد اعطاء اللقاح وتوبع في فترات منتظمة يفصلهما اسبوعين ولغاية الاسبوع الثاني والثلاثين. أجري فحص التلزن الانبوبي وفحص الروزبنكال بانتظام لمتابعة عملية التلزن وفق ما وصفه الباحثون^(١٢،١١).

النتائج والمناقشة

توبعت ١١٩ بقرة حامل جافة غير ملقحة في حينه لعدم توفر اللقاح واعتبرت كسيطرة ووجد ان نسبة الاجهاضات تصل ١٤% كما موضحة في جدول (١). وكان احتباس المشيمة والتهاب الرحم يعقب حالات الاجهاض او في الولادات التي تبدو طبيعية. أما الابقار الملقحة والبالغ عددها ٥٧ فشكلت الاجهاضات نسبة قد تصل الى ١% وكذلك حالات احتباس المشيمة والتهاب بطانة الرحم ١% و ١,٥% لكل منها على التوالي، اما اسباب هلاك الابقار الملقحة فلا علاقة له بداء البروسيلات وانما كانت بسبب الانفراش والتهاب التامور الرضحي، اما في الابقار غير الملقحة فاسباب هلاكها كانت مختلفة اذ شملت ايضا على الانفراش والتهاب التامور الرضحي والتايليريا. وعند تدقيق جدول (٢) يلاحظ ان نسبة الاصابة بداء البروسيلات في الابقار غير الملقحة لم يزد على ٦% ويشكل ٤١% من مجمل حالات الاجهاض،

اما الابقار الملقحة فكانت نسبة الاصابة بداء البروسيلات ٩,٠% وعزلت البروسيلات المجهضة مختبرياً من حالتين فقط في حين عزلت العترة اللقاحية من ثلاث حالات اجهاض، ويبدو ان اللقاح قد اظهر الاصابات الكامنة وهذا ما يتفق فيه الدوريات المنشورة في هذا المجال^(١٤،١٥).

اما الشكلين ١، ٢ المرسومين من النتائج الموضحة في جدول ٣ فيلاحظ ان عقب التلقيح بلقاح س - ١٩ بدأ معيار الاضداد بالارتفاع حتى وصل الى اعلى معيار له في الاسبوع الرابع عشر ثم بدأ بالانخفاض التدريجي حتى بدأ يتقارب في معياره في الاسبوع ٢٨ - ٣٢ وهذا مشابه لما ذكرته الدراسات^(٨٦).

إن العجلات والاباكير اقل تحسناً لجراثيم البروسيلات ولقاحاتها من الابقار لذا يوصي بعض الباحثين باعطاء جرعة مخفضة للابقار ١٤ وان اللقاح بتركيزه الفاعل يجب ان يحوي على ٥٠ مليون بكتريا / مل وتنتهي فاعليته عند التركيز ٢٥ مليون بكتريا / مل لذا اعتمدت دراستنا على اعطاء لقاح يحوي على 3×10^8 لكونها الاقرب الى الجرعة الفاعلة. وان معظم الدراسات التي تنهج نحو تقليل الجرعة هدفها تقليل التفاعلات الجانبية التي قد تعقب اعطاء اللقاح وانه وجد ان الكمية الاكثر عدداً تكون الاكثر نفعاً للعجلات لتزيد فترة فاعلية اللقاح لتمتد الى مرحلة الابقار.

هذا ولا بد من الاشارة الى ان عند اعطاء اللقاح قد يحدث تلف نسيجي موضعي يعقبه غزو خلايا البلاعم للمنطقة نتيجة تحرر مواد الانجذاب الكيميائي من الانسجة التالفة. وتلتهم البلاعم خلايا اللقاح وتنقله الى الغدد اللمفية القريبة من موقع التلقيح حيث تنمو وتستعمر بعض الجراثيم خلاياها والبعض الاخر تنقله البلاعم مرقو اخرى الى خلايا اللف نوع ب، ت. تنقسم خلايا اللف ب لتكون الخلايا البلازمية المصورة التي تصنع اجسام الضد وتبقى خلايا اللف ب - متحفزة. تحرر اللمفوكينات حيث تنشط وتحفز البلاعم الاخرى والتي بدورها تلتهم خلايا اللقاح ليتخلص منها المضيف وعندئذ تشفى الابقار من مرض غير ظاهر - الاصابة بالخلايا اللقاحية. وعند الشفاء منه تتوقف عملية انتاج الاضداد، وخلال انضاج خلايا

فاروق خالد حسن وفلاح خليل العاني

ب، ت تتكون خلايا الذاكرة المناعية والتي تبقى حية وتحفظ الحيوان لسنوات قادمة قد تصل الى سبع سنوات او اكثر حتى ولو دخلت الجسم البروسيل المجهضة المرضية.

إن تربية الابقار والجاموس في العراق في شكلها المنفرد والتي تشمل تربية الابقار في المدن وباعداد قليلة جداً او في الريف وباعداد اكثر وباقل مشاكل لتوفر المساحة واشعة الشمس المباشرة. والتربية المكثفة في محطات تربية الابقار تستدعي الحاجة الى تلقيح هذه الابقار وخاصة الجافة منها بلقاح س - ١٩ في بداية فترة حياتها اضافة الى تلقيح العجلات والاباكير في سن مبكرة. ان تلقيح الابقار كما اوضحت الدراسة تقلل المشاكل التناسلية وتختزلها الى حد كبير وبذا تسهم عملية التلقيح بتقليل الجهد والنفك التي تستدعيها المعالجة البيطرية. كما ان السيطرة على المرض في المضيف الطبيعي يقلل اصابة الانسان بحمي مالطا - احد اهم الامراض المنذرة لصحة الانسان في الوقت الحاضر وتقلل الخسائر الاقتصادية المترتبة على استيطان المرض.

جدول (١) : اصابات احتباس المشيمة والتهاب بطانة الرحم في ابقار

التجربة

عند الابقار	ملقحة بلقاح س ١٩	عند الاجهاض	عدد حالات احتباس المشيمة	التهاب بطانة الرحم	الملاحظات
١١٩	-	١٧	٢١	٢٧	هلكت اربعة ابقار باسباب مختلفة
٥٥٧	+	٥	٦	٩	هلكت واحد ونيفت الاخرى.

جدول (٢) : الغزلات الجرثومية من حالات الاجهاض

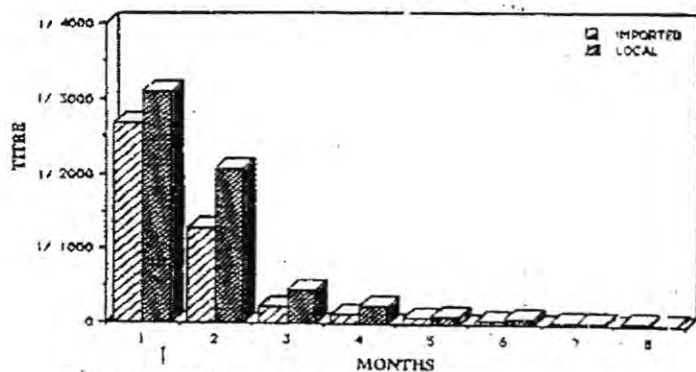
نوع البكتريا المعزولة		عدد حالات داء البروسيلات المثبتة مختبرياً *	ملقحة بلقاح س ١٩	عدد الإبقار
البروسيلات للقاحية	للجهض			
-	٧	٧	-	١١٩
٣	٢	٥	+	٥٥٧

* ثبت داء البروسيلات بالفحوص المصلية وبالنزاع البكتري

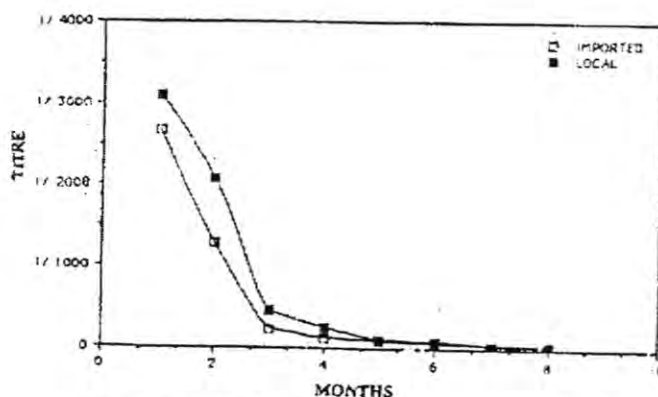
تمنيع الإبقار الحافّة بلقاح البروسيلة المجبنة س - ١٩
فاروق خالد حسن وفلاح خليل العائلي

جدول (٣) : المعيار في الاسابيع

المعيار	عدد الإبقار التي أعطت فحصاً موجباً للتلازن الانبوبي في الأسابيع															
	٢	٤	٦	٨	١٠	١٢	١٤	١٦	١٨	٢٠	٢٢	٢٤	٢٦	٢٨	٣٠	٣٢
صفر											١٠	١٩	٢٩	٣٣	٤٠	٤٠
٤٠ : ١										١٥	٣٣	٦٠	٢٥٥	٢٧٠	٢٨٨	٢٩٥
٨٠ : ١	١٨٨	٢٤	٥						٢٤	٥٦	٧٣	٢٢٣	١٥٩	١٦٦	١٩١	١٩٧
١٦٠ : ١	٢٥٦	١٦٣	٧٩	٦٣	١٣			١٩	٧٧	١١٤	٢١٠	١٥١	٥٧	٧٩	٣٤	٢٣
٣٢٠ : ١	١١٣	٣١٠	١٩٨	١٠٢	٤٨	٥٣	٣٠	٧٣	١٤٣	١٧٦	١١٨	٦٤	٣٣	٥	٢	٢
٦٤٠ : ١		٦٠	٢٢٨	232	١٠١	١٠٥	١١٨	١٥١	١٦٧	١١٧	٦٩	٢٦	١٧	١	١	
١٢٨٠ : ١			٤٧	151	٢١٢	١٤٠	١٥١	١١٩	١٢٥	٧٤	٤٤	١٣	٦			
٢٥٦٠ : ١				9	١٨١	٢٢٧	٢٣٣	١٨٩	٢١	٥						
٥١٢٠ : ١						٣٢	٢٥	٦								



شكل رقم (١) سريان المصلية للمناعة في الأغنياء المحلية والمخترجة من سوريا في العراق



شكل رقم (٢) سريان المصلية للمناعة في الأغنياء المحلية والمخترجة من سوريا في العراق (بالمقارنة)

REFERENCES

1. Farid, A & Al-Hashimi, J. The status of bovin brucellosis in Baghdad as indicated by seroagglutination. Cairo Vet. Med. J. 16 : 1919-194. (1969).
2. Hadad, J.J & Jamalludin N.M. Brucella strains isolated from cattle in Ninevah province. Iraqi J. Vet. Sci, 5: 165-170 (1962).
3. Al-Zahawi S. Brucellosis in Iraq. Bull. Intl. Hygiene Public Health 30:1 (1938).

فاروق خالد حسن وفلاح خليل العاني

4. Nicoletti, P. Bovine Brucellosis : Etiology, Pathogenesis & Diagnosis in International symposium in Brucellosis 18 - 20 October 1988. Pandek - Turkey (1988).
5. Al-Rawi Z.S. Al-Khatteb N., & Khalifa S. J. Brucella arthritis among Iraqi patients. British J. Rheumatology 26 : 24 - 27 (1987).
6. Thimm, B.M. Brucellosis - Distribution in man, Domestic & wild animals, Springer - Verlag, New York. (1982).
7. Sukar F. Some epidemiological aspects of human brucellosis in Iraq & its control., Bull Endemic Dis. 30 : 31-41 (1989).
8. Nicoletti, P. : Vaccination of cattle with Br. abortus strain 19 adminstred by different routes & doses. Vaccine 2; 133-135 (1984).
9. Stemshorn, B.W. Bovine Brucellosis - diagnosis & eradication. Can. Vet. J. 26 : 35-39 (1985).
10. Alton G. G., Jones L. M., Angus R. D. and Verger J. M. : Techniques for the Brucellosis Laboratories. Institut National DELH Recherche Agronomique, Paris (1988).
11. Davis G. : The Rose bengal test Bull Int. Epiz. 76 : 717-720 (1971).
12. Morgan W.J. B., Mackinnon, D.J. Gill, K.P.W., Grower J.G. M. & Norris, P.I. Brusellosis diagnosis standard laboratories 2nd Ed. Central Veterinary Laboratories, Weybridge, Surrey. U.K. (1978).
13. Corbel M.J. Recent Advances in the study of Brucella antigens and their serological cross - reactions. Vet. Bull 55 (12) : 927 - 947 (1985).
14. Alton G. G., Vornor, L.A., & Plackett, P. vaccination of cattle against brucellsis using either reduced dose of strain 19 or one or two doses of 45/20 vaccine. Aust. Vet. J. 60: 175 - 177 (1983).

١٥. الثنوني، أمنة نعمة : انتاج وتقويم لقاح (S-19) ضد داء البروسيلات ،

اطروحة دكتوراه مقدمة الى كلية الطب البيطري - جامعة بغداد

(١٩٩٥).

دراسة تأثير اشعة ليزر النتروجين في حيائية الرؤيسات الأولية لطفيلي المشوكات الحبيبية *Echinococcus granulosus* في الزجاج

امل مصطفى مكي*، خليل ابراهيم حاجم**، اياد غازي اتور**
* الجامعة المستنصرية / كلية العلوم / قسم علوم الحياة
** جامعة بغداد / معهد الليزر والبلازما للدراسات العليا/ قسم الليزر
والاطياف

(سُلم بتاريخ ١٩٩٨/٧/٢٠ وقبل للنشر في ١٩٩٩/١/٢٤)

ABSTRACT

This study involves the investigation of the effects of nitrogen laser at 337.1 nm wave length on bioaspects of protoscolices of *Echinococcus granulosus* *In vitro*. Daughter cysts were obtained from two viable hepatic hydatid cysts of 55 year old patient during surgical operation. Pulsed nitrogen laser system (Molelectron uv/ 24) with (337.1) nm wave length, 1.5 millijoule pulse energy, 10 nanoseconds puls width and repetition rate range of (1 - 50) pulse/ second, was used in the experiments. The samples of protoscolices were exposed to laser beam with (2, 6, 18) pulse / second and for (1, 3, 9, 27) minutes in their respective order. After exposur to laser beam, survival, evagination, vesicularization and posterior bladder formation were examined after 1 min, 1hr, 6hr, 12hr, and daily from exposure. The *In vitro* results show that nitrogen laser have a significant effect on the reduction of the percentage of survival, evagination, vesicularization and posterior bladderr formation. We concluded that the likely effect of the nitrogen laser is the photochemical effect caused by absorption of photons of the laser ray by the chromophores, namly the reduced form of Nicotin Amide Adnine Dinucleotide Phosphate NADP(H). These

chromophores absorbs the light wave length of about (337) nanometer. As a result, dissociation of this compound may occur, leading to the effects on the bioaspects of protoscolices.

الخلاصة

شمل هذا البحث دراسة تأثير اشعة ليزر النتروجين ذات الطول الموجي 337.1 نانومتر في بقاء Survival الرؤيسات الأولية لطفيلي المشوكات الحبيبية والمظاهر الحياتية الأخرى كالانبعاث الى الخارج Evagination والتحوصل Vesiculation وتكوين المثانة الخلفية Posterior bladder من قبل الرؤيسات الحية. تم الحصول على الرؤيسات الأولية من اكياس مائية في كبد مريض بعمر 55 عاما اثناء العملية الجراحية التي اجريت لاستئصال هذه الاكياس. أستعمل في تجارب التشعيع ليزر النتروجين النبضي نوع (Molelectron UV/24) بطول موجي 337.1 نانومتر. وطاقة نبضة 1.5 ملي جول. وعرض نبضة 10 نانو ثانية، وتكرارية نبضات (1 - 50) نبضة / ثانية. أجريت تجارب تشعيع الرؤيسات الأولية باشعة الليزر في الزجاج بتكرارية نبضات (2,6,18) نبضة/ ثانية وزمن تشعيع (1, 3, 9, 27) دقيقة لكل تكرارية نبضة، وتم فحص المظاهر الحياتية للرؤيسات الأولية بعد 1 دقيقة، 1 ساعة، 12 ساعة ويومياً بعد التشعيع. أظهرت نتائج تجارب التشعيع في الزجاج ان لأشعة ليزر النتروجين تأثيراً معنوياً في تقليل النسبة المئوية للبقاء والانبعاث الى الخارج والتحوصل وتكوين المثانة الخلفية في الرؤيسات الحية. من المحتمل أن يكون لأشعة ليزر النتروجين تأثير كيميائي ضوئي ناتج عن امتصاص طاقة فوتونات اشعة ليزر النتروجين من قبل انجزيئات Chromophores الموجودة في خلايا الرؤيس الأولي والمتحصصة لهذا المدى من الطول الموجي، حيث وجد ان المركب NADP (H) يمتص

الضوء عند الطول الموجي 337 نانوميتر، مما قد يؤدي الى تفكك اواصر المركب التي تكون طاقة تفككها مساوية او اقل من طاقة فوتونات اشعة الليزر، وقد يؤدي ذلك بالنتيجة الى حدوث اختلال في الأيض الحيوي و التأثير سلبياً في حيائية الرؤيسات الأولية.

المقدمة

يعد مرض الأكياس المائية Hylatid disease الذي يسببه طفيلي المشوكات الحبيبية *Echinococcus granulosus* من الأمراض المتوطنة في العراق (3).

فضلاً عن ذلك يعد هذا المرض واحداً من أكثر الامراض الطفيلية خطورة في العراق ويشكل مشكلة صحية عامة (1).

تحدث الإصابة بالمرض في الإنسان ولامضائف الوسطية الأخوى عن طريق ابتلاع بيوض الدودة بواسطة المياه والخضروات الملوثة ببراز الكلاب وكذلك عن طريق التماس المباشر مع الكلاب. و يتحرر من هذه البيوض جنين سداسي الاشواك يخترق جدران الامعاء الى الوعية اللمفية ويحمل مع مجرى الدم الى الكبد و الرئتين والدماغ واعضاء الجسم المختلفة، وفي حالة عدم تحطيمه من قبل الخلايا المناعية فإنه يتطور الى كيس مائي وينمو بمعدل 1 سم في السنة، ويسبب كبر حجم الكيس بمرور الزمن اعراضاً سريرية تعتمد على العضو الذي يوجد فيه الكيس، ويتم تشخيص المرض وموقع وحجم الكيس بالفحوصات الصمالية وفحص الامواج فوق الصوتية (4). يعد التداخل الجراحي الطريقة المفضلة في العلاج في الوقت الحاضر، وخاصة في حالة الاكياس الكبيرة الحجم (8).

يدخل الليزر في العلوم التطبيقية المهمة التي شملت فروعاً عديدة في مجال علوم الحياة كالأحياء المجهرية وعلم الخلية والوراثة والمناعة والنبات وكذلك دخل الليزر في المجال الطبي واستخدم لعلاج مختلف الامراض (7).

هناك ستة عوامل تحدد تفاعل شعاع الليزر مع الانسجة⁽²⁾ وتشمل:

١. كمية الطاقة المستعملة خلال مدة التعريض لأشعة الليزر.
٢. مدة التعريض لأشعة الليزر.
٣. استجابة النسيج لطاقة اشعة الليزر (امتصاص، انعكاس).
٤. تركيب النسيج.
٥. العلاقة الهندسية بين حزمة الليزر والنسيج.
٦. الطول الموجي لضوء الليزر.

عند سقوط شعاع الليزر على نسيج ما فإنه سيعاني انعكاساً Reflection او استطارة Scatteing او نفوذاً Transmission او امتصاصاً Absorption.

إذا تم امتصاص الفوتونات من قبل النسيج فإن الذرات والجزيئات الموجودة في النسيج ستتفاعل مع فوتونات الضوء بعدة طرق :-

- ١- التفاعل الكيميائي الضوئي Photochemical reaction
- ٢- التفاعل الحراري الضوئي Photothermal reaction⁽⁵⁾

تهدف الدراسة الحالية الى معرفة نوع وطبيعة وميكانيكية التفاعل بين شعاع الليزر ضمن هذا الطول الموجي وخلايا الرؤيس، وانتوصل الى تركيب الجزيئات Chromophores الموجودة في خلايا الرؤيس والتي امتصت طاقة فوتونات الضوء ضمن الطول الموجي 337.1 نانوميتر وتسببت في حصول التفاعل.

المواد وطرائق العمل

١- تحضير نماذج الرؤيسات الأولية

تم الحصول على الرؤيسات الأولية اثناء عملية جراحية اجريت في مستشفى صدام العام لمرريض بعمر 55 عاماً، تم استخراج الاكياس البنيوية Daughter cyst اثناء العملية ووضعت في حاويات معقمة وغسلت بمحلول كرب رنجر (Kerbs Ringer solution (KRS) المعقم. بعد ذلك تم حفظ الاكياس البنيوية في الوسط الحافظ المعقم المتكون من محلول كرب رنجر مضافاً اليه سائل الكيس المائي (KRS + Hydatid cyst fluid (HCF)) بنسبة (4/1) مع اضافة 100 وحدة / مل من البنسلين و 150 وحدة / مل من الستربتومايسين كمضادات حيوية⁽⁹⁾.

استخرجت محتويات الاكياس من رؤيسات اولية وعلب حضنة Brood Capsules وغسلت ثلاث مرات بمحلول كرب رنجر ورسبت بجهاز الطرد المركزي (1500 دورة / دقيقة لمدة 10 دقائق) بعد ذلك وضع الراسب مع كمية من الوسط الحافظ في دورق معقم.

تم اختبار حيوية الرؤيسات الأولية باستعمال صبغة الايوسين المائية Eosin حيث تكون الرؤيسات الميتة ذات لون احمر لنفاذ صبغة الايوسين عبر جدرانها بينما تكون الرؤيسات الحية ذات لون اخضر براق، وتم حساب عدد الرؤيسات في المليليتر الواحد من العالق بوساطة الممص الدقيق Micropipette اذ اعتمد معدل العد لعشرة مكررات باستخدام 10 مايكروليتر من العالق للحصول على عدد كلي للرؤيسات يقدر بحدود 2000 رؤيس / مل، ثم تم توزيع عالق الرؤيسات الأولية بعبوات معقمة بحجم 1 مل وحفظت بدرجة حرارة 4م° لحين استعمالها.

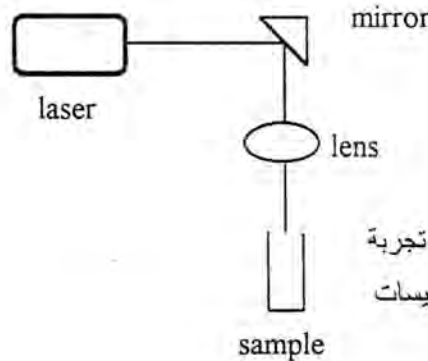
دراسة تأثير اشعة ليزر النتروجين في حيائية الرؤيسات الأولية لطيفيلي المشوكات
الحبيبية *Echinococcus granulosus* في الزجاج
امل مصطفى مكي وجماعتها

٢- جهاز الليزر

تم ساتعمال ليزر النتروجين النبضي Plused Nitrogen Laser نوع (Molelectron UV/24) لغرض اجراء التجارب. يكون الاشعاع المنبعث من هذا الليزر في منطقة الاشعة فوق البنفسجية من الطيف الكهرومغناطيسي بطول موجة مقداره 337.1 نانوميتر، يعمل الجهاز بتكرارية نبضات Repetition Rate تتراوح بين (1 - 50) نبضة / ثانية، وتبلغ طاقة النبضة (Pulse energy) 1.5 ملي جول، ويبلغ عرض النبضة (Pulse width) 10 نانوثانية.

٣- تصميم التجارب

أ- تم تقسيم عالق الرؤيسات المتكون من ٢٠٠٠ رؤيس / مل في عبوات بحجم 1 مل على شكل خمسة مجاميع كل مجموعة تتألف من ستة مكررات.
ب- تم تعريض نماذج الرؤيسات الاولية الى شعاع الليزر كما موضح في شكل (1) حيث ينعكس شعاع الليزر بواسطة مرآة مستوية ليسقط عمودياً ويمر من خلال عدسة لامة ذات بعد بؤري 15سم، ويوضح النموذج الحاوي على الرؤيسات تحت العدسة حيث يسقط شعاع الليزر على النموذج بقطر بقعة يبلغ 8 ملم.



شكل (1) مخطط تجربة
تشعيع نماذج الرؤيسات
الاولية

عرضت مجاميع الرؤيسات الاولى الى اشعة الليزر للمدد (27,9,3,1) دقيقة وتكرارية نبضات (18,6,2) نبضة / ثانية لكل مدة تعريض مع الاحتفاظ بمجموعة سيطرة.

بعد التعريض، حفظت النماذج في الحاضنة بدرجة حرارة $(29+1)^\circ\text{C}$ ، وتم فحص كل عينة بعد 1 دقيقة، 1 ساعة، 6 ساعة، 12 ساعة، ويومياً بعد التعريض مع مراعاة تبديل الوسط الحافظ لكل عينة خلال كل عملية فحص. اذ تم حساب النسبة المئوية لحيوية الرؤيسات الاولى وكذلك النسبة المئوية للانبعاث الرؤيسات الحية الى الخارج مع حساب النسبة المئوية للتحوصل والنسبة المئوية لتكوين المثانة الخلفية من قبل الرؤيسات الحية.

النتائج

اظهرت النتائج ان لاشعة ليزر النتروجين تأثيراً معنوياً في تقليل النسبة المئوية لحيوية الرؤيسات الاولى في الزجاج وكذلك تقليل النسب المئوية للانبعاث للخارج والتحوصل وتكوين المثانة الخلفية من قبل الرؤيسات الحية.

١- تأثير اشعة ليزر النتروجين في حيوية الرؤيسات الاولى

عند تكرارية نبضات 2 نبضة / ثانية لوحظ ان النسبة المئوية لحيوية الرؤيسات تقل تدريجياً بمرور الزمن بعد التشعيع حتى تصل الى (0%) في اليوم الثاني عشر والحادي عشر والتاسع والثامن لمدد التشعيع (27, 9, 3, 1) دقيقة على التوالي، شكل (A 2)، ويزداد التأثير عند تكرارية نبضات 6, 18 نبضة / ثانية، حيث عند تكرارية نبضات 6 نبضة / ثانية تقل الحيوية تدريجياً بمرور الزمن ما بعد التشعيع حتى تصل الى (0%) في اليوم العاشر بالنسبة لمجموعة التشعيع لمدة 1 دقيقة، واليوم الثامن بالنسبة لمجاميع التشعيع 3, 9 دقيقة على التوالي وفي لايوم الخامس بالنسبة لمجموعة التشعيع 27 دقيقة، شكل (B 2)، وعند تكرارية نبضات

18 نبضة / ثانية يكون التأثير اكثر حيث تصل النسبة المئوية للحوية الى ((%)) في اليوم العاشر والثامن والسادس والرابع لمدد التشعيع (1,3,9,27) دقيقة على التوالي، شكل (2.C).

٢- تأثير اشعة الليزر في انبعاث الرؤيسات الاولى

عند تكرارية نبضات 2 / ثانية لوحظ ان النسبة المئوية للانبعاث الرؤيسات تقل تدريجياً بمرور الزمن بعد التشعيع ما عدا المجموعة المشعة لمدة دقيقة واحدة حيث ظهر ارتفاع في النسبة المئوية للانبعاث مقارنة بمجموعة السيطرة ابتداءً من اليوم الاول الى اليوم العاشر لمدة ما بعد التشعيع حيث تقل في اليوم الحادي عشر عن مجموعة السيطرة وتصبح (0%) في اليوم الثاني عشر. اما بالنسبة لبقية مجاميع التشعيع، فنقل النسبة المئوية للانبعاث بزيادة الزمن ما بعد التشعيع حتى تصل الى (0%) في اليوم الحادي والتاسع والثامن لمجاميع التشعيع (3,9,27) دقيقة على التوالي، شكل (3.A).

ويزداد التأثير عند تكرارية نبضات 6 نبضات / ثانية، حيث تكون النسبة المئوية للانبعاث (0%) في اليوم العاشر بالنسبة لمجموعة التشعيع 1 دقيقة. واليوم الثامن بالنسبة لمجاميع التشعيع (3,9) دقيقة واليوم الخامس بالنسبة لمجموعة التشعيع 27 دقيقة، شكل (3.B).

ويزداد التأثير عند تكرارية نبضات 6 نبضة / ثانية، حيث تكون النسبة المئوية للانبعاث (0%) في اليوم العاشر بالنسبة لمجموعة التشعيع 1 دقيقة، واليوم الثامن بالنسبة لمجاميع التشعيع (3,9) دقيقة واليوم الخامس بالنسبة لمجموعة التشعيع 27 دقيقة، شكل (3.B). وعند تكرارية نبضات 18/ ثانية يزداد التأثير حيث تصل النسبة المئوية للانبعاث الى (0%) في اليوم العاشر والثامن والسادس والرابع لمجاميع التشعيع (1,3,9,27) دقيقة على التوالي، شكل (3.C).

٣- تأثير اشعة الليزر في تحوصل الرؤيسات الاولى

عند تكرارية نبضات 2/ ثانية، لوحظ ان النسبة المئوية لتحوصل الرؤيسات الاولى تقل بزيادة زمن التشعيع ومدة ما بعد التشعيع حيث تصبح النسبة المئوية لتحوصل (0%) في اليوم الثاني عشر و الحادي عشر والتاسع والثامن لمجاميع التشعيع (27,9,3,1) دقيقة على التوالي، شكل (4.A) وعند تكرارية نبضات 6/ ثانية يزداد التأثير حيث تصل النسبة المئوية لتحوصل الى (0%) في اليوم العاشر لمجموعة التشعيع ١ دقيقة والثامن لمجاميع التشعيع (9,3) دقيقة و الخامس لمجموعة التشعيع 27 دقيقة، شكل (4.B). وعند تكرارية نبضات 18 / ثانية يكون التأثير اكبر حيث تصل النسبة المئوية لتحوصل الى (0%) في اليوم العاشر والثامن والسادس و الرابع لمجاميع التشعيع (27,9,3,1) على التوالي، شكل (4.C).

٤- تأثير اشعة الليزر في تكوين المثانة الخلفية في الرؤيسات الاولى

عند تكرارية نبضات 2/ ثانية لوحظ ان النسبة المئوية لتكوين المثانة الخلفية من قبل الرؤيسات الاولى تقل بزيادة زمن التشعيع ومدة ما بعد التشعيع وتصبح النسبة المئوية لتكوين المثانة الخلفية (0%) في اليوم الثاني عشر و الحادي عشر والتاسع لمجاميع التشعيع (9,3,1) دقيقة على التوالي، شكل (5.A). وعند تكرارية نبضات 6/ ثانية يزداد التأثير حيث اصبحت النسبة المئوية لتكوين المثانة الخلفية (0%) في جميع مجاميع التشعيع وذلك في اليوم العاشر لفترة ما بعد التشعيع، شكل (5.B). كذلك الحال عند تكرارية نبضات 18/ ثانية حيث يظهر التأثير المعنوي لأشعة الليزر في اليوم الاول لمدة ما بعد التشعيع وتصل النسبة المئوية لتكوين المثانة الخلفية الى (0%) في جميع مجاميع التشعيع وذلك في اليوم العاشر لمدة ما بعد التشعيع، شكل (5.C).

دراسة تأثير اشعة ليزر النتروجين في حيائية الرؤيسات الأولية لطفيلي المشوكات
الحبيبية *Echinococcus granulosus* في الزجاج
امل مصطفى مكي وجباعتها

المناقشة

يتبين من خلال النتائج ان لاشعة ليزر النتروجين تأثيراً سلبياً في
حيائية الرؤيسات الأولية لطفيلي المشوكات الحبيبية. ويزداد هذا التأثير
بزيادة زمن التشعيع وعند النبضات في الثانية الواحدة وكذلك بزيادة المدة
الزمنية لما بعد التشعيع، ان زيادة تأثير اشعة ليزر النتروجين بزيادة عدد
النبضات يعود الى ان معدل القدرة يزداد بزيادة عدد النبضات في الثانية
الواحدة.

حيث ان معدل القدرة = طاقة النبضة \times عدد النبضات في الثانية الواحدة
كذلك يؤدي زيادة عدد النبضات في الثانية الواحدة الى زيادة كثافة القدرة او
الشدة،

حيث ان كثافة القدرة = معدل القدرة / مساحة بقعة حزمة الليزر

ان زيادة زمن التشعيع يؤدي الى زيادة التأثير السلبى لاشعة الليزر في
حيائية الرؤيسات الحية ويمكن تفسير ذلك على اساس ان زيادة زمن التشعيع
يؤدي الى زيادة كثافة الطاقة او التأثير.

طاقة النبضة \times عدد النبضات في الثانية الواحدة \times زمن التشعيع
حيث ان كثافة الطاقة =

مساحة بقعة حزمة الليزر

ان الميكانيكية المحتملة للتفاعل بين اشعة ليزر النتروجين وخلايا الرؤيس
والتي ادت الى حدوث تأثير في حيائية الرؤيس في الزجاج يمكن تفسيرها
في ضوء النظريات الفيزيائية كما يلي :-

قد يكون التأثير الاكثر احتمالاً في هذا الطول الموجي من الاشعة وفي هذا
المدى من الشدة (كثافة القدرة) والتأثير (كثافة الطاقة) هو تأثير كيميائي
ضوئي Photochemical effect، فعند امتصاص الضوء من قبل خلايا

الرؤيس، فإن الجزيئات الموجودة في الخلايا والتي تمتص فوتونات الضوء بطول موجي معين وتسبب حصول التفاعل الكيميائي الضوئي تدعى بالمحسسات الضوئية Photosensitizers أو Chromophores ولهذه الجزيئات خصوصية في امتصاص الضوء ضمن هذا المدى من الطول الموجي للضوء دون سواء من الأطوال الموجية الأخرى.

في حالة امتصاص فوتونات الضوء من قبل جزيئات مركب معين، فإن طاقة الفوتونات سوف تكتسب من قبل الأواصر التي تربط بين ذرات الجزيئة، فإذا كانت طاقة الفوتون أقل من طاقة تفكك الأصرة Dissociation energy وكافية لرفع طاقة الأصرة بصورة تؤدي الى تهيج ذرات الجزيئة ورفعها الى مستوى اعلى من الطاقة (الحالة المثارة) Exited state فتحصل هنا حالة الاثارة Excitation التي قد تؤدي بالنتيجة الى حدوث تحفيز او تنشيط للجزيئات وكما يلي :-



حيث ان (A-B) جزيئة تتكون من ذرتين A , B

hv طاقة الفوتون ، (A - B)* الجزيئة في حالة الاثارة

اما اذا كانت طاقة الفوتون مساوية لطاقة تفكك الأصرة او اعلى منها فان ذلك سيؤدي الى حدوث تفكك للأواصر التي بين الذرات مع تحرير طاقة وكما يلي :-



بما ان الليزر المستخدم في هذه الدراسة ذو طول موجي (337.1) نانوميتر، فمن المحتمل ان يكون المركب المسؤول عن حدوث التفاعل الكيميائي الضوئي هو المركب الذي يمتص الاشعة ضمن هذا الطول الموجي . تم

دراسة تأثير اشعة ليزر النتروجين في حيائية الرؤيسات الأولية لطفيلي المشوكات

الحبيبية *Echinococcus granulosus* في الزجاج

امل مصطفى مكي وجباعتها

التحري عن اطياف الامتصاص للمركبات التي تتعلق بايض رؤيسات الطفيلي، وقد وجد بأن الشكل المختزل Reduced form للمساعد الانزيمي : Coenzyme

Nicotinamide Adenine Diunucleotide Phosphate NADP(H)

يمتص الضوء عند الطول الموجي 337 نانوميتر⁽⁶⁾.

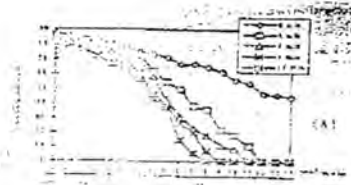
يعمل مركب NADP(H) كواهب لذرات الهيدروجين في

تفاعلات التخليق الحيائي الاختزالية Reductive Biosynthetic Reaction، كما يدخل في مسارات ايض الكاربوهيدرات في دورة كريبس Krebs Cycle وكذلك في مسلك البنتوز فوسفيت Pentose Phosphate لتحرير الطاقة بشكل مركب Adenosin Tri Phosphate (ATP).

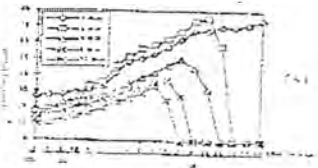
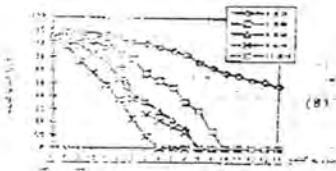
من المحتمل ان يكون تأثير اشعة ليزر النتروجين في حيائية الرؤيسات الأولية لطفيلي المشوكات الحبيبية في الزجاج ناتج عن امتصاص طاقة فوتونات اشعة ليزر النتروجين من قبل الاواصر التي تربط بين ذرات جزيئات مركب NADP (H) التي تكون طاقة تفككها اقل او مساوية لطاقة فوتون اشعة ليزر النتروجين مما قد يؤدي الى تفكك هذه الاواصر والتأثير في الايض الحيائي للرؤيسات من حيث تخليق المركبات الحيوية وتحرير الطاقة.

REFERENCES

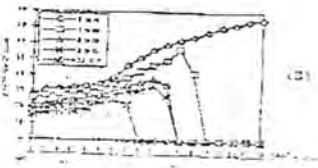
1. Al-Khalili, A.H., Al-Jeboori, T.I. Munir, R. & Al-Sammak, M. Hydatid disease : Acomparative study in the medical teaching hospital after 10 years. Proc. 5th. Sci. Conf. Iraq. Baghdad, 5 : 356-364 (1989).



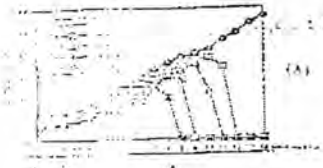
شكل (A) العلاقة بين تركيز المادة ودرجة الحرارة عند ضغط ثابت 100 mmHg ودرجة الحرارة 100 °C. (1) تركيز المادة 1.0، (2) تركيز المادة 1.5، (3) تركيز المادة 2.0، (4) تركيز المادة 2.5.



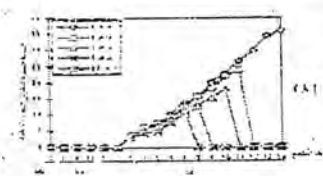
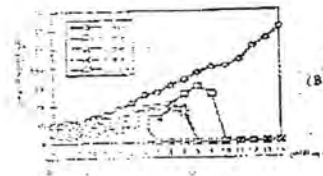
شكل (D) العلاقة بين تركيز المادة ودرجة الحرارة عند ضغط ثابت 100 mmHg ودرجة الحرارة 100 °C. (1) تركيز المادة 1.0، (2) تركيز المادة 1.5، (3) تركيز المادة 2.0، (4) تركيز المادة 2.5.



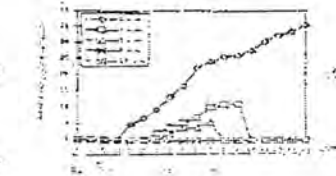
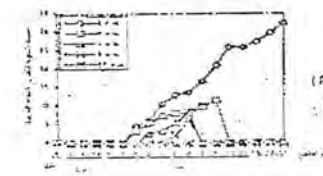
دراسة تأثير اشعة ليزر الفنتروجين في حيائية الرؤسبات الأولية لطيفلي المشوكات
 الحبيبية *Echinococcus granulosus* في الزجاج
 امل مصطفى مكي وجماعتها



شكل (A) تأثير اشعة ليزر الفنتروجين على حيائية الرؤسبات الأولية لطيفلي المشوكات الحبيبية (10-20-30 ميلي واط) في الزجاج (24 ساعة تعريض).



شكل (A) تأثير اشعة ليزر الفنتروجين على حيائية الرؤسبات الأولية لطيفلي المشوكات الحبيبية (10-20-30 ميلي واط) في الزجاج (24 ساعة تعريض).



2. Al-Koubaisy, O.K., Hajim, K.L., & Quzueeny, M.B. Effects of CO₂ laser on arterial tissues. Iraqi medical journal, 42 : 19-23 (1993).
3. Aziz, L.J., Kadir, H.A. & Al-Debbag, M.A. Comparative study on trace elements concentration and enzyme activities of liver hydatid cysts of *Echinococcus granulosus* in different intermediate hosts. Proc. 5th. Sci. Conf. Iraq. Baghdad, 5 : 373-378. (1989).
4. Barons, S. medical Microbiology, third ed. Churchill Livingstone. PP 1101-1103 (1991).
5. Chopra, S. & Chawia, H.M. lasers in chemicals and biological sciences. Wiley eastern limited, newdelhi. PP : 2-182 (1992).
6. Devlin, T.M. Text book of biochemistry with clinical correlations, 2nd ed. A wiley medical publications. PP : 423 (1986).
7. Goldman, L. Applications of the laser. USA. PP : 155-177 (1982).
8. mentes, A., Yuzeer, Y. & Ozbal, O. Omentoplasty versus inflexion for hydatid liver cyst. J.R. Coll. Surg, 38 : 82-85 (1994).
9. Smyth, J.D. *In vitro* culture of *Echinococcus* sp. the proceeding of the 13th international congress of hdatology. p 84-89 (1985).

إيجاد طاقة السطح النووي لنظير السلينيوم $^{74}_{34}\text{Se}$ باستخدام نموذج البوزونات المتفاعلة الأول (IBM-1)

خالد سلمان إبراهيم ، إيمان طارق العلوي وأنعام حاتم خضير
قسم الفيزياء / كلية العلوم / الجامعة المستنصرية
(أستلم بتاريخ ١٠/٦/١٩٩٨ وقبل للنشر في ٢٧/١/١٩٩٩)

ABSTRACT

The interacting boson model (IBM-1) was used to find the potential energy surface $v(\beta, \gamma)$ of Se-74 isotope. The contour lines for triaxial symmetric shapes have been drawn for $(\gamma = 0^\circ, 30^\circ, 60^\circ)$ as a function of β values. A comparison was made between our results and the ideal values of these Symmetric. A very good agreement between them has been found.

الخلاصة

أستخدم نموذج (IBM-1) لإيجاد طاقة السطح النووي $v(\beta, \alpha)$ لنظير السلينيوم (Se-74) من خلال رسم الخطوط الكنتورية للأشكال ذات التناظر المحوري الثلاثي (Triaxial Symmetric) بين $(\gamma = 0^\circ, 30^\circ, 60^\circ)$ كدالة لقيم β . وقد تم مقارنة نتائجنا مع القيم المثالية لهذه التناظرات فكانت متوافقة بصورة جيدة جداً.

المقدمة

إن لكل نواة حالة دنيا من الطاقة تسمى الحالة الأرضية (Ground State) وحالات أعلى من تلك الطاقة تسمى الحالات المثيجة (Excited States) فكثير من المعلومات المتعلقة بالقوى النووية يمكن

إيجاد طاقة السطح النووي لنظير السيلينيوم $^{74}\text{Se}_{40}$ باستخدام نموذج البوزونات المتفاعلة الأول (IBM-1) خالد سلمان إبراهيم وجماعته

معرفتها من خلال دراسة الحالات الأرضية للنوى بغض النظر عن كون هذه النوى مستقرة أم لها القابلية على الانحلال^(6,5,4) إن شكل النواة يحدد بدلالة عاملي التشوه (β, γ) حيث أن قيمة (β) تقترب من الصفر للنوى الكروية (Spherical nuclei) بينما قيمتها لاتساوي صفر $(\beta \neq 0)$ للنوى المشوهة (Triaxially Symmetric) ولوحظ أيضا أن قيمة (γ) تساوي صفرا للتمائثل الثلاثي (Triplet Symmetric) من نوع الـ (Prolate) وقيمتها تساوي 60° لتمامثل ثلاثي من نوع الـ (Oblate)^(12,11,10).

الجزء النظري

إن المعادلة لطاقة جهد السطح تعطى بالعلاقة التالية^(3,2) :

$$E(N, \beta, \gamma) = \frac{N(\epsilon_d + \epsilon_s)\beta^2}{1 + \beta^2} + \frac{N(N-1)}{(1 + \beta^2)^2} (\alpha_1\beta^4 + \alpha_2\beta^3 \cos 3\gamma + \alpha_3\beta^2 + \alpha_4) \dots (1)$$

حيث أن :

N : تمثل العدد الكلي للبوزونات

ϵ_s : تمثل طاقات البوزون المنفرد من (S-boson).

ϵ_d : تمثل طاقات البوزون المنفرد من (d-boson).

$\alpha_1, \alpha_2, \alpha_3, \alpha_4$ عبارة عن الاغومات (Parameters)

أما معادلة مؤثر دالة هاملتون العامة فتكتب كالآتي^(3,2) :

$$\hat{H} = \epsilon \hat{n}_d + \alpha_0 \hat{P}^+ \cdot \hat{P} + a_1 \hat{L} \hat{L} + a_2 \hat{Q} \cdot \hat{Q} + a_3 \hat{T}_3 \cdot \hat{T}_3 + a_4 \hat{T}_4 \cdot \hat{T}_4 \dots (2)$$

إذ إن :

\hat{P} : تمثّل الأزواج (Pairing Operator)

\hat{Q} : تمثّل مؤثر عزم رباعي القطب (Quadrupole Operator)

\hat{L} : يمثّل مؤثر الزخم الزاوي (Angular Momentum Operator)

\hat{T}_3 : مؤثر خماسي القطب (Octupole Operator)

\hat{T}_4 : مؤثر سداسي القطب (Hexadecapole Operator)

كما أن :

عند التحديد $SU(5)-O(6)^{(3,2)}$

$$\hat{H} = \varepsilon \hat{n}_d + a_0 \hat{P}^+ \cdot \hat{P} + a_1 \hat{L} \cdot \hat{L} \quad \dots\dots\dots (3)$$

تعتمد المعادلة (3) على النسبة (ε/a_0) .

وعند التحديد $SU(5) - SU(3)^{(3,2)}$

$$\hat{H} = \varepsilon \hat{n}_d + a_1 \hat{L} \cdot \hat{L} + a_2 \hat{Q} \cdot \hat{Q} \quad \dots\dots\dots (4)$$

وتعتمد المعادلة (4) على النسبة (ε/a_2) .

النتائج والمناقشة

إن طاقة جهد السطح (Potential Energy Surface) تمثّل — $U(\beta, \gamma)$ وقد تم حسابها بعد تحديد قيم المعاملات (Parameters) لدالة مؤثر هاميلتون الجدول (1) يمثّل معاملات A's التي أستخدمت في برنامج حساب $U(\beta, \gamma)$.

يبين الشكل $(2a \leftrightarrow 1a)$ يبين طاقة جهد السطح كدالة لعامل التشويه (Deformed Parameter (β, γ)) التي تظهر فيها الخطوط الكنتورية توافقاً جيداً مع المخطط المثالي ومن خلال رسم التناظر المحوري

ليجاد طاقة السطح النووي لنظير السيلينيوم $^{74}_{34}\text{Se}$ باستخدام نموذج البوزونات المتفاعلة الأول (IBM-1) خالد سلمان إبراهيم وجماعته
(Triaxial Symmetric) بين ($\gamma = 0^\circ, 30^\circ, 60^\circ$) كدالة لقيم β لاحظنا أن هذا النظرير يتصرف بموجب خاصيتين هما :

١. خاصية الـ SU(5)-O(6) كما في الشكل (1b) فعند طاقة الجهد (2Mev) تبلغ قيمة β (0.6) لشكل ببيضوي من نوع (Prolate) وتبلغ القيمة نفسها لشكل ببيضوي من نوع (Oblate) وهذا يتفق مع خاصية SU(5)-O(6) للتناظر المحوري المثالي.

٢. خاصية SU(5)-SU(3) كما في الشكل (2b) حيث نجد أن قيمة (β) تبلغ (0.6) عند طاقة جهد (0.8 MeV) لشكل ببيضوي من نوع (Prdate) بينما بلغت (0.6) أيضاً لكن عند طاقة جهد (1MeV) وهذا يتفق مع خاصية SU(5)-SU(3) للتناظر المحوري المثالي.
جدول (2) يبين الخاصية النهائية التي ينتمي إليها النظرير (Se-74).

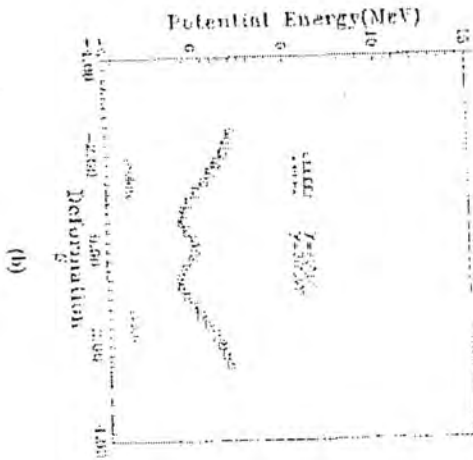
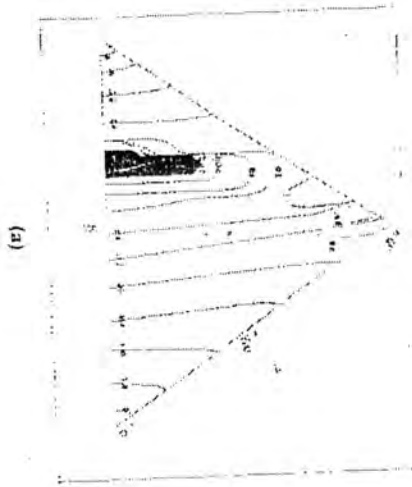
جدول (١) : المعاملات المستخدمة في برنامج حساب $U(\beta, \gamma)$

Isotpe	A1	A2	A3	A4	ϵ_s	ϵ_d
Se-74	0.0000	-0.0070	-0.1600	0.0000	-0.2000	0.6400
	0.2480	0.0000	-0.4950	0.0000	0.0000	1.0780
	0.0020	-0.0070	-0.1650	0.0000	-0.2000	0.5000

جدول (٢) : يوضح تحديد الخاصية للنظير (Se-74)

العدد الكلي للبوزونات [N]	مستويات الطاقة Energy Levels	نسب الطاقات Energy Ratios	حزم الطاقة Energy bands	احتمالية الانتقال الكهربائي رباعي القطب (E2) B(E2)	تحديد الخاصية النهائية	الملاحظات
8	SU(5)-SU(3)	SU(5)	SU(5)	SU(5)-SU(3)	SU(5)-SU(3)	١- إن لهذا النظير خاصية SU(5) والتي تبدأ عند الحالة الأرضية
	SU(5)-O(6)			SU(5)-O(6)	SU(5)-O(6)	٢- تبدأ خاصية التشوه في الحزمة β لأن المستوي O_2^+ أقرب للتحديد SU(3) و O(6) أكثر مما للتحديد SU(5) وهذا يتفق مع (9,7,8)

إيجاد طاقة السطح النووي لنظير السيلينيوم $^{74}\text{Se}_{40}$ باستخدام نموذج البوزونات المتفاعلة الأول (IBM-1)
 خالد سلمان إبراهيم وجماعته



التمثيل (a,b) : 1 : الخطوط المتقطعة والتأثيرات المعزولة للنظير $^{74}\text{Se}_{40}$ عند $\beta=0$

SI(5) - SI(3)

REFERENCES

- 1.D. Bonatsos : Interacting Boson Models of Nuclear Structure. Ed. Hodgson P.E.; Pub. Clarendon Press Oxford (1988).
- 2.F. Iachello and A. Arima : The Interacting Boson Model. Pub. Cambridge University Press Cambridge (1987).
- 3.R.F. Casten and D.D. Warner: The Interacting Boson Approximation. Rev. Mod. Phys. 60,2, 390 (1988).
- 4.K.P. Lieb and J.J. Kolata: Ground-state band in Se-72. Phys. Rev. C15, 3, 939 (1977).
- 5.J.H. Hamilton, H.L.Crowell, R.L.Robinson, A.V. Ramayya, W.E. Collins, R.M. Ronningen, V. Maruhn-Rezwani, J.A. Maruhn, N.C.Singhal, H.J.Kim, R.O. Sayer, T. Magee, and L.C. Whitlock: Life time measurements to test the coexistence of spherical and deformed shapes in Se-74. Phys. Rev. Lett. 36, 340 (1976).
- 6.J. Barrette, M.R.Haroutanion, G.Lamoureux, and R. Monaros: Investigation of the Reorientation effect on ^{122}Te , ^{124}Te , ^{126}Te , ^{128}Te , and ^{130}Te . Phys. Rev. C10, 1166 (1974).
- 7.R. B. Piercey, A. V. Ramayya, R.M. Ronningen, J.H.H.amilton, and V. Maruhn-Rezwani: In-beam gamma-ray spectroscopy of Se-74 following the $^{60}\text{Ni}(^{16}\text{O}, 2\text{p})$, $^{64}\text{Ni}(^{12}\text{C}, 2\text{n})$ and $^{65}\text{Cu}(^{11}\text{B}, 2\text{n})$ reactions. Phys. Rev. C19, 4, 1344 (1979).
- 8.K.S.Krane: E2/M1 multipole mixing ratios of 2-2 gamma transitions in even-even spherical nuclei. Phys. Rev. C10,3,1197 (1974).
- 9.R.Lecomte, S.Landsberger, P.Paradis, and S. Monaro: Static quadrupole moment of the first excited state of Se-74. Phys. Rev. C18, 6, 2801 (1978).
- 10.S.R. Almoney and G.J. Borse: Anharmonic effects in spherical nuclei. Nucl. Phys. A171, 660-670 (1971).
- 11.J.C. Wells, R.L.Robinson, H.J.Kim, R.O.Sayer, R.B.Peircey, A.V. Ramayya, J.H. Hamilton, and C.F.

- Maguire: High-spin states and band structure in Se-76. Phys. Rev. C22, 1126 (1980).
12. A.R.H. Subber, S.J. Robinson, and P. Hungerford: The level structure of Se-76 and Se-78 and the systematics of Selenium isotopes within the framework of the DDM. J. Phys. G: Nucl. Phys. 13, 807 (1987).

تأثير ظاهرة النينو على التغيرات المطري في العراق

نعمة محسن لفتة

المستنصرية / العلوم / الأنواء الجوية

(استلم بتاريخ ١٩٩٩/١٢/٧ وقبل للنشر في ٢٠٠٠/٥/١٦)

ABSTRACT

Teleconnection between El Nino and rainfall variation in Iraq region during the period 1940-1990 were uninvestigated using correlation methods. The pearson product-moment correlation coefficient analysis gives a significant negative correlation between annual values of El Nino and rainfall anomalies in 12 climatological stations in Iraq. It is indicate that El Nino impact in this region is most pronounced. In the normally wet months (N,D,J) & (F,M,A), El Nino intensity was moderate and strong.

الخلاصة

لتحقيق العلاقة بين النينو والتغيرات المطري في منطقة العراق خلال الفترة ١٩٤٠-١٩٩٠ استخدمت طرق الارتباط وتحليلات معاملات الارتباط بطريقة Pearson-product moment. أعطت النتائج ارتباطات مميزة بين القيم السالبة السنوية للنينو والشذوذ بالتساقط المطري الى ١٢ محطة مناخية في العراق. وهذا يشير الى ان ظاهرة النينو تؤثر على القطر العراقي. لقد وجد أن أغلب أشهر الشتاء الممطرة تشترين الثاني و كانون الأول و كانون الثاني (N,D,J)، وأشهر الربيع الممطرة شباط وآذار ونيسان (F,M,A) تحدث فيهما ظاهرة النينو وبشدة متوسطة وقوية.

المقدمة

أن ظاهرة النينو تعود الى تيار مائي ساخن يشرع بالهبوب كل سنة على امتداد سواحل جنوب الأكوادور وشمال البيرو وخلال الصيف لنصف الكرة الجنوبي حينما تضعف الرياح التجارية في الجنوب وسميت الظاهرة بالنينو نسبة الى الطفل يشوع ولظهورها بفترة أعياد المسيح وتزامن ظاهرة النينو مع تردي الجو وضعف الرياح التجارية في نصف الكرة الجنوبي للأرض ويعرف النينو بأنه مفتاح التذبذب المناخي لمركبات المنظومات الجوية المعقدة، وأرتبطت الظاهرة (EN) El Nino مع الذبذبة الجنوبية (SO) ارتباطاً وثيقاً حتى سميت بـ (ENSO) والتعبير عن الذبذبة الجنوبية (SO) أستخدمت لأول مرة من قبل [Walker, 1924] لتصف التذبذب بالأخدود (امتداد المنخفض الجوي بين شمال استراليا - أندونيسيا والضغط العالي الشبه مداري في جنوب المحيط الهادي). [1], [2]

ويعرف [3] دليل اذبذبة الجنوبية [SOI] بأنه الاختلاف بالضغط بين جزيوة استر في جنوب المحيط الهادي وجاكارتا (أندونيسيا).

يعرف [4] دليل الذبذبة الجنوبية بأنه الشذوذ لقيم الضغط عن المعدلات الطبيعية الشهرية بين مدينتي تاهيتي (18S, 150 W) وداروين في أستراليا (12 S, 131 E) يكون الدليل موجب إذا كان الضغط أعلى من المعدل في جنوب الهادي وأقل من المعدل في شمال أستراليا هذه الحالة تسمى سنوات لانينو. وبالعكس الدليل السالب يتماشى مع نزول الضغط عن المعدل الطبيعي في جنوب الهادي وصعوده عن المعدل في شمال أستراليا [5]. في السنوات الأخيرة طور تعريف النينو عندما ادركو بموقع واضح لدورة متذبذبة على المقياس الكبير الجو - المحيط مما تجلب الرياح التجارية القوية وباتجاه الجنوب الشرقي وكذلك الشرقية الاستوائية (زيادة بقيم دليل الذبذبة الجنوبية) [6].

أفترض السبب أو الأسباب للنينو هي غير معروفة رغم أقترح عدة نظريات. أقترح [7] بأنه سبب النينو هو وصول شدة الرياح النطاقية الى

الحدود الدنيا غرب خط طول ١٢٠ درجة غرباً وكذلك وصول شدة الرياح العرضية الى الحدود الدنيا شرق خط طول ١٢٠ درجة غرباً. وربط النقصان بالرياح التجارية الجنوبية قرب البيرو مع النينو وأسستج تزامن النقصان مع تردي الجو على السواحل وبرودة سطح الماء مع رحيل المياه الساخنة على السطح.

آلية ميكانيكية أخرى اقترحها^[3,8] خلال الشروط الطبيعية للانحدار الحراري الانتقال الأفقي بين سطوح المياه الساخنة والأبرد منها تزود المياه العميقة بالطاقة على مقربة من السطوح الشرقية للمحيط الهادي مع تردي الجو على طول الساحل الجنوبي لأمريكا. والمياه الباردة يمكن أن تصل الى سطح البحر. التباين الحراري الأعمق في غرب المحيط الهادي نسبة الى^[9] في السنوات التي تسبق النينو، الضغط العالي شرق تهايتي يكون عميق قوي والمنخفض في أندوسيا يتعمق ومع بعضهم يشتد وتظهر الرياح التجارية الجنوبية على خط الاستواء من المحيط الهادي.

عامل اخر لخلق النينو اقترحها^[10] بتعريفه خلية الدورة الافقية المسماة دورة ولكر التي تتبع بين الذبذبة الجنوبية ودرجات حرارة سطح البحر في خط الاستواء المحيط الهادي وتتصف صعود الهواء فوق أندوسيا ونزول هواء غرب الهادي هذا ينتج على السطح شرقيات وفي أعالي الجو غربيات فوق خط الاستواء للمحيط الهادي وعند التسخين تحدث الشرقيات للهادي وتتناقص درجة حرارة سطح البحر وتضعف الرياح التجارية وينتج تغير بالضغط بين الشرقيات والغربيات لخط الاستواء للمحيط الهادي وهو أحد العوامل الرئيسية بالحساب فيما اذا تتطور أم لا تتطور النينو^[9] ويعتبر النينو هو المؤثر القوي على مناخ الكرة الأرضية ويعتقد بانه عامل مهم بالتصحر والجفاف في صحراء افريقيا استراليا والهند وكذلك الفيضانات في الأكوادور وبيرو^[11].

الغرض من هذا البحث لأختبار العلاقة بين ظاهرة النينو والتغاير المطري للقطر العراقي.

تحليل البيانات

تسقط أمطار غزيرة في العراق في بعض السنين بينما تكون شحيحة في سنوات أخرى وهذا ما يسمى بالتذبذب المطري والحالتين تشكل خطورة على المحاصيل بالإضافة الى الأضرار على المدن والقرى والطرق. ولدراسة التغيرات المطري بالعراق وعلاقته بظاهرة النينو العالمية أختيرت (١٢) محطة موزعة جغرافياً بشكل جيد على مناطق القطر مع الأخذ بنظر الاعتبار التوزيع الطبوغرافي لما له من أهمية بالغة في التساقط المطري. تم أخذ القراءات للتساقط المطري للمحطات العراقية من هيئة الأنواء الجوية العراقية وحسب التساقط المطري خلال الأشهر الشتوية الثلاثة (ت ٢، ك ١، ك ٢) والأشهر الربيعية الثلاثة (شباط، آذار، نيسان) والانحراف المعياري (SD) والنسبة المئوية للتغيرات المطري (%CV) وتم عمل أحصائيات الى كل من هذين المجموعتين الأولى والثانية نسبة الى شدة التأثير لظاهرة النينو.

كما وأخذت قراءات دليل الذبذبة الجنوبية (SOI) لأشهر السنة (١٩٤٠ - ١٩٩٧) ورسمت بالحاسوب الى كل شهر كما في الرسومات ، الشكل رقم (٥ - أ).

النتائج والمناقشة

١. تلعب التضاريس الأرضية دوراً مهماً في زيادة التساقط المطري ويتضح هذا في الجنول رقم (١) والشكل رقم (١) حيث يكون التساقط المطري في منطقة السهل الرسوبية ومنطقة الهضبة الغربية أقل ما يمكن ويزداد التساقط المطري مع الاتجاه الشمالي والشمال الشرقي حيث يصل الى قيمه العظمى في المناطق الجبلية لذا أهملنا هذه المحطات الجبلية لدخول عامل التضاريس بنسبة عالية، كما نعتقد بأن تأثير ظاهرة النينو لا يصل الى خطوط عرض تزيد على ٣٥ درجة شمال وجنوب خط الاستواء.

٢. عند رسم المعدلات الشهرية للمحطات المناخية للعراق الشكل رقم (٢) تبين وجود أربعة أشهر يندر فيها التساقط المطري في جميع أنحاء القطر وهي (حزيران - تموز - آب - ايلول) في حين يكون شهر مايس وتشرين الاول قليل التساقط وبهذا يمكن تقسيم أو حصر الموسم المطري في ستة أشهر. ثلاثة أشهر شتوية هي تشرين الثاني و كانون الاول و كانون الثاني [N,D,J] وثلاثة أشهر ربيعية هي شباط وآذار ونيسان [F,M,A] والتي تم عليهما أجراء الأحصائيات والدراسة.

٣. لتقديم الفائدة لأكثر عدد ممكن من الباحثين وضعت قيم دليل الذبذبة الجنوبية (SOI) لأشهر السنة وللفترة المحصورة ما بين (١٨٧٦ - ١٩٩٧) في ملحق البحث ولكون الفترة تزيد على ١٢٠ سنة ولأنعدام قراءات التساقط المطري في المحطات العراقية لهذا المدى الطويل أنحصرت أحصائياتنا وتحليل البيانات والدراسة والمناقشة للفترة المحصورة بين (١٩٤٠ - ١٩٩٠) حيث ضمنت ٢٣ سنة نينو كما في الجدول رقم (٢) موزعة الى أربعة أنواع^(١) ما بين ضعيفة جداً بالتأثير على الجو وتحت الرقم (١) الى ضعيفة الشدة بالرقم (٢) ومتوسطة الشدة تحت الرقم (٣) وشديدة تحت الرقم (٤) حسب تصنيف^[1].

٤. لوحظ من النتائج ان الأمطار السنوية للعراق تتميز بتعاقب فترات زمنية غزيرة الأمطار وأخرى قليلة وكذلك بالفراق الكبير بين أدنى كمية للأمطار السنوية وأعلى كمية. ومن خلال استعراضنا لتساقط المطري السنوي شكل (٣) لفترة طويلة أتضح ان أعلى معدل للتساقط المطري كان في المنطقة الشمالية (الجبليّة والمتوجة) الشكل رقم (١) فبالنسبة للمنطقة الجبلية كان معدل التساقط المطري ما بين (٨٤٠-٦٢٩) ملم في زاخو وعقرة على التوالي. أما في المنطقة المتموجة فكانت المعدلات للتساقط المطري ما بين (٤١٥-٣٣٣) ملم في طوزخورماتو وأربيل على التوالي. اما بالنسبة للمنطقة الوسطى والجنوبية فكان التساقط المطري السنوي محصور ما بين (٩٨-١٥٤) ملم. الجدول رقم (١).

نعمه محسن لفته

٥. يلاحظ من السلسلة الزمنية للتساقط المطري التذبذب حول المعدل (زيادة أو نقصان عن المعدل) وتختلف هذه الزيادة أو النقصان من محطة الى أخرى، ألا أن هناك سنوات تشترك فيها كل المحطات بالزيادة أو النقصان عن المعدل كما في الشكل رقم (٣) وعند مقارنته مع السلسلة الزمنية لذبذبة الجنوبية الشكل رقم (٤). وجد ان هناك توافق بين الموجتين المطرية وموجة الذبذبة الجنوبية وهذه اول نقطة توحي بوجود تأثير لظاهرة النينو على الموجة المطرية للمحطات العراقية.

٦. الجدول رقم (٣) يوضح عدد المحطات التي يكون فيها التساقط المطري أعلى من المعدل (Above Norm., AN) أو أقل من المعدل (Bellow Norm.; BN) للأشهر الممطرة الشتوية (N,D,J) وللأشهر الممطرة الربيعية (F,M,A) مع سنوات النينو الضعيفة جداً أو الضعيفة أو المتوسطة أو الشديدة التأثير وسنوات اللانينو . فنلاحظ من الجدول أن محطتين كان التساقط المطري فيها دون المعدل وعشرة محطات فوق المعدل في سنوات النينو الضعيفة جداً بينما ٨ محطات يكون التساقط المطري أعلى من المعدل واربعة محطات دون المعدل هذا الى المجموعة الممطرة الشتوية (ت ٢، ك ١، ك ٢).

وللمجموعة الممطرة الثانية (شباط ، آذار ، نيسان) يكون التساقط المطري فوق المعدل الى ٣ محطات و ٩ محطات دون المعدل مع سنوات النينو الضعيفة جداً و ٩ محطات فوق المعدل و ٣ محطات دون المعدل في حالة التأثير الشديد لظاهرة النينو ويمكن القول بأن التأثير الضعيف جداً والضعيف للنينو يؤدي الى نقصان المطري للعراق وزيادة بالتساقط المطري مع سنوات النينو الشديدة التأثير (ومن هذه الفقرة نستنتج بان الشدة الظاهرة تؤثر على التغيرات المطري).

٧. الجدول رقم (٤) يبين النسبة المئوية للمعامل التغيرات الى المحطات العراقية لجميع سنوات النينو البالغة (٢٣) سنة خلال الـ (٥٠) سنة المدروسة ويشاهد بوضوح بأن النسبة للمعامل التغيرات يتناسب عكسياً مع

خطوط العرض للأشهر الممطرة الأولى وللأشهر الممطرة الثانية وهذا ما يزيد الاعتقاد بأن جنوب العراق ووسطه يتأثر بظاهرة النينو حيث يكون النسبة المئوية لمعامل التغير في مدينة البصرة للمجموعة الممطرة الأولى ١٠٤% و ١٢٤% للمجموعة الممطرة الثانية وتبدأ النسبة المئوية لمعامل التغير بالنقصان مع زيادة خطوط العرض الى ان تصبح ٦٨% و ٦٥% لمدينة الموصل.

أما الانحراف المعياري للمحطات الاثنى عشر حول الرقم (٢٠-٣٠) عند غرض النظر عن المحطات الجبلية فإن الانحراف المعياري لا يعطي لنا فروقات بين محطة وأخرى. وضعت هذه القيم في الجدول كأشارة للقارئ بان الانحراف تم حسابه لكنه يعطي مؤشرات واضحة حول موضوع البحث.

الاستنتاجات

١. التساقط المطري معروف لدى المهتمين والاختصاصيين في العراق يزداد مع الاتجاه الشمالي والشمالي الشرقي نتيجة وجود السلاسل الجبلية في شمال العراق ويمكن اعتبار الأشهر الممطرة ستة أشهر، ثلاثة شتوية هي تشرين الثاني وكانون الأول وكانون الثاني وثلاثة ربيعية هي شباط وآذار ونيسان وأشهر السنة الباقية أربعة صيفية يندر التساقط فيها وهي مايس وحزيران وتموز وآب وشهرين خريفيين يكون التساقط قليل وهي أيلول وتشرين الأول.
٢. ان ظاهرة النينو تؤثر على التغير المطري في العراق من خلال العلاقة الواضحة بين معامل الذبذبة الجنوبية والسلاسل المطرية الشتوية والربيعية والسنوية.
٣. ان شدة الظاهرة تؤثر على الشذوذ بالتغير المطري (زيادة أو نقصان عن المعدل) من خلال الأحصائيات في الجدول رقم (٣).

نعمه محسن لقنه

٤. ان جنوب العراق ووسطه يتأثر بظاهرة النينو وذلك من خلال الجدول (٤) النسبة المئوية للتغيرات المطرية في المحطات الجنوبية والوسطى. أما المحطات الشمالية فتكون النسبة المئوية للتغيرات المطري قليلة.

جدول رقم (١)

الموقع والمعدل السنوي للتساقط المطري الى (١٢) محطة مناخية للعراق خلال الفترات المسجلة أمامها

المدينة	الموقع	معدل التساقط المطري السنوي (mm)	الفترة المسجلة
البصرة	٣٧ ٤٧	٣٠ ٣٤	١٩٩٠-١٩٤١
العمارة	١٧ ٤٧	٣١ ٨٥	١٩٩٠-١٩٥٨
النجف	٣٢ ٤٤	٣١ ٩٨	١٩٩٠-١٩٦٢
الكويت	٠٣ ٤٦	٣٢ ١٠	١٩٩٠-١٩٤١
بغداد	١٤ ٤٤	٣٣ ١٤	١٩٩٠-١٩٤١
طوزخرماتو			١٩٩٠-١٩٥٢
كركوك	٢٤ ٤٤	٣٥ ٢٨	١٩٩٠-١٩٤١
السليمانية	٤٣ ٤٥	٣٥ ٥٥	١٩٩٠-١٩٤١
أربيل	٢٠ ٤٤	٣٦ ٣٨	١٩٩٠-١٩٤٩
الموصل	٠٩ ٣٤	٣٦ ١٩	١٩٩٠-١٩٤١
عقرة			١٩٩٠-١٩٤٧
زاخو	٦٨ ٤٢	٣٧ ١٣	١٩٩٠-١٩٥٣

جدول رقم (٢): مستهل السنوات لأنواع حدوث النينو خلال الفترة (١٩٤٠-١٩٩٧) وتصنيف الحدث نسبة الى الشدة (ضعيف جداً رقم (١)، ضعيف (٢)، متوسط (٣) شديدة (٤))

السنة	شدة الحدث	السنة	شدة الحدث
١٩٤٠	٢	١٩٦٩	٢
١٩٤١	٤	١٩٧٢	٤
١٩٤٣	٢	١٩٧٣	٤
١٩٤٤	٢	١٩٧٥	١
١٩٤٦	١	١٩٧٦	٣
١٩٤٨	١	١٩٨٢	٤
١٩٥١	٢	١٩٨٣	٤
١٩٥٣	٣	١٩٨٦	٣
١٩٥٧	٤	١٩٨٧	٢
١٩٥٨	٤	١٩٩٢	٤
١٩٦٣	١	١٩٩٧	٤
١٩٦٥	٣		

المصدر : [Rasmusson, 1984 and Andrade & Sellers, 1988]

جدول رقم (٣): الأرقام تعبر عن عدد المحطات المناخية التي فيها تساقط مطري فوق المعدل AN وتحت المعدل BN خلال الفترة المدروسة كدالة لشدة تأثير النينو

السنة الكاملة		شباط آذار نيسان		ت ٢ ك ١ ك ٢		الشدة
BN	AN	BN	AN	BN	AN	
١٠	٢	٩	٣	١٠	٢	ضعيفة جداً
٤	٨	٥	٧	٩	٣	ضعيفة
٢	١٠	٨	٤	١٠	٢	متوسطة
٣	٩	٣	٩	٤	٨	شديدة
٥	٧	٢	١٠	٥	٧	سنوات النينو

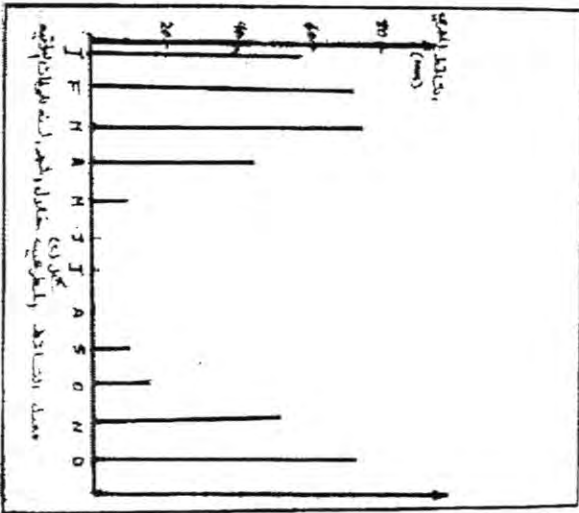
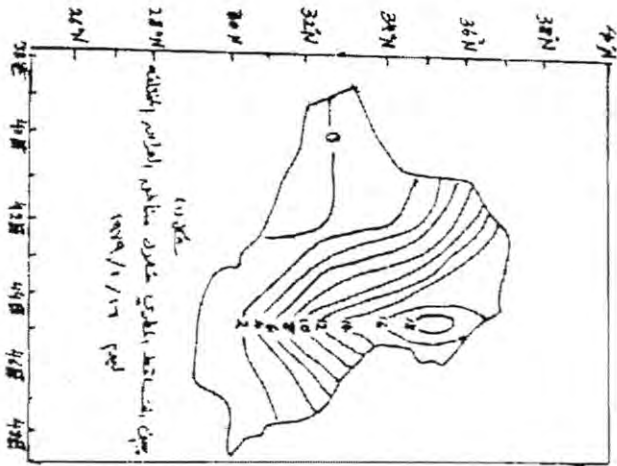
نعمه محسن لقنه

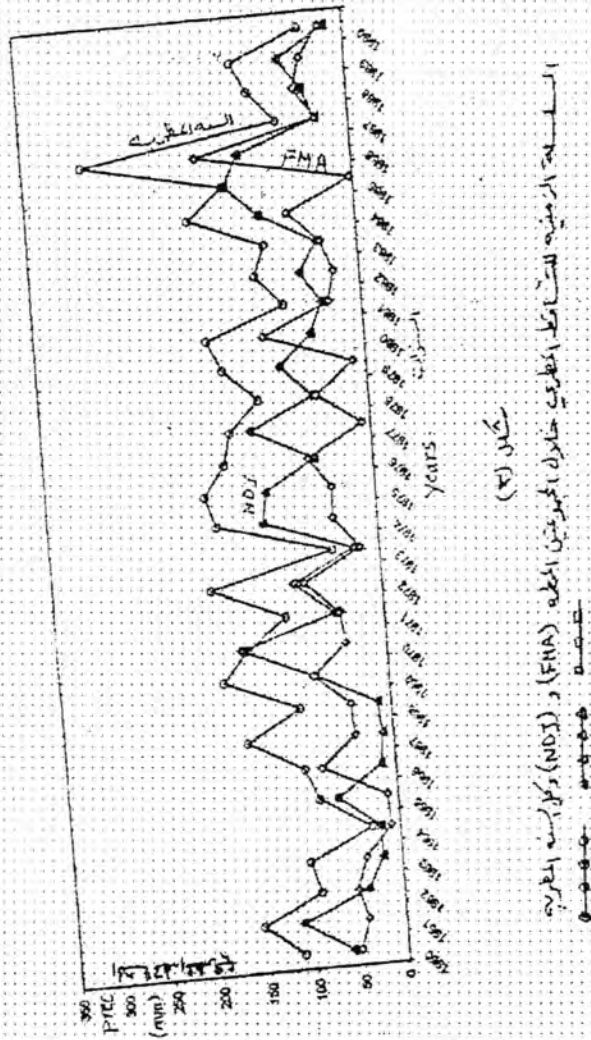
جدول رقم (٤): النسبة المئوية لمعامل التغيرات والانحراف المعياري للمحطات العراقية في سنوات النينو

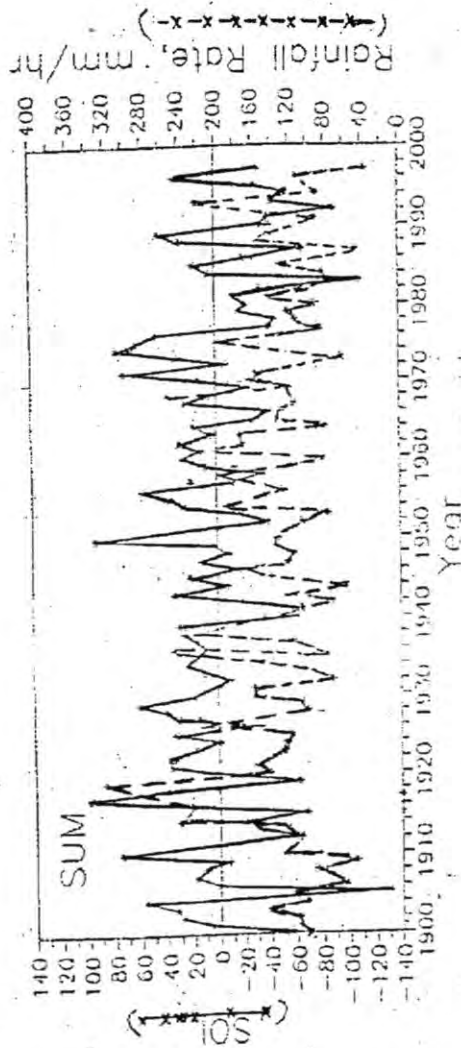
النسبة المئوية لمعامل التغيرات CV%		الانحراف المعياري SD		المحطات
FMA	NDJ	FMA	NDJ	
١٢٤	١٠٤	٢١	٢٥	البصرة
١٢٠	١٠٣	٢١	٢٨	العمارة
١٣٣	١٢٧	١٦	١٩	النجف
١٢١	١٠٥	١٥	١٨	الكويت
١٠٥	٨٦	٢٣	١٨	بغداد
١٠٩	١١٤	٤٢	٣٨	طوزخورماتو
٧١	٧٤	٤٤	٣٧	كركوك
٥٨	٦٣	٦٤	٦٠	السيمانية
٧٠	٩٨	٤٧	٥٤	أربيل
٦٥	٦٨	٣٨	٣٥	الموصل
٨٩	٨٢	١٢٢	١٠٣	عقراء
٦٥	٨٠	٦٢	٧١	زاخو

REFERENCES

1. Andrade, E.R. And Sellers, W.D. : EL-Nino and its effect on precipitation in Arizona and western new mexico, J. of Climat, Vol. 8, 403-410 (1988).
2. Philander, S.G. and Rasmusson, E.M. The Southern Oscillation and Elnio, Adr. Geophys, 28, 197-215 (1985).



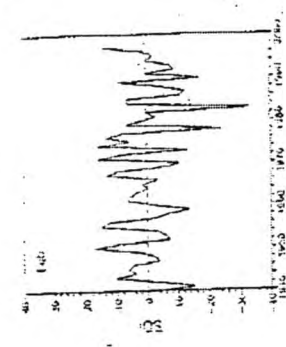
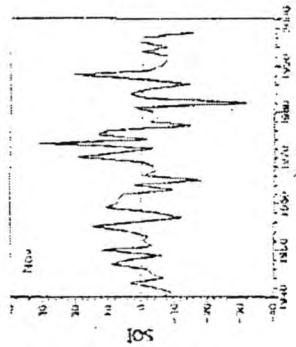
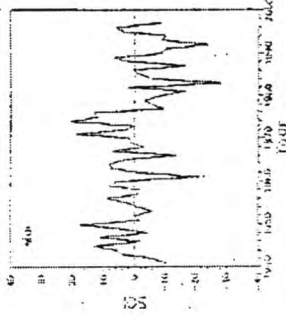
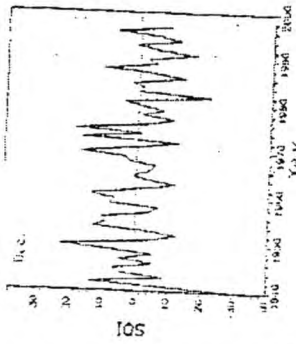
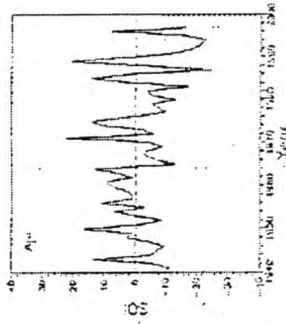
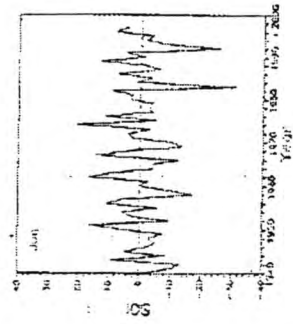




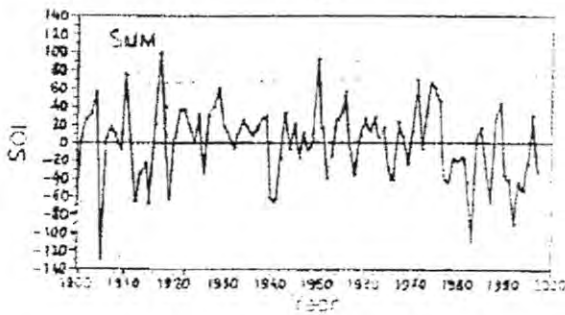
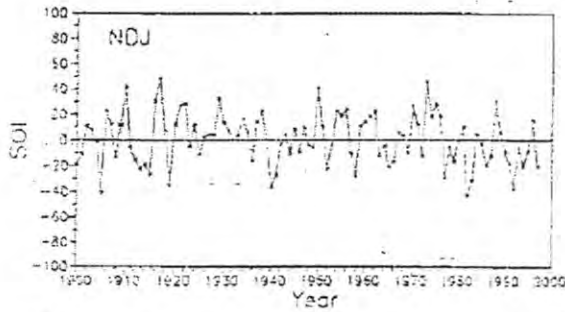
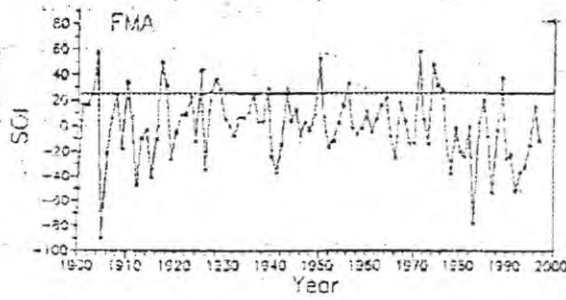
شكل (٤)
السلسلة الزمنية لطريقه التغيرات العراقية خلال الفترة المذكورة والسلسلة الزمنية لـ SOI

تأثير ظاهرة النينو على التغيرات المطري في العراق

نعمة محسن لفته



دليل النينو اكنوسيه
501 لا شهر السنه الملهه خلال نتره الدماسه
شكل [٣٥]



شكل (٥ ب)

دليل التذبذب الجنوبي SOI للشهر الربيعي FMA، والتنبؤ NDJ،
والتنبؤ SUM.

نعمه محسن لفته

- Walker, G.T. and Bliss, E.W. : World weather V. Mem. R. met. Soc., Vol. 36, 53-84. world Meterological Organization, (1983-1988), the Global Climate system, world climate date programme, Who, Geneve. (1932).
3. Chen W.Y : Assessment of southern oscillation sea-level pressure indices", Mon. Wea Rev, 110, 800-807 (1982).
4. GLANTS, N.H : Floods, Fires and Famine; is EL-Nino to blame ? Oceanus, 27, 14-19 (1984).
5. Bjerkens, J. : Atmospheric teleconnections from the equatorial pacific, Mon. Wea. Rev. Vol. 97, 163-172 (1969).
6. Hickey, B. : The relationship between Fluctuation in sea level, wind stress, and sea surface temperature in the equatorial pacific, J. Phys. Oceanogr. 5, 46-475 (1975).
7. Walker, G.T. : Correlation in seasonal variations of weather, 1x : A further study of world, Mem. Ind. met. Dept., 24, 275-332 (1924).
8. Wyrski K. : ElNino : The dynamic response of the equatorial pacific ocean to atomosphenic forcing. J. phys. Oceanogr., 5, 572-584 (1975).
9. Quinn, W.H. : Monitoring and prediciting Elnino invasions, Joun, Appl. Metero., 13, 825-830 (1974).
10. World Weather Records, Monthly climatic : Date for the world, from (1900-1988) U.S. Dept of Commerce, Wachington, D.C.